UNIVERSITY OF CANTERBURY

Department of Mechanical Engineering
Christchurch, New Zealand

Wind Turbine Noise

by

Andrew J Mitchell

Master of Engineering
Thesis

May 2004

Wind Turbine Noise

by

Andrew J Mitchell

A thesis submitted in

partial fulfilment of the requirements for

the Degree of Master of Engineering

in the

Department of Mechanical Engineering

University of Canterbury

Christchurch, New Zealand

May 2004

Abstract

The objectives of this thesis were (i) to investigate the main sources and paths of noise on modern utility size wind turbines; (ii) to explore methods of reducing the noise; (iii) to assess our current ability to accurately predict and measure wind turbine noise. The accomplishment of these objectives would enable quieter wind turbines to be developed and allow them to be located near residential dwellings with greater confidence that the noise would not be a nuisance.

A comprehensive review of the current literature was carried out and the findings were used as a basis for the investigative work conducted. It was found that wind turbine noise could be classed as either aerodynamically produced noise or mechanically produced noise. Aerodynamically produced noise on wind turbines arises mainly from the interaction of the flow over the blade with the surrounding air. Mechanically produced noise arises from a number of sources such as the gearbox, generator and hydraulic pumps. The noise can be radiated directly from the noisy component (airborne) and / or transferred through the structure of the turbine and radiated elsewhere (structure-borne) such as the tower.

The prototype Windflow 500 wind turbine near to Christchurch was used for the majority of the investigative work carried out, and to assess the predictions made. The main radiators of noise from the turbine were identified as the blades (86 – 90% of the total sound power), the tower (initially 8 – 12% but later reduced to ~4% of the total sound power), and the nacelle cladding (1% of the total sound power). A prominent tone in the sound power spectrum from the turbine was observed in the 315 Hz 1/3 octave band. This was shown to be predominantly caused by gear meshing in the second stage of the gearbox at 311 Hz. The presence of the tone was significant because under commonly used standards a tonal penalty would be applied to the measured sound pressure level from the turbine to account for the extra annoyance caused by the tone. This in turn would mean that any potential wind farms would need to be sited further from residential dwellings than would otherwise be necessary in order to comply with noise regulations.

Investigations were carried out that addressed the noise radiated from each of the main contributors outlined above. The sound power level radiated from the tower was found to be effectively reduced by attaching rubber tiles at strategic locations inside the tower. Noise radiated from the nacelle was reduced with a combination of acoustic insulation and acoustic absorption inside the nacelle. An investigation into the gearbox noise was also carried out. Attempts to reduce the tonal noise caused by gear meshing were made with little success but the investigation provided a good basis upon which to conduct further work.

Preliminary investigations into both structure-borne and aerodynamically generated blade noise were carried out. The structure-borne blade noise investigation showed that the blades readily vibrated at a range of frequencies, the result being that structurally transmitted noise radiated from the blades was likely to be present at high levels. Research showed that the structure-borne noise radiated from the blades could be significantly reduced by partially filling the internal cavity of the blades with foam. The investigation of aerodynamically produced noise was carried out on a section of Windflow 500 blade in the low noise wind tunnel at the University of Canterbury. The tests showed that the blade generated noise at a range of frequencies including those in the 315 Hz 1/3 octave band. This suggested that the tonal noise measured from the blades was not only due to structurally transmitted noise from the gearbox but was also contributed to by aerodynamically produced noise. It was found that the noise from the blade section could be reduced by up to 4.5 dB at certain frequencies by attaching serrated strips to the trailing edge of the aerofoil.

Empirical equations for prediction of wind turbine sound power levels were evaluated and found to be in good agreement with measured data. It was found that accurate spectral predictions of the sound power level were much more difficult. However given spectral data for a turbine, it was found that accurate predictions of the noise propagation from the turbine could be made, taking into account meteorological effects and the effect of complex topography. It was found that the CONCAWE propagation model was well suited to the prediction of noise propagation from wind turbines because of its superior handling of meteorological effects. In an investigation carried out which modelled the Gebbies Pass site of the

Windflow 500 it was found that the CONCAWE model could predict sound pressure levels from the turbine to within 2 dB at distances of up to 1400 m.

Further work in the area of wind turbine noise should be focused on the reduction of blade noise. This is especially relevant to the Windflow 500 since blade noise was found to be by far the largest contributor to total noise radiated from the turbine. Acoustic treatments elsewhere would therefore produce only small reductions in the total sound power emitted by the turbine.

Acknowledgements

I would like to thank Dr John Pearse and Professor Cliff Stevenson of the Department of Mechanical Engineering, University of Canterbury for their guidance, support and encouragement. The leadership and expertise that they have provided is embodied in this thesis.

I wish to extend special thanks to Windflow Technology for the use of their wind turbine and facilities. In particular I would like to thank Geoff Henderson, Warwick Payne and Wernher Roding for their ideas, assistance and 'real world' engineering support.

I would like to thank my parents for providing me with the wealth of opportunities with which I grew up. The opportunities they provided have ultimately led me to where I am today. I would like to express my gratitude to both my parents and my wife Neroli for their support and understanding during the course of my studies.

I also wish to thank my good friend and fellow acoustics student Aaron, who has undoubtedly made my time here more enjoyable with his dry sense of humour, mischievous antics and amusing propensity to break things that were not meant to be broken.

Finally I would like to convey my thanks to my brother David, for providing many hours of assistance with the wind tunnel work, my friend Mess for the use of his handheld GPS unit, and to all of the other people who have provided technical advice and practical assistance during the course of my studies.

Preface

This Masters thesis is primarily concerned with the prediction, measurement and reduction of wind turbine noise. Much of the work in this thesis was based on the Windflow 500, a prototype turbine that was installed near Christchurch in early 2003 by the New Zealand wind turbine manufacturer Windflow Technology.

1. Motivation

In order to construct the prototype turbine, Windflow Technology was required to obtain a resource consent, for which it was necessary that the noise levels produced by the turbine were modelled in the surrounding area. The WEG MS3, a similar wind turbine that was built in the UK in the early 1990's, provided an estimate of the sound power level that would be produced by the turbine. The sound pressure levels at a number of critical points around the Gebbies Pass area were then calculated from this using the propagation model specified in NZS 6808:1998 "Acoustics - The Assessment and Measurement of Sound from Wind Turbine Generators".

A number of issues were raised by the residents of nearby McQueen's Valley during the resource consent process including the accuracy of the sound power estimate, the accuracy of the propagation model and how likely the sound was to be masked by the background noise level. These issues and the convenience of a wind turbine within an hour's drive from the University campus prompted this research into wind turbine noise.

After installation of the turbine, Windflow Technology was required to ensure that the noise levels from the turbine were within the predicted levels. Upon discovering that the turbine noise was above the allowable levels, remedial work was required to be carried out, providing further motivation for the research.

2. Aims and Objectives

The main objectives of this thesis fall into three categories – prediction, measurement and reduction of wind turbine noise. The objectives within each category are described below.

2.1 Prediction

- Assess the accuracy of current empirical wind turbine noise prediction models and if possible improve them.
- Research and develop models for the propagation of sound over complex terrain and assess their accuracy with regards to the Windflow 500.
- Gain a sufficient understanding of wind turbine noise to allow prediction of the resulting sound pressure levels to within 1-2 dB at distances of up to 2km from the turbine site.

2.2 Measurement

- Measure the noise levels of the Windflow 500 for a range of different wind speeds and directions.
- Quantify the proportions of structure-borne versus airborne noise.
- Test and evaluate modifications made to the turbine to reduce its noise level.

2.3 Reduction

- Investigate the effect of blade parameters on the noise produced by the turbine blade.
- Investigate techniques of reducing both the structure-borne and the airborne components of the mechanical noise from the turbine.

3. Conventions and Terminology

3.1 General Conventions

The measured data in this thesis is in 1/3 octave bands, and hence should be referred to frequency bands. To avoid needless repetition much of the discussion refers to frequencies and frequency ranges instead of frequency bands and frequency band ranges.

The prototype Windflow 500 turbine studied in this thesis was located at Gebbies Pass near to Christchurch. It is often referred to as the "Windflow 500", "the wind turbine" or simply "the turbine".

This thesis is presented in chapters. A table of contents, list of figures, and a list of tables contained within each chapter are presented at the beginning of each chapter. A bibliography and list of references is provided at the end of each chapter where appropriate. Nomenclature for equations and formulas has been defined in full following each equation or set of equations.

3.2 Anatomy of a Wind turbine

Figure P1 below shows the main components of a typical horizontal axis wind turbine –

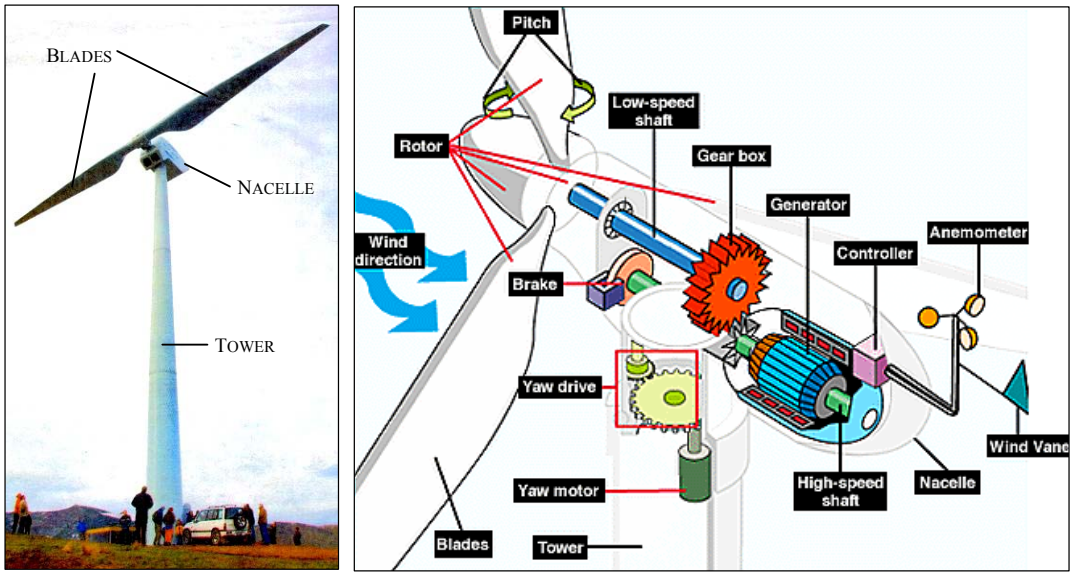

Figure P1 – Anatomy of a Wind Turbine

3.3 Definitions and Abbreviations

A list of the more commonly used terms and abbreviations from this thesis is shown below with the definition as used in the thesis.

Term	Definition as Used in Thesis
Aero-acoustic noise	Noise generated due to the interaction of the flows over an aerofoil or around an object.
Aerodynamic noise	See *Aero-acoustic noise.*
AGL	Above ground level.
Airborne noise	Noise radiated directly to the air from a noise source.
Blade	The aerodynamic part of the rotor used to turn the hub.
Blade pitch	Angle of attack of the blades.
GMF	Gear meshing frequency.
Mechanical noise	Noise originating from mechanical sources and machinery.
Nacelle	Usually refers to the system of machinery contained the top enclosure of the turbine, but can be used more generally to include the machinery and the enclosure itself.
Nacelle cladding	The housing (walls, floor and roof) that encloses the nacelle machinery.
Overall noise	The noise generated by the turbine as a whole.
Pallet	Chassis upon which the machinery in the nacelle is mounted to the tower.
Rotor	The assembled blades and hub.
Rotor hub	Centre of the rotor. Part to which the blades are attached and through which the rotor is attached to the gearbox input shaft.
SIL	Sound intensity level.
SPL	Sound pressure level.
STL	Sound transmission loss.
Structure-borne noise	Noise transmitted from a noise source structurally as vibration, later being radiated to the surroundings.
SWL	Sound power level.

Teeter	The ability of the rotor to rock at the hub to reduce fatigue loads on the structure of the turbine.
TL	1) Torque limiting. 2) Transmission loss.
TLG	Torque limiting gearbox.
Total noise	1) The logarithmically added total of each of the frequency bands in a noise measurement. 2) See *Overall noise.*
Tower	The upright structure of the turbine that supports the nacelle.
Yaw	Rotation of the direction of the nacelle so as to face the turbine into the wind.

Table of Contents

Chapter 9

Modelling and Validation of Sound Propagation from the Wind Turbine

Summary

This chapter describes the investigation that was carried out into predicting the propagation of wind turbine noise over complex terrain and in various meteorological conditions.

Three propagation models were investigated in depth - i) ISO 9613 [1],[2], ii) the CONCAWE model [4], and iii) NORD2000 – the Nordic General Prediction Method [6],[7],[8]. SoundPLAN^{TM} noise modelling software was used to expediently calculate the predictions from each model at a number of receiver locations. A three dimensional terrain model of the area surrounding the Windflow 500 wind turbine was constructed in SoundPLAN and the sound power level of the wind turbine was set to be the same as that determined experimentally. The sound pressure level at a number of receiver locations in the area was calculated using each model, for a range of meteorological conditions. The results were validated using measured data and were compared to predictions calculated using the simpler method employed in NZS 6808 [3].

The results showed that the CONCAWE model was the most accurate model for use where the wind speed and direction has a significant influence on the sound pressure level at a receiver location. It was found that the CONCAWE model could usually predict the sound pressure level at a given location to within 1 – 2 dBA of measured data. Given the accuracy and repeatability of the measured data, the prediction of the CONCAWE model (or any model for that matter) could not have realistically been expected to be more accurate.

The ISO method of calculation, while not quite as accurate, was found to be the fastest. The Nordic method was the slowest and in this application did not prove to be any more accurate than the ISO method.

Table of Contents

List of Figures

List of Tables

1. Introduction

1.1 Background

One of the goals of this research was to establish if a method existed for accurately predicting the noise level from a wind turbine at receiver distances of up to 2 km. More specifically it was envisaged that the method would be capable of adjusting for the effects on sound propagation of complex topography and meteorological conditions.

1.2 Modelling Methods Investigated

Three modelling methods that met the above specifications were identified. These were -

- ISO 9613: Acoustics -- Attenuation of Sound During Propagation Outdoors Pt 1 & 2 [1], [2]
- CONCAWE Model [4]
- NORD2000 – Nordic General Prediction Method [6], [7], [8]

A brief description of each model can be found in Chapter 1, section 4.6. From a general viewpoint each model has its advantages and disadvantages. The Nordic and CONCAWE methods employ calculations based on octave bands whereas the ISO method does not allow for influences on different frequencies. The ISO method may therefore be used for any frequency but in some circumstances may not calculate the spectral content of the noise very accurately. The CONCAWE method is especially suited for assessments where prevailing winds and other meteorological conditions do not fit the conditions for which the other methods were developed. CONCAWE is the only method that allows the meteorological influence to be assessed in detail. The strength of the Nordic method is in accommodating topographical effects and screening, but it makes no allowance for the effect of differing meteorological conditions. It is the only method available for accurate frequency dependent calculations of ground effects. The ISO calculation method is much faster than the Nordic or the CONCAWE methods, making it particularly suitable for noise mapping of large areas.

The three models described above were also compared with the less complex noise prediction method of NZS 6808:1998 [3] (see chapter1, section 4.6) in order to establish if the use of the more complex models was justified.

1.3 Modelling Software

In order to facilitate faster calculation of predicted noise levels, an environmental noise modelling computer software package was used. Several different programs were available for this task, but SoundPLAN v6.1 was selected for its capability to make predictions using all three of the calculation methods investigated, and because of its widespread use in industry.

In SoundPLAN a geometrical terrain model is constructed and various parameters such as source and receiver properties are set in order to simulate conditions in the area to be modelled. After selecting a calculation method or standard, the user can then adjust the parameters specific to the chosen method of calculation, such as those which account for the influence of meteorological and topographical effects on the sound propagation. SoundPLAN can then be used to predict the noise levels from the source(s) either at selected receiver locations or over the entire calculation area (i.e. construct a noise map of the area). SoundPLAN calculates the noise levels according to the rules defined in the calculation method being used.

1.4 Objective

The aim of the investigation was to establish which, if any, of the propagation models described in section 1.2 were accurate enough to predict the sound levels from a wind turbine to within ± 2 dBA at distances of up to 2km.

2. Model Description

2.1 General Parameters

As mentioned in section 1.3, SoundPLAN v6.1 environmental noise modelling software was used to calculate the sound pressure levels in the vicinity of the wind turbine according to the ISO, CONCAWE

and NORD2000 modelling methods. The simulations were run from Microsoft Windows 2000 Professional™ on an Intel Pentium 4™ 2.4 GHz processor with 512 megabytes of ram. Calculations using the NZS 6808:1998 method were done by hand at selected receiver locations.

2.1.1 Area Modelled

The Gebbies Pass site of the Windflow 500 wind turbine was modelled for the investigation. The area used was rectangular in shape and spanned 2 km from north to south, 4 km from east to west and was centred on the turbine site as shown in figure 9.2.1.

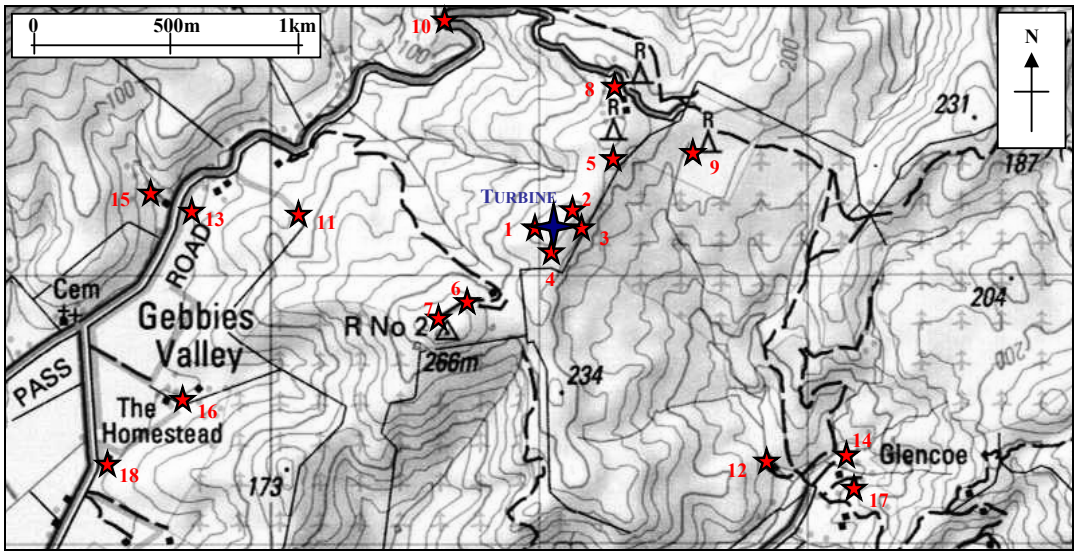

Figure 9.2.1 – Area Modelled

Receivers were placed at houses near the turbine and at a number of other easily recognisable landmarks in the area (as shown in figure 9.2.1). Table 9.2.1 details the location and description of each receiver along with its distance from the turbine.

Table 9.2.1 – Receiver Locations

Receiver	Landmark	Distance from Turbine (m)	Direction from Turbine
1	Ring of tussock	30	W
2	Met mast	66	NE
3	Access road	90	E
4	Steep part of access road	100	S
5	Top gate on access road	320	N
6	Gate of House 1	400	SW
7	House 1	527	SW
8	House 2	551	NNE
9	Hut near RNZ mast	630	NE
10	Hairpin corner main road	840	NW
11	House 3	966	W
12	House 4	1255	SE
13	House 5	1263	W
14	House 6	1393	SE
15	House 7	1514	W
16	House 8	1544	SW
17	House 9	1572	SE
18	House 10	1852	SW

2.1.2 Terrain Model

A three dimensional model of the terrain surrounding the Gebbies Pass wind turbine site was developed in SoundPLAN based on 20m contour lines from a 1:50000 topographical of the area (see figure 9.2.2).

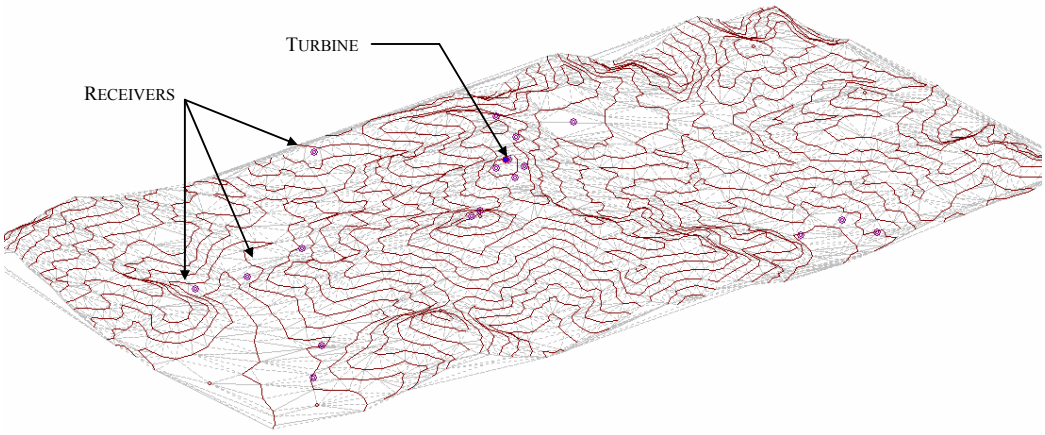

Figure 9.2.2 – Three Dimensional Terrain Model

A ground absorption coefficient of 0.5 dBA/km was applied to the entire calculation area to represent the ground attenuation resulting from the mix of open grass and tussock farmland, hard clay soils, and rocky outcrops that were present in the area surrounding the turbine.

2.1.3 Air Absorption

The attenuation due to air absorption for each of the modelling methods was calculated using ISO 9613-1 [1].

2.1.4 Meteorological Conditions

The noise propagation was modelled for a range of different meteorological conditions. The effects of wind speed and direction were studied comprehensively, but the effects of humidity, temperature and atmospheric temperature inversion (as sometimes occurs at night) were also investigated. Table 9.2.2 shows details of the combinations of meteorological conditions modelled.

Table 9.2.2 – Meteorological Conditions Modelled

Run #	Simulated Condition	Wind Dirn	Wind Spd (m/s)	Humidity (%)	Temp (^{o}C)
1	Light northerly wind, average summer day	N	6	55	20
2	Northerly wind, average summer day	N	7	55	20
3	Northerly wind, average summer day	N	8	55	20
4	Northerly wind, average summer day	N	9	55	20
5	Strong northerly wind, average summer day	N	10	55	20
6	Strong northerly wind, humid summer day	N	10	80	20
7	Strong northerly wind, average winter day	N	10	55	10
8	Light northerly wind, winter night	N	6	55	3
9	Light southerly wind, average summer day	S	6	55	20
10	Southerly wind, average summer day	S	8	55	20
11	Strong southerly wind, average summer day	S	10	55	20
12	Strong southerly wind, average winter day	S	10	55	10
13	Light southerly wind, winter night	S	6	55	3
14	Light easterly wind, average summer day	E	6	55	20
15	Easterly wind, average summer day	E	8	55	20
16	Strong easterly wind, average summer day	E	10	55	20
17	Light westerly wind, average summer day	W	6	55	20
18	Westerly wind, average summer day	W	8	55	20
19	Strong westerly wind, average summer day	W	10	55	20

All models assumed an atmospheric pressure of 101.3 kPa.

2.1.5 Turbine Emission Data

The sound power level of the Windflow 500 wind turbine was previously measured at wind speeds of 6 and 10 m/s. These measurements formed the basis of the emission data for the models. For wind speeds between 6 and 10 m/s the sound power levels were linearly interpolated. At wind speeds above 10 m/s, it was found experimentally that the noise level of the turbine remained approximately constant. The sound power level of the wind turbine operating in a 10m/s wind was therefore also used in the simulations where the wind speed was above 10 m/s. Table 9.2.3 shows the sound power levels that were used at each wind speed. Note that no directivity was assigned to the source data for the turbine.

Table 9.2.3 – Turbine Emission Data

Sound Power Emission from Windflow 500 (dBA)					
1/3 Octave Band	**Windspeed (m/s)**				
Centre Frequency (Hz)	**6**	**7***	**8***	**9***	**10**
50	68.4	72.6	76.7	80.9	85.0
63	71.6	75.3	79.0	82.7	86.4
80	74.5	77.9	81.2	84.6	87.9
100	73.6	77.5	81.3	85.1	88.9
125	77.9	80.4	82.9	85.3	87.8
160	83.1	84.4	85.6	86.8	88.0
200	85.6	86.6	87.6	88.6	89.6
250	88.5	89.5	90.6	91.6	92.6
315	99.0	100.0	100.9	101.8	102.7
400	94.0	95.0	95.9	96.9	97.8
500	91.0	92.3	93.6	94.8	96.1
630	90.5	91.5	92.5	93.5	94.5
800	90.5	91.3	92.0	92.8	93.5
1k	90.6	91.9	93.1	94.3	95.5
1.25k	90.3	91.2	92.1	92.9	93.8
1.6k	89.8	90.3	90.8	91.2	91.7
2k	88.9	89.5	90.1	90.7	91.3
2.5k	89.3	89.8	90.3	90.7	91.2
3.15k	90.8	91.3	91.8	92.2	92.7
4k	92.4	92.6	92.7	92.8	92.9
5k	91.7	92.0	92.2	92.5	92.7
6.3k	88.3	88.8	89.3	89.8	90.3
8k	80.2	82.2	84.1	86.1	88.0
10k	74.7	76.9	79.1	81.3	83.5
12.5k	70.1	72.1	74.1	76.0	78.0
Total	104.1	105	105.9	106.8	107.7

* Interpolated values

2.1.6 Computational Parameters

All calculations were done with an 'A' frequency weighting applied. The SoundPLAN computational parameters were left at their default settings as follows –

- Angle increment for calculations *1 degree*
- Maximum number of reflections calculated *3*
- Reflection depth *0*
- Maximum radius of search for sources *5000m*
- Side diffraction *Disabled*

An explanation of the purpose of each of these settings follows –

Angle Increment

SoundPLAN uses a sector method to partition the calculation area. Starting from the receiver, search "rays" scan the geometry for sources, reflections, screens and geometry modifying the ground attenuation. The scanning rays use a constant angular increment to complete a 360^{o} scan around the receiver. The finer the increments, the more accurate the calculations, but the slower they become.

Maximum Number of Reflections and Reflection Depth

These two parameters are relevant for the reflection calculation. The number of reflections depicts how many consecutive reflections of a search ray are permitted until the operation is stopped. The reflection depth defines the number of potential reflecting surfaces that the search ray may pass over before a reflected ray can no longer be found. Figure 9.2.3 below shows two examples that explain the effect of these parameters.

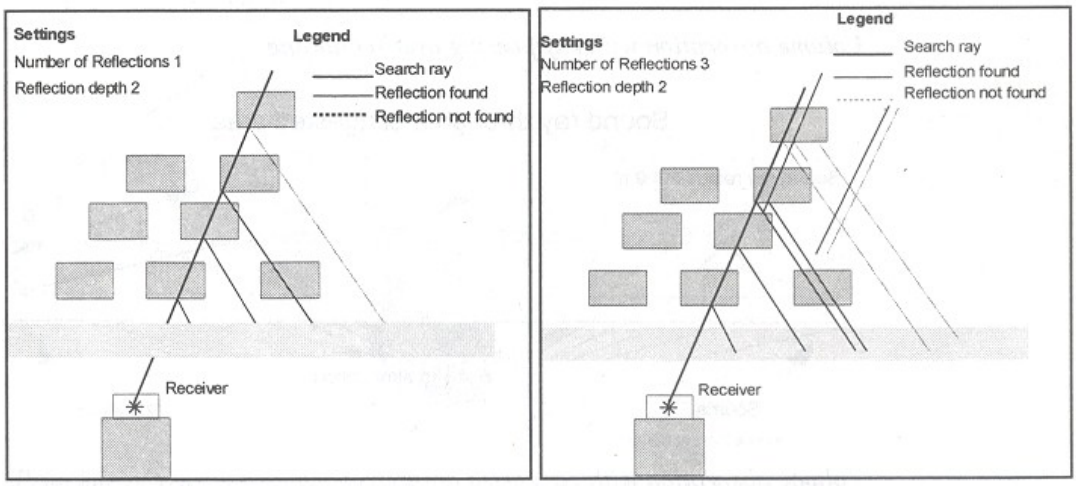

Figure 9.2.3 – Maximum Number of Reflections and Reflection Depth

Maximum Radius of Search for Sources

During the calculation SoundPLAN searches for sources within a set distance around the receiver. The maximum search radius sets how far a source can be from the receiver and still contribute to the noise level at the receiver.

Side Diffraction

In normal operations, SoundPLAN evaluates the diffraction of sound over a screen. Diffraction around the sides of obstacles is only processed if the calculation standard used has made provisions for it and if side diffraction is enabled. For big noise maps, the use of this option usually results in a significant increase calculation time with minimal changes in the results.

2.2 ISO 9613 Specific Model Set-Up

2.2.1 Diffraction Parameters

The diffraction parameters were set as follows –

- Limitation of single diffraction *20 dB*
- Limitation of multiple diffraction *25 dB*
- Diffraction constant C_1 *3*
- Diffraction coefficient C_2 *20*

- Diffraction coefficient C_3 *1*

The above values were the SoundPLAN defaults and were determined from the standard to be suitable in this situation. The definition of each parameter follows –

Limitation of Single Diffraction

This value is the maximum attenuation allowable due to diffraction of the sound over a single barrier (see figure 9.2.4).

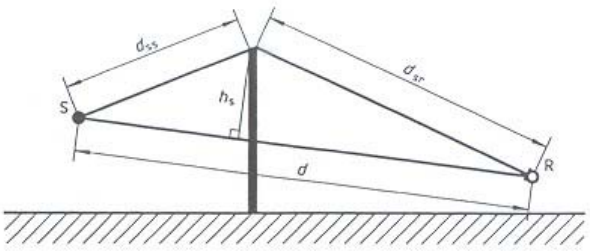

S = Source, R = Receiver

d_{ss} = Distance from source to barrier (m)

d_{sr} = Distance from barrier to receiver (m)

d = Direct distance from source to receiver (m)

h_s = Effective height of barrier (m)

Figure 9.2.4 – Diffraction Over a Single Barrier

Limitation of Multiple Diffraction

This value is the maximum attenuation allowable due to diffraction of the sound over multiple barriers (see figure 9.2.5)

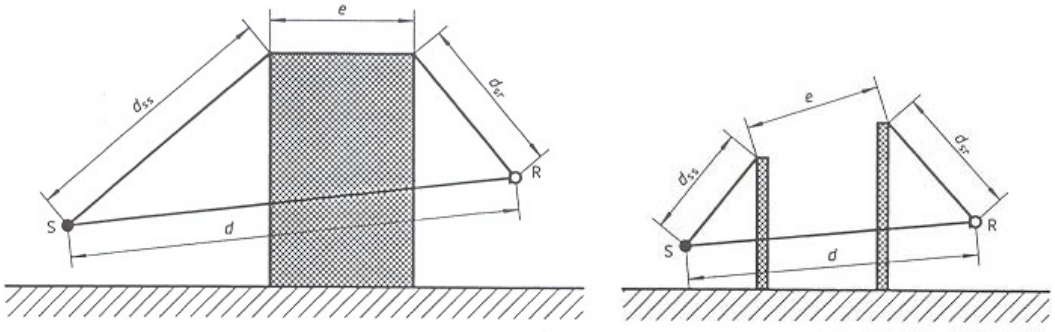

S = Source; R = Receiver; d_{ss} = Distance from source to barrier (m); d_{sr} = Distance from barrier to receiver (m); d = Direct distance from source to receiver (m); e = Distance between barriers (m)

Figure 9.2.5 – Diffraction Over a Double Barrier

Diffraction Parameters C_1, C_2, C_3

ISO 9613 uses the following formula to calculate the barrier attenuation –

$$D_Z = 10\log_{10}\left[C_1 + \left(\frac{C_2}{\lambda}\right)C_3 z K_{Met}\right] \tag{9-1}$$

where

D_Z is the attenuation of the sound due to a barrier.

C_1 is a constant equal to 3.

C_2 is a coefficient equal to 20 for normal calculations and includes the effect of ground reflections. In special cases where ground reflections are taken into account separately by image sources, $C_2 = 40$.

λ is the wavelength of the sound in metres.

C_3 is a coefficient equal to 1 for single diffraction. For double diffraction with distance e between the screens C_3 is given by –

$$C_3 = \left[1 + \left(\frac{5\lambda}{e}\right)^2\right] \Big/ \left[\frac{1}{3} + \left(\frac{5\lambda}{e}\right)^2\right] \tag{9-2}$$

z is the path length difference between the directed and diffracted sound as calculated by equations (9-3) and (9-4).

For single diffraction

$$z = \left[\left(d_{ss} + d_{sr}\right)^2 + a^2\right]^{1/2} - d \tag{9-3}$$

For double diffraction

$$z = \left[\left(d_{ss} + d_{sr} + e\right)^2 + a^2\right]^{1/2} - d \tag{9-4}$$

where

d_{ss} is the distance from the source to the (first) diffraction edge in metres as shown in figures 9.2.4 and 9.2.5.

d_{sr} is the distance from the (second) diffraction edge to the receiver in metres as shown in figures 9.2.4 and 9.2.5.

a is the horizontal distance between the source and the receiver in metres.

d is the distance in a straight line between the source and receiver in metres (the direct path length) as shown in figures 9.2.4 and 9.2.5.

K_{Met} is a correction factor for meteorological influences on the diffraction around the barrier, and is given by –

$$K_{Met} = \exp\left(-\frac{1}{2000}\sqrt{d_{ss}d_{sr}\frac{d}{2z}}\right) \quad (9\text{-}5)$$

2.2.2 Meteorological Correction

The ISO 9613 calculation method was designed for use with downwind sound propagation at wind speeds of up to 5 m/s. At speeds above 5 m/s the method may no longer be as accurate. For the case of unfavourable propagation conditions from the source to the receiver (upwind propagation) the standard makes use of a meteorological correction factor (C_{met}). This factor is calculated based on source and receiver height, the distance between the source and receiver, and a coefficient related to local wind speeds and temperature gradients (C_0). For cases with upwind propagation (wind direction within ±45 degrees of the direction from source to receiver) C_0 was set to 1; for all other cases C_0 was set to 0. These values were selected based on generic information supplied in the standard.

2.3 CONCAWE Specific Model Set-Up

2.3.1 Diffraction

The diffraction parameters were set as follows –

- Limitation of single diffraction *20 dB*
- Limitation of multiple diffraction *25 dB*

The above values were the SoundPLAN defaults and were determined to be suitable in this situation. The parameters are defined as for ISO 9613 (see section 2.2.1).

2.3.2 Meteorological Correction

The CONCAWE method makes corrections for meteorological effects using a meteorological correction factor (K_4). The factor is frequency dependent and determined from a series of meteorological categories based on the Pasquill Stability Categories [5]. The Pasquill Stability Categories define the state of the lower atmosphere in terms of wind, cloud cover, and solar radiation to allow an estimate of temperature gradient to be made without recourse to actual measurement. The categories are as follows -

"A" Extremely Unstable Weather conditions are very unpredictable. Wind speed averages 1 m/s but is gusty. The temperature rapidly decreases with altitude. This condition is called superadiabatic. It is common on a hot sunny day.

"B" Moderately Unstable Weather conditions are still unpredictable, but less so than with category "A". Wind speed averages 2 m/s, and is not gusty. The temperature still decreases with altitude, but not as rapidly as for category "A". This condition is common on a warm sunny day.

"C" Slightly Unstable Weather conditions are somewhat unpredictable. Wind speed averages 5 m/s. Some gustiness may be expected. The temperature still decreases with altitude but less quickly than for category "A" and "B". This usually occurs on an average day, with slightly cloudy skies.

"D" Neutral Weather conditions are more predictable. Wind speed averages 5 m/s or more, with no expected gustiness. The temperature still decreases with altitude, but the change is less pronounced than for categories "A", "B" and "C". At this point, the condition name changes from superadiabatic to adiabatic. This condition is common on an overcast day or night (heavy overcast)

"E" Slightly Stable Weather conditions are more predictable than with "D". Wind speeds average 3 m/s. The temperature does not change with altitude. This condition is called isothermic. This condition generally occurs at night, and is considered an average night (partly cloudy).

"F" Moderately Stable Weather conditions become very predictable. Wind speeds average 2 m/s. Temperatures increase with altitude (temperature inversion). This condition is opposite of a Category "A".

"G" Extremely Stable This condition is very predictable, but rarely occurs. No winds blow and the temperature increases rapidly with altitude. This condition sometimes occurs over a city at night.

Table 9.2.3 shows how the Pasquill Stability Categories are determined.

Table 9.2.3 – Pasquill Stability Categories

Wind Speed*	**Day Time Incoming Solar Radiation (mW/cm^2)**				**One Hour Before Sunset**	**Night Time Cloud Cover (octas***)**		
(m/s)	**> 60**	**30 - 60**	**< 30**	**Overcast**	**or After Sunrise**	**0 - 3**	**4 - 7**	**8**
< 1.5	A	A - B	B	C	D	F or G**	F	D
2.0 - 2.5	A - B	B	C	C	D	F	E	D
3.0 - 4.5	B	B - C	C	C	D	E	D	D
5.0 - 6.0	C	C - D	D	D	D	D	D	D
> 6.0	D	D	D	D	D	D	D	D

* Measured to nearest 0.5 m/s
** Category G is restricted to night-time with less than 1 octa of cloud and a windspeed of less than 0.5 m/s
*** 1 octa of cloud cover means that 1/8th of the celestial dome is covered by cloud

The CONCAWE method further simplifies these categories into the six meteorological categories shown in table 9.2.4.

Table 9.2.4 – CONCAWE Meteorological Categories

Meteorological Category	Pasquill Stability Category		
	A, B	C, D, E	F, G
1	v* < -3.0	-	-
2	-3 < v < -0.5	v < -3.0	-
3	-0.5 < v < 0.5	-3.0 < v < -0.5	v < -3.0
4**	0.5 < v < 3.0	-0.5 < v < 0.5	-3.0 < v < -0.5
5	v > 3.0	0.5 < v < 3.0	-0.5 < v < 0.5
6	-	v > 3.0	0.5 < v < 3.0

* Where 'v' is velocity. Negative velocity indicates upwind propagation
** Category with assumed zero meteorological influence

After determining the meteorological category the CONCAWE method assigns the meteorological attenuation value K_4 according to category, frequency and receiver distance.

In SoundPLAN the user enters the Pasquill Stability Category, the wind speed and the wind direction, from which SoundPLAN calculates K_4. For all of the meteorological conditions modelled the wind speed was 6 m/s or above and therefore the Pasquill Stability Category was always set to D. Wind speed and direction were altered according to the conditions being modelled.

2.4 Nord2000 Specific Model Set-Up

2.4.1 Diffraction

The diffraction parameters were set as follows –

- Limitation of single diffraction *20 dB*
- Limitation of multiple diffraction *40 dB*

The above values were the SoundPLAN defaults and were determined from the standard to be suitable in this situation. The diffraction parameters are defined as for ISO 9613 (see section 2.2.1).

2.4.2 Terrain Effects and Ground Absorption

The rules for calculation of the terrain effects and ground absorption using the Nordic General Prediction Method are embedded in SoundPLAN. The method does not require the use of empirical correction

factors and therefore does not require any specific set-up to be performed other than the construction of an accurate terrain model.

2.5 Validation Method

In order to validate the calculated results of the models the sound pressure levels at each receiver location were measured. Unfortunately, because the Windflow 500 was a prototype turbine it was often not operational and this along with resource consent compliance resulted in it only being able to be run for short periods for sound measurements to be taken. During the time available for the measurements the range of meteorological conditions included some but not all of the conditions modelled. This meant that the data could be validated only for some scenarios at some receiver locations. In order to maximise the data gathered during the measurement period two kinds of sound pressure level measurements were made-

- Continuous logged measurements
- Single measurements

2.5.1 Continuous Logged Measurements

Sound pressure levels (L_{95} and L_{eq}) were measured in ten minute averaging intervals over a period of two weeks. The measurements were conducted approximately 1400m from the turbine at House 6 (see table 9.2.1 and figure 9.2.1). Figure 9.2.6 shows the approximate location of the microphone in relation to House 6 and the turbine.

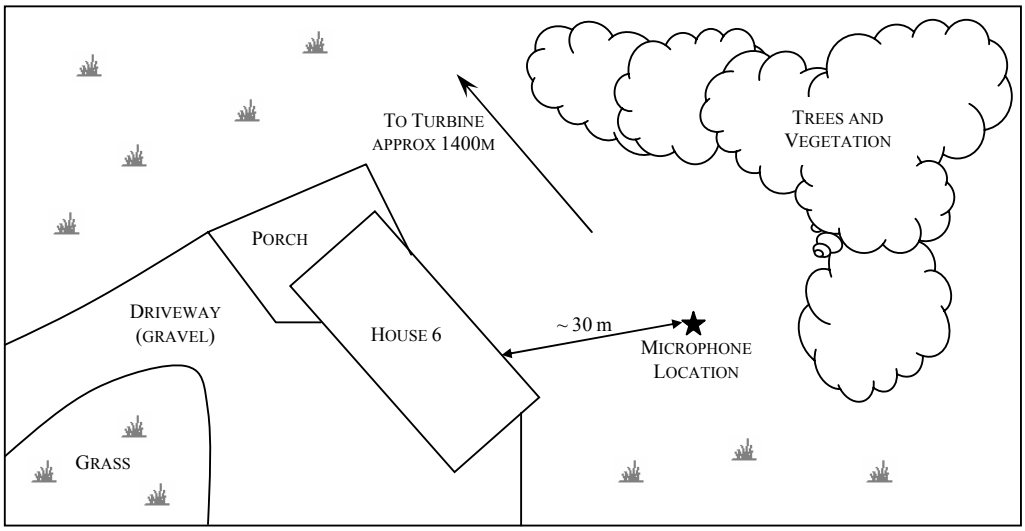

Figure 9.2.6 – Microphone Location on House 6 Property

The measurement equipment was set up in accordance with NZS 6808:1998 [3] except that the microphone was not placed on the boundary of the property nearest the turbine as the equipment could not be conveniently operated at this location. The sound level meter used was a Bruel and Kjaer 2260 Investigator with a Type 4189 pre-polarised microphone. The microphone was covered with a Bruel and Kjaer 100mm spherical foam windscreen. Sound pressure levels were recorded with an 'A' frequency weighting and a 'fast' time weighting.

The wind speed 30m above ground level at the turbine site was also monitored. This was done using the vane anemometer on the meteorological mast located 66.4m northeast of the turbine. The wind data was averaged over 10 minute intervals.

During the measurement period the turbine was run in a range of winds and meteorological conditions. A number of measurements were also taken with the turbine parked in order to determine the background noise levels present for various conditions.

2.5.2 Single Measurements

Sound pressure levels (30 second L_{eq}) were measured at various points around the turbine using a Bruel and Kjaer 2260 Investigator and a Type 4189 pre-polarised microphone covered by a 100mm spherical foam windscreen. The meter was hand held facing the turbine with the microphone positioned at arms

length approximately 1.5m above the ground. Sound pressure levels were recorded with an 'A' frequency weighting and a 'fast' time weighting.

Measurement positions were the same as the receiver locations shown previously in table 9.2.1. In certain meteorological conditions some receiver locations were unsuitable for measuring the sound pressure level because of excessive wind turbulence and background noise.

3. Results

A full set of tabulated experimental results can be found in Appendix B. The results shown in this section are representative of the general trends observed in the complete set of results.

3.1 Effect of Distance on Model Accuracy

To examine the effect of distance from the turbine on model accuracy, receiver locations downwind of the turbine were selected for analysis. The receiver locations represented short, middle and long distances from the turbine. The data shown below in table 9.3.1 was predicted and measured with a 10m/s northerly wind at approximately 20^{o}C and 55% humidity.

Table 9.3.1 – Effect of Distance on Model Accuracy

Receiver	Distance from Turbine (m)	Direction from Turbine	Predicted Sound Pressure Level (dBA)				Measured Sound Pressure Level (dBA)
			ISO	CONCAWE	NORD2000	NZS 6808	
4	100	S	54.7	58.1	54.2	59.2	57.8
6	400	SW	41.4	45.5	43.4	45.7	46.1*
14	1393	SE	29.3	32.4	29.6	29.9	32.5

* Wind / background noise level high relative to turbine noise level

The results showed that the ISO and Nordic models tended to under-predict the measured sound pressure level. The magnitude of the discrepancy was largely dependent on the wind speed. At the highest wind speed modelled (10 m/s) it was found the ISO and Nordic models under-predicted the measured value by approximately 3 dB. The CONCAWE model was found to provide the best fit to the measured data – often being within ± 0.5 dB even at considerable distances from the turbine. The NZS 6808 model

generally over-predicted the measured sound pressure level at short distances and under-predicted the level at long distances – however at long distances the NZS 6808 model over-predicted the measured noise level in some circumstances since it did not account for the effects of the terrain or meteorological conditions on the propagation of the noise.

3.2 Effect of Wind Speed on Model Accuracy

Table 9.3.2 shows the effect of wind speed on model accuracy. The data in the table was predicted and measured at receiver location 5, 320m north of the turbine, with a northerly wind, approximately 20^{o}C and 55% humidity.

Table 9.3.2 – Effect of Wind Speed on Model Accuracy

Wind Speed (m/s)	Predicted Sound Pressure Level (dBA)				Measured Sound Pressure Level (dBA)
	ISO	CONCAWE	NORD2000	NZS 6808	
6	40.3	43.9	42.4	44.4	43.4
8	42.2	45.9	44.4	46.2	45.6
10	44.4	47.9	46.4	48.0	47.9

The accuracy of each prediction was not found to change significantly with wind speed. Again the ISO and Nordic models were found to under-predict the sound pressure level at each receiver location while the CONCAWE model provided the best prediction, within ± 0.5 dB in most cases. The NZS 6808 model was found to be of reasonable accuracy at low wind speed but as the wind speed increased, and hence its effects on the propagation of noise from the turbine, the NZS 6808 model became decreasingly accurate, particularly at locations far from the turbine.

3.3 Effect of Wind Direction on Model Accuracy

The effect of wind direction on the accuracy of the models was investigated by changing the direction of the wind so as to place the receiver of interest upwind or downwind of the turbine. Table 9.3.3 shows the predicted and measured levels for selected receivers upwind and downwind of the turbine in a 10 m/s wind.

Table 9.3.3 – Effect of Wind Direction on Model Accuracy

Receiver	Distance from Turbine (m)	Direction from Turbine	Predicted Sound Pressure Level (dBA)				Measured Sound Pressure Level (dBA)
			ISO	CONCAWE	NORD2000	NZS 6808	
Receiver Upwind of Turbine							
4	100	S	54.7	57.8	54.2	59.2	57.1
5	320	N	44.4	47.9	46.4	48.0	47.9
6	400	SW	41.1	45.2	43.4	45.7	46.0*
14	1393	SE	28.5	26.3	29.6	29.9	30.8*
Receiver Downwind of Turbine							
4	100	S	54.7	58.1	54.2	59.2	57.8
5	320	N	44.4	48.4	46.4	48.0	48.4
6	400	SW	41.4	45.5	43.4	45.7	46.1*
14	1393	SE	29.3	32.4	29.6	29.9	32.5

* Wind / background noise level high relative to turbine noise level

As can be seen from the table, the wind direction was found to change the measured level by only fractions of a decibel near to the turbine, but further away the disparity between the levels measured with the wind blowing from different directions increases. This trend was correctly calculated by the ISO and CONCAWE models, but the inability of the Nordic and NZS 6808 models to compensate for wind direction meant that the results from these models were unchanged regardless of whether the receiver was upwind or downwind of the turbine. Of the four models, the CONCAWE model was found to most accurately compensate for the effect of wind direction, especially when the receivers were upwind of the source. The CONCAWE model was generally in good agreement with the measured data while the other models were accurate within 1 – 3 dB of the measured data.

3.4 Effect of Temperature and Humidity on Model Accuracy

At short distances, changes in atmospheric temperature and humidity were found to have negligible effect on the calculated and measured sound pressure levels. At longer distances, where the effects of atmospheric sound absorption became more significant, small changes in the predicted and measured levels were observed. Table 9.3.4 shows the effect that changes in the atmospheric temperature and humidity had on the models and measured data.

Table 9.3.4 – Effect of Temperature and Humidity on Model Accuracy at 1393m

Condition	Predicted Sound Pressure Level (dBA)				Measured Sound Pressure Level (dBA)
	ISO	CONCAWE	NORD2000	NZS 6808	
20°C, 55% humidity	29.3	32.4	29.6	29.9	32.5
10°C, 55% humidity	29.4	32.6	29.8	29.9	32.9
20°C, 80% humidity	29.8	33.1	30.3	29.9	33.2

The table shows that the effect of the changes in atmospheric temperature and humidity amounted to less than 1 dB change in sound pressure level at a distance of 1393m. The sound pressure level at this distance could not be repeatably measured to a sufficient accuracy in order to determine if it had actually changed as a result of changes in the atmospheric temperature and humidity. It could therefore be concluded that the effect of temperature and humidity on the accuracy of the models was negligible in comparison to the effects of the other parameters investigated.

3.5 Spectral Prediction

Spectral predictions of noise propagation from the turbine were carried out using each method (except NZS 6808) and analysed with reference to a measured spectrum at receiver locations 4, 5 and 14 with a 10 m/s northerly wind at 20°C and 55% humidity. This combination of receiver locations covered short, middle and long distances along with upwind and downwind propagation.

Figure 9.3.1 shows the predicted and measured spectrums at receiver 4, 100m south (downwind) of the turbine.

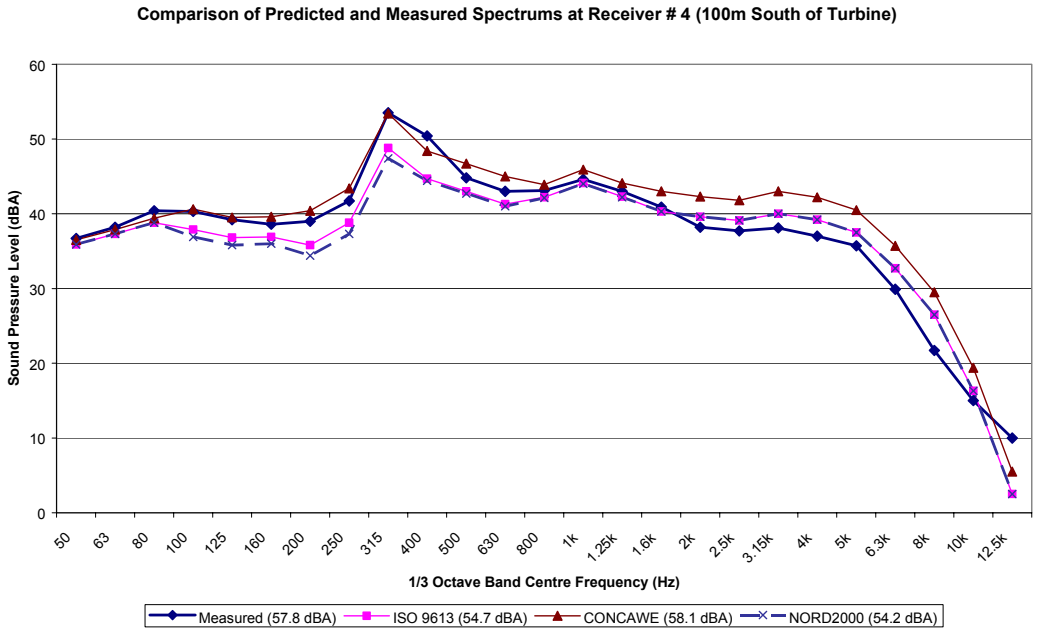

Figure 9.3.1 – Spectral Prediction at Receiver # 4

All three models agree well with the measured data being within 5 dB of the measured sound pressure level at each frequency. At this relatively short distance from the turbine it can be seen that the ISO and the Nordic methods provided almost the same prediction. This is what would be expected given that they are based on similar calculations apart from the calculation of terrain effects and at this short distance the terrain effects would be small. The CONCAWE method accurately predicted the sound pressure level up to 1 kHz, but above this frequency it significantly over-predicted the sound pressure level. However, this was to be expected since the CONCAWE method was not designed for use at short distances.

Figure 9.3.2 shows the spectrums predicted by each model 320m north (upwind) of the turbine at receiver 5.

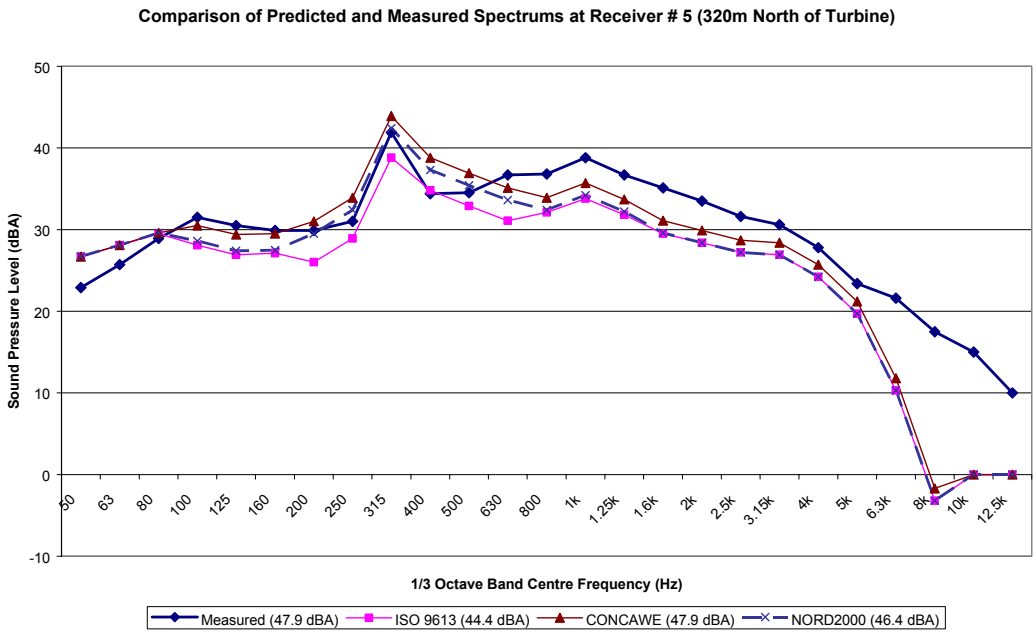

Figure 9.3.2 – Spectral Prediction at Receiver # 5

Again, at this distance the general trends in sound pressure level at each frequency were predicted well by all three models. The CONCAWE model provided the closest fit to the measured data, but all three models significantly under-predicted the sound pressure level at frequencies above 630 Hz. However, at higher frequencies the measured spectrum was probably affected by background noise resulting in an increased sound pressure level.

The predicted and measured spectrums at receiver 14, 1393m south east (downwind) of the turbine, are shown in figure 9.3.3.

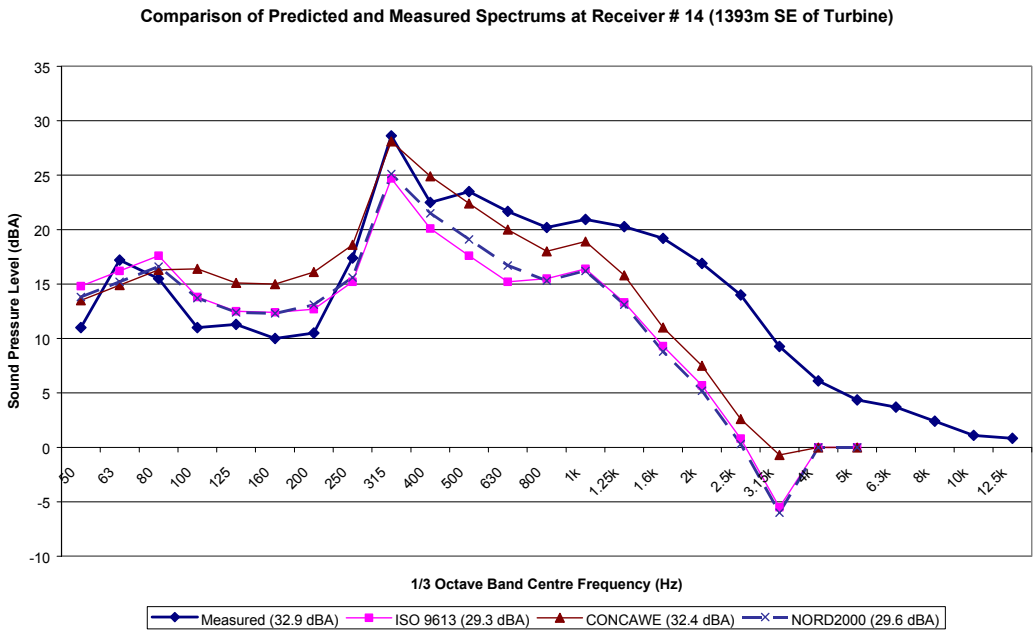

Figure 9.3.3 – Spectral Prediction at Receiver # 14

At longer distances from the turbine the influence of background noise on the measured values becomes increasingly difficult to avoid since the sound pressure level from the turbine is reduced to levels comparable to those of the background and wind noise. As can be seen from the figure, all three models predicted that above 1 kHz the sound pressure level drops rapidly to 0 dBA. However, while the measured level decreases, it does not drop away as abruptly as the predicted levels. This is probably due to the influence of background or wind noise on the measurement.

In general, the trends observed in the measured and predicted levels are in agreement. Again the CONCAWE model was on the whole the most accurate except between the frequencies of 80 and 200 Hz where the measured level decreases significantly and was considerably over-predicted by the CONCAWE model, and to a lesser extent by the ISO and Nordic models.

3.6 Noise Mapping and Computation Time

Figures 9.3.4, 9.3.5 and 9.3.6 show noise maps calculated using the ISO, CONCAWE and Nordic calculation methods respectively. The maps were generated for a 10 m/s northerly wind at 20^{o}C and 55% humidity.

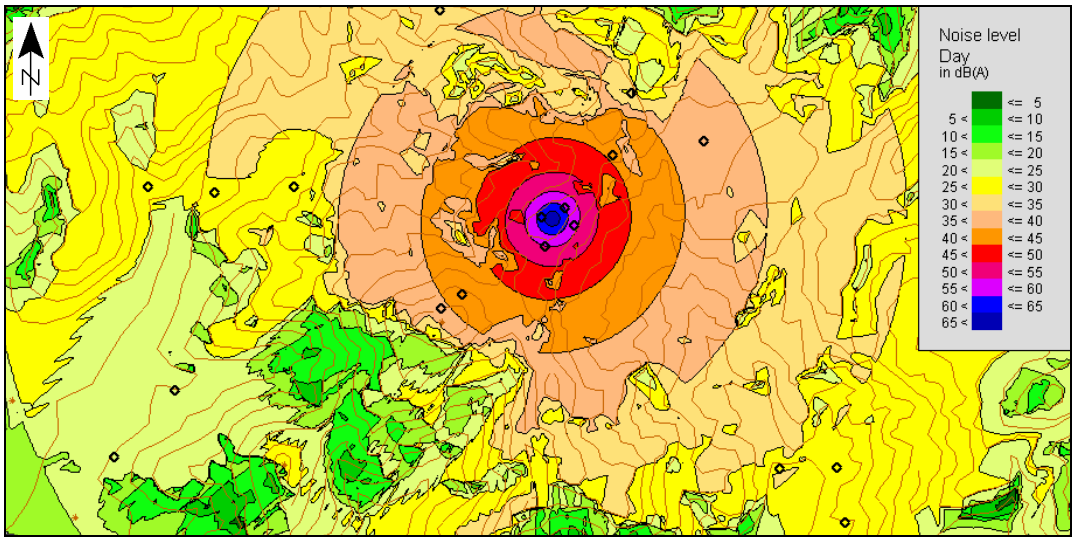

Figure 9.3.4 – Noise Map Using ISO Model

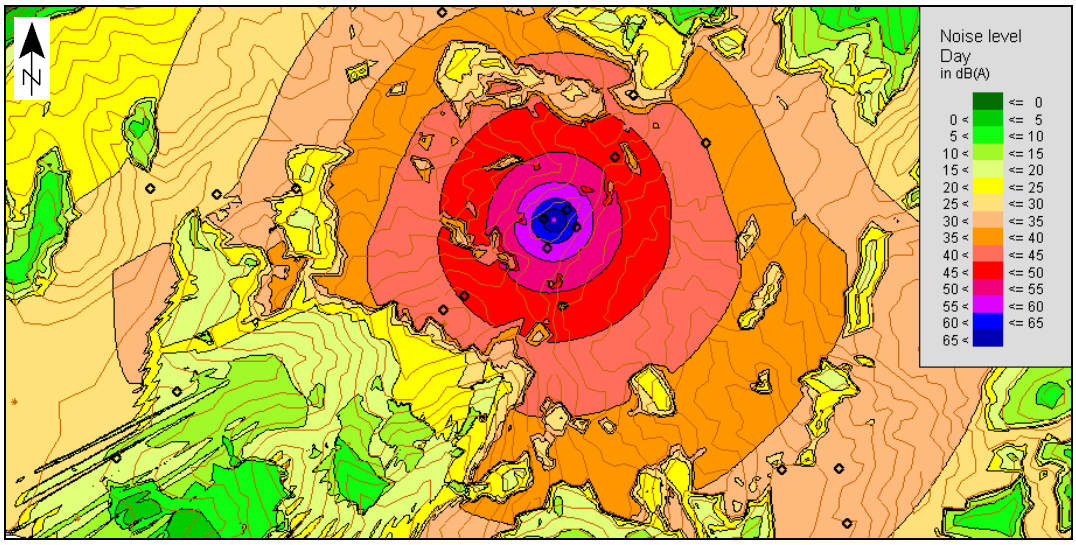

Figure 9.3.5 – Noise Map Using CONCAWE Model

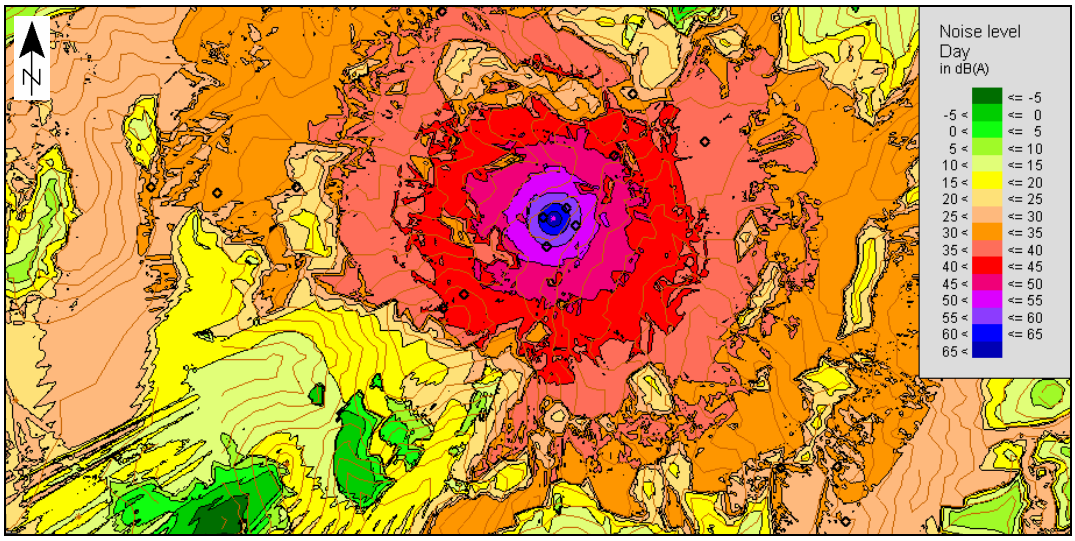

Figure 9.3.6 – Noise Map Using NORD2000 Model

The noise contours on the map constructed using the ISO calculation method distinctively show a circular pattern around the source, which results from the spherical sound divergence formula that the calculation is based upon. On the map generated using the CONCAWE model, the circular pattern of the noise contours is compressed to the north of the turbine and elongated to the south when compared with the map made using the ISO model. This reflects the ability of the CONCAWE model to compensate for wind speed and direction in its calculations. Finally in the map generated using the Nordic model, the circular pattern of the noise contours is far more irregular as a result of the enhanced calculation of the terrain effects.

Computation times for each of the noise maps are shown in table 9.3.5.

Table 9.3.5 – Time to Calculate Noise Map

Computation Time (hrs:mins:secs)		
ISO	CONCAWE	NORD2000
2:14:52	2:18:49	4:31:21

The ISO method proved to be the fastest at four minutes quicker than the CONCAWE method. The Nordic model took over twice as long to complete the calculation as the ISO model. The calculation times reflect the increasing complexity of the models from the simple ISO model through to the relatively complex NORD2000 model.

4. Discussion

Each of the calculation methods predicted the noise propagation from the turbine remarkably well. Even at large distances from the turbine all of the methods generally predicted the level to within 5 dBA. The most successful model was the CONCAWE method, which was normally within ± 1-2 dB of the measured sound pressure level at a given receiver. The ISO and Nordic models were generally found to under-predict the sound pressure levels, while the simple formula used in the NZS 6808 method was normally found to be a conservative method – over-predicting the sound pressure level.

On analysis of the spectral predictions, the CONCAWE model again proved to be the most accurate, while the ISO and Nordic models provided very similar results to one another. However, accurate spectral predictions require good knowledge of the spectral sound power level of the wind turbine. Without first knowing the spectral sound power level of the wind turbine, none of the calculation methods would provide accurate predictions. This may seem obvious, but it is of the utmost importance if prediction of the propagation of noise from the wind turbine is to be accurately modelled.

Similarly, the set-up of the model also plays an important role in the accuracy of the outcome. Parameters such as ground absorption, and in the case of the ISO model the meteorological correction factor, must be estimated from tables or previous experience since there is no definitive scientific method of establishing them. Therefore each model ultimately requires validation before further modelling work can be confidently carried out. This somewhat limits the ability of the models to be used for prediction where experience is limited and/or the model cannot be verified. Had the meteorological correction factor of the ISO model in this investigation been studied in more detail, it may have been possible for the ISO model to produce a better result.

In this instance it was found that the CONCAWE model was the best fit to the experimental data and it is plausible to expect that because its sound level predictions can be accurately corrected for meteorological conditions, it would generally be the model most suited to modelling the noise propagation from wind turbines given the high wind speeds that would be expected. The accuracy of the CONCAWE model in SoundPLAN could perhaps be improved even further by the addition of wind speed modelling. At present the CONCAWE modelling method in SoundPLAN assumes a constant wind speed and direction

over the entire calculation area. If the wind speed and direction over the terrain was allowed to vary subject to certain boundary conditions, then a more accurate representation of the wind speed in each part of the calculation area could be developed, which would probably result in a more accurate sound level prediction.

The major limitation of the Nordic model is that it makes very few corrections for meteorological factors. However, it clearly has a much more advanced terrain effect calculation method. In the situation of the single turbine at Gebbies Pass the terrain effects did not play a significant role in the observed sound pressure levels compared with factors such as wind speed and direction. However, in a situation where an entire wind farm exists i.e. multiple sources spread over a large area, the effect of terrain shape may play a larger role in the way in which the sound propagates – especially if the terrain is hilly and highly irregular. In these circumstances the Nordic model may also be quite suitable for modelling of the sound propagation from wind turbines.

Ultimately the calculation method that is selected for prediction of the noise propagation must be suited to the source, the area and meteorological conditions to be modelled. While the ISO model will provide a fast and reasonably accurate calculation over a large area with relatively simple topography and light winds, it will not work as well as the CONCAWE model at higher wind speeds. In situations where there is highly complex terrain and large source to receiver distances, it may be advantageous to use the Nordic model at the expense of accurate representation of meteorological effects in order to utilise its more advanced terrain effect calculations. In a commercial environment where computation time is important, the longer calculation times of the Nordic model may however make it unsuitable for regular use.

As mentioned previously, validation of the model constructed is very important to ensure any empirical correction factors are correctly calibrated. In the measurement of noise from a wind turbine there are issues with wind induced background noise, general background noise, and wind induced pseudo-noise on the microphone. Wind induced pseudo noise can be reduced in a number of ways which include the use of vertical measuring and ground boards, multiple microphone cross-correlation techniques and microphone wind screens (see Chapter 1, section 5.2). For the purposes of this investigation it was found that the use of a 100mm spherical foam windscreen on the microphone along with careful selection of

receiver locations that were sheltered from the wind, was sufficient to reduce the wind induced microphone pseudo-noise to an acceptable level. It was also found that the use of an A-weighted rather than un-weighted spectrum increased the repeatability of the total sound pressure levels measured (all frequencies added) since the wind induced pseudo-noise was found to effect mainly the heavily weighted frequencies below 160 Hz.

Near to the turbine, the signal to noise ratio was large enough that the measurement remained for the most part unaffected by any background noise. Further from the turbine though, the sound of trees and other vegetation moving in the wind was found to influence the measurements. As the distance from the turbine increased the influence of background and wind noise was increasingly difficult to avoid in the measurements. It was found from logging of the background sound pressure levels at receiver location 14 (House 6) that the lowest background noise levels usually occurred from 11pm until 4am. With a northerly wind blowing at the turbine site, the property was sheltered from the wind by the hills and the background noise level at night was found to regularly be as low as 19 dBA, even with a 10 m/s wind at the turbine site. This meant that the noise from the turbine could be assessed between the hours 11pm and 4am in a northerly wind without significant influence from background noise. This sort of approach to measuring the noise a long distance from the turbine provided highly repeatable results far from the turbine where its noise was at very low levels. Given the level of repeatability of the results, the influence of background noise and the general accuracy of the measuring equipment used, it was estimated that the sound pressure levels used for validation purposes were accurate to ± 1 – 2 dBA.

5. Conclusions and Recommendations

The objective of this investigation was to determine if a method existed that was capable of predicting the sound pressure level from a wind turbine to within ± 2 dBA at distances of up to 2 km. Models of the Gebbies Pass wind turbine site were constructed in SoundPLAN and predictions made using the calculation methods of ISO 9613, CONCAWE, NORD2000 and NZS 6808. The results of the models were validated at distances of up to 1400m. Beyond 1400m the sound pressure level from the wind turbine was found to be too low to be accurately measured without undue influence from background noise.

Based on the results of the investigation it can be concluded that the CONCAWE model was the most accurate in the case of the Windflow 500 located at Gebbies Pass. This model is probably the one most suited to the modelling of wind turbine noise, where the effects of wind speed and direction significantly influence the way in which the sound propagates from the turbine.

It was found that the total sound pressure level predicted by the CONCAWE model was generally within 1 - 2 dBA of the measured data, but the predictions at individual frequencies were less accurate and fundamentally dependent on the sound power level attributed to the turbine in the model.

The measured levels were estimated to have a repeatability of ± 1 - 2 dBA given the influence of wind and background noise, and the variability of the turbine sound power level. With this degree of repeatability of the measured sound pressure levels it would be unrealistic to expect a model to more accurately predict the sound pressure levels from a wind turbine than the CONCAWE model has in this investigation.

6. References

[1] "Acoustics -- Attenuation of sound during propagation outdoors -- Part 1: Calculation of the absorption of sound by the atmosphere," ISO 9613-1, 1993.

[2] "Acoustics -- Attenuation of sound during propagation outdoors -- Part 2: General method of calculation," ISO 9613-2, 1996.

[3] "NZS 6808:1998 Acoustics - The Assessment and Measurement of Sound from Wind Turbine Generators."

[4] Manning C., "The Propagation of Noise from Petroleum and Petrochemical Complexes to Neighbouring Communities," CONCAWE 4/81, 1981.

[5] Pasquill F., *Atmospheric Diffusion*, Revised Edition ed: J. Wiley, 1976.

[6] Plovsing B. and Kragh J., "Nord2000. Comprehensive Outdoor Sound Propagation Model. Part 1: Propagation in an Atmosphere without Significant Refraction.," Delta Acoustics and Vibration AV 1849/00, 2001.

[7] Plovsing B. and Kragh J., "Nord2000. Comprehensive Outdoor Sound Propagation Model. Part 2: Propagation in an Atmosphere with Refraction," Delta Acoustics and Vibration AV 1851/00, 2001.

[8] Plovsing B., Kragh J., et al., "Nordic Environmental Noise Prediction Methods, Nord2000 Summary Report. General Nordic Sound Propagation Model and Applications in Source Related Prediction Methods," Delta Acoustics and Vibration AV 1719/01, 2002.

Chapter 10
Project Conclusion

1. Conclusions of the Work

1.1 Windflow 500 Acoustic Characteristics

The sound power level of the Windflow 500 was found to be approximately 108 dBA and was not changed significantly by the acoustic treatments implemented during the course of this work. The blades were found to radiate 86 - 90% of the total sound power. The tower initially radiated 8 – 12% of the total sound power but this was later reduced to approximately 4% as a result of the acoustic treatment applied to the tower wall. Approximately 1% of the noise was radiated from the nacelle cladding. These results agreed well with figures stated in the literature.

Spectral analysis of noise measurements from the Windflow 500 showed a tone in the 315 Hz 1/3 octave band. The tone was found to originate from a 311 Hz gear meshing frequency in the gearbox. This was significant as tonality increases the annoyance factor of the noise.

1.2 Mechanical Noise

The investigation of tower noise found that the noise was predominantly transmitted structurally from the machinery in the nacelle. In order to inhibit the vibration of the tower wall and hence the noise transmitted, rubber tiles were glued to the inner wall of the tower at the locations of maximum acceleration. This was found to reduce the sound pressure level inside the base of the tower by approximately 9 dBA and the sound intensity level measured at the base of the tower on the outside wall by 5 dBA/m^2. However due to the dominance of blade noise, no significant noise reduction was observed at a distance.

It was found that installation of an acoustic barrier material in the nacelle increased the transmission loss of the nacelle wall above 400 Hz by up to 12dB at some frequencies. The addition of $12m^2$ of sound absorbing material inside the nacelle was found to reduce the sound pressure level inside the nacelle by approximately 2dBA which would translate to a similar noise reduction outside (ignoring the presence of the other greater noise sources).

The flexible coupling installed on the high speed shaft between the gearbox and the generator was found to produce a small reduction in the sound pressure level inside the nacelle at frequencies above 800 Hz but no appreciable difference in the 315 Hz 1/3 octave band where the tone from the gearbox second stage gear meshing frequency was dominant. The oil additive that was added to the gearbox reduced the noise in the 315 Hz 1/3 octave band by about 1.6dB but was most effective between 80 and 200 Hz. At some frequencies (1 kHz, 1.6 kHz and 2.5 kHz bands) the noise from the gearbox was increased. The reason for the increases was unclear but it could be concluded that the additive was not performing as intended.

The modifications made to the gearbox to correct the abnormal wear identified were found to be ineffective in reducing the 311 Hz tone.

Resonance of the gearbox or its one of its mating components was also cited as a possible reason for the prominent gearbox tone. Noise measurements made on the turbine at varied rotor speeds showed that the turbine produced the highest levels of noise and vibration when the second stage gear meshing frequency was in the region of 318 to 330 Hz (rotor speed of 49 – 51 rpm). This coincided closely with the second stage gear meshing frequency of 311 Hz and indicated that a component or system resonance near to the normal operating speed of 48 rpm could be adversely affecting the noise and vibration levels produced by the gearbox.

1.3 Aerodynamic Noise

It was found experimentally that the section of the blade near to the tip was producing noise across a wide range of frequencies, with certain frequencies exhibiting tonal character. Perhaps most significantly in the context of the other work conducted, the blade was found to be producing a significant level of noise

in the 315 Hz 1/3 octave band. This indicated that aerodynamically produced blade noise was probably contributing to the 315 Hz tone observed in noise from the turbine.

It was found that the noise produced by the aerofoil increased slightly with angle of incidence and was reduced by up to 4.5 dB at certain frequencies with the addition of a serrated trailing edge. At low angles of incidence a large toothed trailing edge produced a larger noise reduction, but with the aerofoil set at 9 and 12 degrees angle of incidence, a small toothed serration performed slightly better. At frequencies above 4 kHz both serrated trailing edges were found to increase the noise produced by the aerofoil. The results were largely in agreement with previous experimental observations.

1.4 Prediction of Noise Levels and Sound Propagation

Empirical equations for prediction of wind turbine sound power levels were evaluated and found to be in good agreement with measured data. As turbine technologies progress noise levels from wind turbines will be reduced and empirical equations will need adjustment to remain accurate, however as a conservative guide to the sound power level for preliminary calculations the current equations should be adequate. Spectral predictions of aerodynamic noise can be made using semi-empirical formulas based on blade parameters and atmospheric conditions but the spectral characteristics of the mechanical noise sources are much harder to predict as they are generally a function of the specifications of the equipment in the nacelle and the way in which it interacts as a system.

The accuracy of the ISO, CONCAWE and NORD2000 methods for prediction of sound propagation were investigated in a range of meteorological conditions for the Gebbies Pass site of the Windflow 500. Based on the results of the investigation the CONCAWE model was found to be the most accurate, generally predicting the total sound pressure level to within 1 - 2 dBA of the measured data at distances of up to 1400m. It was determined to be the calculation method most suited to the modelling of wind turbine noise, where the effects of wind speed and direction significantly influence the way in which the sound propagates from the turbine.

2. Further Work and Recommendations

2.1 Acoustic Characterisation

Further work could be done to refine the techniques used for measuring the sound power level of the turbine and the relative contributions of each component. An acoustic parabola (to focus the sound) could be trialled to measure noise from different parts of the blades on the operating turbine. This would aid in the investigations of mechanical noise as well as aerodynamic noise. A scanning laser Doppler vibrometer may be able to be used to track specific points on the rotating blades to provide data on the vibration of the blades during operation. Any further work should however employ narrow band analysis of the sound and vibration.

2.2 Mechanical Noise

Further work to reduce the noise generated by the turbine should include an investigation into preventing the transmission of noise from the gearbox to the blades, and an investigation of the effects of blade vibration damping. Without reducing the noise from the blades it is unlikely that noise reduction efforts elsewhere (other than relating to the gearbox itself) would be effective.

To reduce the noise from the gearbox the number of planets in the second stage could be increased, thereby reducing the gear tooth forces and hence the magnitude of vibration. This may also change the gear meshing frequency, so it would be important to ensure that the new gear meshing frequency did not coincide with any system resonances of the turbine.

Another area that could be investigated is the possibility of mounting the gearbox on flexible mounts so as to provide a degree of vibration isolation between the gearbox and the pallet and tower, and introduce additional vibration energy absorption into the system as a whole.

2.3 Aerodynamic Noise

Future investigations of aerodynamic blade noise could study the noise produced by other sections of the blade nearer to the hub. This would however require a much larger wind tunnel outlet area than was used

for the investigation described in this thesis, as both the chord length and the thickness of the blade would be much greater nearer to the hub and as a result tunnel blockage effects would become more significant. The investigation should also make more extensive use of flow visualization techniques than was used in the preliminary investigation, in order to better establish the mechanisms generating the aero-acoustic noise.

Further research into reducing the aero-acoustic blade noise could investigate the effect on trailing edge noise produced by altering the size, shape and spacing of serrations on the trailing edge of the blade. It is possible that optimum tooth parameters will vary along the length of the blade because of the increasing tangential velocity with distance from the hub. Other blade parameters that could be investigated include trailing edge shape and bluntness, aerofoil shape, and the effect of flow trips. Investigations into blade modifications to reduce the aero-acoustic noise should be run in parallel with extensive flow measurements in order to establish the effect of modifications on the aerodynamic performance of the blade.

2.4 Prediction of Noise Levels and Sound Propagation

Further work investigating the accuracy of the three noise propagation models could be carried out at a different turbine site, perhaps with multiple turbines. This would better allow the effect of the terrain shape and source location on the accuracy of each model to be assessed. The results of further investigations could be used to further develop the existing prediction models, perhaps by incorporating the NORD2000 method for predicting terrain effects into the CONCAWE model.

In validation of the noise levels at receiver locations, care needs to be taken to avoid the influence of background noise in the measurements. Measurement locations should be selected so as to be sheltered from strong winds and away from noisy vegetation. Where this is not possible the use of measuring boards is strongly recommended. It was also found that high background noise levels could be best avoided by measuring at night between the hours of 11pm and 4am.

Appendix A

Results of Experimental Investigation into the Effect of Serrated Trailing Edges on Blade Noise

This appendix contains a set of graphed comparisons between the noise generated by the unmodified aerofoil and the two serrated trailing edges investigated (see Chapter 8).

List of Figures

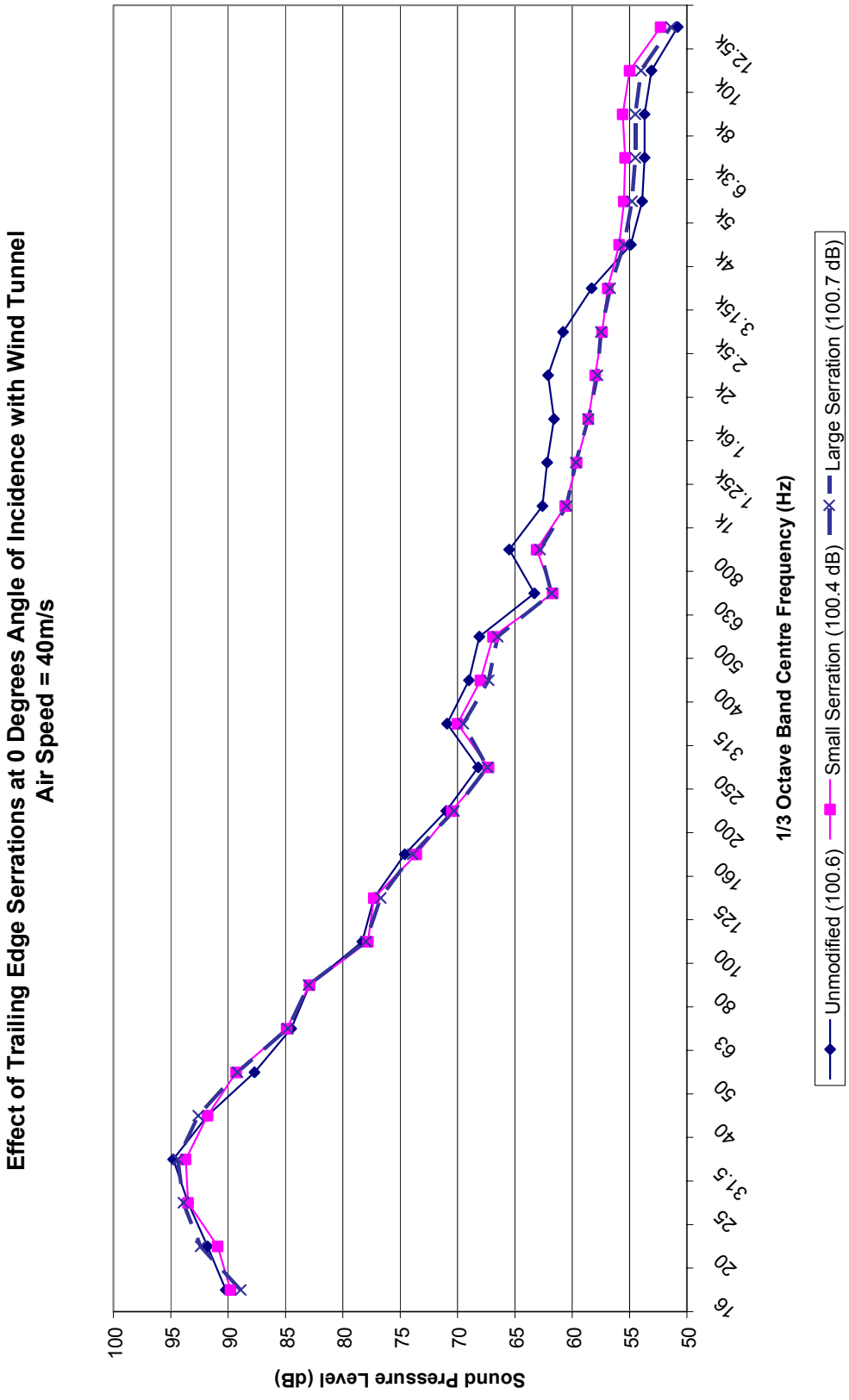

Figure A1 – Sound Pressure Levels at 0 Degrees Angle of Incidence (40m/s)

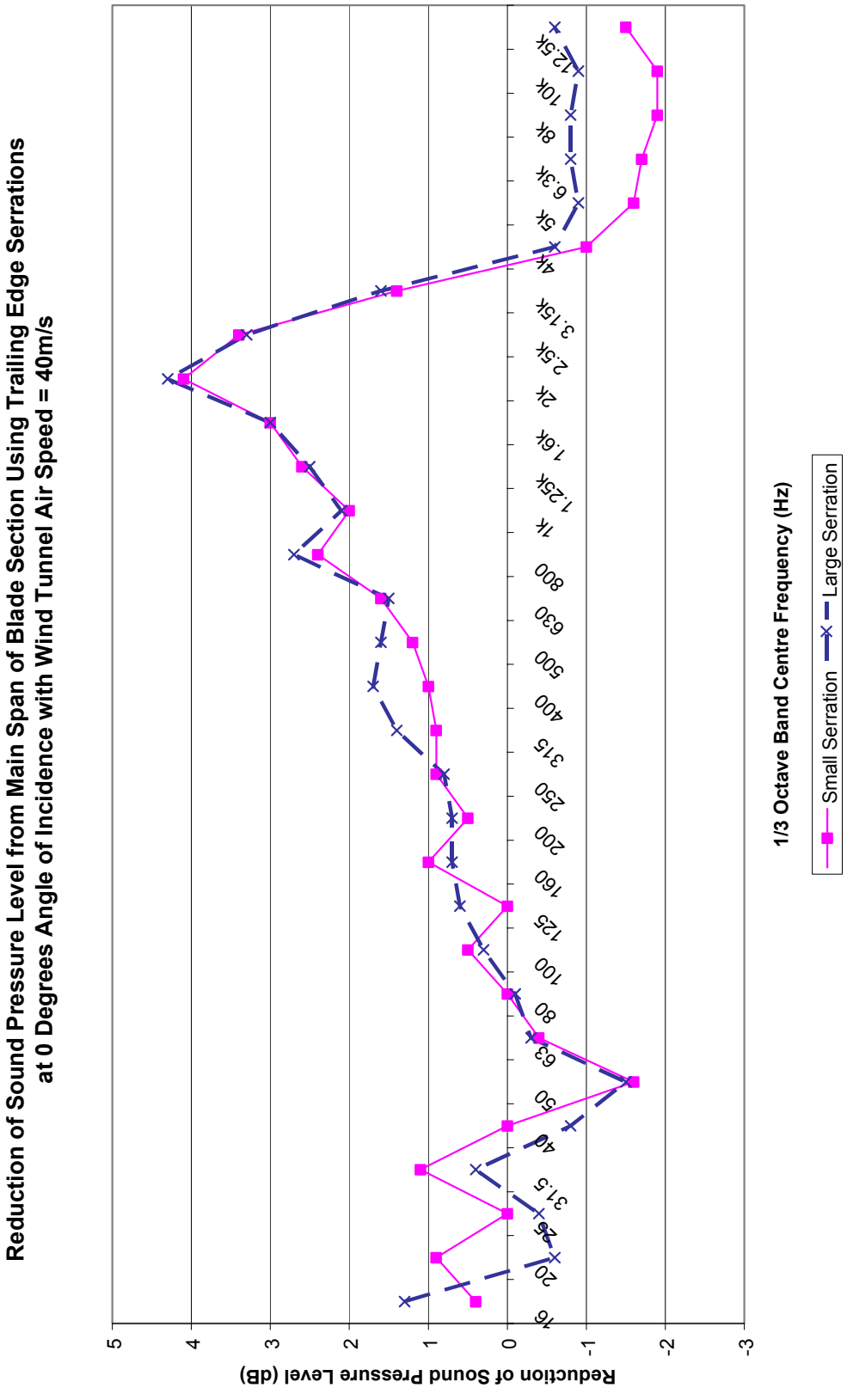

Figure A2 – Noise Reductions at 0 Degrees Angle of Incidence (40m/s)

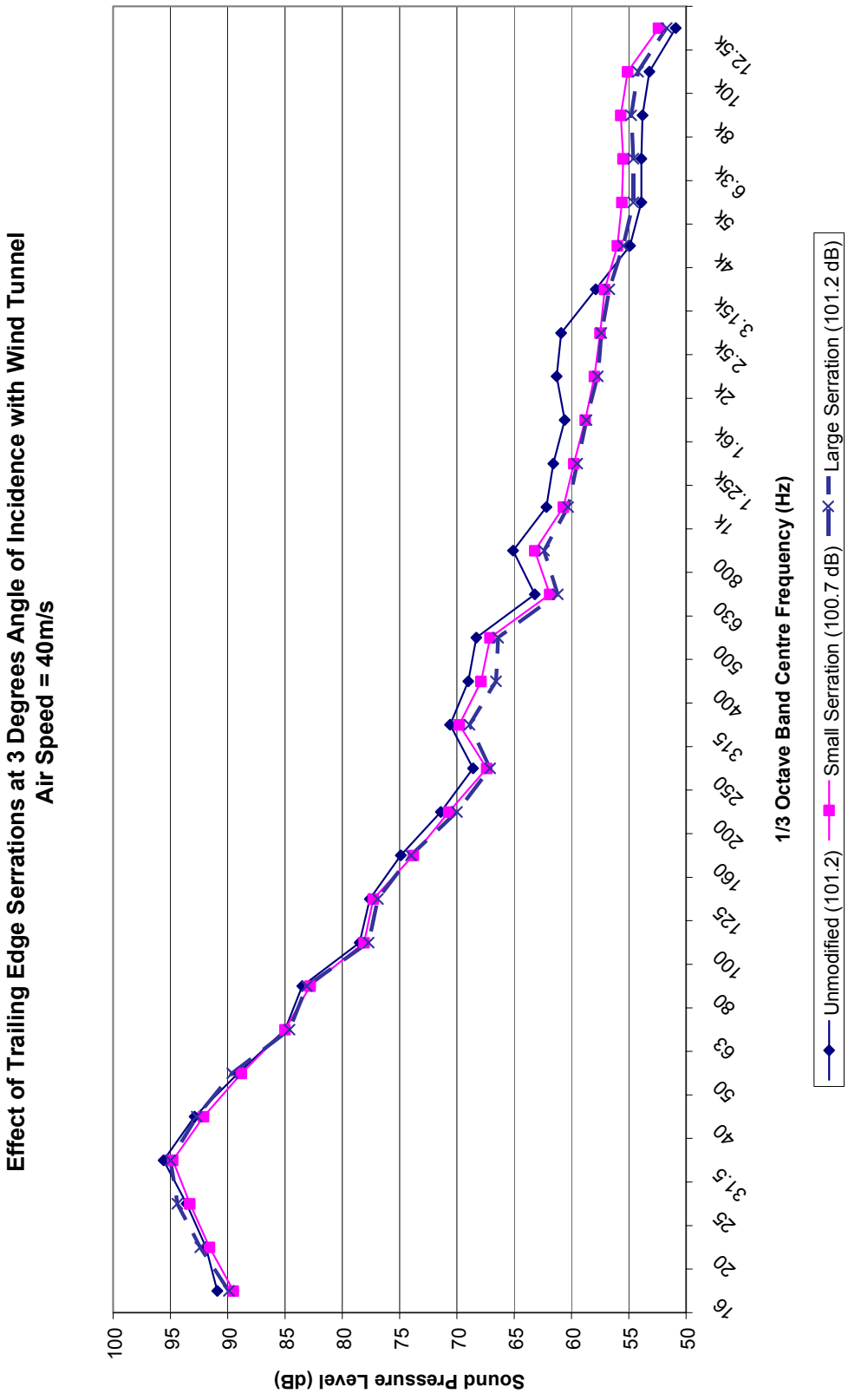

Figure A3 – Sound Pressure Levels at 3 Degrees Angle of Incidence (40m/s)

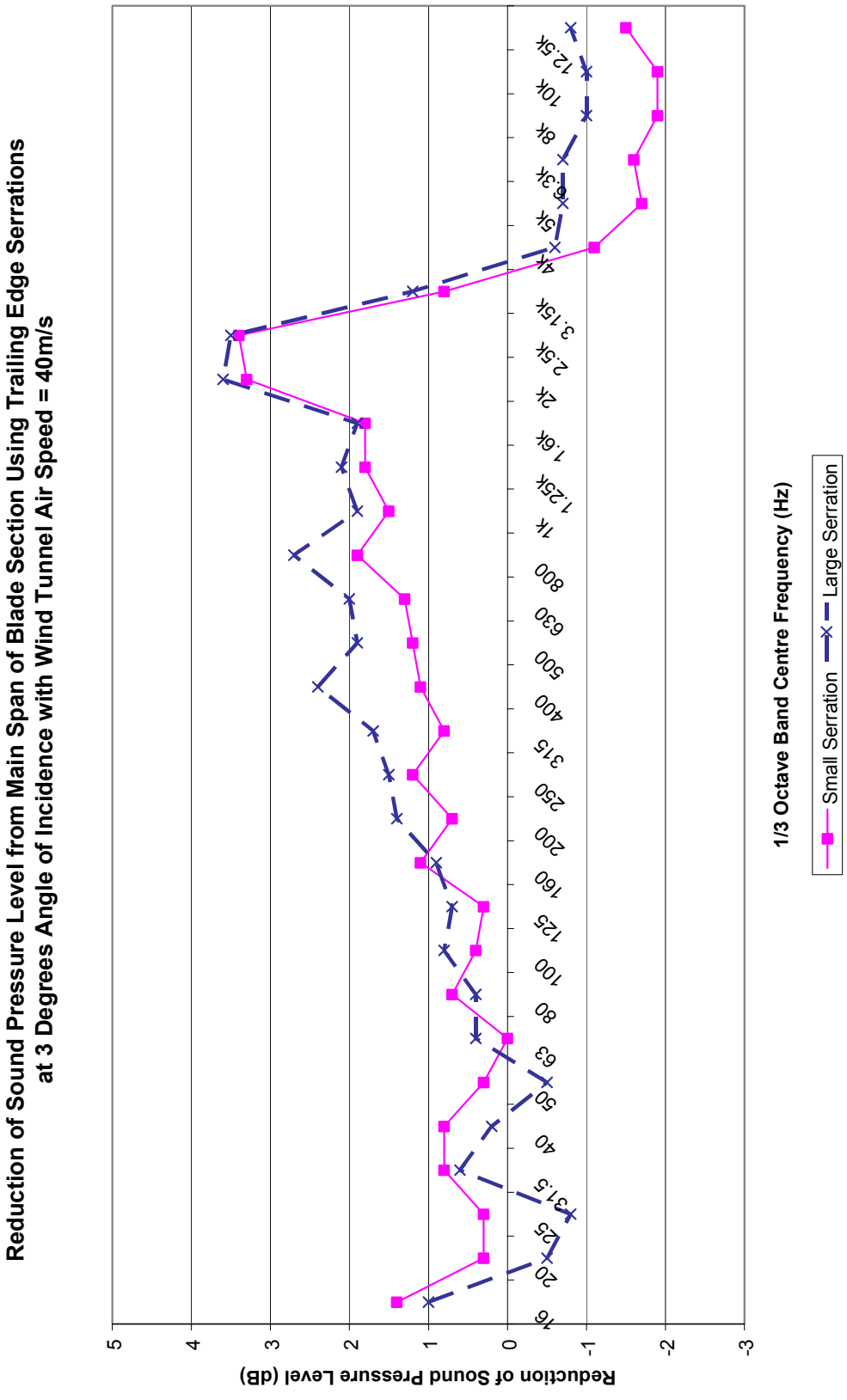

Figure A4 – Noise Reductions at 3 Degrees Angle of Incidence (40m/s)

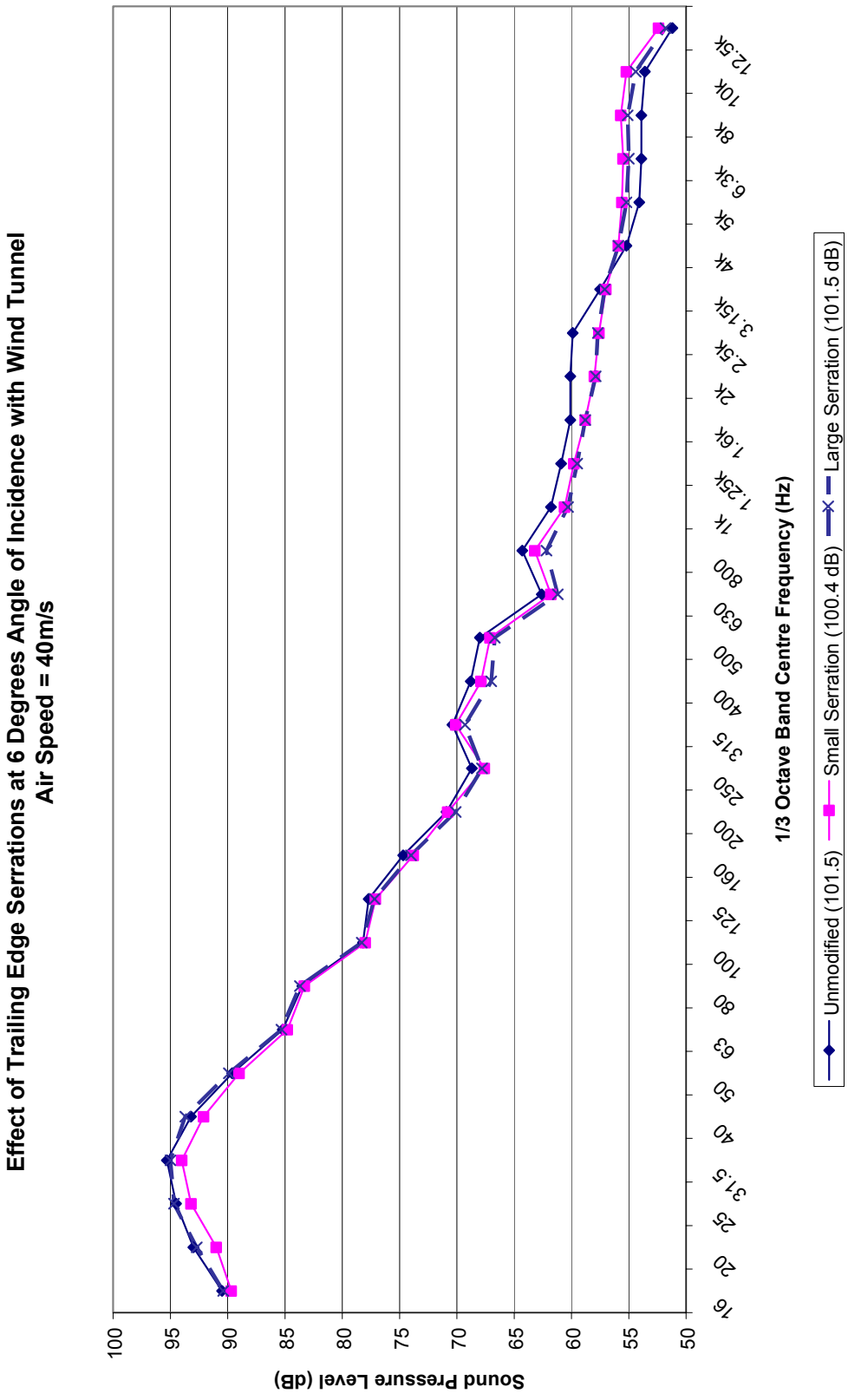

Figure A5 – Sound Pressure Levels at 6 Degrees Angle of Incidence (40m/s)

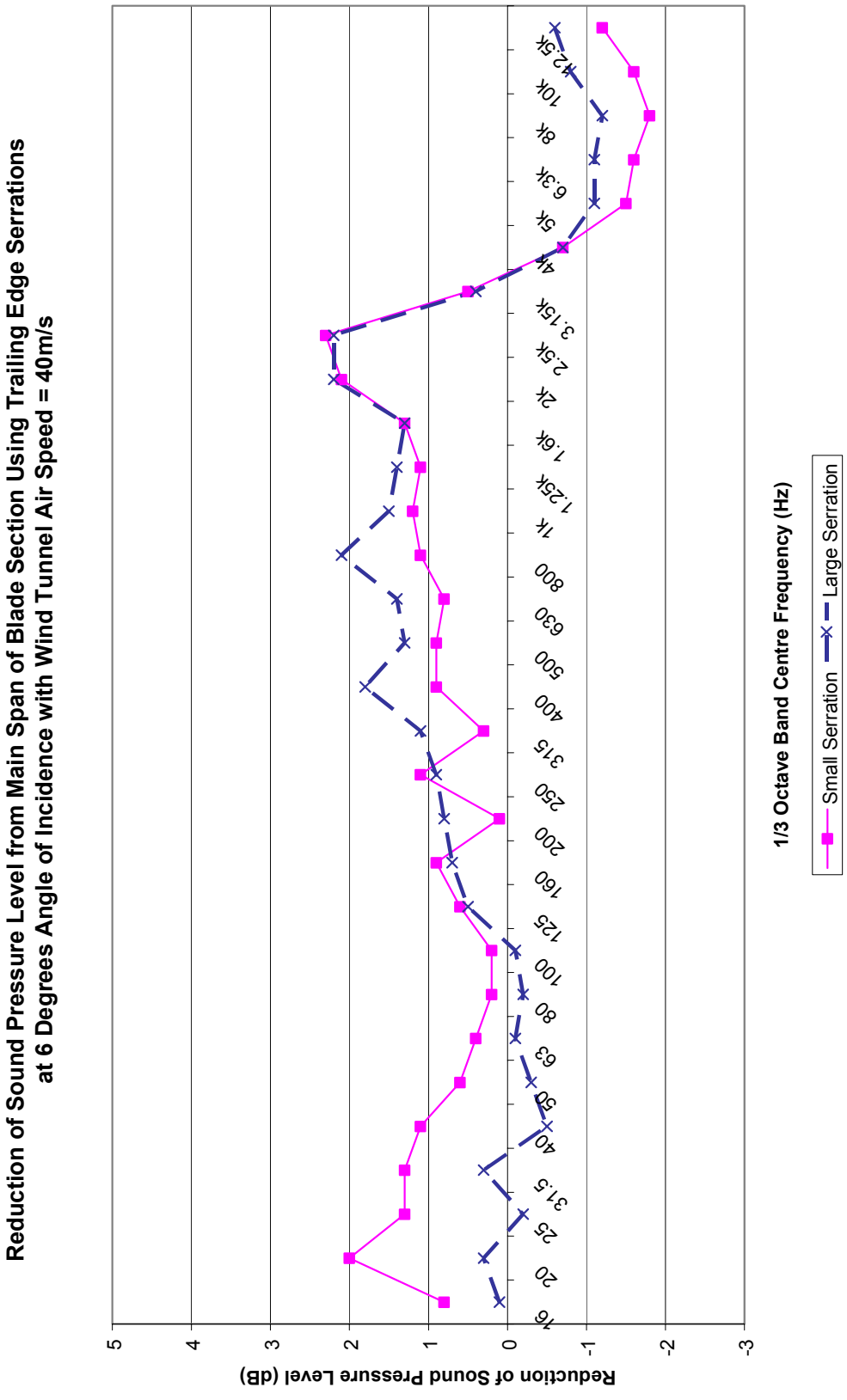

Figure A6 – Noise Reductions at 6 Degrees Angle of Incidence (40m/s)

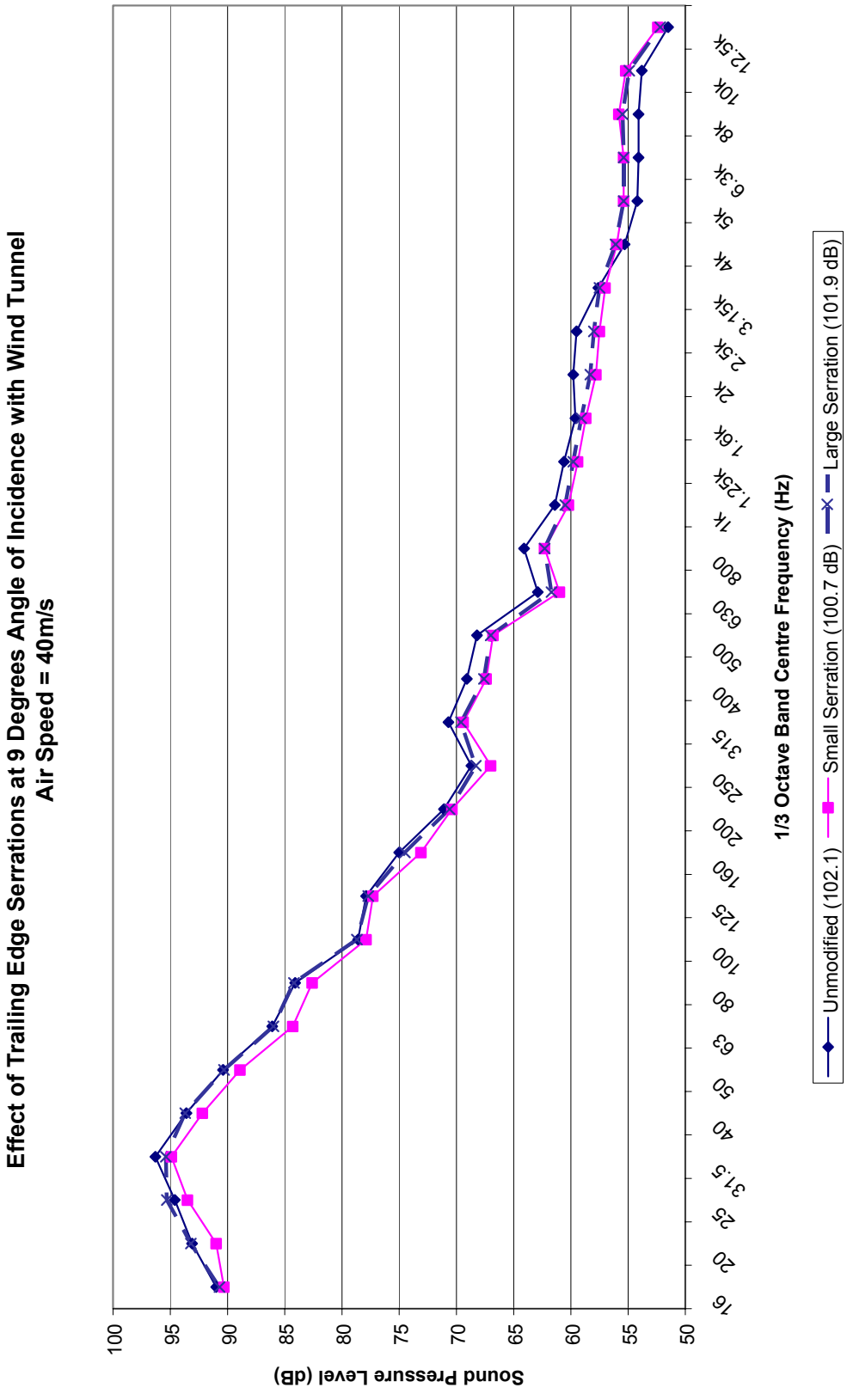

Figure A7 – Sound Pressure Levels at 9 Degrees Angle of Incidence (40m/s)

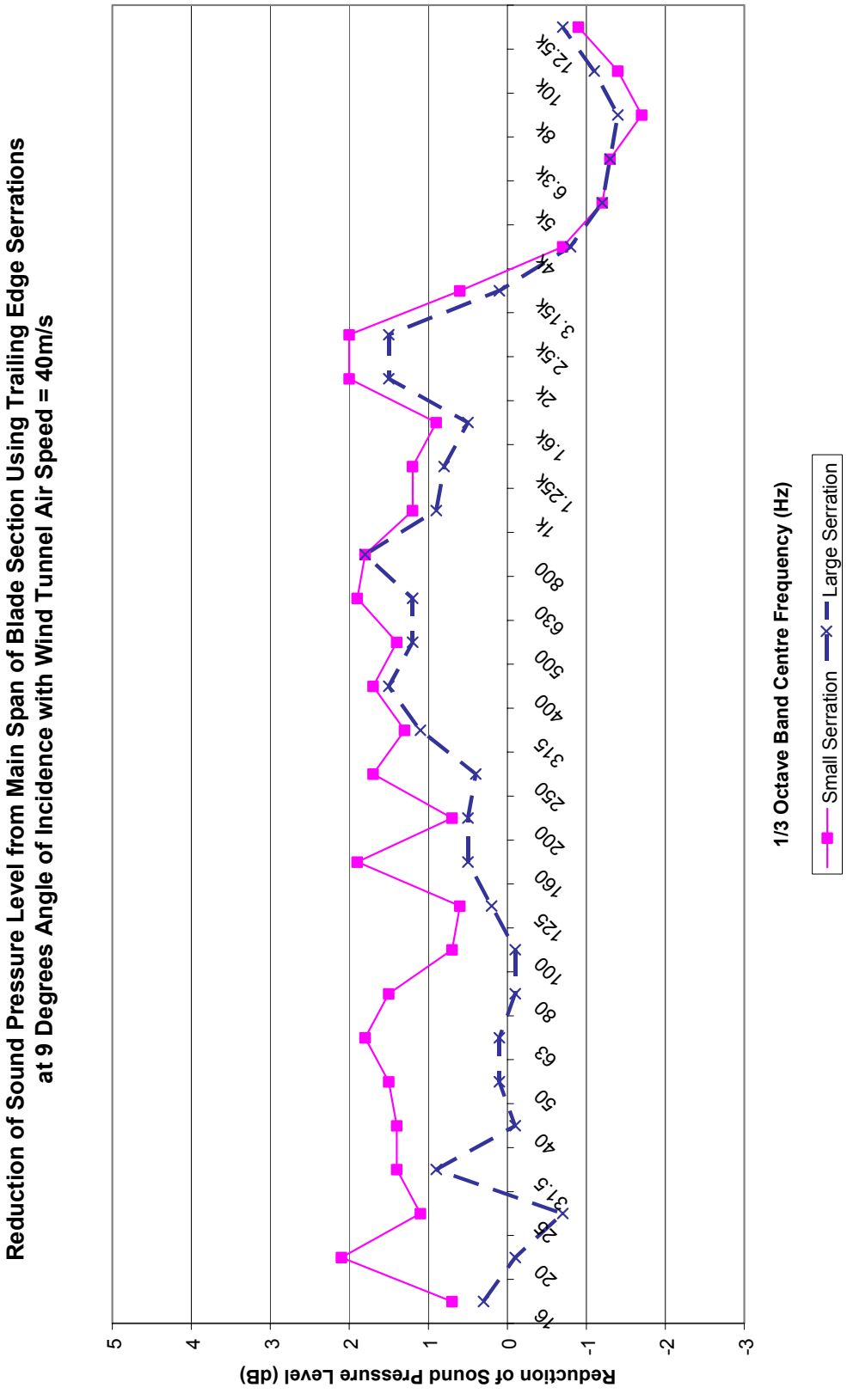

Figure A8 – Noise Reductions at 9 Degrees Angle of Incidence (40m/s)

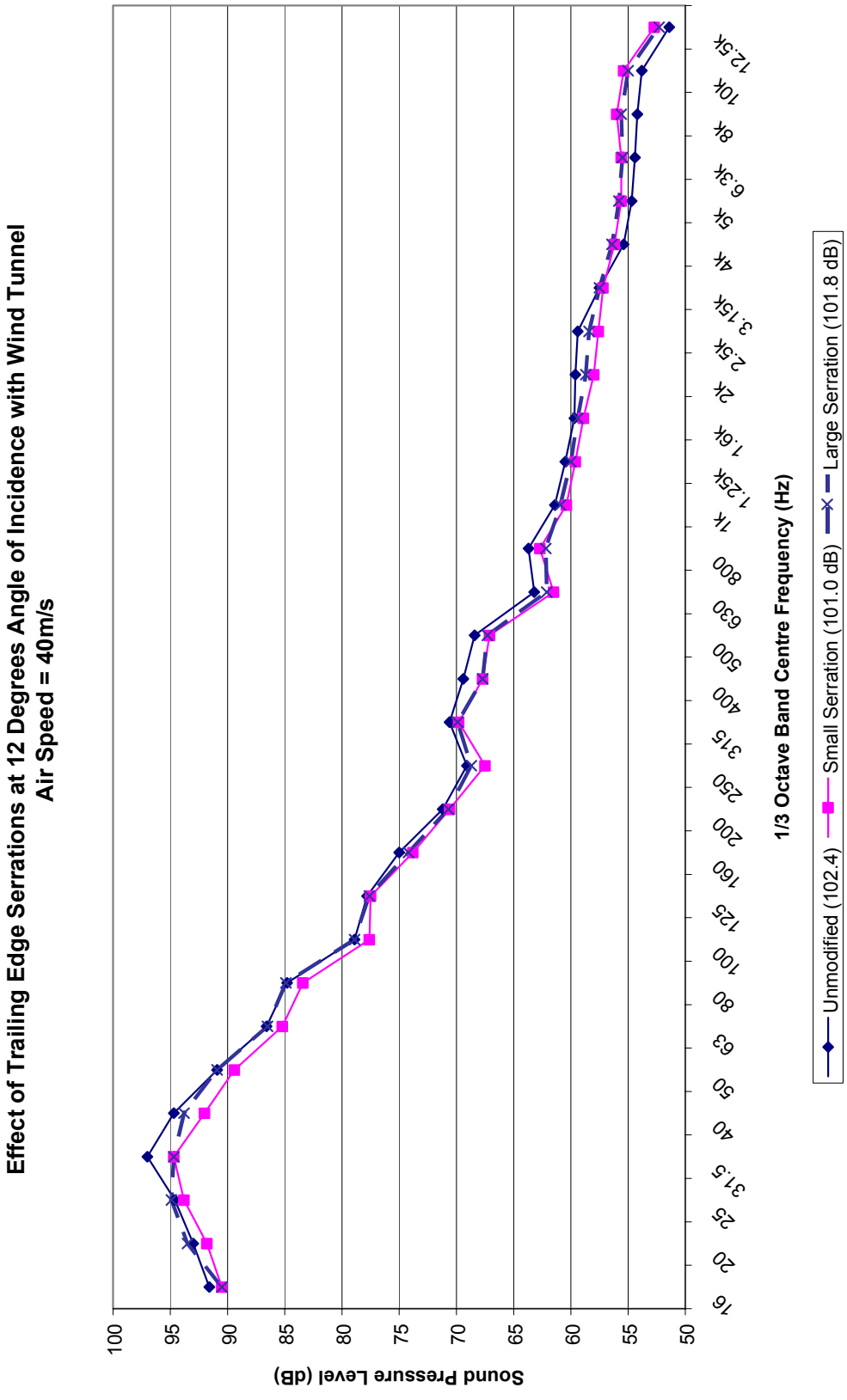

Figure A9 – Sound Pressure Levels at 12 Degrees Angle of Incidence (40m/s)

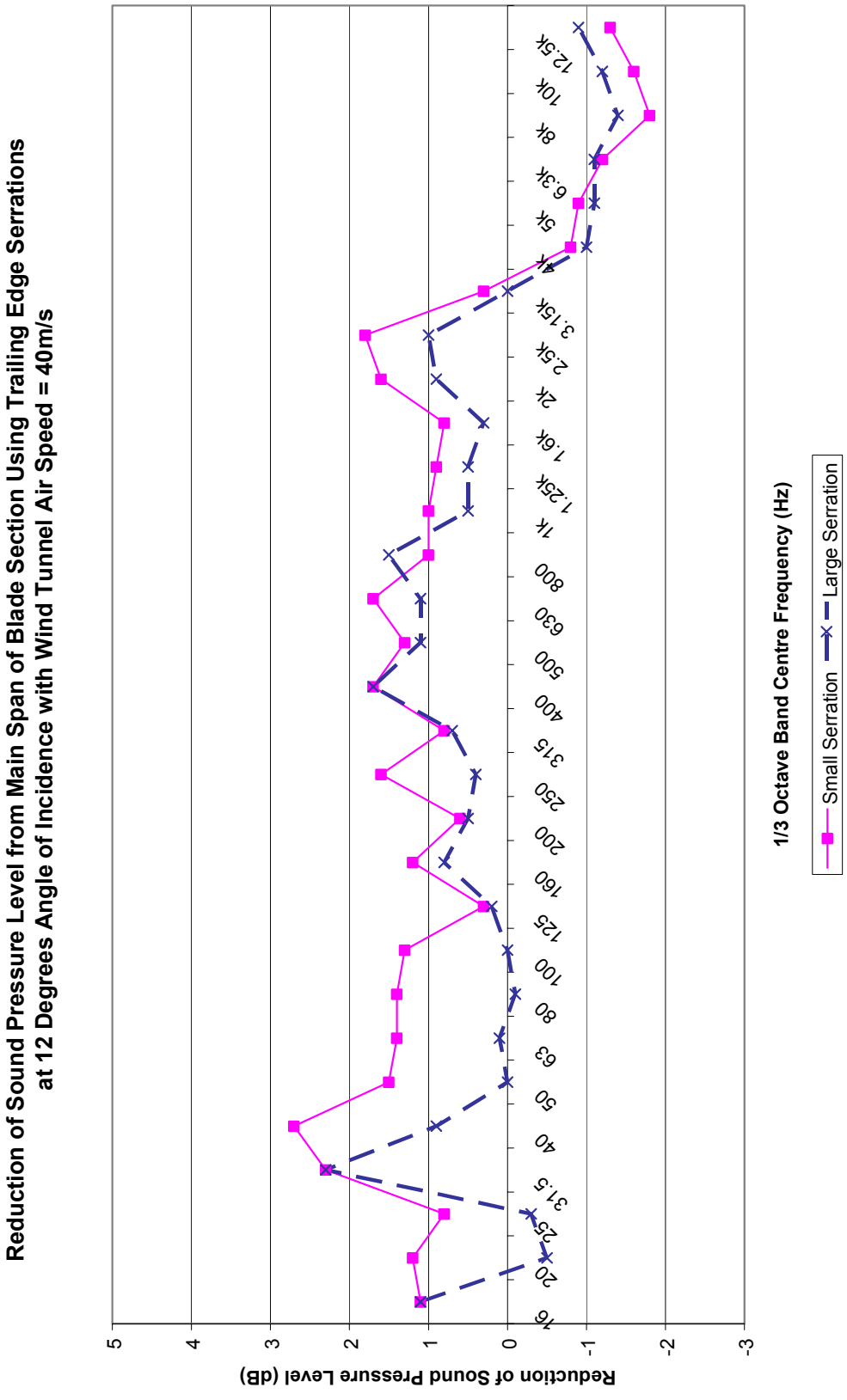

Figure A10 – Noise Reductions at 12 Degrees Angle of Incidence (40m/s)

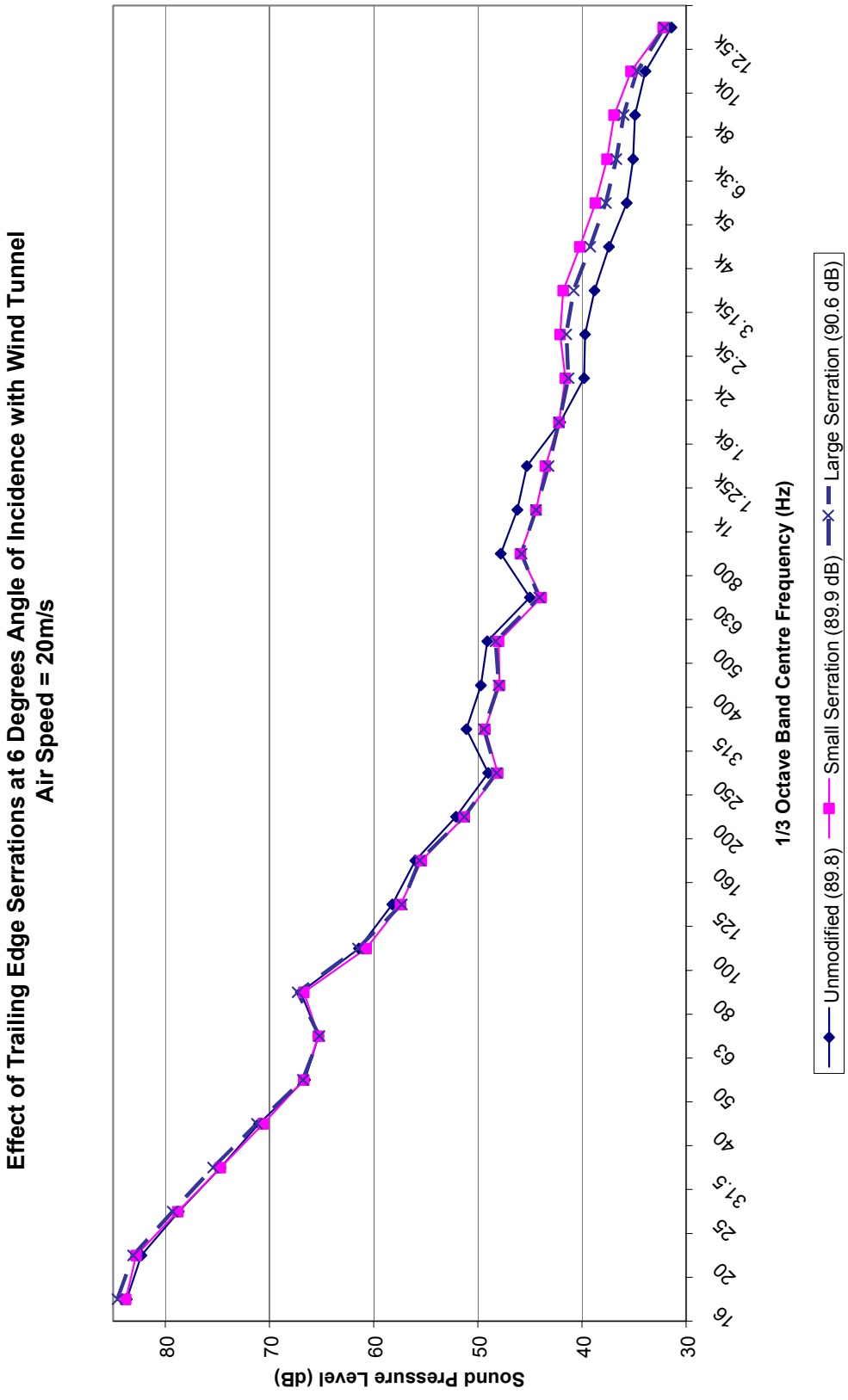

Figure A11 – Sound Pressure Levels at 6 Degrees Angle of Incidence (20m/s)

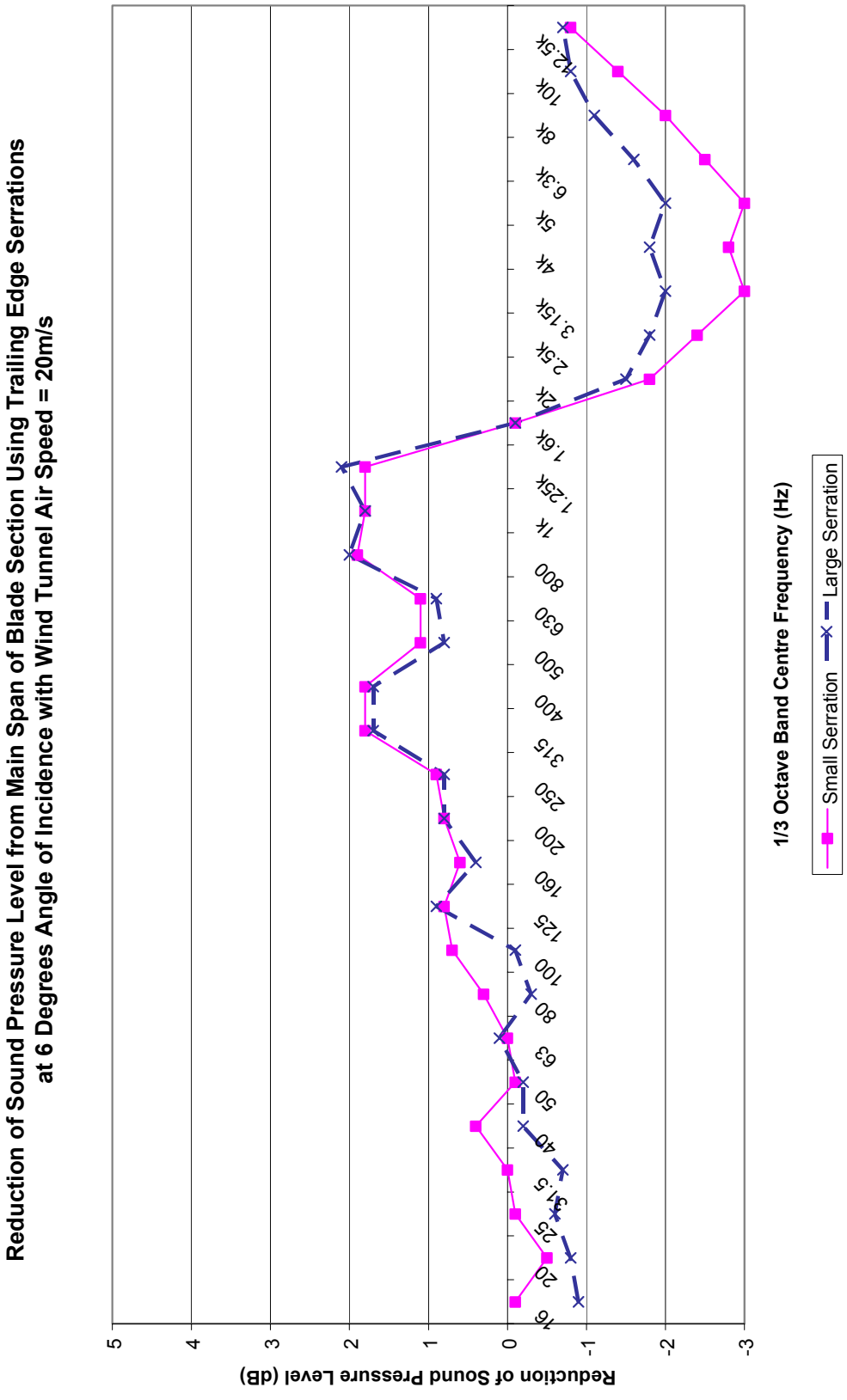

Figure A12 – Noise Reductions at 6 Degrees Angle of Incidence (20m/s)

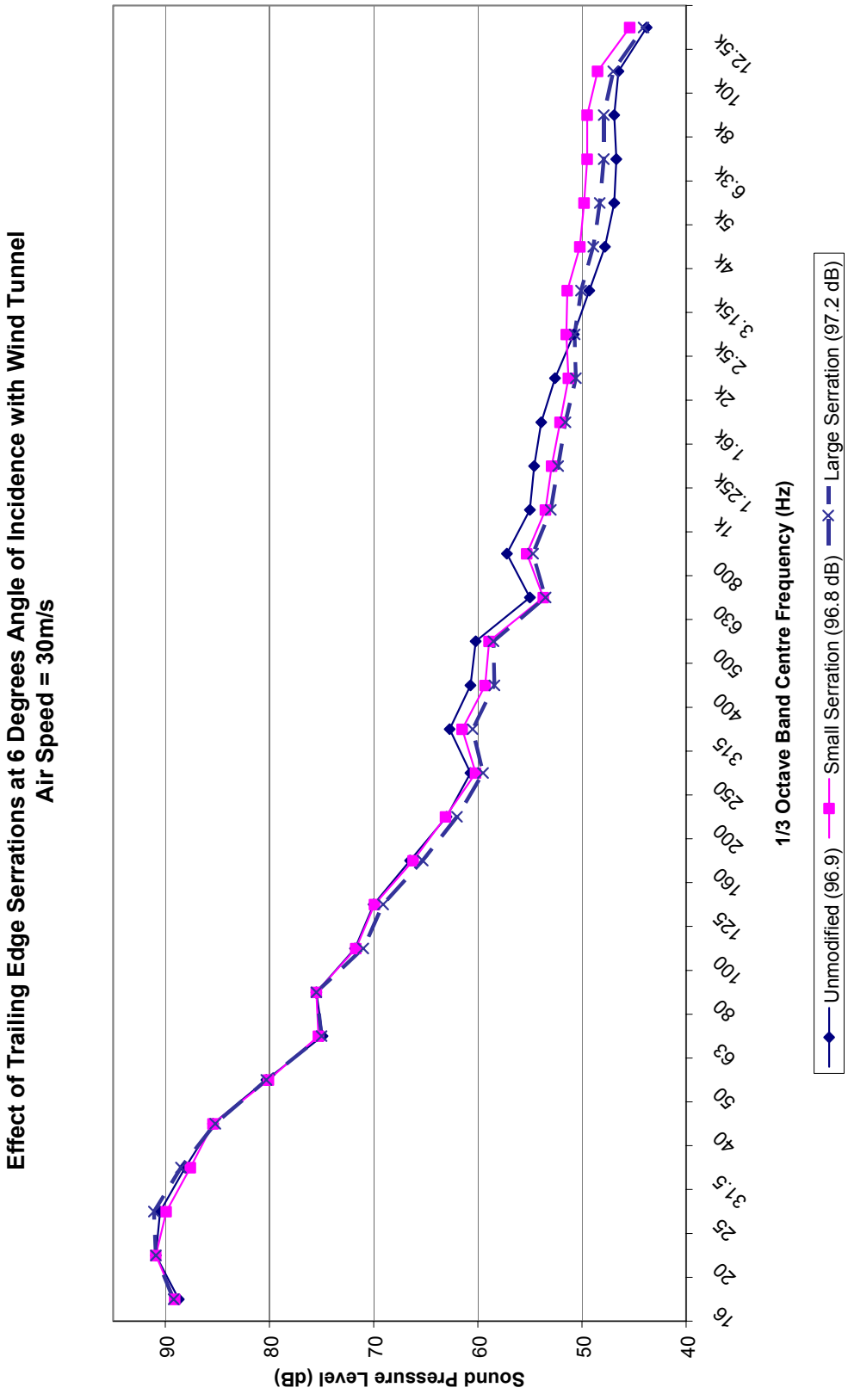

Figure A13 – Sound Pressure Levels at 6 Degrees Angle of Incidence (30m/s)

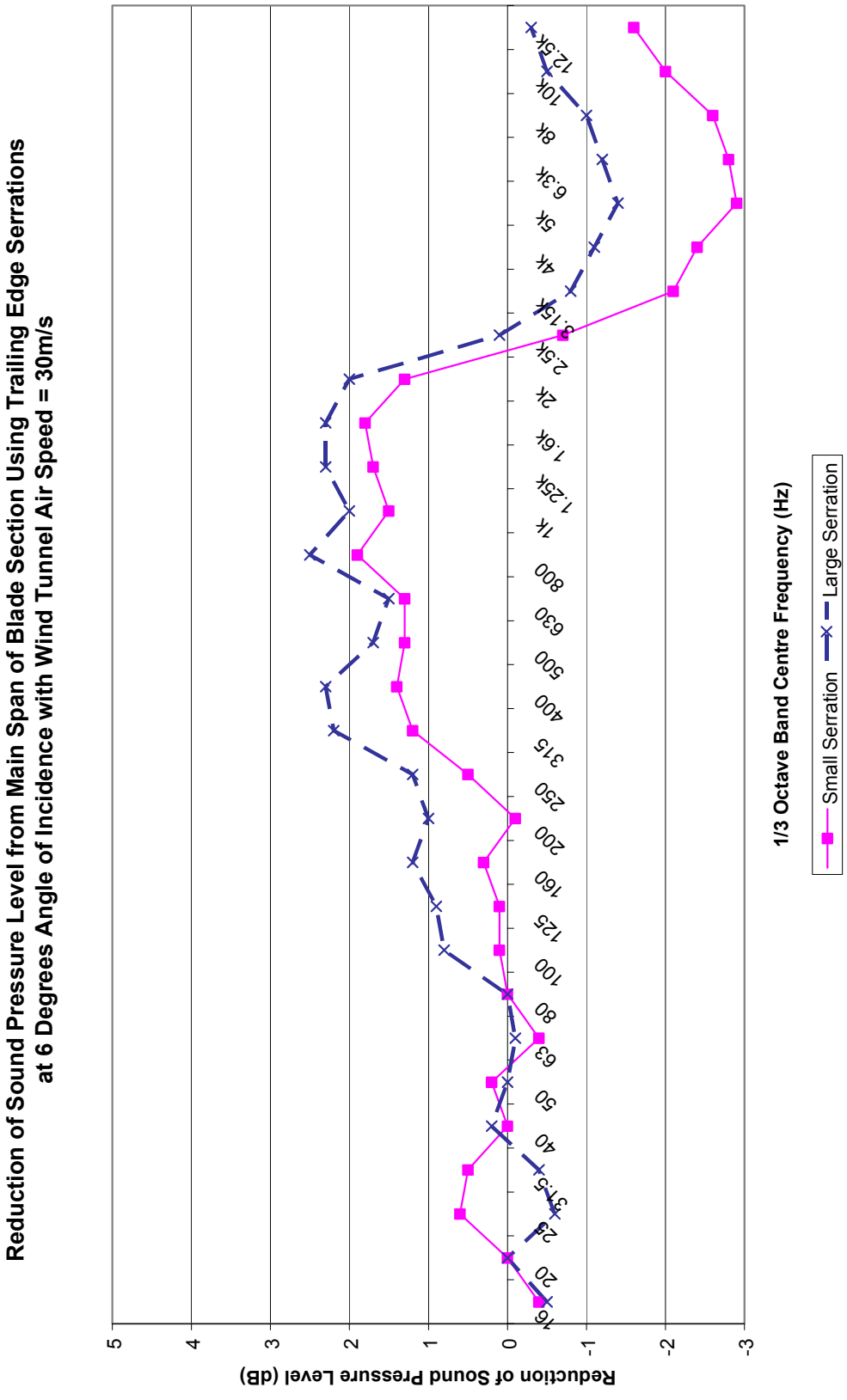

Figure A14 – Noise Reductions at 6 Degrees Angle of Incidence (30m/s)

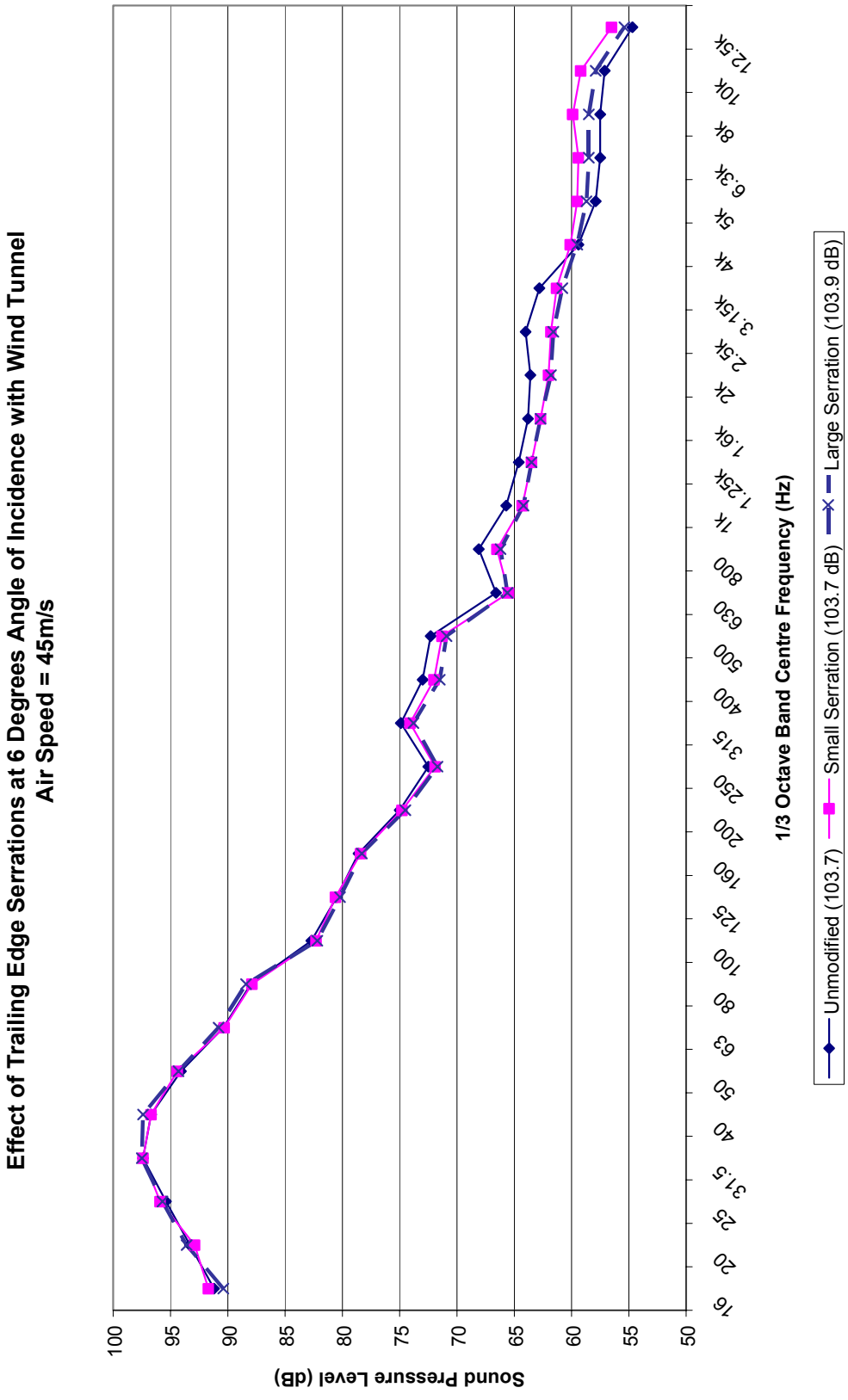

Figure A15 – Sound Pressure Levels at 6 Degrees Angle of Incidence (45m/s)

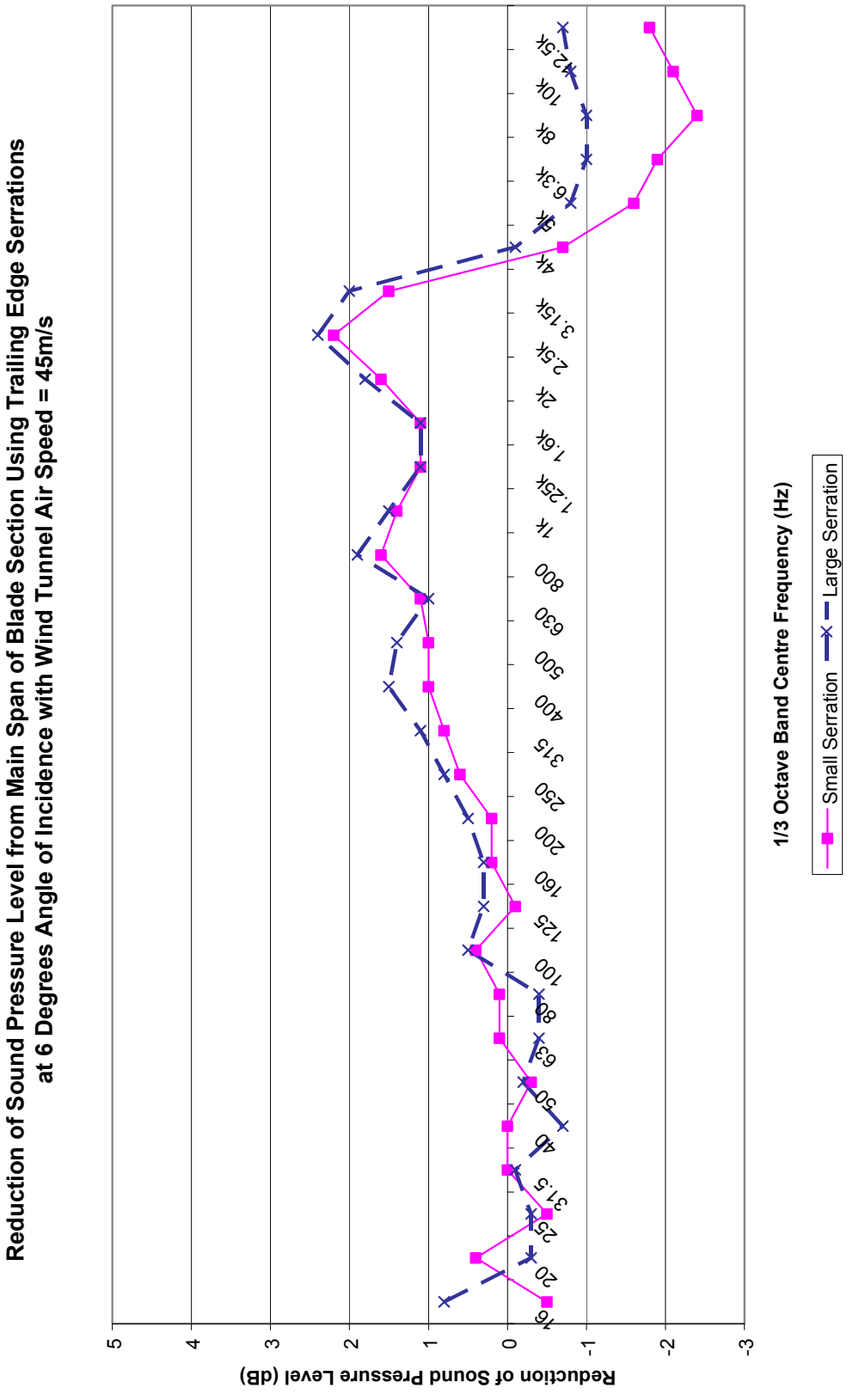

Figure A16 – Noise Reductions at 6 Degrees Angle of Incidence (45m/s)

Appendix B

Environmental Noise Modelling Results

This appendix contains a set of environmental noise modelling and validation results. For a methodology of the modelling and discussion of the results refer to Chapter 9.

List of Tables

Run # 1 **Simulated Condition:** 6m/s northerly wind, 20 deg C, 55% humidity

Receiver	Landmark	Distance from Turbine (m)	Direction from Turbine	Predicted Sound Pressure Level (dBA)				Measured Sound Pressure Level (dBA)
				ISO	CONCAWE	NORD2000	NZS 6808	
1	Ring of tussock	30	W	58.1	61.3	58.1	66.4	61.6
2	Met mast	66	NE	55.9	58.7	55.9	59.4	59.0
3	Access road	90	E	51.8	55.7	51.7	56.6	55.2
4	Steep part of access road	100	S	51.0	54.4	50.5	55.6	54.7
5	Top gate on access road	320	N	40.3	43.9	42.4	44.4	43.4
6	Gate of House 1	400	SW	37.2	41.5	39.3	42.1	43.0*
7	House 1	527	SW	35.2	39.4	37.5	39.0	**
8	House 2	551	NNE	26.9	23.4	22.7	38.5	**
9	Hut near RNZ mast	630	NE	32.7	35.6	33.3	37.0	40.1*
10	Hairpin corner main road	840	NW	28.8	29.8	30.7	33.4	39.9*
11	House 3	966	W	24.6	23.0	24.7	31.6	**
12	House 4	1255	SE	21.7	29.4	25.3	27.9	**
13	House 5	1263	W	21.7	25.5	28.0	27.8	**
14	House 6	1393	SE	24.5	28.1	25.1	26.3	26.6
15	House 7	1514	W	24.9	22.8	25.9	24.9	**
16	House 8	1544	SW	19.3	11.2	10.6	24.6	**
17	House 9	1572	SE	23.3	26.7	25.4	24.3	**
18	House 10	1852	SW	17.2	9.5	8.8	21.5	**

* Wind / background noise level high relative to turbine noise level

** Not measured

Note: Temperature and humidity at time of measurement approximate only.

Table B1 – Results of Calculation Run #1

Table B2 – Results of Calculation Run #2

Run # 2 **Simulated Condition:** 7m/s northerly wind, 20 deg C, 55% humidity

Receiver	Landmark	Distance from Turbine (m)	Direction from Turbine	Predicted Sound Pressure Level (dBA)				Measured Sound Pressure Level (dBA)
				ISO	CONCAWE	NORD2000	NZS 6808	
1	Ring of tussock	30	W	58.9	62.2	58.9	67.3	**
2	Met mast	66	NE	56.8	59.6	56.8	60.3	**
3	Access road	90	E	52.6	56.7	52.6	57.5	**
4	Steep part of access road	100	S	51.9	55.3	51.4	56.5	**
5	Top gate on access road	320	N	41.2	44.9	43.4	45.3	**
6	Gate of House 1	400	SW	38.2	42.4	40.4	43.0	**
7	House 1	527	SW	36.2	40.4	38.5	39.9	**
8	House 2	551	NNE	27.9	24.5	23.8	39.4	**
9	Hut near RNZ mast	630	NE	33.8	36.6	34.3	37.9	**
10	Hairpin corner main road	840	NW	29.9	30.9	31.8	34.3	**
11	House 3	966	W	25.7	23.9	25.7	32.5	**
12	House 4	1255	SE	22.8	30.5	26.3	28.8	**
13	House 5	1263	W	22.7	26.5	29.0	28.7	**
14	House 6	1393	SE	25.6	29.2	26.2	27.2	28.0
15	House 7	1514	W	26.0	23.7	27.0	25.8	**
16	House 8	1544	SW	20.4	12.4	11.8	25.5	**
17	House 9	1572	SE	24.4	27.8	26.4	25.2	**
18	House 10	1852	SW	18.2	10.7	10.0	22.4	**

* Wind / background noise level high relative to turbine noise level
** Not measured

Note: Temperature and humidity at time of measurement approximate only.

Run # 3 **Simulated Condition:** 8m/s northerly wind, 20 deg C, 55% humidity

Receiver	Landmark	Distance from Turbine (m)	Direction from Turbine	Predicted Sound Pressure Level (dBA)				Measured Sound Pressure Level (dBA)
				ISO	CONCAWE	NORD2000	NZS 6808	
1	Ring of tussock	30	W	59.7	63.1	59.7	68.2	63.9
2	Met mast	66	NE	57.7	60.5	57.7	61.2	65.3*
3	Access road	90	E	53.5	57.6	53.4	58.4	57.4
4	Steep part of access road	100	S	52.7	56.2	52.2	57.4	55.0
5	Top gate on access road	320	N	42.2	45.9	44.4	46.2	45.6
6	Gate of House 1	400	SW	39.2	43.4	41.3	43.9	45.0*
7	House 1	527	SW	37.2	41.3	39.5	40.8	**
8	House 2	551	NNE	29.0	25.6	24.9	40.3	**
9	Hut near RNZ mast	630	NE	34.8	37.6	35.3	38.8	**
10	Hairpin corner main road	840	NW	30.9	31.9	32.8	35.2	**
11	House 3	966	W	26.7	24.8	26.8	33.4	**
12	House 4	1255	SE	23.8	31.5	27.3	29.7	**
13	House 5	1263	W	23.8	27.4	30.1	29.6	**
14	House 6	1393	SE	26.7	30.2	27.2	28.1	30.6
15	House 7	1514	W	27.0	24.6	28.0	26.7	**
16	House 8	1544	SW	21.4	13.6	13.0	26.4	**
17	House 9	1572	SE	25.5	28.8	27.5	26.1	**
18	House 10	1852	SW	19.3	11.9	11.3	23.3	**

* Wind / background noise level high relative to turbine noise level

** Not measured

Note: Temperature and humidity at time of measurement approximate only.

Table B3 – Results of Calculation Run #3

Table B4 – Results of Calculation Run #4

Run # 4 **Simulated Condition:** 9m/s northerly wind, 20 deg C, 55% humidity

Receiver	Landmark	Distance from Turbine (m)	Direction from Turbine	Predicted Sound Pressure Level (dBA)				Measured Sound Pressure Level (dBA)
				ISO	CONCAWE	NORD2000	NZS 6808	
1	Ring of tussock	30	W	60.6	64	60.6	69.1	**
2	Met mast	66	NE	58.6	61.4	58.6	62.1	**
3	Access road	90	E	54.4	58.5	54.4	59.3	**
4	Steep part of access road	100	S	53.7	57.1	53.2	58.3	**
5	Top gate on access road	320	N	43.2	46.8	45.4	47.1	**
6	Gate of House 1	400	SW	40.2	44.4	42.3	44.8	**
7	House 1	527	SW	38.3	42.4	40.5	41.7	**
8	House 2	551	NNE	30.1	26.8	26.2	41.2	**
9	Hut near RNZ mast	630	NE	35.9	38.6	36.4	39.7	**
10	Hairpin corner main road	840	NW	32.1	33	33.9	36.1	**
11	House 3	966	W	27.7	25.8	27.9	34.3	**
12	House 4	1255	SE	24.9	32.5	28.4	30.6	**
13	House 5	1263	W	24.8	28.4	31.1	30.5	**
14	House 6	1393	SE	27.9	31.3	28.4	29.0	31.6
15	House 7	1514	W	28.2	25.7	29.1	27.6	**
16	House 8	1544	SW	22.5	15	14.4	27.3	**
17	House 9	1572	SE	26.7	29.9	28.6	27.0	**
18	House 10	1852	SW	20.4	13.2	12.7	24.2	**

* Wind / background noise level high relative to turbine noise level
** Not measured

Note: Temperature and humidity at time of measurement approximate only.

Run # 5 **Simulated Condition:** 10m/s northerly wind, 20 deg C, 55% humidity

Receiver	Landmark	Distance from Turbine (m)	Direction from Turbine	Predicted Sound Pressure Level (dBA)				Measured Sound Pressure Level (dBA)
				ISO	CONCAWE	NORD2000	NZS 6808	
1	Ring of tussock	30	W	61.6	65.0	61.6	70.0	64.6
2	Met mast	66	NE	59.6	62.4	59.6	63.0	66.2*
3	Access road	90	E	55.4	59.6	55.4	60.2	60.1
4	Steep part of access road	100	S	54.7	58.1	54.2	59.2	57.8
5	Top gate on access road	320	N	44.4	47.9	46.4	48.0	47.9
6	Gate of House 1	400	SW	41.4	45.5	43.4	45.7	46.1*
7	House 1	527	SW	39.4	43.4	41.6	42.6	**
8	House 2	551	NNE	31.3	28.2	27.6	42.1	**
9	Hut near RNZ mast	630	NE	37.1	39.8	37.6	40.6	45.7*
10	Hairpin corner main road	840	NW	33.3	34.2	35.1	37.0	40.4*
11	House 3	966	W	28.8	27.1	29.1	35.2	**
12	House 4	1255	SE	26.0	33.5	29.5	31.5	**
13	House 5	1263	W	26.0	29.5	32.3	31.4	**
14	House 6	1393	SE	29.3	32.4	29.6	29.9	32.5
15	House 7	1514	W	29.5	26.8	30.3	28.5	**
16	House 8	1544	SW	23.7	16.5	16.2	28.2	**
17	House 9	1572	SE	28.1	31.1	29.8	27.9	**
18	House 10	1852	SW	21.6	14.8	14.5	25.1	**

* Wind / background noise level high relative to turbine noise level
** Not measured

Note: Temperature and humidity at time of measurement approximate only.

Table B5 – Results of Calculation Run #5

Table B6 – Results of Calculation Run #6

Run # 6 **Simulated Condition:** 10m/s northerly wind, 20 deg C, 80% humidity

Receiver	Landmark	Distance from Turbine (m)	Direction from Turbine	Predicted Sound Pressure Level (dBA)				Measured Sound Pressure Level (dBA)
				ISO	CONCAWE	NORD2000	NZS 6808	
1	Ring of tussock	30	W	61.7	65.0	61.7	70.0	64.5
2	Met mast	66	NE	59.7	62.4	59.7	63.0	66.4*
3	Access road	90	E	55.5	59.6	55.5	60.2	60.1
4	Steep part of access road	100	S	54.8	58.2	54.3	59.2	57.8
5	Top gate on access road	320	N	44.4	48.0	46.5	48.0	48.0
6	Gate of House 1	400	SW	41.5	45.6	43.5	45.7	46.1*
7	House 1	527	SW	39.5	43.5	41.7	42.6	**
8	House 2	551	NNE	31.3	28.3	27.7	42.1	**
9	Hut near RNZ mast	630	NE	37.1	39.9	37.7	40.6	**
10	Hairpin corner main road	840	NW	33.4	34.3	35.2	37.0	**
11	House 3	966	W	29.0	27.2	29.2	35.2	**
12	House 4	1255	SE	26.2	33.7	29.6	31.5	**
13	House 5	1263	W	26.1	29.7	32.5	31.4	**
14	House 6	1393	SE	29.4	32.6	29.8	29.9	32.9
15	House 7	1514	W	29.6	27.0	30.5	28.5	**
16	House 8	1544	SW	23.8	16.7	16.4	28.2	**
17	House 9	1572	SE	28.3	31.2	30.0	27.9	**
18	House 10	1852	SW	21.8	15.0	14.7	25.1	**

* Wind / background noise level high relative to turbine noise level
** Not measured

Note: Temperature and humidity at time of measurement approximate only.

Table B7 – Results of Calculation Run #7

Run # 7 **Simulated Condition:** 10m/s northerly wind, 10 deg C, 55% humidity

Receiver	Landmark	Distance from Turbine (m)	Direction from Turbine	Predicted Sound Pressure Level (dBA)				Measured Sound Pressure Level (dBA)
				ISO	CONCAWE	NORD2000	NZS 6808	
1	Ring of tussock	30	W	61.5	64.9	61.5	70.0	63.9
2	Met mast	66	NE	59.5	62.3	59.5	63.0	66.2*
3	Access road	90	E	55.3	59.5	55.2	60.2	59.9
4	Steep part of access road	100	S	54.6	58.0	54.1	59.2	57.8
5	Top gate on access road	320	N	44.4	48.0	46.5	48.0	47.9
6	Gate of House 1	400	SW	41.5	45.5	43.6	45.7	46.1*
7	House 1	527	SW	39.6	43.6	41.8	42.6	**
8	House 2	551	NNE	31.5	28.4	27.8	42.1	**
9	Hut near RNZ mast	630	NE	37.3	40.0	37.8	40.6	45.7*
10	Hairpin corner main road	840	NW	33.6	34.6	35.5	37.0	40.4*
11	House 3	966	W	29.3	27.5	29.5	35.2	**
12	House 4	1255	SE	26.6	34.2	30.1	31.5	**
13	House 5	1263	W	26.6	30.1	32.9	31.4	**
14	House 6	1393	SE	29.8	33.1	30.3	29.9	33.2
15	House 7	1514	W	30.2	27.5	31.0	28.5	**
16	House 8	1544	SW	24.3	17.1	16.6	28.2	**
17	House 9	1572	SE	28.8	31.9	30.5	27.9	**
18	House 10	1852	SW	22.4	15.5	15.0	25.1	**

* Wind / background noise level high relative to turbine noise level
** Not measured

Note: Temperature and humidity at time of measurement approximate only.

Table B8 – Results of Calculation Run #8

Run # 8 **Simulated Condition:** 6m/s northerly wind, 3 deg C, 55% humidity

Receiver	Landmark	Distance from Turbine (m)	Direction from Turbine	Predicted Sound Pressure Level (dBA)			Measured Sound Pressure Level (dBA)
				ISO	CONCAWE	NORD2000	NZS 6808	
1	Ring of tussock	30	W	57.7	61.0	57.7	66.4	**
2	Met mast	66	NE	55.5	58.4	55.5	59.4	**
3	Access road	90	E	51.2	55.4	51.1	56.6	**
4	Steep part of access road	100	S	50.4	54.0	49.9	55.6	**
5	Top gate on access road	320	N	39.9	43.8	42.3	44.4	**
6	Gate of House 1	400	SW	37.0	41.2	39.3	42.1	**
7	House 1	527	SW	35.1	39.3	37.6	39.0	**
8	House 2	551	NNE	27.1	23.7	22.9	38.5	**
9	Hut near RNZ mast	630	NE	32.7	35.8	33.3	37.0	**
10	Hairpin corner main road	840	NW	29.1	30.2	31.0	33.4	**
11	House 3	966	W	25.1	23.5	25.2	31.6	**
12	House 4	1255	SE	22.5	30.1	25.9	27.9	**
13	House 5	1263	W	22.4	26.2	28.7	27.8	**
14	House 6	1393	SE	25.2	28.9	25.9	26.3	27.0
15	House 7	1514	W	25.7	23.6	26.8	24.9	**
16	House 8	1544	SW	20.2	12.1	11.5	24.6	**
17	House 9	1572	SE	24.1	27.7	26.3	24.3	**
18	House 10	1852	SW	18.3	10.7	9.9	21.5	**

* Wind / background noise level high relative to turbine noise level
** Not measured

Note: Temperature and humidity at time of measurement approximate only.

Run # 9 **Simulated Condition:** 6m/s southerly wind, 20 deg C, 55% humidity

Receiver	Landmark	Distance from Turbine (m)	Direction from Turbine	Predicted Sound Pressure Level (dBA)				Measured Sound Pressure Level (dBA)
				ISO	CONCAWE	NORD2000	NZS 6808	
1	Ring of tussock	30	W	58.1	61.3	58.1	66.4	**
2	Met mast	66	NE	55.9	58.9	55.9	59.4	**
3	Access road	90	E	51.8	55.6	51.7	56.6	**
4	Steep part of access road	100	S	51.0	54.1	50.5	55.6	**
5	Top gate on access road	320	N	40.3	44.5	42.4	44.4	**
6	Gate of House 1	400	SW	36.9	41.2	39.3	42.1	**
7	House 1	527	SW	34.8	38.4	37.5	39.0	**
8	House 2	551	NNE	27.3	24.3	22.7	38.5	**
9	Hut near RNZ mast	630	NE	33.2	37.4	33.3	37.0	**
10	Hairpin corner main road	840	NW	29.5	33.7	30.7	33.4	**
11	House 3	966	W	23.9	25.0	24.7	31.6	**
12	House 4	1255	SE	21.0	23.5	25.3	27.9	**
13	House 5	1263	W	20.9	27.3	28.0	27.8	**
14	House 6	1393	SE	23.7	21.6	25.1	26.3	29.9*
15	House 7	1514	W	24.1	25.0	25.9	24.9	**
16	House 8	1544	SW	18.5	5.0	10.6	24.6	**
17	House 9	1572	SE	22.5	19.7	25.4	24.3	**
18	House 10	1852	SW	16.3	2.3	8.8	21.5	**

* Wind / background noise level high relative to turbine noise level
** Not measured

Note: Temperature and humidity at time of measurement approximate only.

Table B9 – Results of Calculation Run #9

Table B10 – Results of Calculation Run #10

Run # 10 **Simulated Condition:** 8m/s southerly wind, 20 deg C, 55% humidity

Receiver	Landmark	Distance from Turbine (m)	Direction from Turbine	Predicted Sound Pressure Level (dBA)				Measured Sound Pressure Level (dBA)
				ISO	CONCAWE	NORD2000	NZS 6808	
1	Ring of tussock	30	W	59.7	63.1	59.7	68.2	**
2	Met mast	66	NE	57.7	60.7	57.7	61.2	**
3	Access road	90	E	53.5	57.4	53.4	58.4	**
4	Steep part of access road	100	S	52.7	55.9	52.2	57.4	**
5	Top gate on access road	320	N	42.2	46.4	44.4	46.2	**
6	Gate of House 1	400	SW	38.9	43.2	41.3	43.9	**
7	House 1	527	SW	36.8	40.4	39.5	40.8	**
8	House 2	551	NNE	29.4	26.5	24.9	40.3	**
9	Hut near RNZ mast	630	NE	35.3	39.4	35.3	38.8	**
10	Hairpin corner main road	840	NW	31.6	35.7	32.8	35.2	**
11	House 3	966	W	26.0	27.5	26.8	33.4	**
12	House 4	1255	SE	23.1	25.6	27.3	29.7	**
13	House 5	1263	W	23.0	29.8	30.1	29.6	**
14	House 6	1393	SE	25.9	23.8	27.2	28.1	30.3*
15	House 7	1514	W	26.2	27.5	28.0	26.7	**
16	House 8	1544	SW	20.6	7.4	13.0	26.4	**
17	House 9	1572	SE	24.7	21.9	27.5	26.1	**
18	House 10	1852	SW	18.4	5.0	11.3	23.3	**

* Wind / background noise level high relative to turbine noise level
** Not measured

Note: Temperature and humidity at time of measurement approximate only.

Run # 11 **Simulated Condition:** 10m/s southerly wind, 20 deg C, 55% humidity

Table B11 – Results of Calculation Run #11

Receiver	Landmark	Distance from Turbine (m)	Direction from Turbine	Predicted Sound Pressure Level (dBA)				Measured Sound Pressure Level (dBA)
				ISO	CONCAWE	NORD2000	NZS 6808	
1	Ring of tussock	30	W	61.6	65	61.6	70.0	62.4
2	Met mast	66	NE	59.6	62.5	59.6	63.0	65.1
3	Access road	90	E	55.4	59.4	55.4	60.2	59.5
4	Steep part of access road	100	S	54.7	57.8	54.2	59.2	57.1
5	Top gate on access road	320	N	44.4	48.4	46.4	48.0	48.4
6	Gate of House 1	400	SW	41.1	45.2	43.4	45.7	46.0*
7	House 1	527	SW	39	42.5	41.6	42.6	**
8	House 2	551	NNE	31.7	29.2	27.6	42.1	**
9	Hut near RNZ mast	630	NE	37.6	41.6	37.6	40.6	**
10	Hairpin corner main road	840	NW	33.9	37.9	35.1	37.0	**
11	House 3	966	W	28.2	30	29.1	35.2	**
12	House 4	1255	SE	25.3	27.8	29.5	31.5	**
13	House 5	1263	W	25.2	32.3	32.3	31.4	**
14	House 6	1393	SE	28.5	26.3	29.6	29.9	30.8*
15	House 7	1514	W	28.7	30.2	30.3	28.5	**
16	House 8	1544	SW	22.9	11.1	16.2	28.2	**
17	House 9	1572	SE	27.3	24.5	29.8	27.9	**
18	House 10	1852	SW	20.7	8.8	14.5	25.1	**

* Wind / background noise level high relative to turbine noise level

** Not measured

Note: Temperature and humidity at time of measurement approximate only.

Table B12 – Results of Calculation Run #12

Run # 12 **Simulated Condition:** 10m/s southerly wind, 10 deg C, 55% humidity

Receiver	Landmark	Distance from Turbine (m)	Direction from Turbine	Predicted Sound Pressure Level (dBA)				Measured Sound Pressure Level (dBA)
				ISO	CONCAWE	NORD2000	NZS 6808	
1	Ring of tussock	30	W	61.5	64.9	61.5	70.0	62.5
2	Met mast	66	NE	59.5	62.5	59.5	63.0	65.6
3	Access road	90	E	55.3	59.3	55.2	60.2	59.1
4	Steep part of access road	100	S	54.6	57.8	54.1	59.2	57.1
5	Top gate on access road	320	N	44.4	48.4	46.5	48.0	48.5
6	Gate of House 1	400	SW	41.2	45.4	43.6	45.7	**
7	House 1	527	SW	39.2	42.7	41.8	42.6	**
8	House 2	551	NNE	31.9	29.4	27.8	42.1	**
9	Hut near RNZ mast	630	NE	37.8	41.8	37.8	40.6	**
10	Hairpin corner main road	840	NW	34.3	38.3	35.5	37.0	**
11	House 3	966	W	28.6	30.5	29.5	35.2	**
12	House 4	1255	SE	25.9	28.3	30.1	31.5	**
13	House 5	1263	W	25.8	32.9	32.9	31.4	**
14	House 6	1393	SE	29.1	26.9	30.3	29.9	30.3*
15	House 7	1514	W	29.4	30.9	31.0	28.5	**
16	House 8	1544	SW	23.5	11.4	16.6	28.2	**
17	House 9	1572	SE	28.0	25.1	30.5	27.9	**
18	House 10	1852	SW	21.6	9.2	15.0	25.1	**

* Wind / background noise level high relative to turbine noise level
** Not measured

Note: Temperature and humidity at time of measurement approximate only.

Run # 13 **Simulated Condition:** 6m/s southerly wind, 3 deg C, 55% humidity

Table B13 – Results of Calculation Run #13

Receiver	Landmark	Distance from Turbine (m)	Direction from Turbine	Predicted Sound Pressure Level (dBA)				Measured Sound Pressure Level (dBA)
				ISO	CONCAWE	NORD2000	NZS 6808	
1	Ring of tussock	30	W	57.7	61.3	57.7	66.4	**
2	Met mast	66	NE	55.5	58.9	55.5	59.4	**
3	Access road	90	E	51.2	55.6	51.1	56.6	**
4	Steep part of access road	100	S	50.4	54.1	49.9	55.6	**
5	Top gate on access road	320	N	39.9	44.5	42.3	44.4	**
6	Gate of House 1	400	SW	36.7	41.2	39.3	42.1	**
7	House 1	527	SW	34.6	38.4	37.6	39.0	**
8	House 2	551	NNE	27.5	24.3	22.9	38.5	**
9	Hut near RNZ mast	630	NE	33.2	37.4	33.3	37.0	**
10	Hairpin corner main road	840	NW	29.7	33.7	31.0	33.4	**
11	House 3	966	W	24.4	25.0	25.2	31.6	**
12	House 4	1255	SE	21.7	23.5	25.9	27.9	**
13	House 5	1263	W	21.6	27.3	28.7	27.8	**
14	House 6	1393	SE	24.4	21.6	25.9	26.3	27.2*
15	House 7	1514	W	25.0	25.0	26.8	24.9	**
16	House 8	1544	SW	19.4	5.0	11.5	24.6	**
17	House 9	1572	SE	23.3	19.7	26.3	24.3	**
18	House 10	1852	SW	17.5	2.3	9.9	21.5	**

* Wind / background noise level high relative to turbine noise level

** Not measured

Note: Temperature and humidity at time of measurement approximate only.

Table B14 – Results of Calculation Run #14

Run # 14 **Simulated Condition:** 6m/s easterly wind, 20 deg C, 55% humidity

Receiver	Landmark	Distance from Turbine (m)	Direction from Turbine	Predicted Sound Pressure Level (dBA)				Measured Sound Pressure Level (dBA)
				ISO	CONCAWE	NORD2000	NZS 6808	
1	Ring of tussock	30	W	58.1	61.5	58.1	66.4	**
2	Met mast	66	NE	55.9	58.7	55.9	59.4	**
3	Access road	90	E	51.8	55.6	51.7	56.6	**
4	Steep part of access road	100	S	51.0	54.1	50.5	55.6	**
5	Top gate on access road	320	N	40.3	43.9	42.4	44.4	**
6	Gate of House 1	400	SW	36.9	41.5	39.3	42.1	**
7	House 1	527	SW	35.2	39.4	37.5	39.0	**
8	House 2	551	NNE	26.9	23.4	22.7	38.5	**
9	Hut near RNZ mast	630	NE	32.7	35.6	33.3	37.0	**
10	Hairpin corner main road	840	NW	29.5	33.7	30.7	33.4	**
11	House 3	966	W	24.6	26.1	24.7	31.6	**
12	House 4	1255	SE	21.0	23.5	25.3	27.9	**
13	House 5	1263	W	21.7	29.4	28.0	27.8	**
14	House 6	1393	SE	23.7	21.6	25.1	26.3	**
15	House 7	1514	W	24.9	27.2	25.9	24.9	**
16	House 8	1544	SW	19.3	11.3	10.6	24.6	**
17	House 9	1572	SE	22.5	19.7	25.4	24.3	**
18	House 10	1852	SW	17.2	9.5	8.8	21.5	**

* Wind / background noise level high relative to turbine noise level
** Not measured

Note: Temperature and humidity at time of measurement approximate only.

Run # 15 **Simulated Condition:** 8m/s easterly wind, 20 deg C, 55% humidity

Receiver	Landmark	Distance from Turbine (m)	Direction from Turbine	Predicted Sound Pressure Level (dBA)				Measured Sound Pressure Level (dBA)
				ISO	CONCAWE	NORD2000	NZS 6808	
1	Ring of tussock	30	W	59.7	63.2	59.7	68.2	**
2	Met mast	66	NE	57.7	60.5	57.7	61.2	**
3	Access road	90	E	53.5	57.4	53.4	58.4	**
4	Steep part of access road	100	S	52.7	56.0	52.2	57.4	**
5	Top gate on access road	320	N	42.2	45.9	44.4	46.2	**
6	Gate of House 1	400	SW	39.2	43.4	41.3	43.9	**
7	House 1	527	SW	37.2	41.3	39.5	40.8	**
8	House 2	551	NNE	29.0	25.6	24.9	40.3	**
9	Hut near RNZ mast	630	NE	34.8	37.6	35.3	38.8	**
10	Hairpin corner main road	840	NW	31.6	35.7	32.8	35.2	**
11	House 3	966	W	26.7	28.2	26.8	33.4	**
12	House 4	1255	SE	23.1	25.6	27.3	29.7	**
13	House 5	1263	W	23.8	31.5	30.1	29.6	**
14	House 6	1393	SE	25.9	23.8	27.2	28.1	**
15	House 7	1514	W	27.0	29.3	28.0	26.7	**
16	House 8	1544	SW	21.4	13.6	13.0	26.4	**
17	House 9	1572	SE	24.7	21.9	27.5	26.1	**
18	House 10	1852	SW	19.3	11.9	11.3	23.3	**

* Wind / background noise level high relative to turbine noise level

** Not measured

Note: Temperature and humidity at time of measurement approximate only.

Table B15 – Results of Calculation Run #15

Table B16 – Results of Calculation Run #16

Run # 16 **Simulated Condition:** 10m/s easterly wind, 20 deg C, 55% humidity

Receiver	Landmark	Distance from Turbine (m)	Direction from Turbine	Predicted Sound Pressure Level (dBA)				Measured Sound Pressure Level (dBA)
				ISO	CONCAWE	NORD2000	NZS 6808	
1	Ring of tussock	30	W	61.6	65.1	61.6	70.0	64.3
2	Met mast	66	NE	59.6	62.4	59.6	63.0	64.1*
3	Access road	90	E	55.4	59.4	55.4	60.2	58.4
4	Steep part of access road	100	S	54.7	58.0	54.2	59.2	57.1
5	Top gate on access road	320	N	44.4	47.9	46.4	48.0	48.0
6	Gate of House 1	400	SW	41.4	45.5	43.4	45.7	**
7	House 1	527	SW	39.4	43.4	41.6	42.6	**
8	House 2	551	NNE	31.3	28.2	27.6	42.1	**
9	Hut near RNZ mast	630	NE	37.1	39.8	37.6	40.6	**
10	Hairpin corner main road	840	NW	33.9	37.9	35.1	37.0	**
11	House 3	966	W	28.8	30.5	29.1	35.2	**
12	House 4	1255	SE	25.3	27.8	29.5	31.5	**
13	House 5	1263	W	26.0	33.7	32.3	31.4	**
14	House 6	1393	SE	28.5	26.3	29.6	29.9	**
15	House 7	1514	W	29.5	31.5	30.3	28.5	**
16	House 8	1544	SW	23.7	16.5	16.2	28.2	**
17	House 9	1572	SE	27.3	24.5	29.8	27.9	**
18	House 10	1852	SW	21.6	14.8	14.5	25.1	**

* Wind / background noise level high relative to turbine noise level
** Not measured

Note: Temperature and humidity at time of measurement approximate only.

Run # 17 **Simulated Condition:** 6m/s westerly wind, 20 deg C, 55% humidity

Receiver	Landmark	Distance from Turbine (m)	Direction from Turbine	Predicted Sound Pressure Level (dBA)				Measured Sound Pressure Level (dBA)
				ISO	CONCAWE	NORD2000	NZS 6808	
1	Ring of tussock	30	W	58.1	61.3	58.1	66.4	**
2	Met mast	66	NE	55.9	58.9	55.9	59.4	**
3	Access road	90	E	51.8	55.9	51.7	56.6	**
4	Steep part of access road	100	S	51.0	54.1	50.5	55.6	**
5	Top gate on access road	320	N	40.3	44.5	42.4	44.4	**
6	Gate of House 1	400	SW	36.9	41.2	39.3	42.1	**
7	House 1	527	SW	34.8	38.4	37.5	39.0	**
8	House 2	551	NNE	27.3	24.3	22.7	38.5	**
9	Hut near RNZ mast	630	NE	33.2	37.5	33.3	37.0	**
10	Hairpin corner main road	840	NW	28.8	29.9	30.7	33.4	**
11	House 3	966	W	23.9	21.8	24.7	31.6	**
12	House 4	1255	SE	21.7	29.4	25.3	27.9	**
13	House 5	1263	W	20.9	23.4	28.0	27.8	**
14	House 6	1393	SE	24.5	28.1	25.1	26.3	**
15	House 7	1514	W	24.1	20.5	25.9	24.9	**
16	House 8	1544	SW	18.5	4.8	10.6	24.6	**
17	House 9	1572	SE	23.3	26.7	25.4	24.3	**
18	House 10	1852	SW	16.3	2.2	8.8	21.5	**

* Wind / background noise level high relative to turbine noise level

** Not measured

Note: Temperature and humidity at time of measurement approximate only.

Table B17 – Results of Calculation Run #17

Table B18 – Results of Calculation Run #18

Run # 18 **Simulated Condition:** 8m/s westerly wind, 20 deg C, 55% humidity

Receiver	Landmark	Distance from Turbine (m)	Direction from Turbine	Predicted Sound Pressure Level (dBA)				Measured Sound Pressure Level (dBA)
				ISO	CONCAWE	NORD2000	NZS 6808	
1	Ring of tussock	30	W	59.7	63.1	59.7	68.2	**
2	Met mast	66	NE	57.7	60.7	57.7	61.2	**
3	Access road	90	E	53.5	57.7	53.4	58.4	**
4	Steep part of access road	100	S	52.7	55.9	52.2	57.4	**
5	Top gate on access road	320	N	42.2	46.4	44.4	46.2	**
6	Gate of House 1	400	SW	38.9	43.2	41.3	43.9	**
7	House 1	527	SW	36.8	40.4	39.5	40.8	**
8	House 2	551	NNE	29.4	26.5	24.9	40.3	**
9	Hut near RNZ mast	630	NE	35.3	39.4	35.3	38.8	**
10	Hairpin corner main road	840	NW	30.9	31.9	32.8	35.2	**
11	House 3	966	W	26.0	24.0	26.8	33.4	**
12	House 4	1255	SE	23.8	31.5	27.3	29.7	**
13	House 5	1263	W	23.0	25.6	30.1	29.6	**
14	House 6	1393	SE	26.7	30.2	27.2	28.1	**
15	House 7	1514	W	26.2	22.7	28.0	26.7	**
16	House 8	1544	SW	20.6	7.4	13.0	26.4	**
17	House 9	1572	SE	25.5	28.8	27.5	26.1	**
18	House 10	1852	SW	18.4	5.0	11.3	23.3	**

* Wind / background noise level high relative to turbine noise level
** Not measured

Note: Temperature and humidity at time of measurement approximate only.

Run # 19 **Simulated Condition:** 10m/s westerly wind, 20 deg C, 55% humidity

Receiver	Landmark	Distance from Turbine (m)	Direction from Turbine	Predicted Sound Pressure Level (dBA)				Measured Sound Pressure Level (dBA)
				ISO	CONCAWE	NORD2000	NZS 6808	
1	Ring of tussock	30	W	61.6	65.0	61.6	70.0	**
2	Met mast	66	NE	59.6	62.5	59.6	63.0	**
3	Access road	90	E	55.4	59.6	55.4	60.2	**
4	Steep part of access road	100	S	54.7	57.8	54.2	59.2	**
5	Top gate on access road	320	N	44.4	48.4	46.4	48.0	**
6	Gate of House 1	400	SW	41.1	45.2	43.4	45.7	**
7	House 1	527	SW	39.0	42.5	41.6	42.6	**
8	House 2	551	NNE	31.7	29.2	27.6	42.1	**
9	Hut near RNZ mast	630	NE	37.6	41.6	37.6	40.6	**
10	Hairpin corner main road	840	NW	33.3	34.2	35.1	37.0	**
11	House 3	966	W	28.2	26.4	29.1	35.2	**
12	House 4	1255	SE	26.0	33.5	29.5	31.5	**
13	House 5	1263	W	25.2	28.1	32.3	31.4	**
14	House 6	1393	SE	29.3	32.4	29.6	29.9	**
15	House 7	1514	W	28.7	25.2	30.3	28.5	**
16	House 8	1544	SW	22.9	11.1	16.2	28.2	**
17	House 9	1572	SE	28.1	31.1	29.8	27.9	**
18	House 10	1852	SW	20.7	8.8	14.5	25.1	**

* Wind / background noise level high relative to turbine noise level

** Not measured

Note: Temperature and humidity at time of measurement approximate only.

Table B19 – Results of Calculation Run #19

Chapter 1
Literature Survey

Summary

Wind turbine noise can be separated into two distinct categories – aerodynamically generated and mechanically generated noise. Mechanically generated noise is produced by the machinery inside the nacelle of the turbine with the gearbox usually being the largest contributor. The noise is either radiated directly from the nacelle or transmitted to the tower and blades as structure-borne noise. The reduction of mechanical noise from wind turbines can largely be achieved using conventional techniques such as sound insulation of the nacelle, vibration isolation of rotating machinery, and well designed and accurately made componentry such as the gearbox. However, aerodynamically generated noise is still a significant area of research. It is thought that aerodynamic (or aero-acoustic) noise from the blades arises from a number of different mechanisms that are related to the way in which the flow over the aerofoil interacts with the surrounding air. Techniques for prediction of the noise produced by an aerofoil are usually based on theoretical principles but use empirically derived components to achieve better agreement with what is observed in practice. Research into the reduction of aerodynamic noise from wind turbines has mainly focused on the use of serrated trailing edges, different trailing edge and tip shapes, and different aerofoil profiles.

The environmental aspects of wind turbine noise relate to how it propagates over the terrain surrounding the wind turbine and to how the noise is interpreted by people. The noise produced by wind turbines is often impulsive and tonal, both of which can add to the annoyance factor of the sound. Several standards for calculation of the propagation of the sound are widely used and range from basic calculations that assume hemispherical propagation, to complex calculations designed to be done computationally which take into account the effects of terrain shape, barriers, wind speed and direction, atmospheric temperature

profile, humidity, and air and ground absorption. Complex calculations such as these are regarded as being acceptably accurate at distances of up to 3000m from the turbine.

The accurate measurement of wind turbine noise can be difficult due to fluctuations in wind speed and direction, fluctuation in power produced and high levels of wind induced background and microphone pseudo-noise. However, measurement techniques and guidelines for noise emissions from wind turbines are well documented in several standards. Common techniques for improving the signal to noise ratio for wind turbine noise measurement include the use of a secondary windscreen, ground or vertical measuring boards, an acoustic parabola, or through use of multiple microphone cross-correlation to separate wind noise from turbine noise. However there appears to a lack of agreement over the duration over which a measurement should be taken. Longer durations of up to 10 minutes allow time to produce a more accurate average but the argument is that a shorter period of measurement of as little as 10 seconds might be more appropriate so as to measure the noise generated by the turbine without the variability produced by fluctuations in the speed and direction of the wind.

Table of Contents

List of Figures

1. Introduction

This chapter is a review of the current literature and is intended to introduce the reader to the important aspects of wind turbine noise.

The noise generated by a wind turbine falls into two main classes [51] –

1. Mechanical noise
2. Aerodynamic noise

In the subsequent parts of this chapter the noise sources from within each of these classes are identified, and reduction and prediction of the noise level for each source is discussed with regards to previous work. Research done into the propagation of noise to surrounding areas is then examined and both the human perception of noise and methods for prediction of the noise level at a distance from the turbine are discussed. The chapter concludes with a section on measurement techniques for gathering field data.

2. Mechanical Noise

2.1 Overview

The mechanical noise from a wind turbine is widely regarded as a less important area of research than that of aerodynamic noise [39, 51]. This is largely because the mechanical noise can be controlled using conventional techniques such as vibration isolation and sound insulation and absorption.

Pinder [43] identified the following main sources of mechanical noise from a wind turbine:

- Gearbox
- Generator
- Cooling fans
- Auxiliaries (oil coolers, hydraulic power packs, etc.)

Figure 1.2.1 below shows the relative contributions of each component to the overall sound power level of a typical wind turbine.

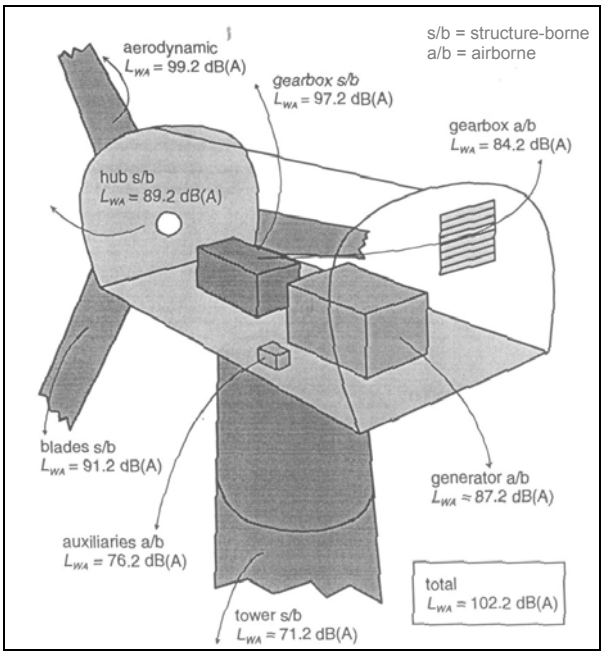

Figure 1.2.1 – Contribution of Individual Components to Overall Sound Power Level [51]

The noise generated by these sources can be propagated either directly from the surface of the component (airborne), or first transmitted along a structural component such as a blade or the tower, then radiated from another surface (structure-borne).

Pinder states that the dominant source of mechanical noise is the gearbox. Typically this will produce a broadband noise spectrum containing several prominent tones. The broadband noise is thought to originate from random errors in the shape of the gear teeth whilst the tonal peaks are due to rotation frequency harmonics and gear tooth meshing frequencies.

2.2 Noise Prediction

Prediction formulas for the mechanical noise of wind turbines are not readily available in either an empirical or theory based form. Mechanical noise is generally included as a part of empirical equations for the total sound power such as the class I prediction formulas cited in [51]. However, a rough estimate of mechanical noise can be obtained at the design stage by summing the sound power levels (known from testing or manufacturers' data) of each of the main noise emitting components. This technique will

however tend to underestimate the total mechanical noise because of the amplification that can often occur within the structure of the wind turbine, which is not allowed for.

2.3 Noise Reduction

The most effective means of reducing the mechanical noise radiated by a wind turbine is through vibration isolation of rotating or vibrating components, and insulation of the nacelle. Pinder's study showed that the mechanical noise propagated from a wind turbine could be reduced by up to 15 dB in this way.

In modern wind turbines, sound insulation often plays only a minor role since noise emission problems are generally treated at the source[39]. For example a structural dynamics analysis is often carried out on the wind turbine to ensure that the vibrations of various components do not interact with the structure to amplify the sound. Another example is the specification of quiet gearboxes, which use gears of an accurate cut and with a flexible core, capable of damping out vibrations.

3. Aerodynamic Noise

3.1 Overview

3.1.1 Introduction

Aerodynamic or aero-acoustic noise is considered to be the dominant noise source on modern large-scale wind turbines [51]. Experience with conventional fans and propellers has shown that the noise generated by the blades increases as approximately the fifth power of the blade tip speed [18], however reducing the tip speed is often not a commercially attractive option since the power produced is approximately proportional to the cube of the tip speed.

Lighthill's acoustic analogy [32], [33] forms the basis of much aero-acoustic theory – effectively relating the pressure fluctuations in real flows to acoustic wave generation. This theory is used extensively in the prediction of aerodynamic noise from wind turbine blades. The size of wind turbine blades and limitations of computational speed often mean that a fully theoretical approach cannot be used to predict

the noise produced by the blades. For this reason semi-empirical formulas based on Lighthill's theory are more widely used.

3.1.2 Lighthill's Theory

Lighthills theory states that aerodynamic sound is generated from fluid flow, which is governed by the mass conservation and Navier-Stokes momentum equations (Equations (1) and (2) below).

$$\frac{\partial \rho}{\partial t} + \frac{\partial}{\partial x_i}\left(\rho u_i\right) = 0 \tag{1-1}$$

$$\frac{\partial}{\partial t}\left(\rho u_i\right) + \frac{\partial}{\partial x_j}\left(\rho u_i u_j + p_{ij}\right) = 0 \tag{1-2}$$

where ρ is density, u_i and u_j are the velocity components, p_{ij} is the stress tensor and is defined as:

$$p_{ij} = -\sigma_{ij} + \delta_{ij} p \tag{1-3}$$

where p is the static pressure of the flow field, δ_{ij} the Kronecker delta, and σ_{ij} is the viscous stress tensor:

$$\sigma_{ij} = \mu\left\{\frac{\partial u_i}{\partial x_i} + \frac{\partial u_j}{\partial x_i} - \frac{2}{3}\left(\frac{\partial u_i}{\partial x_i}\right)\delta_{ij}\right\} \tag{1-4}$$

Equations of sound propagation are derived by use of the above mass and momentum conservation equations as:

$$\frac{\partial^2 \rho}{\partial t^2} - a_0^2 \nabla^2 \rho = \frac{\partial^2}{\partial x_i \partial x_j} T_{ij} \tag{1-5}$$

where T_{ij} is given by:

$$T_{ij} = \rho u_i u_j + p_{ij} - a_0^2 \rho \delta_{ij} \tag{1-6}$$

Mathematically, equation 1-5 is a hyperbolic partial differential equation, which describes a wave propagating at the speed of sound a_0 in a medium at rest, on which fluctuating forces are externally applied in the form described by the right hand side of equation 5. Physically, this means that sound is generated by the fluid flow's fluctuating internal stresses acting on an acoustic medium at rest (without flow), and propagated at the speed of sound.

Lighthill's analogy separates the analysis of aerodynamic acoustics into two steps. The first step is sound generation induced by fluid flow in any real continuous medium. The second step is sound propagation in an acoustic medium at rest, exerted by external fluctuating sources which are a function of T_{ij}, known from the first step.

The equation of sound propagation has been solved by Lighthill [32] and Curle [12] in the form:

$$\begin{aligned}\rho'(x,t) &= \rho(x,t) - \rho_0 \\ &= \frac{1}{4\pi a_0^2}\frac{\partial^2}{\partial x_i \partial x_j}\int_V \frac{T_{ij}\left(y, t - R/a_0\right)}{R} dV(y) + \ldots \\ &\quad \ldots \frac{1}{4\pi a_0^2}\frac{\partial}{\partial x_i}\int_S \frac{l_j p_{ij}\left(y, t - R/a_0\right)}{R} dS(y)\end{aligned} \qquad (1\text{-}7)$$

where x is the acoustic observation point where acoustic quantities are measured.

y is the point in the flow field where sound is generated.

$R = /x - y/$ is therefore the distance between the acoustic observation point and the point in the flow field where sound is generated. (Usually, it is assumed that $/x/>>/y/$).

l_j is the unit direction vector of the solid boundary, pointing toward the fluid.

t is the current observation time measured at x.

This equation relates fluctuating stresses in a flow field to the acoustic density oscillation with which conversion from the kinetic energy of fluctuating shearing motion in the flow to the acoustic energy of oscillating longitudinal sound wave can be calculated.

There are some assumptions to this formulation that limit its applicability. These are as follows -

- The sound is radiated into free space.
- The sound induced by the fluid flow is weak (ie. the backward-interaction of acoustic phenomena on the fluid flow is negligible).
- The fluid flow is not sensitive to the sound induced by the fluid flow.

Lighthill's acoustic analogy is therefore only applicable to the analysis of energy escaping from subsonic flows as sound, and not to the analysis of the change in character of generated sound, which is often observed in transitions to supersonic flow due to high frequency emission associated with shock waves. In most wind turbine applications, this will be of no consequence as generally only lower Mach number flows are dealt with.

ρ'(x) can be transformed into a simpler and numerically more tractable form:

$$\begin{aligned}\rho'(x,t) &= \rho(x,t) - \rho_0 \\ &= \frac{1}{4\pi a_0^4}\int_V \frac{(x_i - y_i)(x_j - y_j)}{R^3}\frac{\partial^2}{\partial t^2}T_{ij}(y,t')dV(y) + \ldots \\ &\quad \ldots \frac{1}{4\pi a_0^3}\int_S \frac{(x_i - y_i)l_i}{R^2}\frac{\partial p(y,t')}{dt'}dS(y) + \ldots \\ &\quad \ldots \frac{1}{4\pi a_0^2}\int_S \frac{(x_i - y_i)l_i}{R^3}p(y,t')dS(y)\end{aligned} \tag{1-8}$$

The first term is derived from the volume integrand in equation 1-7, neglecting short distance terms (proportional to inverse of R^4 and R^5). The remaining two terms are derived from the surface integrand in equation 1-7. When R is large, the third term is damped faster than the second term. Therefore the second and the third term are called the long and short distance terms respectively. Usually, the distance between the observer's location and the location at which sound generation occurs is large, and the short distance term will not appear in the following formulations.

Pressure variation can be derived by using the isentropic relation –

$$dp = a_0^2 d\rho \tag{1-9}$$

as –

$$\begin{aligned}\rho'(x,t) &= \rho(x,t) - \rho_0 \\ &= \frac{1}{4\pi a_0^2}\int_V \frac{(x_i - y_i)(x_j - y_j)}{R^3}\frac{\partial^2}{\partial t^2}T_{ij}(y,t')dV(y) + \ldots \\ &\quad \ldots\frac{1}{4\pi a_0}\int_S \frac{(x_i - y_i)l_i}{R^2}\frac{\partial p(y,t')}{dt'}dS(y)\end{aligned} \tag{1-10}$$

where ρ_0 is constant atmospheric density.

However, to accurately predict the noise generated by a given aerofoil it is necessary to study each noise source on the aerofoil individually.

3.2.3 Sources of Aero-Acoustic Noise

The aero-acoustic noise can be grouped into six main categories [19] –

- Turbulent boundary layer trailing edge noise
- Separated flow noise
- Laminar boundary layer vortex shedding noise
- Tip vortex formation noise
- Trailing edge bluntness vortex shedding noise
- Turbulent inflow noise

Dassen et al. [13] identifies turbulent boundary layer trailing edge noise followed by turbulent inflow noise to be the main contributors to the overall aerodynamic noise of modern wind turbines.

This section provides a brief description of the generation mechanisms, and discusses aerodynamic noise prediction and reduction methods found in the literature.

3.2 Turbulent Boundary Layer Trailing Edge Noise

3.2.1 Mechanisms

When the attached turbulent boundary layer convects into the wake of the aerofoil, the resulting interaction of the turbulence produces turbulent boundary layer trailing edge noise (TBL-TE). This is illustrated below in figure 1.3.1.

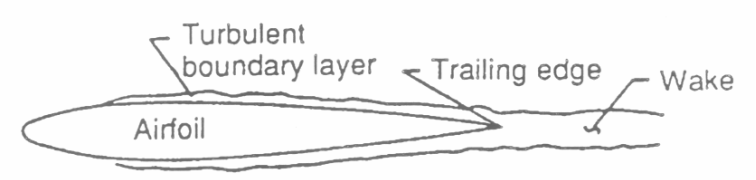

Figure 1.3.1 – Turbulent Boundary Layer Trailing Edge Noise Generation [19]

Fuglsang and Madsen [19] identify the frequency spectrum from TBL-TE noise to be broadband. They also state that the contribution of TBL-TE noise to the overall sound pressure level observed from the aerofoil is unimportant at low Reynolds numbers, but becomes more significant for high Reynolds numbers. Wagner et al. [51] states that TBL-TE is generally perceived as a swishing sound, with peak frequencies typically in the range of 500 – 1500 Hz.

3.2.2 Noise Prediction

The prediction theories found for TBL-TE noise were mainly based on the edge-scatter formulation by Fowcs Williams and Hall [18], which is valid for low Mach number flows. Fuglsang and Madsen successfully used equations 1-12 and 1-13 (which are based on the theory by Fowcs Williams and Hall) to predict the TBL-TE noise of a number of aerofoils –

$$\left(L_p\right)_{TBL-TE} = 10\log\left(10^{\left(L_p\right)_\alpha/10} + 10^{\left(L_p\right)_s/10} + 10^{\left(L_p\right)_p/10}\right) \tag{1-11}$$

where

$(L_p)_{TBL\text{-}TE}$ is the sound pressure level due to TBL-TE noise

$(L_p)_s$, $(L_p)_p$ are the sound pressure levels from the suction and pressure side of the aerofoil at zero angle of attack and are calculated using equation 1-12 below.

$(L_p)_\alpha$ is the sound pressure level due to an angle of attack not equal to zero and is calculated using equation 1-12 below.

$$L_p = 10\log\left(\frac{\delta^* M^5 L\overline{D}_h}{r_e^2}\right) + A\left(\frac{St}{St_1}\right) + (K_1 - 3) + \Delta K_1 \qquad (1\text{-}12)$$

where

L_p is the sound pressure level from the suction or pressure side of the aerofoil or due to a non zero angle of attack.

$\delta^* = \delta^*(\alpha, Re)$ is the boundary layer displacement thickness

where α is the angle of attack and Re is the Reynolds number based on the chord

$M = U/c$ is the Mach number

where U is the free stream velocity, c is the speed of sound

L is the length of the span

D_h is the directivity of the source

r_e is the retarded observer distance (using a retarded co-ordinate system which corrects for Doppler related frequency shifts due to the relative motion between the source and the observer).

$A(\,)$ is the universal frequency spectrum shape

where $St = (f\delta^*)/U$ is the Strouhal number based on the displacement thickness, where f is the frequency

$St_1 = 0.02M^{-0.6}$

$K_1 = K_1(Re)$ and $\Delta K_1 = \Delta K_1(\alpha, Re)$ are empirical functions

A number of other trailing edge noise theories based on Lighthill's acoustic analogy, the solution of linearized hydro-acoustic equations and other ad hoc models are presented by Howe in [26].

3.2.3 Noise Reduction

In a theoretical investigation into trailing edge noise reduction, Howe [25] presented theory which showed that the use of a serrated trailing edge would lead to a reduction of the noise emission. According to the theory, the reduction obtained was dependent on the aspect ratio of the serrations and their length along the trailing edge. An experimental investigation into the reduction of noise by using serrated trailing edges [21] found that Howe's theory underestimated the reduction at low frequencies and

overestimated it for high frequencies. It was found during the study that reductions of up to 4.5 dB could be achieved for frequencies below 1250 Hz, while frequencies above 2000 Hz experienced an increase of up to 7 dB – however, this still resulted in an overall reduction of 2 dB.

In an investigation into different tooth shapes [9], the reduction due to straight, bent and curved serrations (see figure 1.3.2) was studied. It was found that bent serrations were capable of producing an additional reduction in noise over straight and curved serrations, bringing the overall reduction to approximately 3.5 dB.

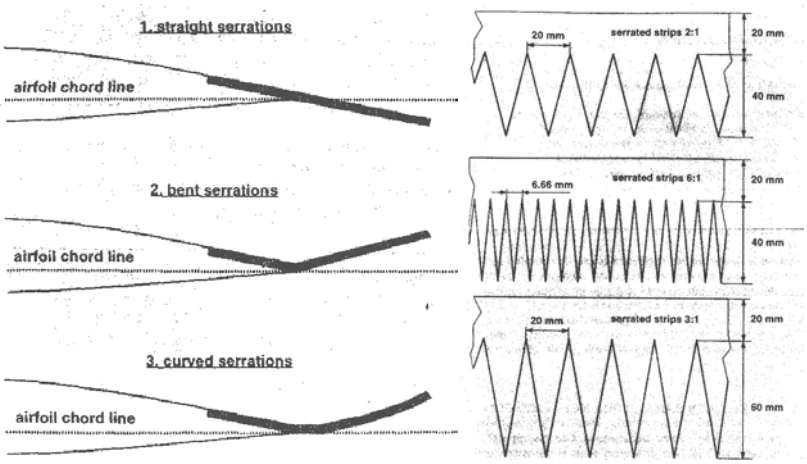

Figure 1.3.2 – Trailing Edge Serration Profiles and Aspect Ratios [9]

Investigations into trailing edge noise by Jakobsen and Andersen [27] compared several different trailing edge configurations. The results of the study showed that a porous trailing edge was capable of producing a similar effect to that of a serrated trailing edge – however very few other investigations of blade noise reduction using porous trailing edges have been done.

3.3 Separated Flow Noise

3.3.1 Mechanisms

At medium to high angles of attack the aerofoil may begin to form a zone of separated flow on the suction side. Air in the zone of separation has low momentum and the flow is highly unsteady. Noise from the separation zone originates from the shedding of vortices from the aerofoil trailing edge into the wake as

shown below in figure 1.3.3. As the angle of incidence increases the turbulence scale becomes larger until unsteady flow exists across the entire suction side. The noise is then radiated from the chord as a whole.

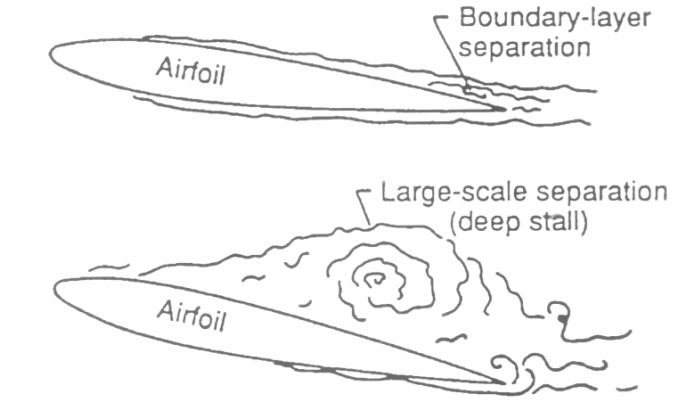

Figure 1.3.3 – Separated Flow Noise Generation [19]

Fuglsang and Madsen [19] state that the noise produced is broadband in nature and only significant for high angles of attack. Wagner et al. [51] describes a study that found an increase of more than 10 dB for stalled flow, relative to TBL-TE noise for low angles of attack.

3.3.2 Noise Prediction

No prediction methods specifically for separated flow noise were found to exist. However, Fuglsang and Madsen used a modified form of equations 1-11 and 1-12 with some success to predict the separated flow noise for a range of angles.

3.3.3 Noise Reduction

Wagner et al. [51] states that the only method of reducing separated flow noise is to avoid stalled flow by limiting the angles of attack of the aerofoil.

3.4 Laminar Boundary Layer Vortex Shedding Noise

3.4.1 Mechanisms

For a rotor blade operating at Reynolds numbers less than 10^6, laminar flow regions which extend up to the trailing edge may exist on either side of the aerofoil. In this situation a resonant interaction of the trailing edge noise with the unstable laminar-turbulent transition can occur [51]. The acoustic wave travels upstream from the trailing edge and couples to the Tollimen-Schlicting instabilities in the upstream boundary layer. From here the waves travel downstream growing rapidly until finally they regenerate an upstream acoustic wave upon reaching the trailing edge – see figure 1.3.4 below.

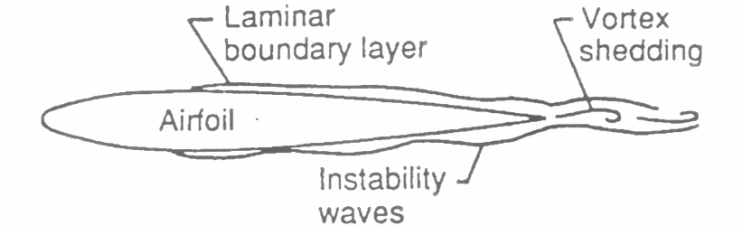

Figure 1.3.4 – Laminar Boundary Layer Vortex Shedding Noise Generation [19]

The resulting noise spectrum from laminar boundary layer vortex shedding noise (LBL-VS) is tonal, and typically of frequencies 1000 – 5000 Hz depending on Reynolds number and angle of attack [19].

3.4.2 Noise Prediction

Fuglsang and Madsen [19] developed the following equation for prediction of LBL-VS noise, based on the work of Fowcs Williams and Hall [18], and found it to be of reasonable accuracy –

$$(L_p)_{LBL-VS} = 10\log\left(\frac{\delta_P M^5 L\overline{D}_h}{r_e^2}\right) + G_1\left(\frac{St'}{St_{peak}}\right) + G_2\left(\frac{\mathrm{Re}_c}{(\mathrm{Re}_c)_0}\right) + G_3(\alpha) \qquad (1\text{-}13)$$

where

$(L_p)_{LBL-VS}$ is the sound pressure level due to LBL-VS noise

δ_p is the pressure side boundary layer thickness

$M = U/c$ is the Mach number

where U is the free stream velocity, c is the speed of sound

L is the length of the span

D_h is the directivity

r_e is the retarded observer distance

$G_1(\,), G_2(\,), G_3(\,)$ are empirical functions

where $St' = St'(Re_c)_0$ is the Strouhal number

$St'_{peak} = St'_{peak}(\alpha)$ is the peak Strouhal number

$(Re_c)_0 = (Re_c)_0(\alpha)$ is a reference Reynolds number

3.4.3 Noise Reduction

Since most large modern wind turbines operate at much higher local Reynolds numbers than 10^6, LBL-VS noise is not usually a major contributor to the overall aerodynamic noise. However, for cases where LBL-VS noise is a problem Wagner et al. [51] cites tripping of the boundary layer well upstream of the trailing edge as a possible solution. Another solution cited by Wagner et al. is the use of leading edge serrations.

3.5 Tip Vortex Formation Noise

3.5.1 Mechanisms

At the tip of an aerofoil, pressure differences between the suction and pressure sides cause cross flow over the side edge of the tip resulting in the formation of a tip vortex. Brooks, Pope and Marcolini [11], suggest that the tip vortex interacts with the trailing edge in the same manner as the boundary layer turbulence does for trailing edge noise – see figure 1.3.5.

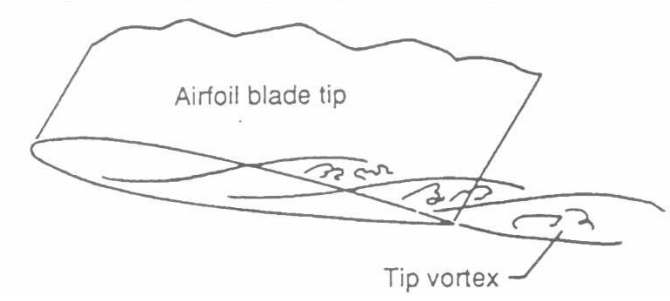

Figure 1.3.5 – Tip Vortex Noise Generation [19]

Tip noise is usually broadband in character but dominated by higher frequencies, typically around 4000 Hz, depending on tip speed [19]. Brooks, Pope and Marcolini [11] estimate the contribution of tip noise to be 1-2 dB in some parts of the frequency range.

3.5.2 Noise Prediction

In an investigation by Brooks and Marcolini [10], the following semi-empirical tip noise prediction formula was developed –

$$\left(L_P\right)_{TIP} = 10\log\left(\frac{M^2 M_{\max}^5 l^2 \overline{D}_h}{r_e^2}\right) - 30.5\left(\log St'' + 0.3\right)^2 + 126 \qquad (1\text{-}14)$$

where

$(L_p)_{TIP}$ is the sound pressure level due to tip vortex formation noise

$M = U/c$ is the Mach number

where U is the free stream velocity, c is the speed of sound

$M_{max} = M_{max}(\alpha_{tip})$ is the maximum Mach number in the vicinity of the tip vortex

where α_{tip} is the angle of attack of the tip

D_h is the directivity

r_e is the retarded observer distance

$l = l(\alpha_{tip})$ is the spanwise extent of the separation zone and depends on whether tip edge is rounded or sharp

$St'' = fl/U_{max}$ is the Strouhal number

where U_{max} is the maximum velocity in the vicinity of the tip vortex

f is the frequency

3.5.3 Noise Reduction

Methods of reducing tip noise are mainly based on a tip shape that reduces the interaction of the turbulent vortex core with the edges of the aerofoil. In a wind tunnel investigation into blade tip modifications [8] three different tip shapes were studied – a reference tip, an ogee, and a shark tip (see figure 1.3.6).

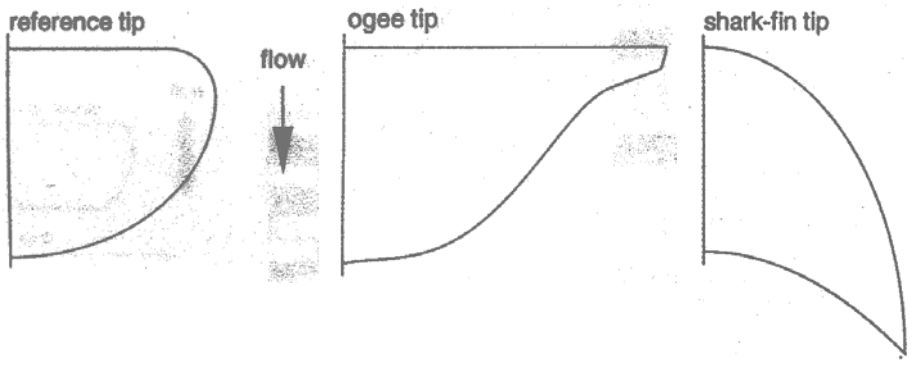

Figure 1.3.6 – Tip Shapes [8]

It was found that the reference tip was 1-2 dB quieter than the ogee and 1-5 dB quieter than the shark tip. Jakobsen and Andersen [27] tested the effects of using an elliptical rounded tip against those of a square tip on an actual wind turbine. It was found that the rounded tip was slightly quieter than square one, but conclusive results were not drawn. In another test by Klug [28], several other tip shapes were investigated with results as shown below in figure 1.3.7.

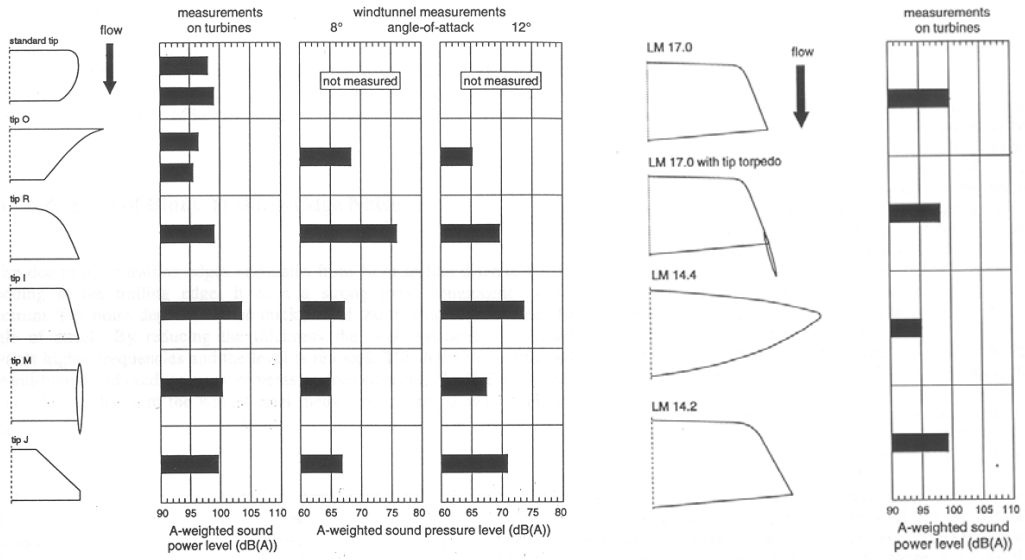

Figure 1.3.7 – Results of Tip Shape Experiments [28]

As can be seen from the above results, reductions of up to 8 dB were achieved by varying the tip shape.

3.6 Trailing Edge Bluntness Vortex Shedding Noise

3.6.1 Mechanisms

Vortex shedding from a blunt trailing edge causes a fluctuating surface pressure differential across the trailing edge – see figure 1.3.8 below. This results in the radiation of tonal noise at the trailing edge.

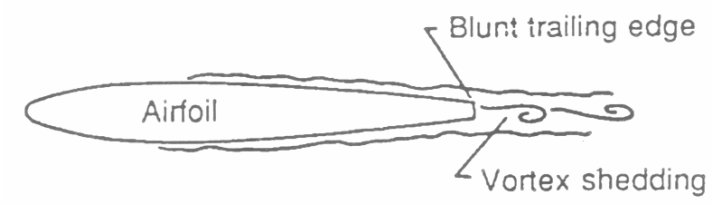

Figure 1.3.8 – Trailing Edge Bluntness Vortex Shedding Noise Generation [19]

3.6.2 Noise Prediction

Howe [26] discusses the theory of blunt trailing edge noise. Other models such as that of Grosveld [20] build on this theory. Fuglsang and Madsen [19] found the model developed by Brooks, Pope and Marcolini [11] to be accurate. The basic model is shown below –

$$\left(L_P\right)_{TEB-VS} = 10\log\left(\frac{hM^{5.5}L\overline{D}_h}{r_e^2}\right) + G_4\left(\frac{h}{\delta^*_{avg}}, \Psi\right) + G_5\left(\frac{h}{\delta^*_{avg}}, \Psi, \frac{St'''}{St'''_{peak}}\right) \qquad (1\text{-}15)$$

where

$(L_p)_{TEB\text{-}VS}$ is the sound pressure level due to TEB-VS noise

h is the trailing edge thickness

$M = U/c$ is the Mach number

where U is the free stream velocity, c is the speed of sound

L is the length of the span

D_h is the directivity

r_e is the retarded observer distance

δ^*_{avg} is the average displacement thickness of the boundary layer for the suction and pressure sides

Ψ is the solid angle between the sloping surfaces upstream of the trailing edge

St''' = fh/U is the Strouhal number

where f is the frequency

St'''_{peak} is the peak Strouhal number

3.6.3 Noise Reduction

Sharpening the trailing edge is the best method of reducing blunt trailing edge noise [51]. Reducing the thickness of the trailing edge has the effect of shifting the peak frequency to higher frequencies and lowering its level. According to Howe's theory , it should be possible to achieve reductions of up to 4 dB at higher frequencies by bevelling the trailing edge. An investigation by Braun et al. [8] seemed to verify this. Blake [6] investigated the effects of trailing edge shape on the generation of aero-acoustic noise. It was found that the relative amplitude of tones in the noise was greatly influenced by the shape of the trailing edge. Some of Blake's results are shown below in figure 1.3.9.

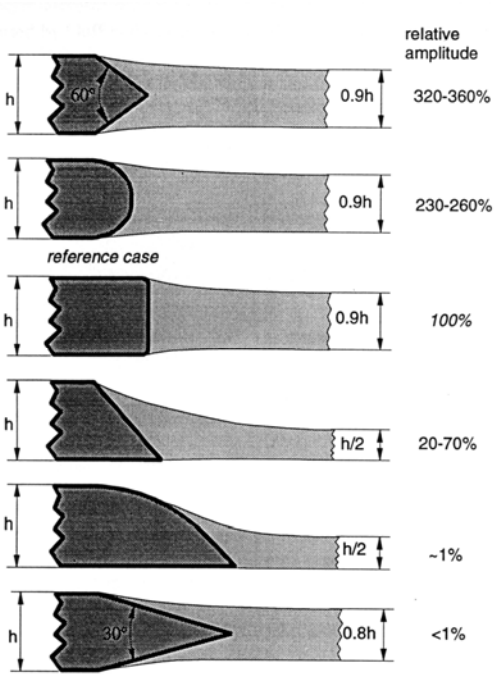

Figure 1.3.9 – Trailing Edge Noise Comparison [51]

3.7 Turbulent Inflow Noise

3.7.1 Mechanisms

Turbulence in the natural wind causes unsteady pressures on the wind turbine blades, leading to the radiation of noise – however the exact mechanisms behind inflow turbulence noise are not yet fully understood [51].

If the scale of the atmospheric turbulence is large in comparison to the blade chord, the blade will respond with low frequency noise, and conversely if the scale of the atmospheric turbulence is small in comparison to the blade cord, the blade will respond with high frequency noise.

At high power levels or high wind speeds inflow turbulence is normally the largest contributor to the overall noise of the wind turbine [37].

3.7.2 Noise Prediction

For high frequency inflow turbulence noise, Lowson [37] and Fuglsang and Madsen [19] both used a model based on theory by Amiet [4] for an infinitely thin flat plate. The model is presented below in equation 1-16 –

$$\left(L_P\right)_{INFLOW-H} = 10\log\left(\rho_0^2 c_0^2 l \,{}^{d}\!/_{r_e^2}\, M^3 u^2 I^2 K^3 \left(1+K^2\right)^{-7/3}\right) + 58.4 \qquad (1\text{-}16)$$

where

$(L_P)_{INFLOW-H}$ is the high frequency sound pressure level due to inflow turbulence

ρ_0 is the air density

c_0 is the speed of sound

l is the overall scale of the turbulence

d is half the length of the span of the aerofoil

r_e is the retarded observer distance

$M = U/c$ is the Mach number

where U is the free stream velocity, c is the speed of sound

u is the mean wind speed

I is the turbulence intensity

$K = \pi fc/U$ is the wave number

where f is the frequency

Another well known model for inflow turbulence noise is that of Grosveld [20] – as with the model based on Amiet's theory, this model is of semi empirical form.

For low frequency inflow turbulence noise the blade can be regarded as acoustically compact. This simplifies the computation of the noise significantly because it can be modelled as an acoustic point dipole with strength being equal to the net force on the blade [51]. However Amiet [4] developed the following expression which uses a the high frequency prediction method with a low frequency correction factor to predict the low frequency turbulent inflow noise -

$$\left(L_P\right)_{INFLOW-L} = \left(L_P\right)_{INFLOW-H} + 10\log\left(\frac{LFC}{1+LFC}\right) \tag{1-17}$$

where

$(L_P)_{INFLOW-L}$ is the low frequency sound pressure level due to inflow turbulence

$(L_P)_{INFLOW-H}$ is the high frequency sound pressure level due to inflow turbulence

$LFC = 10S^2MK^2\beta^{-2}$ is the low frequency correction factor

where $S^2 = \left[\frac{2\pi K}{\beta^2} + \left(1 + 2.4\frac{K}{\beta^2}\right)^{-1}\right]^{-1}$ is the compressible Sears function

$\beta^2 = 1\text{-}M^2$

$M = U/c$ is the Mach number

where U is the free stream velocity, c is the speed of sound

$K = \pi fc/U$ is the wave number

where f is the frequency of the wave

3.7.3 Noise Reduction

Inflow turbulence noise is primarily a function of atmospheric boundary layer turbulence, which cannot effectively be influenced to control the noise radiation. Indications are that the nose radius of the aerofoil has some bearing on the amount of inflow turbulence noise produced, however the exact geometric details of the blade that affect inflow turbulence noise have not yet been investigated in depth.

4. Noise Propagation

4.1 Overview

The propagation of noise from a wind turbine to surrounding areas is a complex issue. Whilst a simple geometrical spreading model forms the basis of many prediction methods, a number of factors can cause the actual sound pressure level observed to deviate from what would be calculated simply assuming geometrical spreading alone. Important factors include terrain and ground effects, atmospheric absorption and meteorological conditions.

This section describes in more detail the factors affecting the propagation of sound outdoors and examines the human perception of noise. The section finishes with a discussion of the various models available for predicting the noise propagation from a wind turbine.

4.2 Terrain and Ground Effects

A receiver may hear the sound of a source from both a direct ray, and a ground reflected ray (as shown in figure 1.4.1). In this way the actual sound pressure at the receiver could be doubled compared with what would be expected from only the direct ray.

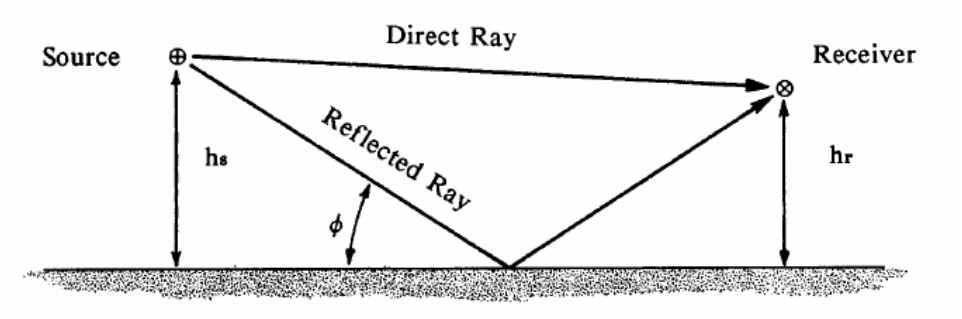

Figure 1.4.1 – Reflection of Sound from Level Ground [31]

Ground attenuation is a result of the absorption and scattering effects of the ground plane. Furthermore, interference between the incident and reflected waves can produce additional attenuation of the sound [41].

The important parameter in determining the attenuation due to the ground is the ground impedance. Ground impedance can be estimated by assuming the ground to be a fibrous absorbent material and calculating the impedance from its flow resistivity as outlined in the flow resistivity model developed by Delany and Bazley [14]. Surfaces such as moss or snow that have a low flow resistivity will have a higher impedance than surfaces with a high flow resistivity such as compacted soil or asphalt.

Vegetation and other terrain features can provide further attenuation. Roots from plants have the effect of increasing the attenuation due to ground absorption since their presence in the ground effectively increases the porosity of the ground. Significant attenuation of higher frequencies due to scattering, occurs where the dimensions of plant leaves become comparable to that of the wavelength of the sound [42].

Where foliage is very dense or other terrain features present significant obstructions to the path of the sound wave, screening effects may also be present. If an obstacle blocks the line of sight between the source and receiver there will be an area behind the obstacle where the sound level is lower than the surrounding area. At high frequencies the sound wave passes the obstacle with only minimal diffraction, which creates a 'shadow zone' with near zero sound behind the obstacle (see figure 1.4.2a below). At wavelengths (λ) comparable to the size of the obstacle (l), the wave diffracts more around the obstacle,

reducing the size of the shadow zone (figure 1.4.2b). For wavelengths much greater than the size, the obstacle becomes insignificant in comparison to the size of the wave and no shadow zone occurs.

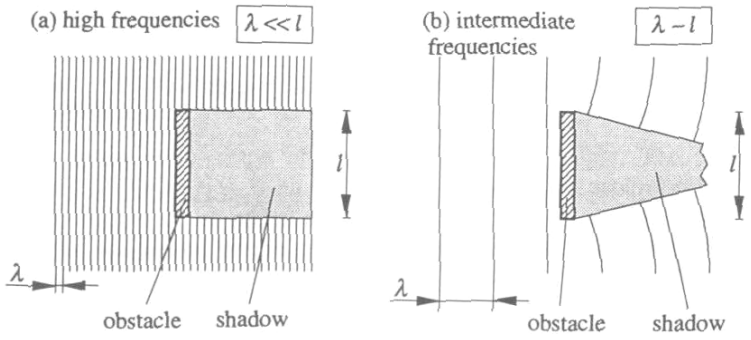

Figure 1.4.2 – Diffraction Around a Barrier [51]

4.3 Atmospheric Absorption

For distances less than approximately 200 metres the effect of atmospheric conditions is usually negligible. However as the sound propagates over larger distances, atmospheric absorption can have a much more significant effect [52].

Atmospheric attenuation is caused by air molecules absorbing energy from the sound wave. The absorption is related to the shear viscosity and thermal conductivity of the air along with its mass and thermal diffusion properties. Additional absorption results from rotational and vibrational relaxation of oxygen and nitrogen molecules in the air [42]. This relationship results in the atmospheric absorption being primarily a function of relative humidity but also of temperature and pressure. The general trend observed is for atmospheric absorption to decrease with increasing temperature and humidity [38].

Various models exist to predict atmospheric absorption. Most are theoretically based but with empirical correction factors included. A widely used example is ISO 9613-1 [1]. This method predicts the attenuation coefficients for pure tones from 50 Hz – 10 kHz and is generally regarded as being of acceptable accuracy [41, 44, 48].

It has been observed both experimentally and theoretically [42] that the attenuation due to atmospheric absorption is most predominant at high frequencies.

4.4 Meteorological Effects

Metrological effects, particularly wind and temperature, can play a major role in the way in which sound propagates.

4.4.1 Temperature Effects

The speed of sound in air is mainly dependent on temperature and increases with increasing temperature. In a normal atmosphere, the air temperature decreases with increasing height. The change in temperature and hence change in the speed of the sound with height causes the wave to refract as it propagates.

If a point source is placed above the ground under normal atmospheric conditions the refraction of the sound wave can cause a shadow zone to be created on the ground. Conversely where a temperature inversion is present (i.e. increasing temperature with increasing height - as is often found at night) the sound wave will refract in the opposite direction causing a concentration of sound on the ground. The effect of the atmospheric temperature profile is demonstrated in figure 1.4.3 below with the sound shown as rays for clarity.

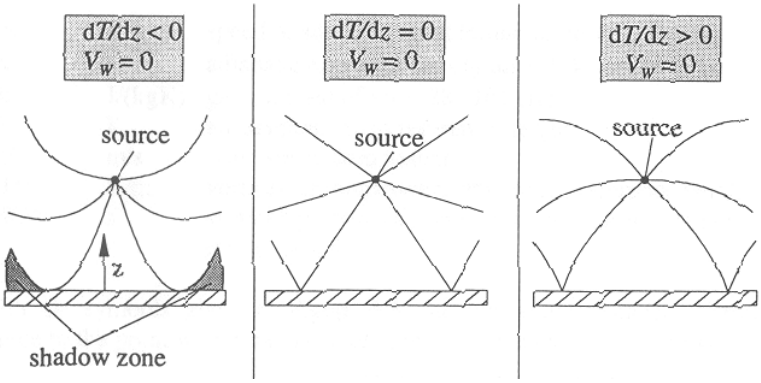

T = Temperature, z = Height, V_w = Windspeed

Figure 1.4.3 – Effect of Atmospheric Temperature Profile on Sound Propagation [51]

4.4.2 Wind Effects

With a wind blowing, the velocity of the sound from a source is superimposed onto the velocity of the wind. Since the velocity of the wind is lower near the ground due to viscous effects, the sound wave refracts as it propagates.

The effect of the wind velocity profile is to cause the sound rays to curve upwards upwind of the source, and downwards downwind of it, as shown in figure 1.4.4 below.

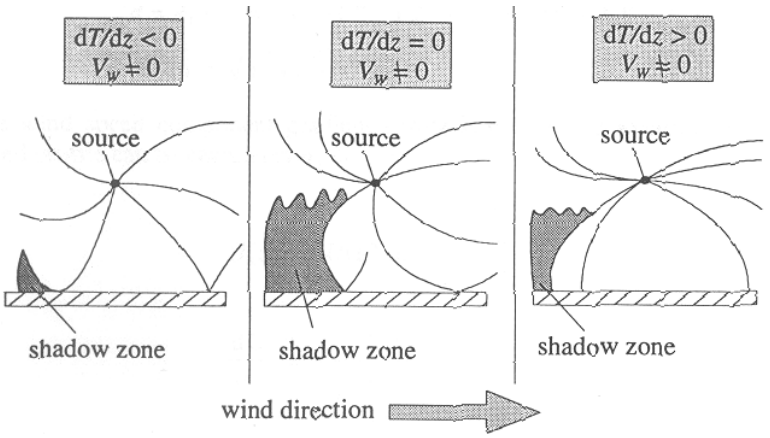

T = Temperature, z = Height, V_w = Windspeed

Figure 1.4.4 – Effect of Wind and Temperature Profile on Sound Propagation [51]

As can be seen in figure 1.4.4, the refraction of the sound waves produces a shadow zone upwind of the source. Under the right conditions the sound attenuation in this zone can be up to 30dB [41], however turbulent velocity fluctuations that are normally present in the atmosphere mean that the exact position and attenuation observed of the shadow zone constantly varies.

4.5 Human Perception of Noise

Although the noise from a wind turbine may propagate to surrounding areas, the way in which the sound is actually interpreted is a function of the response of the human ear, the background noise level, the tonality of the sound, and of a number of psychological factors.

4.5.1 Response of the Human Ear

The human ear perceives loudness as a subjective response to the amplitude of sound. It is not linearly related to either sound pressure, sound pressure level (SPL) or sound power level (SWL). Doubling the sound power (Watts) results in a 3 dB increase in sound pressure level, but does not noticeably increase the loudness of the sound. An increase in SPL of approximately 5 dB is required for the ear to notice a clear increase in loudness. To double the perceived loudness an increase in SPL of approximately 10 dB is required [30]. This implies that to halve the perceived loudness, the sound energy must be decreased by 90% - which is very difficult to achieve in practice.

At a given sound pressure level, the ear does not perceive all frequencies to be of equal loudness. The normal hearing range of the human ear is 20 Hz – 20 kHz, while the ear is most sensitive in the 3 – 4 kHz region. Figure 1.4.5 shows the contours of equal loudness that were determined by Robinson and Dadson [47]. The contours were developed by asking listeners to adjust the volume of single pure tones of various frequencies so that they sounded as loud as a 1000 Hz reference tone.

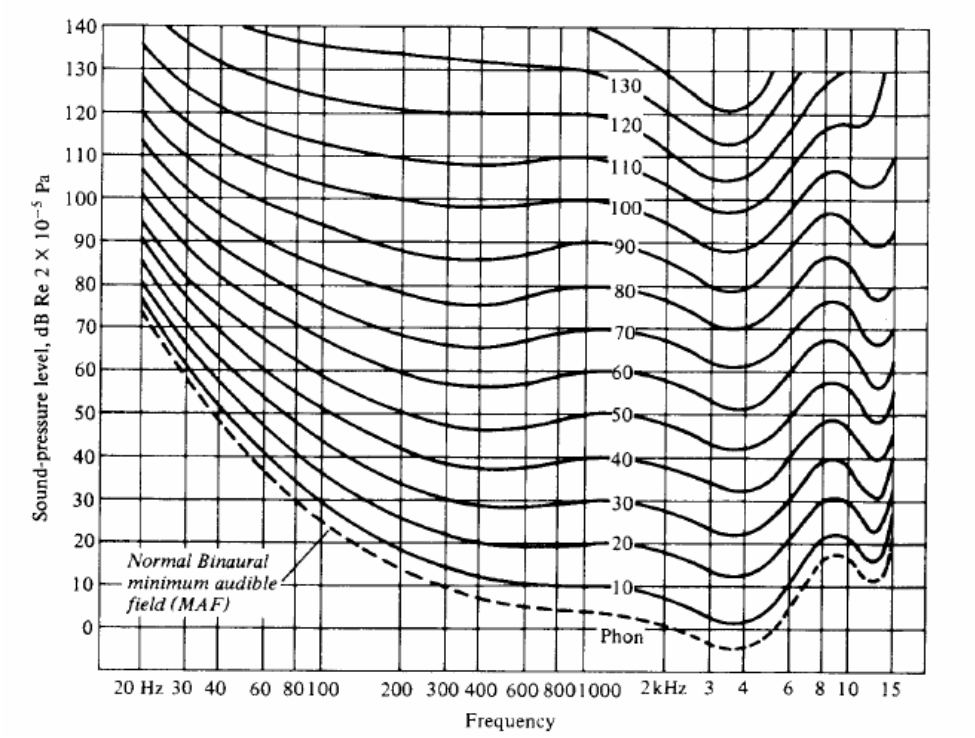

Figure 1.4.5 – Free Field Loudness Contours for Pure Tones [47]

4.5.2 Noisiness and Annoyance

Noise is by definition, unwanted sound. While loudness plays a part in the noisiness of a sound, a number of other factors also contribute. Lamancusa [30] identifies five physical aspects of sound that contribute to noisiness and annoyance. These are –

1.) Spectrum Content and Level

A louder noise is likely to be more annoying than a quieter one [23].

2.) Spectrum Complexity and Existence of Pure Tones

Broadband sound is generally less annoying than sounds that contain pure tones [23].

3.) Time Duration

A noise that is short in duration will be less annoying than one that is ongoing - except perhaps in the case where the noise is repetitive [23].

4.) Amplitude and Frequency of Level Fluctuations

Fluctuations in noise level have been found to be more annoying than noise of a constant level [23].

5.) *Rise Time of Impulsive Sounds*

Sudden noises are likely to startle the receiver and hence are often more annoying than noises with a slower rise time [30].

The actual annoyance caused by a noise, is often a function of both the nature of the noise itself and a number of physiological factors. Studies conducted in Sweden on the impacts of wind power [22] [40] found a correlation between the general attitude of a person towards wind power and their level of annoyance. For example, a shareholder in a turbine may find the noise from it reassuring rather than annoying, whereas a summer resident who has gone to the countryside seeking peace and quiet would probably find it more of a disturbance.

Pederson's study [40] found that the most annoying noise heard from wind turbines was a swishing noise, followed by whistling and then pulsating and throbbing noises. It was also observed that the percentage of people annoyed increased as the noise levels increased.

4.5.3 Noise Perceived from Wind Turbine Sites

Wind and terrain shape play a major role in the way noise from a wind turbine is interpreted by the human ear. Noise from a wind turbine can often be masked by background and vegetation noise, or by wind noise (pseudo-noise caused by turbulent pressure fluctuations rather than actual sound waves). Fégeant [17] provides a measure of detectability of the noise called the detectability index, which is based on the signal to noise ratio.

Conversely, the noise apparent to a listener could actually be increased under certain circumstances. For example in the situation where the wind turbine is on a hill and the receptor site is somewhere at the base of the hill screened from the wind, the wind speed on top of the hill is likely to be 1.5 – 2 times the wind speed at the receptor site. This would reduce the background noise at the receptor site, and the wind turbine noise would thus appear to be more prominent [50].

4.6 Prediction Methods

Several validated methods exist for predicting the propagation of noise from a wind turbine to the surrounding area. These methods range from simple empirical estimations to advanced numerical solutions and achieve varying degrees of accuracy. A number of the more commonly used methods are described briefly below. There are various software packages available for prediction of noise propagation from wind turbines, however these are not discussed here as many of them are based on one or more of the models outlined in this section.

4.6.1 CONCAWE Method [38]

The CONCAWE method was originally developed for use predicting the propagation of noise from petroleum and petrochemical plants. A semi-empirical model is used as follows –

$$L_p = L_w + D - \Sigma K \qquad (1\text{-}18)$$

Where L_p is the sound pressure level at a given distance from the source [dB]

L_w is the sound power level of the source [dB]

D is the directivity index [dB]

K_n are correction factors [dB]

The CONCAWE method includes correction factors for geometrical spreading, atmospheric absorption (calculated from tables of experimental data), ground attenuation, meteorological correction (weather type classified into one of six categories), source/receiver height correction, barrier attenuation, and plant screening.

A statistical analysis carried out in the CONCAWE report [38] found that the method could calculate the sound pressure level with 95% confidence to within 7 dB(A) for most situations – however comparison with experimental data showed it to be considerably more accurate than this.

4.6.2 ISO 9613–1 [1], ISO 9613–2 [2]

This standardised method of calculating sound propagation is widely used and of reasonable accuracy under certain conditions. Sound pressure levels at a given distance from the source are calculated through a series of equations that take into account geometrical divergence, atmospheric absorption, ground effects, wind speed and direction, screening, and reflections.

The accuracy of the model is quoted as 1-3 dB at distances up to 1000m from the source. However, the quoted accuracy is for downwind propagation over flat terrain with a wind speed of 1-5 m/s – outside of this situation the accuracy is not stated. Given that the wind speeds in areas where wind turbines are situated are likely to be higher than 1-5 m/s and the terrain often hilly, this model may not be reliable when applied to wind turbine noise.

4.6.4 NORD2000 [44], [45], [46]

This is probably the most comprehensive model currently available for the calculation of noise propagation over complex terrain. The model is based around the following equation –

$$L_R = L_W + \Delta L_d + \Delta l_\alpha + \Delta L_t + \Delta L_s + \Delta L_r \qquad (1\text{-}19)$$

where

L_R is the sound pressure level at the receiver [dB]

L_W is the sound power level of the source within the considered frequency band [dB]

ΔL_d is the propagation effect of spherical divergence [dB]

Δl_α is the propagation effect of air absorption [dB]

ΔL_t is the propagation effect of the terrain (ground and barriers) [dB]

ΔL_s is the propagation effect of scattering zones [dB]

ΔL_r is the propagation effect of obstacle dimensions and surface properties when calculating a contribution from sound reflected by an obstacle [dB]

In the model, the attenuation due to atmospheric absorption is calculated as in ISO 9613-1. A large portion of the model is dedicated to terrain effects. These are handled by approximating the ground surface and barriers as a series of flat segments, then applying calculations using Fresnel zones (as investigated by Hothersall and Harriot [24]). Ground impedance is divided into a series of groups based on flow resistivity of the ground. Part 2 of the model [45] describes modifications to the basic method to account for refraction in the atmosphere due to meteorological effects (temperature and wind profiles).

The model has been validated to be within ±2 dB for distances up to 200m over complex terrain and is claimed to be 'acceptably' accurate up to 3000m.

4.6.6 Numerical Solutions

Various propagation models can be found in the literature, which are based on either the numerical solution of the acoustic wave equation or the numerical solution of the linearized Euler equations (for example [5], [7], [15]). The acoustic wave equation algorithms generally use either a ray tracing method, the parabolic wave equation or a Hankel transform of the Helmholtz equation.

Most of the numerical propagation techniques are capable of producing models of high accuracy when correctly applied, however they do have some limitations. For example, models based on the parabolic equation require the effects of wind and temperature gradients to be combined into one parameter called vertical sound speed gradient, which leads to differences from the actual situation. Another example is

that of ray tracing methods, which require a significant approximation to be made when considering the diffraction effects of screens. Instead of the wave equation, the linearized Euler equations are sometimes used to compute sound propagation, because they are not restricted to homogeneous media and can handle refraction and reflection of the sound waves. The major drawback of using numerical techniques however is that they are computationally expensive and hence usually only practical for modelling simple situations or in circumstances where a high level of accuracy is absolutely necessary.

4.6.7 NZS 6808 [9]

Whilst not widely used internationally, it was considered appropriate to make mention of the New Zealand standard for "The Assessment and Measurement of Sound from Wind Turbine Generators". The prediction method in this standard utilises the simple semi-empirical propagation model show below.

$$L_p = L_w - 10\log(2\pi R^2) - \Delta L_a \qquad (1\text{-}20)$$

Where L_p is the sound pressure level at distance R from the source [dB(A)]

L_w is the sound power level of the source [dB(A)]

R is the distance between the source and receiver [m]

$\Delta L_a = \alpha R$ where α is the attenuation of sound due to air absorption as defined in ISO 9613-1

This model only takes into account geometrical divergence and atmospheric absorption in its calculation, and hence will not be particularly accurate in many situations.

5. Noise Measurement Techniques

5.1 Overview

The measurement of acoustic emissions from wind turbines is often complicated by unsteady levels of wind and background noise. To counter this, a variety of specialist techniques for use in wind turbine noise measurements have been developed. This section contains a brief review of the most widely used techniques.

5.2 Microphone Set-up

The primary objective in setting up the microphone for acoustic measurements of a wind turbine is to avoid the corruption of measurements by wind induced pseudo-noise and hence optimise the signal to noise ratio. Several set-ups are used, each with its own advantages and disadvantages as described below.

5.2.1 Ground Board

Ground boards (as shown below in figure 1.5.1) are often used in the determination of the total sound power level of a wind turbine or for the measurement of sound pressure levels at a given distance from the turbine.

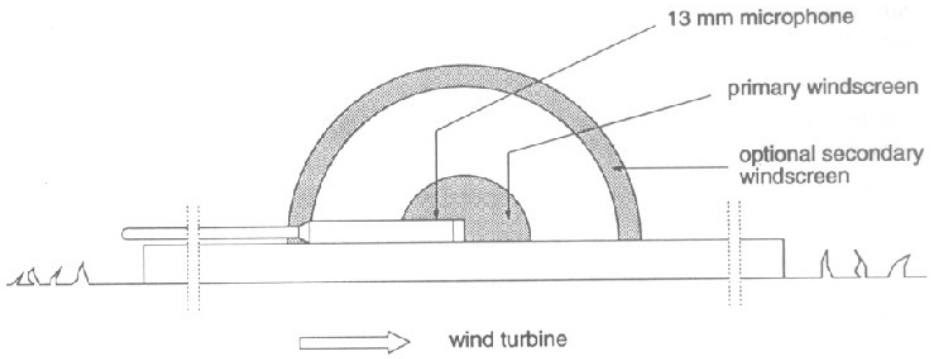

Figure 1.5.1 – Ground Board (Vertical Cut) [51]

Using the ground board set-up, the microphone is placed at a specified position on an acoustically hard board. Recommendations for board size and microphone position can be found in [3].

The main advantage of this technique is that it allows measurements to be made that are independent of the reflective and absorptive properties of the ground surrounding the test site. Another advantage of this technique is that placing the microphone near to the ground reduces the wind noise, since the wind velocity increases with distance from the ground.

5.2.2 Vertical Measuring Boards

Mounting the microphone on a vertical measuring board as shown below in figure 1.5.2 is another technique used to improve signal to noise ratio.

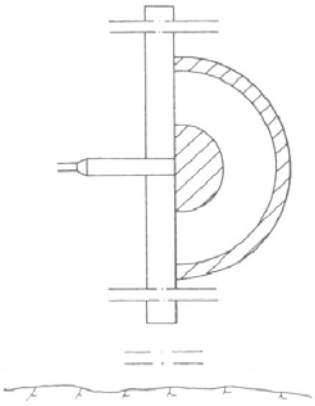

Figure 1.5.2 – Vertical Measuring Board (Vertical Cut) [34]

In a study by Fegeant [16], it was found that the board caused a pressure doubling (3 dB increase) in front of the microphone while reducing the local wind speed (and hence wind induced pseudo-noise). In addition to these effects, the board acted as a barrier to background noise from behind the microphone, further improving the signal to noise ratio.

Recommended dimensions and microphone positions for vertical measurement boards can be found in [34].

5.2.3 Secondary Windscreens

Placing a secondary windscreen over the microphone in addition to a primary windscreen is regarded as one of the most practical methods of reducing wind induced noise [49]. A study conducted into the performance of windscreens of various constructions [49] found that the best windscreens were able to reduce wind noise by 8 – 13 dB and made the interesting observation that the anti-bird spikes used on some secondary windscreens can actually increase the wind induced noise due to a whistling sound produced by the spikes.

5.2.4 Other Set-ups

Two Microphone Cross Correlation [29]

By placing two microphones some distance apart, the noise signals from the two microphones can be analysed using a correlation technique to remove wind induced noise components, which are uncorrelated in the two signals.

Acoustic Parabola [51]

An acoustic parabola is a structure placed around the microphone to focus sound waves onto the microphone. The amount of amplification of the signal is largely dependent on the shape of the parabola and the device must therefore be calibrated before initial use.

The acoustic parabola finds most use in wind turbine noise measurement where specific noise sources are required to be identified during operation – for example, measuring the contribution of selected sections of blade to the overall blade noise of the turbine.

The main limitations of the acoustic parabola are that it is usually bulky (typically 1.8m diameter) and tends to have low resolution for low frequencies (below 500 Hz for a 1.8m diameter parabola).

5.3 Measurement Location

Recommendations have been made of the best measurement locations for use in determining the directivity and sound power level of noise from wind turbines. An example is shown in figure 1.5.3.

Most guidelines recommend the use of more measurement points downwind of the turbine since the noise propagation upwind of the turbine is generally less due to atmospheric refraction. The IEA Recommended Practices for Wind Turbine Measurements [34], [35] and IEC 61400-11 [3] contain further details on the locations where measurements should be made.

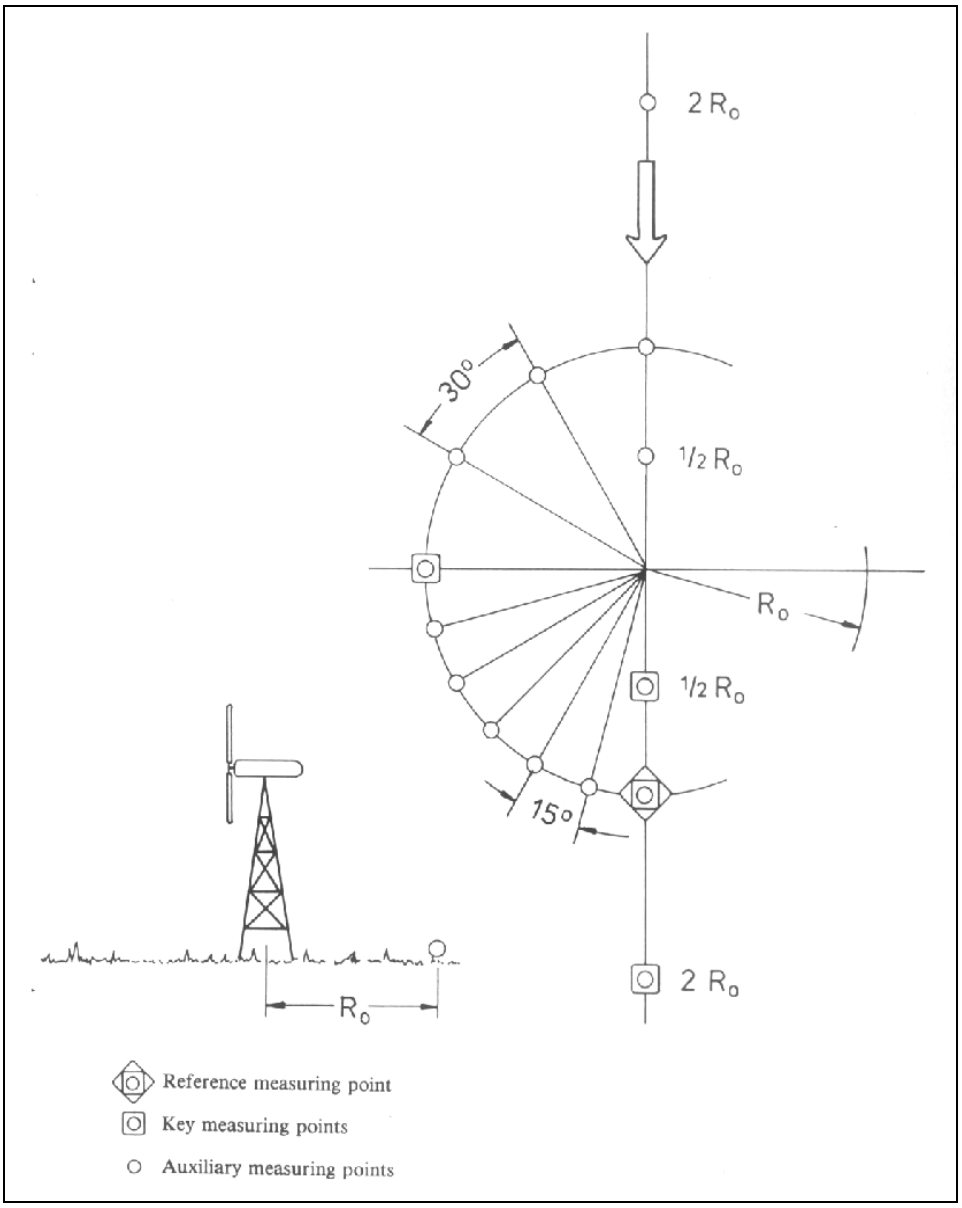

Figure 1.5.3 – Recommended Measurement Locations [35]

5.4 Measurement Duration

In order to obtain a noise level measurement of suitable accuracy, the IEA Recommended Practices for Wind Turbine Measurements Part 10 [34] states that the L_{eq} should be measured over a 1 - 10 minute interval in which wind speed deviates by less than ±2 m/s from the target wind speed. However, experimental studies by Lowson [36] showed that it would be more appropriate to average the readings over 10 – 30 seconds since conditions such as the wind speed and direction, and the speed of the turbine were much more likely to remain stable over this period than the longer period recommended by the IEA.

6. References

[1] "Acoustics -- Attenuation of sound during propagation outdoors -- Part 1: Calculation of the absorption of sound by the atmosphere," ISO 9613-1, 1993.

[2] "Acoustics -- Attenuation of sound during propagation outdoors -- Part 2: General method of calculation," ISO 9613-2, 1996.

[3] "Wind Turbine Generator Systems - Part 11: Acoustic Noise Measurement Techniques," IEC 61400-11.

[4] Amiet R.K., "Acoustic Radiation from an Airfoil in a Turbulent Stream," *J. Sound and Vib.*, vol. 41, pp. 407 - 420, 1975.

[5] Berengier M. and Gauvreau B., "Calculation of Meteorological Conditions Effects on Outdoor Sound Propagation Using Parabolic Equation," presented at Internoise 2000, Nice, France, 2000.

[6] Blake W. K., *Mechanics of Flow Induced Sound and Vibration, Vol II: Complex Flow -*: ACADEMIC Press Inc., Harcourt Brace Jovanovich, Publishers, 1986.

[7] Blumrich R. and Heimann D., "A Linearized Eulerian Sound Propagation Model for Studies of Complex Meteorological Effects," *J. Acoust. Soc. Am.*, vol. 112, pp. 446 - 455, 2002.

[8] Braun K., Arnold H., et al., "Some Blade Tip Modifications and Their Influence on Aeroacoustics," presented at EWEA Conference, Goteborg, 1996.

[9] Braun K., et al., "Serrated Trailing Egde Noise (STENO)," presented at EWEA Conference, Nice, France, 1999.

[10] Brooks T. and Marcolini M., "Airfoil Tip Vortex Formation," *AIAA Journal*, vol. 24, pp. 246 - 252, 1986.

[11] Brooks T., Pope D., and Marcolini M., "Airfoil Self Noise and Prediction," NASA RP 1218, 1989.

[12] Curle N., "The Influence of Solid Boundaries Upon Aerodynamical Sound.," *Proc. Roy. Soc. London, A231, page 505, 1955.*

[13] Dassen T., Parchen R., et al., "Comparison of Measured and Predicted Airfoil Self-Noise with Application to Wind Turbine Noise Reduction," presented at EWEA Conference, Dublin Castle, Ireland, 1997.

[14] Delany M.E. and Bazley E.N., "Acoustical Properties of Fibrous Absorbent Materials," *Applied Acoustics*, vol. 3, pp. 105 - 117, 1970.

[15] Eketerinaris J. and Kampanis N., "A Numerical Prediction of Acoustic Fields Generated by Wind Turbines," *Systems Analysis Modelling Simulation*, vol. 39, pp. 49 - 73, 2000.

[16] Fegeant O., "Measurements of Noise Immision from Wind Turbines at Receptor Locations: Use of a Vertical Microphone Board to Improve the Signal-To-Noise Ratio," presented at EWEA Conference, Dublin Castle, Ireland, 1997.

[17] Fegeant O., "On the Masking of Wind Turbine Noise by Ambient Noise," presented at EWEA Conference, Nice, France, 1999.

[18] Ffowcs Williams J. and Hall L., "Aerodynamic Sound Generation by Turbulent Flow in the Vicinty of a Scattering Half Plane," *J. Fluid Mech.*, vol. 40, pp. 657 - 670, 1970.

[19] Fuglsang P. and Madsen H., "Implementation and Verification of an Aeroacoustic Noise Prediction Model for Wind Turbines," Risϕ National Laboratory, Roskilde, Denmark Riso-R-867(EN), 1996.

[20] Grosveld F., "Prediction of Broadband Noise from Horizontal Axis Wind Turbines," *J. Propulsion and Power*, vol. 1, pp. 292 - 299, 1985.

[21] Hagg F., van Kuik G., Parchen R., and van der Borg N., "Noise Reduction on a 1MW Size Wind Turbine with a Serrated Trailing Edge," presented at EWEA Conference, Dublin Castle, Ireland, 1997.

[22] Hammarlund K., "The Social Impacts of Wind Power," presented at EWEA Conference, Goteborg, Sweden, 1997.

[23] Hassall J.R. and Zaveri K., *Acoustic Noise Measurements*, 5th ed: Bruel & Kjaer, 1988.

[24] Hothersall D.C. and Harriott J.N.B., "Approximate Models for Sound Propagation Above Multi-Impedance Plane Boundaries," *J. Acoust. Soc. Am.*, vol. 97, pp. 918 - 926, 1995.

[25] Howe M., "Noise Produced by a Sawtooth Trailing Edge," *J. Acoust. Soc. Am.*, vol. 90, pp. 482 - 487, 1991.

[26] Howe M., "A Review of the Theory of Trailing Edge Noise," *J. Sound and Vib.*, vol. 61, pp. 437 - 465, 1978.

[27] Jakobsen J. and Andersen B., "Aerodynamical Noise from Wind Turbines - Experiments with Full Scale Rotors, Change of Pitch, Trailing Edges, and Tip Shapesq," DELTA Acoustics and Vibration AV 590/95, 1995.

[28] Klug H., Osten T., et al., "Aerodynamic Noise from Wind Turbines and Rotor Blade Modification," presented at EWEA Conference, Goteborg, Sweden, 1996.

[29] Kragh J., et al., "Noise Immission from Wind Turbines," National Engineering Laboratory ETSU W/13/00503/REP, 1999.

[30] Lamancusa J.S., "Engineering Noise Control - 3. Human Response to Sound," in *Pennsylvania State University, ME458 Course Notes*, 2000.

[31] Lamancusa J.S., "Engineering Noise Control - 10. Outdoor Sound Propagation," in *Pennsylvania State University, ME458 Course Notes*, 2000.

[32] Lighthill M.J., "On Sound Generated Aerodynamically; I. General Theory," presented at Royal Society of London, 1952.

[33] Lighthill M.J., "On Sound Generated Aerodynamically; II. Turbulence as a Source of Sound," presented at Royal Society of London, 1954.

[34] Ljunggren S., "Recommended Practices for Wind Turbine Testing - 10. Measurement of Noise Immission from Wind Energy at Noise Receptor Locations," IEA 1997.

[35] Ljunggren S., Gustafsson A., Trenka A.,, "Recommended Practices for Wind Turbine Testing - 4. Acoustics. Measurement of Noise from Wind Energy Conversion Systems (WECS)," IEA 1984.

[36] Lowson J., "A New Approach to Wind Turbine Noise Measurement," presented at EWEA Conference, Goteborg, Sweden, 1996.

[37] Lowson M.V. and Lowson J.V., "Systematic Comparison of Prediction and Experiment for Wind Turbine Aerodynamic Noise," ETSU W/13/00363/REP, 1993.

[38] Manning C., "The Propagation of Noise from Petroleum and Petrochemical Complexes to Neighbouring Communities," CONCAWE 4/81, 1981.

[39] Oerlemans S., Schepers J., Guidati G., and Wagner S., "Experimental Demonstration of Wind Turbine Noise Reduction Through Optimised Airfoil Shape and Trailing Edge Serrations," presented at EWEA Conference, Copenhagen, Denmark, 2001.

[40] Pedersen E., Persson Waye K., "The Impact of Wind Turbines in Sweden with Special Reference to Noise Annoyance," presented at EWEA Conference, Copenhagen, Denmark, 2001.

[41] Penton S., Chadder D., Stiebert S., and Sifton V., "The Effect of Meteorology and Terrain on Noise Propagation - Comparison of Five Modelling Methodologies," *Canadian Acoustics*, vol. 30, pp. 30 - 33, 2002.

[42] Piercy J.E., Embleton T.F.W., and Sutherland L.C., "Review of Noise Propagation in the Atmosphere," *J. Acoust. Soc. Am.*, vol. 61, pp. 1403 - 1418, 1977.

[43] Pinder J.N., "Mechanical Noise from Wind Turbines," *Wind Engineering*, vol. 16, pp. 158 - 168, 1992.

[44] Plovsing B. and Kragh J., "Nord2000. Comprehensive Outdoor Sound Propagation Model. Part 1: Propagation in an Atmosphere without Significant Refraction.," Delta Acoustics and Vibration AV 1849/00, 2001.

[45] Plovsing B. and Kragh J., "Nord2000. Comprehensive Outdoor Sound Propagation Model. Part 2: Propagation in an Atmosphere with Refraction," Delta Acoustics and Vibration AV 1851/00, 2001.

[46] Plovsing B., Kragh J., et al., "Nordic Environmental Noise Prediction Methods, Nord2000 Summary Report. General Nordic SOund Propagation Model and Applications in Source Related Prediction Methods," Delta Acoustics and Vibration AV 1719/01, 2002.

[47] Robinson D. and Dadson R., "A Re-determination of Equal Loudness Relations for Pure Tones," *British J. Applied Acoustics*, vol. 7, pp. 166 - 181, 1956.

[48] Sutherland L., "Overview of Outdoor Sound Propagation," presented at Internoise 2000, Nice, France, 2000.

[49] Theofiloyiannakos D., Kragh J., Fragoulis A.,, "Investigation of the Reduction of the Wind Induced Microphone Noise by the Use of Supplementary Wind Screens," presented at EWEA Conference, Dublin Castle, Ireland, 1997.

[50] Theofiloyiannakos D., Zorlos P., Agoris D., "Current Practices for the Prediction and Assessment of the Environmental Impact from Wind Energy Projects in Greece," presented at EWEA Conference, Copenhagen, Denmark, 2001.

[51] Wagner S., Bareiss R., and Guidati G., *Wind Turbine Noise*: Springer, 1996.

[52] Wilson K. and Noble J., "Putting Meteorology into Outdoor Sound Propagation Calculations," presented at Internoise 2000, Nice, France, 2000.

Chapter 2

The Wind Turbine – Description and Acoustic Characterisation

Summary

This project was concerned with the Windflow 500 wind turbine which is a 500 kW two bladed prototype turbine designed by Christchurch based company Windflow Technology Ltd. The prototype turbine was located on a hilltop site at Gebbies Pass, about 35 km south of Christchurch.

The acoustic significance of the turbine's location was due to its proximity to local residential dwellings along with the unique meteorology and topography of the area. The nearest house to the turbine was 527m away however it was considered that the houses in McQueens valley, 1200m – 1400m south of the turbine were the most likely to be affected by noise from the turbine. This was due to the terrain, wind direction and quiet rural background noise levels in the valley combining to produce very little noise masking even with strong winds at the turbine site.

Several features of the turbine's design had significant acoustical issues associated with them. The gearbox and generator were solid mounted to the pallet. This reduced the design and construction costs however it also meant that there was a good path for vibration to travel to the tower and other componentry creating additional radiated noise.

Initial analysis of the noise produced by the wind turbine showed that it was producing a total sound power level of 108 dBA. This agreed well with the predictions that had been made using simple empirical formulas. A more detailed analysis of the noise showed that 8 -12 % of the total noise was radiated by the tower while over 86 % of the total noise was radiated from the blades. Spectral analysis showed a prominent tone at 311 Hz, which originated from the gearbox.

Table of Contents

List of Figures

List of Tables

1. Introduction

This chapter provides information about the wind turbine that was studied in this project. It contains a brief overview of the specifications of the wind turbine, including its location and relevant noise issues.

Later in the chapter the acoustic characteristics of the turbine are analysed in more detail, identifying the significant noise paths and sources along with features of the noise spectrum which would be likely to increase the annoyance factor of the turbine noise.

2. The Windflow 500

2.1 General

The Windflow 500 is a prototype 500 kW wind turbine generator designed and manufactured in New Zealand by Windflow Technology Ltd. The Windflow 500 turbine combines two innovative features which give it a technological advantage in the wind energy industry. These are the torque limiting gearbox (TLG) system of power control and the pitch regulated two-bladed teetering rotor with pitch-teeter coupling.

Through a system of hydraulics, the torque limiting gearbox is used to control the torque applied to the generator input shaft. This system allows the power produced by the generator to be accurately limited. The advantage of this becomes apparent when the situation of a conventionally controlled wind turbine is considered. For a conventionally controlled wind turbine the componentry specified must be rated to cope with short periods operating in overload conditions. This means for example, that a turbine with a nominal design rating of 500 kW might actually need componentry capable of handling 750 or perhaps even 1000 kW. The torque limiting gearbox prevents the overload situations occurring meaning componentry with a lower power rating can be specified than would otherwise be possible – see figure 2.2.1.

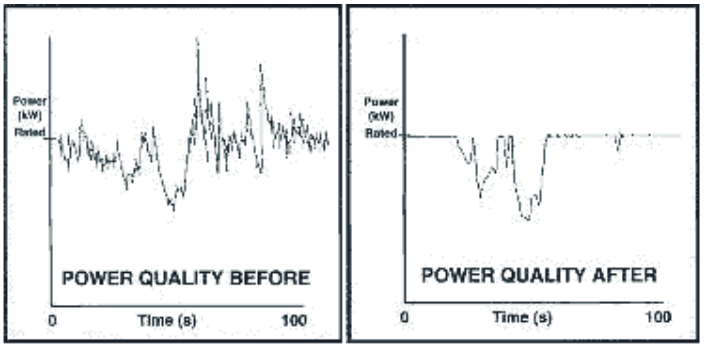

Figure 2.2.1 – Power Quality Before and After Installation of TLG

The pitch regulated, two-bladed teetering rotor allows the rotor speed to be accurately controlled by adjusting the pitch on the blades, while the teeter mechanism allows the blades to rock slightly at the hub (see figure 2.2.2). This reduces the effects of the fatigue loads on the blades and tower that arise from the abrupt change in air pressure which occurs as the blades pass the tower.

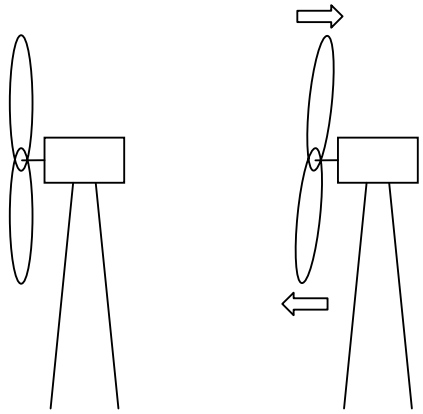

Figure 2.2.2 – Teeter Motion

With the TLG and the pitch regulated two bladed teetering rotor, the Windflow 500 can be specified with lighter componentry and associated structure. This gives the Windflow 500 a considerable cost advantage over turbines of similar size.

2.2 Technical Specifications

2.2.1 General Specifications

A brief list of the technical specifications of the Windflow 500 follows in Table 2.2.1.

Table 2.2.1 – Windflow 500 Technical Specifications

Windflow 500 Technical Specifications	
Blade:	
Make:	Wind Blades Ltd
Material:	Laminated wood/epoxy
Air Brake:	Full-span pitch
Weight:	925 kg
Rotor:	
Number of Blades:	2
Rotor Diameter:	33.2 m
Rotor Speed:	48-50 rpm
Swept Area:	863 m^2
Hub Height:	30 m
Orientation:	Upwind
Regulation:	Full-span pitch
Hub:	Teetering (pitch-coupled)
Weight (Hub and Blades):	4000 kg
Hydraulic System:	
Power Unit:	5 kW gear pump
Yawing:	9 kN.m geared motor
Pitch Actuation:	Linear actuator
Braking:	Fail-safe caliper
Torque Limiting:	3.3 kN.m radial piston motor
Gear Box:	
Type:	Hicks Planetary/parallel TLG
Design:	AH Gears Ltd
No of Stages:	4
Overall Ratio:	1:31.1
Rated Torque:	108 kN.m
Generator:	
Type:	Synchronous
Rated Power:	520 kW
Speed:	1500 rpm
Voltage:	415 V
Frequency:	50 Hz
Tower:	
Type:	Tubular Steel
Height:	28.5 m
Weight:	15000 kg
Controller:	
Make:	Bremca Industries Ltd
Cut in System:	Auto-Synch
Logic System:	PLC

Windflow 500 Technical Specifications (cont'd)	
Performance:	
Low Wind Cut-In:	5.9 m/s
Rated Power At:	13.7 m/s
Maximum Power:	500 kW
High Wind Cut-Out:	30 m/s
Total Weight:	
Nacelle & Rotor:	13,000 kg
Total (lattice tower):	18,500 kg
Total (tubular tower):	25,500 kg
Costs (NZ$):	
Prototype	$2.4m
Production (Estimated)	$675 000

2.2.2 Meteorological Mast

To monitor wind speed and direction at site and allow a comparison to be drawn with the turbine mounted anemometer, a 30m tall meteorological mast was erected 66.4m northeast of the wind turbine on the same level. The mast had calibrated vane anemometers placed at 10m and 30m above ground level.

2.2.3 Acoustic Specifications

There was little evidence within the wind turbine of acoustic considerations. The tower and blades were large undamped hollow structures, and major rotating components such as the gearbox and generator were not in any way vibration isolated from these structures.

An attempt had been made to make the nacelle cladding an effective acoustic enclosure. In order to minimise possible structure-borne noise arising from vibrations transmitted to the cladding by the machinery inside the nacelle, the cladding was mounted to the pallet using flexible mounts. To minimise the airborne noise transmission from the nacelle, several treatments had been applied. The first was the selection of a suitable nacelle cladding material. The cladding was manufactured from fibreglass using a 35mm thick sandwich construction (see figure 2.2.3). The core material used was selected not only for its structural properties but also for its acoustic properties based on a series of sound transmission loss tests that were conducted at the University of Canterbury using different core materials.

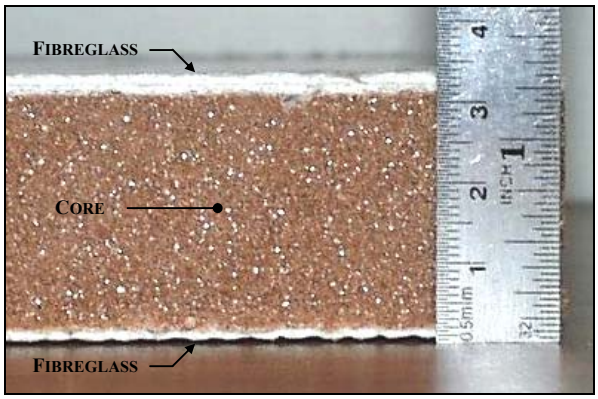

Figure 2.2.3 – Nacelle Cladding Material Cross-Section

To further prevent airborne sound transmission from the nacelle, all hatches, doors, gaps and openings were sealed with either foam-rubber sealing tape or specially manufactured seals. Cooling air for the machinery in the nacelle was drawn up the tower through a louvred door at the tower base instead of directly through a duct in the cladding.

The generator cooling fan exit duct was also acoustically treated. Two 90 degree bends were incorporated into the shape of the duct in order to increase the sound attenuation of the duct as much as possible. In addition to this the duct was partially lined with a sound absorbing material (6/24 Multigrade™ supplied by Latimer Acoustics), while the remainder of the duct (which was subject to water infiltration) was lined with a 30 mm thick water resistant sound absorber (Quash™ manufactured by Dow Industries). The duct exit was on the top surface of the nacelle so as to direct sound from the duct away from receivers on the ground.

2.3 Location

The turbine was located on a hilltop site on private farm land at Gebbies Pass, approximately 35km south of Christchurch. The site was selected for the prototype because of its average annual wind speed of 7 m/s (30m AGL) along with its close proximity to power lines and the short distance to Windflow Technology's Christchurch office.

The location of the site meant that it was close to several residential dwellings - the nearest of which was 527m. Figure 2.2.4 and Table 2.2.2 below show the locations of the houses and their distances from the turbine.

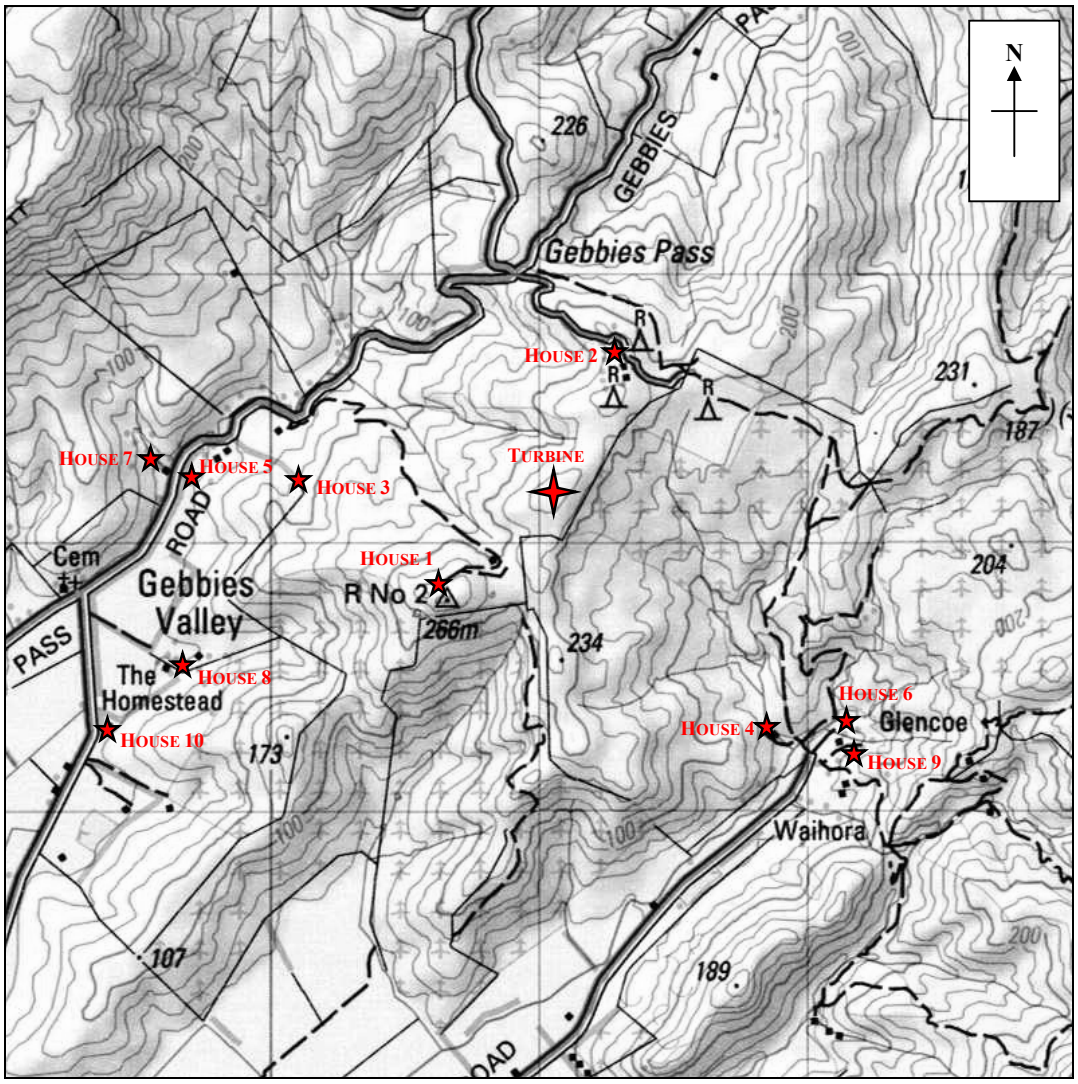

Figure 2.2.4 – House Location Map

Table 2.2.2 – House Location Details

House #	Longitude	Latitude	Distance to Turbine (m)
1	172° 38.14561' E	43° 42.07502' S	527
2	172° 38.66914' E	43° 41.64462' S	551
3	172° 37.73770' E	43° 41.83072' S	966
4	172° 39.07417' E	43° 42.40187' S	1255
5	172° 37.51435' E	43° 41.84080' S	1263
6	172° 39.25701' E	43° 42.35407' S	1393
7	172° 37.32835' E	43° 41.82940' S	1514
8	172° 37.40029' E	43° 42.23465' S	1544
9	172° 39.25966' E	43° 42.51042' S	1572
10	172° 37.23569' E	43° 42.36912' S	1852
Turbine	172° 38.45183' E	43° 41.89776' S	0

While not the closest houses to the turbine, houses 4, 6 and 9 nestled below the turbine in McQueens Valley (Glencoe) were considered to be highly likely to be effected by noise from the turbine. The reasons for this arose mainly from the unique topography and meteorology of the area. Firstly, houses 4, 6, and 9 had direct line of sight to the turbine so there were no barriers in the path of the noise between the turbine and the houses (see figure 2.2.5).

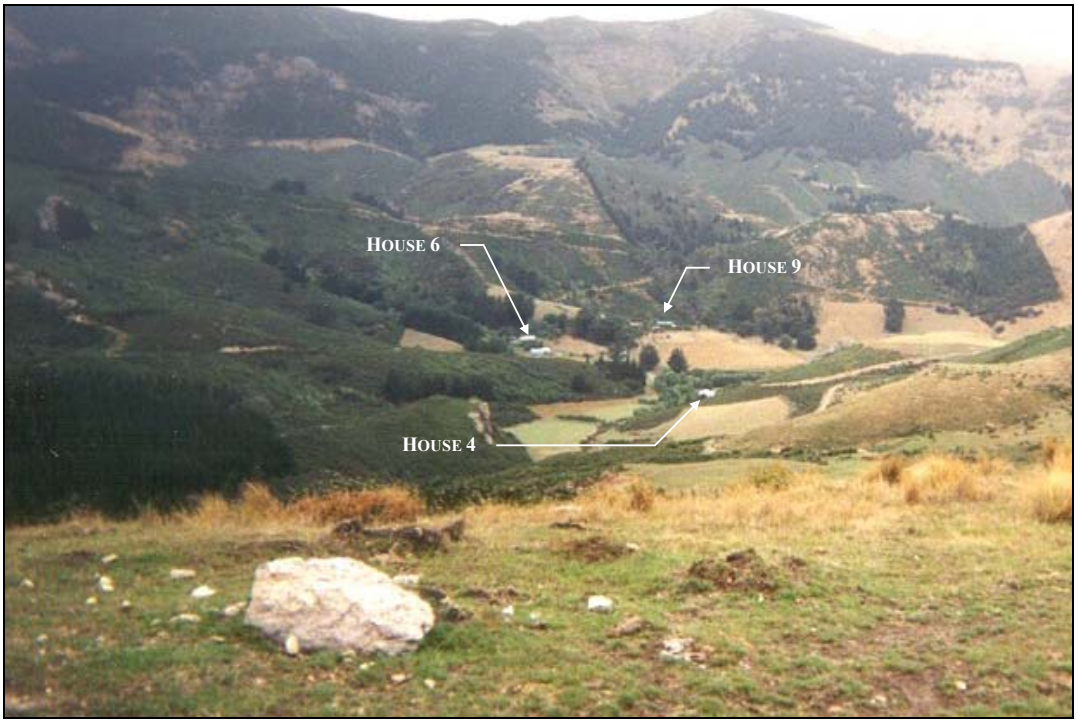

Figure 2.2.5 – View from Turbine Site to McQueens Valley

Secondly, the prevailing wind at the site was from a northerly direction, meaning that the houses in McQueens Valley were approximately downwind of the turbine. The significance of this was that the sound would travel further with the wind than against it, so the noise observed in McQueens Valley would be likely to be greater than that estimated for a no wind situation. Finally, the shape of the terrain was such that the houses in McQueens Valley were often sheltered from the wind, while up at the wind turbine site the turbine could be generating at a high output. The masking effect that would usually be experienced due to wind induced noise was therefore often not present in McQueens Valley. These factors in combination with the rural setting meant that daytime background sound pressure levels were often in the range of 30 – 35 dBA while during the night the sound pressure levels frequently dropped as low as 19 dBA.

3. Acoustic Characteristics

3.1 Sound Power Level

Being a prototype, the expected sound power level of the Windflow 500 was unknown before being built and measured. The following empirical formulas from Wagner et al. [1] were used to predict the sound power level from the turbine –

$$L_{WA} = 10\log_{10} P_{WT} + 50 \tag{2-1}$$

$$L_{WA} = 22\log_{10} D + 72 \tag{2-2}$$

$$L_{WA} = 50\log_{10} V_{Tip} + 10\log_{10} D - 4 \tag{2-3}$$

where

L_{WA} is the predicted A-weighted sound power level (dBA)

P_{WT} is the rated power of the wind turbine (W)

D is the rotor diameter of the turbine (m)

V_{Tip} is the tip velocity of the turbine rotor (m/s)

Given the 500 kW power rating of the Windflow 500, the 33.2 m rotor diameter and the 83.44 m/s rotor tip velocity, the above equations give the results shown below in table 2.3.1.

Table 2.3.1 – Empirically Predicted Sound Power Levels of Windflow 500

Equation	LWA (dBA)
1	107.0
2	105.5
3	107.3

Once the wind turbine was built, its sound power level was calculated from sound pressure levels that were measured at various points around the turbine with the turbine generating in 10 – 12 m/s wind (above this wind speed the noise from the turbine was found not to increase significantly). For each calculation, hemispherical propagation from a point source was assumed and an air absorption coefficient of 0.004 dBA/m was used. Ground absorption, terrain effects and meteorological effects were neglected. This allowed equation 2-4 below to be used -

$$L_{WA} = L_{PA} + 10\log_{10}(2\pi R) + \alpha R \qquad (2\text{-}4)$$

where

L_{WA} is the calculated A-weighted sound power level (dBA)

L_{PA} is the measured A-weighted sound pressure level at a distance from the turbine (dBA)

R is the distance from the turbine at which L_{PA} is measured (m)

α is the air absorption coefficient (= 0.004 dBA/m)

Table 2.3.2 shows the measured sound pressure levels and the sound power levels that were calculated –

Table 2.3.2 – Sound Power Levels of Windflow 500 Calculated from Measured SPLs

R (m)	L_{PA} (dBA)	L_{WA} (dBA)
30	66.3	103.9
66	67.0	111.6
90	61.0	108.4
100	57.0	105.4
320	49.9	109.3
1400	31.2	107.7
Average		107.7

The results show that the sound power level produced by the turbine was approximately 107.7 dBA. Near to the turbine the assumption of propagation from a point source does not hold. The sound power levels calculated from the SPL measurements near the turbine (30m, 66m) are therefore likely to be less accurate than those further away. If the measurements from 30m and 66m are excluded from the averaging, the average calculated sound power level remains at 107.7 dBA. Given the level of repeatability of the SPL measurements and the consequent variability in the calculated sound power levels it was estimated that the average calculated sound power level was accurate to ±2 dBA.

These results agreed well with what was predicted using the simple empirical prediction formulas, which provided confidence that the levels calculated from the SPLs around the turbine were of reasonable accuracy.

3.2 Identification of Main Noise Sources and Paths

3.2.1 Method

In order to establish the most important sources and paths of noise from the turbine, sound intensity measurements were conducted on the major exterior components of the wind turbine. The contribution of each component to the total sound power level was therefore able to be determined. The intensity measurements were made using a Bruel and Kjaer Type 2260 Investigator with a Type 3595 sound intensity probe kit. The directionality of the Bruel and Kjaer intensity probe allowed measurements to be made from each exterior component without being significantly influenced by noise radiated from the other components.

Measurements were made with the turbine generating in a relatively constant wind of 10 – 12 m/s. At this wind speed the noise from the wind turbine was found to be approximately constant and near its maximum level.

The intensity measurements were performed by sweeping the probe at constant speed (see figure 2.3.1) just above the surface of interest in order to obtain an average value of intensity from the surface.

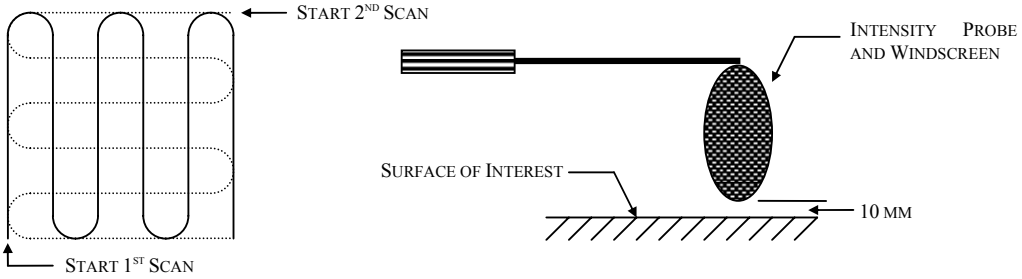

Figure 2.3.1 – Probe Sweep Path

The main exterior components studied were the nacelle, generator duct exit, cooler housing (located directly under the nacelle), tower and blades. In the case of the blade noise measurement the probe was held stationary while the blades rotated.

From the intensity measurements, the sound power level was calculated using equation 2-5.

$$L_{WA} = 10\log_{10}\left[\left(10^{L_{IA}/10}\right) \times A\right] \qquad (2\text{-}5)$$

where

L_{WA} is the A-weighted sound power level (dBA)

L_{IA} is the A-weighted measured sound intensity level (dBA)

A is the surface area of the component measured (m^2)

Given the difficulty of taking accurate sound intensity measurements from the moving blades two methods were used to calculate the sound power emitted from the blades. These were as follows –

Method 1 – Back Calculation

Sound power contributions from each of the main exterior components (excluding the blades) were calculated from sound intensity measurements. The total sound power level of the wind turbine was calculated from sound pressure level measurements at a distance (see section 3.1). The difference between the total sound power contribution from the main exterior components (blades excluded) and the total sound power level of the turbine was attributed to noise from the blades.

Method 2 – Direct Measurement

The intensity probe was placed on the end of a 4m boom from the side of the nacelle and held stationary near to the trailing edge of the passing blades while the turbine was generating. The intensity measurement was averaged over approximately 24 rotations of the blade. The intensity measurement and the swept area of the blade were then used to calculate the sound power emitted from the blades.

Possible inaccuracies in this measurement may have arisen because of the difficulties involved in maintaining a consistent and short distance from the microphone to the blade. This would have decreased the apparent sound intensity when compared with that which would have been measured under ideal conditions. Furthermore the microphone would have been subjected to a large amount of buffeting and possible wind induced pseudo-noise each time the blade passed. This would have had the effect of increasing the noise level measured from the blade – especially at lower frequencies.

3.2.2 Results

Tabulated below in table 2.3.2 is a summary of the results of the investigation using each of the methods outlined above. The results are for the turbine in the original 'as built' condition with no additional acoustic treatment.

Table 2.3.2 – Contribution Investigation Results

	L_{WA} (dBA)		**Contribution to Total L_{WA} (%)**	
Component	**Method 1**	**Method 2**	**Method 1**	**Method 2**
Nacelle	88.7	88.7	1.3	0.9
Duct Exit	79.8	79.8	0.2	0.1
Cooler Housing	78.6	78.6	0.1	0.1
Tower	98.6	98.6	12.1	8.4
Blades	107.1	108.9	86.3	90.5
Total	107.7	109.3	100.0	100.0

Each method of calculation produced very similar results. The results showed that the blades were the major contributor to the total noise from the turbine and contributed approximately 86 – 91% of the sound power level observed. The next largest contributor was the tower, which was found to contribute 8 – 12% of the total sound power of the turbine. The nacelle contributed 0.9 – 1.3%, and the duct exit and cooler housing were found to contribute only 0.1% of the total sound power level of the turbine (the sound intensity levels measured in the regions of the duct exit and cooler housing were actually relatively high but due to their comparatively small surface areas their sound power contributions were small).

These results provided a basis for noise reduction work, showing that blade and tower noise would be the most important to reduce. What the experiment did not determine was whether the sound radiated from the blades and tower originated from structure-borne or airborne mechanisms.

3.3 Spectral Analysis

Analysis of the sound spectrum produced by the Windflow 500 showed that a tone was present in the 315 Hz 1/3 octave band and to a lesser degree in the 1000 Hz 1/3 octave band. Figure 2.3.2 below shows a sound pressure level spectrum measured 1400m from the turbine at house 6, which illustrates the strength of the 315 Hz tone.

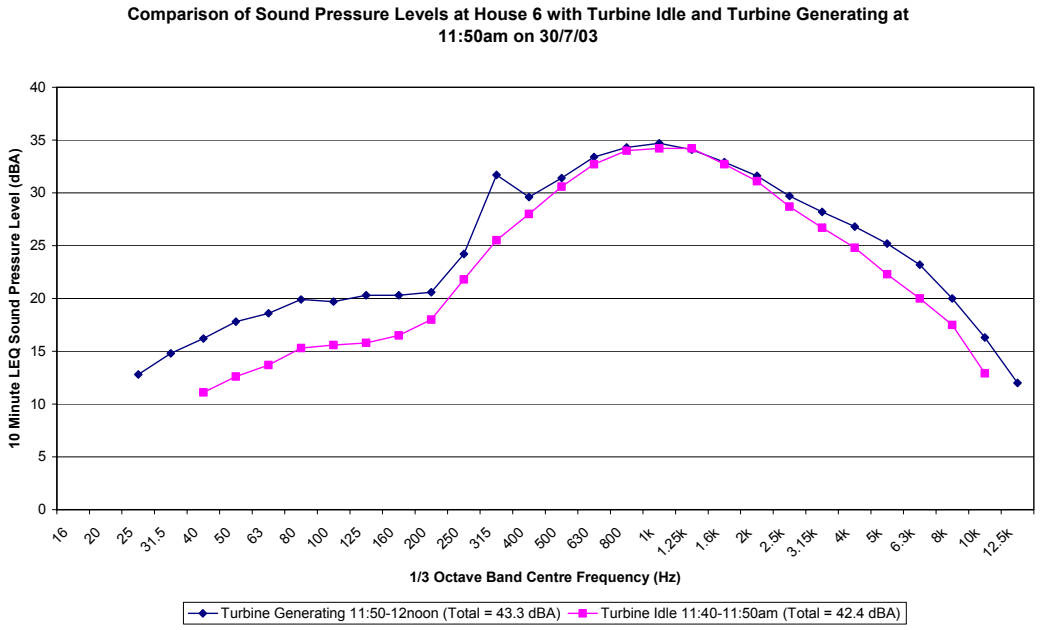

Figure 2.3.2 – Sound Spectrum at House 6, 1400m from Turbine

The presence of the tones is important because it is generally accepted that a noise with tonal character is more likely to be found annoying by people than one without. As a result of this, the New Zealand Standard for the Assessment of Wind Turbine Noise (NZS 6808:1998) [1] states that in the case where the noise from the turbine exhibits a tonal character, there must be a 5 dBA penalty added to the measured sound pressure level to compensate for the additional annoyance factor. This in turn has implications for the wind turbine operator, as it means that the minimum distance that a wind turbine may be located from a residential dwelling is markedly increased if an equivalent sound pressure level is to be achieved at the dwelling when compared to a case where no tonal character is exhibited.

Possible origins of the tones were investigated. Several possible contributing sources to the 315 Hz tone were identified. These were as follows –

- Gearbox 2nd Stage Gear Meshing Frequency (GMF) = 311 Hz
- Generator fan blade passing frequency = 325 Hz
- Rotor blade vortex shedding in the frequency range of 282 – 355 Hz

Rotor blade vortex shedding in the frequency range of 282 – 355 Hz was considered unlikely to be occurring to a large extent, given the geometry of the blade. The noise from the generator fan was measured at the exit of the duct, but the tone produced by the passage of the fan blades was found to be insignificant when compared with the magnitude of the tone observed in the 315 Hz 1/3 octave band at a distance. This left the gearbox 2nd stage GMF of 311 Hz as the most likely source of the tone. This was confirmed when accelerometer measurements were taken at several points on the nacelle cladding and tower wall and it was found that the 311 Hz frequency was dominant in the spectrum.

For the tone observed in the 1000 Hz band, the only possible source identified was the 985 Hz GMF of the gearbox final stage. Again, this frequency came through strongly in accelerometer measurements taken from various points on the turbine which provided confidence that the gearbox was the source of this tone.

3.4 Other Characteristics

Another important feature of the noise from the turbine was that it was modulated by the motion of the blades creating an impulsive sound. Figure 2.3.3 below is a time-frequency plot of the sound pressure level (magnitude depicted by colouration) measured on the ground near to the turbine. The figure illustrates the impulsive nature of the sound.

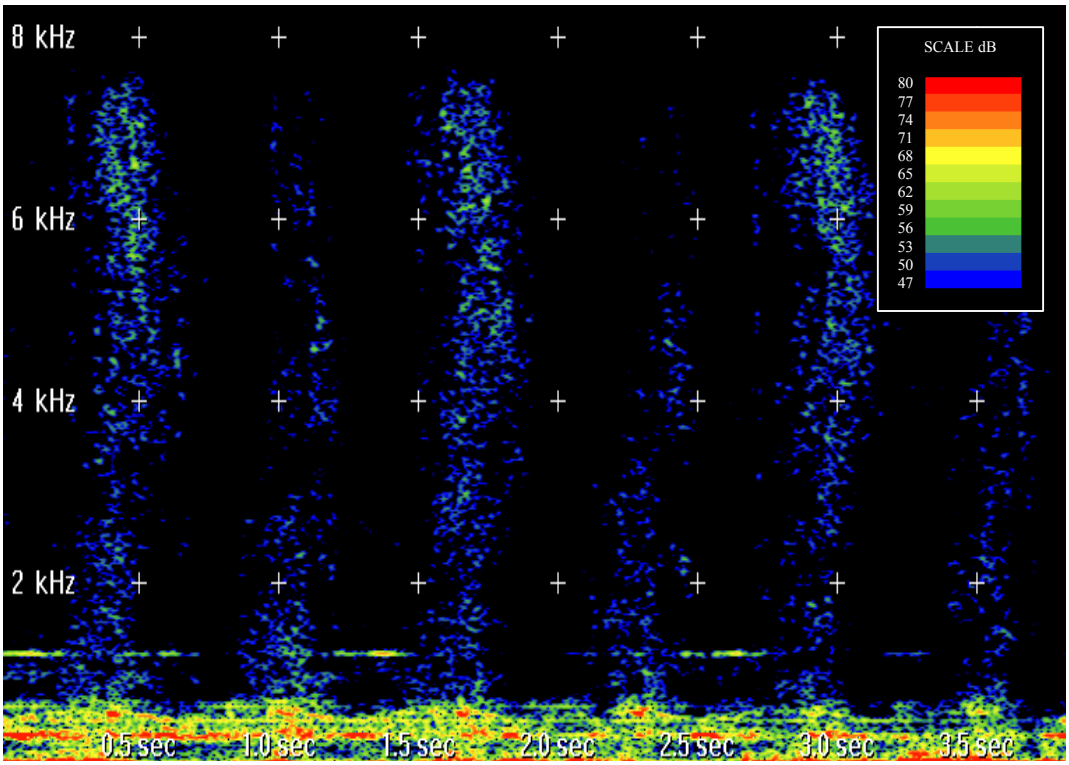

Figure 2.3.3 – Time-Frequency Plot of SPL Near the Turbine

Impulsiveness is generally regarded as having the effect of increasing the annoyance factor of the noise however unlike tonal noise no penalty is applied by NZS 6808:1998.

Another interesting phenomenon which was easily observable with the human ear and can be seen on the time-frequency plot above is the difference in noise produced by each of the two blades of the turbine. One blade clearly produced more noise than the other in the region of 5 kHz – 8 kHz. Given that each of the blades were supposedly manufactured to identical specifications, the noise difference begs the questions to what tolerance were the blades manufactured, how closely matched are their angles of

incidence during operation and what degree of blade imperfection is allowable before the noise produced is altered significantly.

4. Conclusions and Recommendations

This chapter has presented information regarding the location and specifications of the wind turbine studied in this thesis, with reference to the acoustic significance of the set-up. Furthermore, an initial investigation aimed at quantifying the relative proportions of noise from each major component on the wind turbine was carried out and reported.

It was found that the total sound power level of the wind turbine was 108 dBA. It was found that the blades and tower were the main components providing the greatest contributions to the total noise of the turbine, with 86 – 91% of the noise being radiated from the blades and 8 – 12% being radiated from the tower.

It was found that the sound spectrum produced by the generating turbine was dominated by two tones which originated from the gearbox. The noise was modulated by the blades creating an impulsive signal.

Further work could be conducted to ascertain the reason why the second stage of the gearbox in particular created such a prominent tone. In addition to this, an investigation could be carried out to determine why one blade was noisier that the other, and establish guidelines for the degree of manufacturing imperfection allowable in the blades before the noise produced in altered significantly.

5. References

[1] NZS 6808:1998 Acoustics - The Assessment and Measurement of Sound from Wind Turbine Generators.

[2] Wagner S., Bareiss R., and Guidati G., *Wind Turbine Noise*: Springer, 1996.

Chapter 3
Design and Evaluation of a Dissipative Muffler

Summary

Airborne noise transmission from the nacelle to the inside of the tower was thought to be responsible for the high sound pressure levels observed inside and to a lesser extent outside the tower of the Windflow 500 wind turbine. An expansion chamber muffler containing dissipative material was designed and built into the top of the tower to reduce the airborne noise transmission while still allowing the flow of cooling air to the nacelle via the tower. Two configurations of the muffler were tested – one with a tower 'lid' to provide a more favourable inlet contraction, and one without.

The muffler was evaluated using pink noise from a speaker placed in the nacelle. It was found to perform better than predicted from theory except between 630 and 1000 Hz, achieving an overall transmission loss of approximately 20dB. The lidded configuration was found to perform significantly better at frequencies above 2000 Hz.

The effectiveness of the muffler for reducing the transmission of airborne noise from the nacelle to the tower was not realised with the turbine generating. It was found that the sound pressure levels inside the tower and at points outside around the turbine were not reduced. This indicated that either the tower noise was being structurally transmitted from the nacelle, or that there was another greater source of noise that had not been accounted for.

Table of Contents

List of Figures

List of Tables

1. Introduction

1.1 Background

Initial acoustic measurements conducted on the turbine showed that the inside of the tower was highly reverberant (see figure 3.1.1). It was thought that the airborne noise produced by the machinery inside the nacelle was propagating easily down the reverberant tower where it was being transmitted through the tower wall to the outside. This was assumed (incorrectly) to be a large contributor to the sound pressure levels that were measured around the base of the tower.

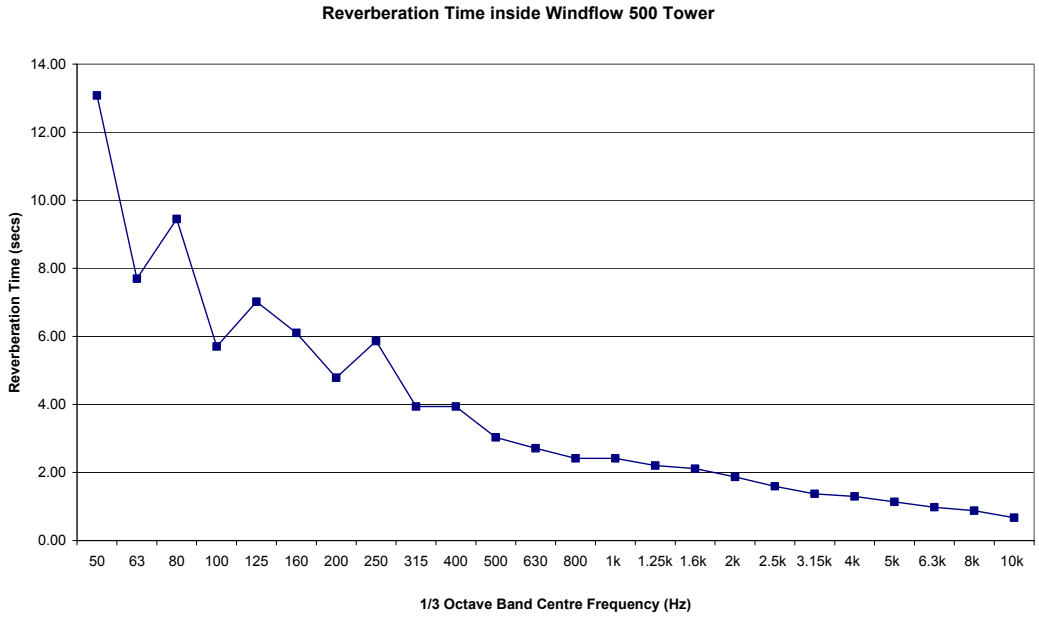

Figure 3.1.1 –Reverberation Time Inside Windflow 500 Tower

In order to reduce the airborne noise being transmitted to the tower from the nacelle a dissipative muffler was designed and installed in the top of the tower. This chapter is concerned with the design and testing of the muffler.

1.2 Muffler Theory

The simplest type of muffler is the expanded cross-section muffler, as shown below in figure 3.1.2.

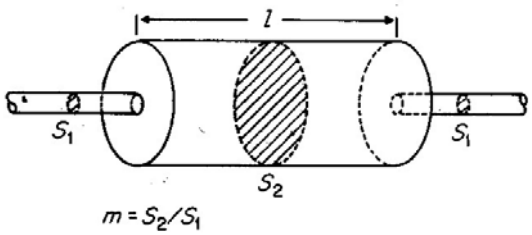

Figure 3.1.2 – Single Expansion Chamber Muffler

The expansion muffler works primarily by reflection and secondly by scattering of the incident sound waves. At very low frequencies or whenever the length of the muffler is equal to λ/2, λ, 3λ/2, etc., a standing wave system is produced with enhanced sound pressures at the end walls of the cavity. This increases the characteristic impedance of the expanded cross-section to exactly that of the inlet and outlet pipes. Because of the perfect impedance match at these frequencies a resonance occurs in the muffler and the sound transmission loss is zero.

Beranek [1] derives the following equation for the transmission loss of an unlined single expansion chamber muffler –

$$TL_{Unlined} = 10\log_{10}\left[1+\frac{1}{4}\left(m-\frac{1}{m}\right)^2 \sin^2 kl\right] \quad \text{(dB)} \qquad (3\text{-}1)$$

where

$TL_{Unlined}$ is the transmission loss of an unlined expansion chamber (dB).

m is the expansion ratio = S_2/S_1 where S_2 is the cross-sectional area of the expanded section of muffler and S_1 is the cross-sectional area of the inlet / outlet to the muffler.

k is the wave number = $2\pi f/c$ where f is the frequency of the sound and c is the speed of sound in air.

l_e is the length of the expanded section.

The use of equation 1 produces the frequency – expansion ratio relationship for transmission loss as shown in figure 3.1.3 below.

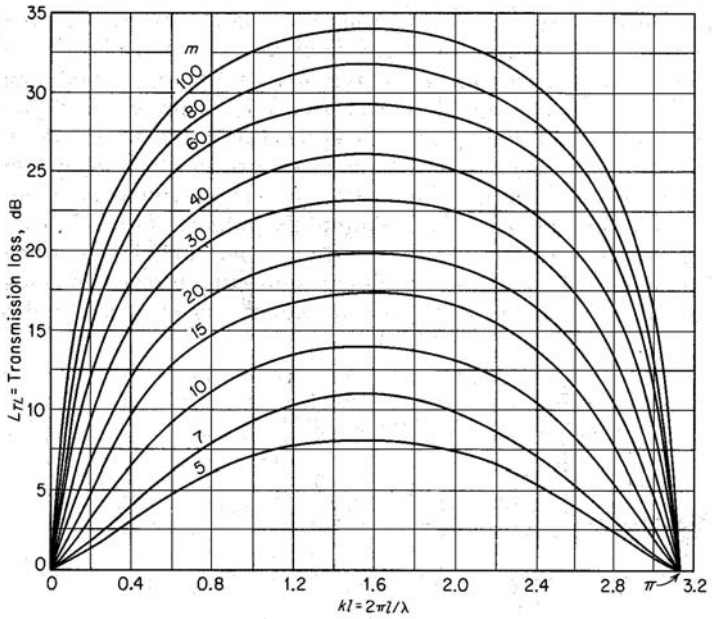

Figure 3.1.3 – Effect of Expansion Ratio on Muffler Transmission Loss

By introducing a sound-absorbing medium into the expansion chamber, further improvements in the transmission loss of the muffler can be achieved at most frequencies including those at which resonance usually would occur in the unlined expansion chamber.

In the case where the expansion chamber is lined the attenuation due to the lining is often found to be the dominant mechanism in reducing the sound transmitted. Beranek states that for a lined expansion chamber the total transmission loss is often greater than sum of the attenuation due to the lining plus the reflection and scattering due to the expansion. Beranek gives the following expression for the transmission loss of a lined expansion chamber

$$TL_{Lined} = 10\log_{10}\left\{\begin{array}{l}\left[\cosh\frac{\sigma l_e}{2}+\frac{1}{2}\left(m+\frac{1}{m}\right)\sinh\frac{\sigma l_e}{2}\right]^2\cos^2 kl_e+\ldots\\ \ldots\left[\sinh\frac{\sigma l_e}{2}+\frac{1}{2}\left(m+\frac{1}{m}\right)\cosh\frac{\sigma l_e}{2}\right]^2\sin^2 kl_e\end{array}\right\}\ \text{(dB)} \qquad (3\text{-}2)$$

where

TL_{Lined} is the transmission loss of a lined expansion chamber (dB).

m, k, and l_e are as defined for equation 1.

σ is the energy attenuation per unit length of the lining = IL/4.34 where IL is the insertion loss of the lining in dB/m.

Figure 3.1.4 below shows a graphical representation of the effect of expansion ratio and lining attenuation on the transmission loss of the muffler.

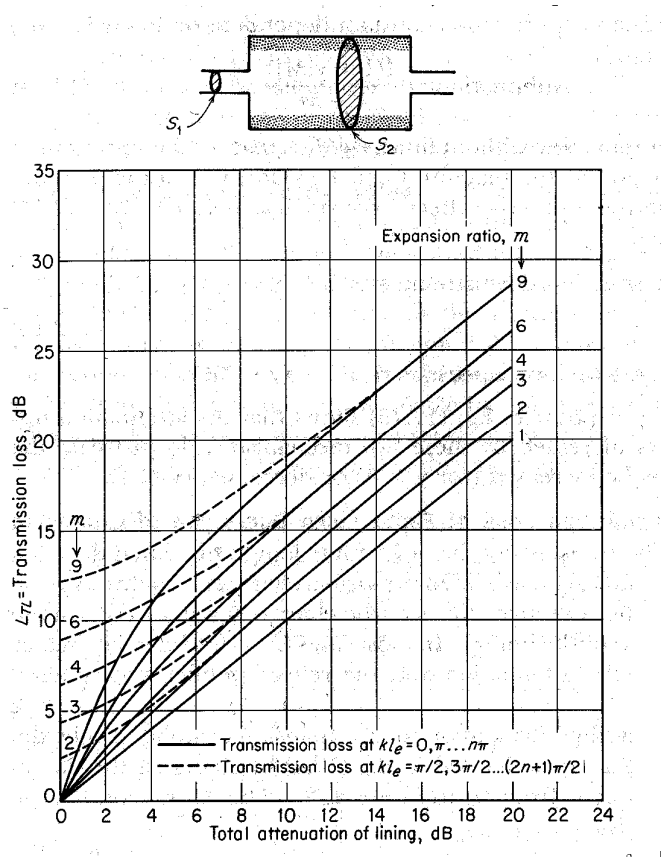

Figure 3.1.4 – Transmission Loss of a Lined Expansion Chamber

2. Design

2.1 Requirements

The muffler was required to reduce the airborne noise in the tower as much as possible within the space available.

Cooling air for the generator is drawn up the tower at a maximum rate of 1 cubic metre per second, and this airflow could not be obstructed. The muffler had to be designed so that it would not interfere with the movement of the pendant cable during yawing of the turbine, or any of the machinery inside the nacelle and the design had to allow easy access to the inside of the nacelle to be maintained.

The muffler had to fit within the confines of the turbine and had to be able to be easily installed.

2.2 Solution

From figures 3.1.3 and 3.1.4 it can be seen that the larger the expansion ratio of the muffler, the more effective it becomes. Given the geometric constraints of the tower and the operating airflow requirements of the wind turbine, the muffler was designed with an approximately 10:1 expansion ratio. The muffler was designed so as to make use of the existing structure of the turbine as much as possible so as not to require extensive construction or modification work.

2.2.1 Inlet (Top)

In order to achieve the required expansion ratio at the inlet to the muffler a tower lid was constructed. This was shaped to fit on the top of the tower while still being able to be easily removed to allow access to the nacelle. The resulting tower lid shape is shown in figure 3.2.1

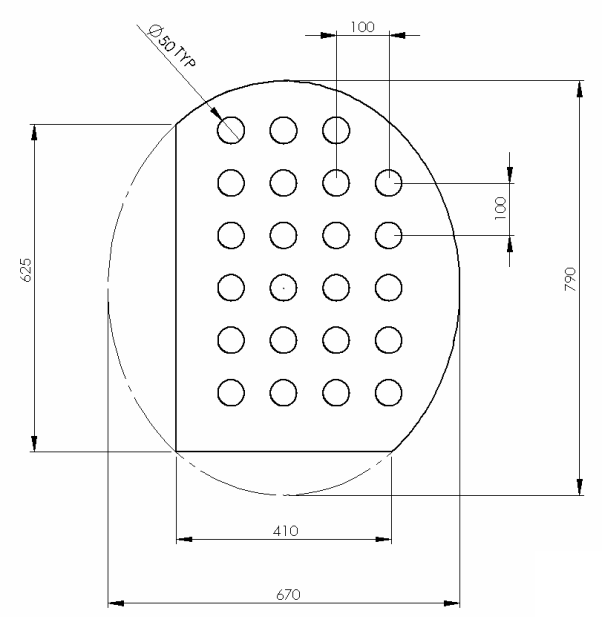

Figure 3.2.1 - Tower Lid

The lid was manufactured from two sheets of 18 mm medium density fibreboard glued together so that the total thickness of the lid was 36 mm.

2.2.2 Outlet (Bottom)

The muffler used the existing platform 2m below the top of the tower to create the outlet contraction – see figure 3.2.2 below.

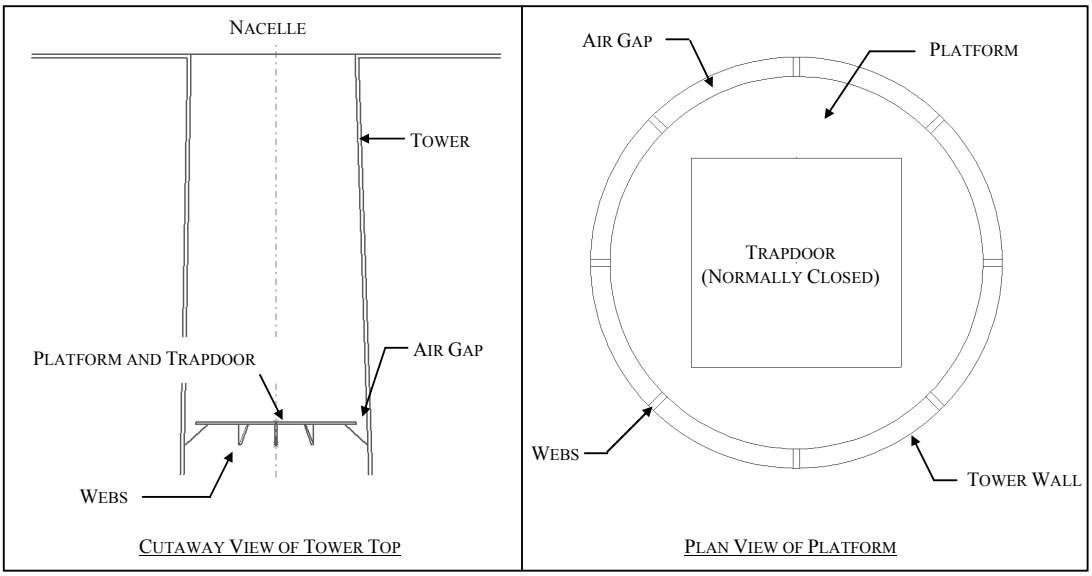

Figure 3.2.2 – Tower Platform / Muffler Outlet Schematic

2.2.3 Sound Absorbing Medium

To increase the transmission loss of the muffler, the walls of the expansion chamber were lined with 50 mm thick acoustic grade polyurethane foam. In addition to this the top surface of the trapdoor and platform was covered with a loop-pile rubber backed carpet, while the walls through the outlet and the underside of the trapdoor and platform were covered with 25 mm thick acoustic grade polyurethane foam – see figure 3.2.3. The 25 mm foam and carpet were glued in place while the 50 mm foam was supported against the tower wall by the ladder rungs at the top of the tower.

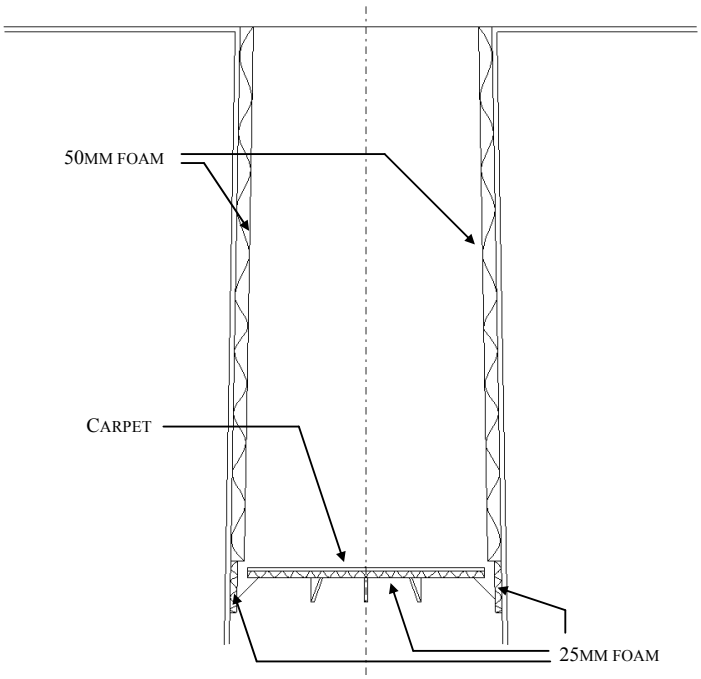

Figure 3.2.3 – Lined Areas

2.3 Transmission Loss Calculation

The transmission loss of the muffler was predicted using equation 3-2. The effects of the carpet and 25 mm foam were neglected in the calculation. Table 3.2.1 contains the insertion loss values that were used in the prediction. These are based on insertion loss figures derived experimentally by Pettersson [2] for the same type of 50 mm foam as used in the muffler.

Table 3.2.1 – 50mm Thick Polyurethane Foam Insertion Loss Values

1/3 Octave Band Centre Frequency (Hz)	Insertion Loss (dB/m)
100	4.6
125	4.2
160	3.2
200	3.7
250	5.3
315	6.5
400	8.1
500	9.5
630	17.2
800	17.6
1000	17.2
1250	11.6
1600	9.7
2000	14.6
2500	16.9
3150	10.9
4000	12.3
5000	12.1

Figure 3.2.4 below shows the predicted transmission loss characteristics of the muffler.

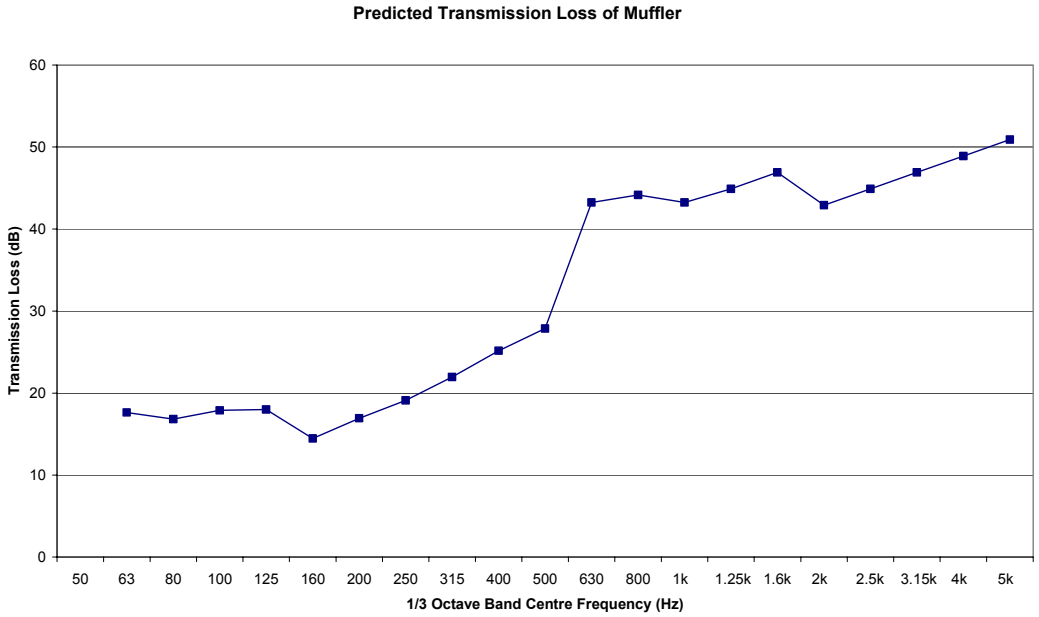

Figure 3.2.4 – Predicted Transmission Loss of Muffler

It should be noted that in application to this particular muffler design, the accuracy of the theories derived by Beranek will be somewhat limited for the following reasons –

1. Beranek assumes a constant cross-section along the length of the expansion chamber, whereas the tower muffler is actually a conical shape with its circular cross-section increasing in area with distance down the tower.
2. Beranek derives the theory for the inlet / outlet configuration shown in figure 3.2.5a below, whereas the way in which the tower is constructed limits the actual inlet / outlet to a configuration as shown in figure 2.5b.

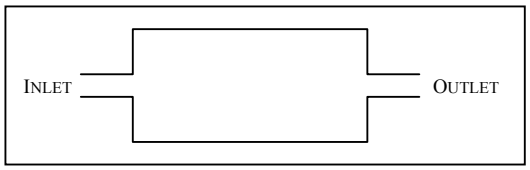

Figure 3.2.5a – Assumed Configuration

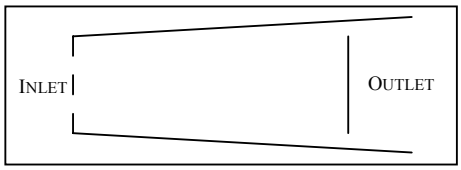

Figure 3.2.5b – Actual Configuration

3. Beranek's theory does not take into account the effects of airflow up the tower.

3. Evaluation Method

A Neutrik Minirator MR1 audio generator was used to create pink noise played through a JBL EON 10" powered speaker that was placed in the nacelle as shown in figure 3.3.1. The speaker was set so as to produce a sound power level of 110 dB inside the nacelle.

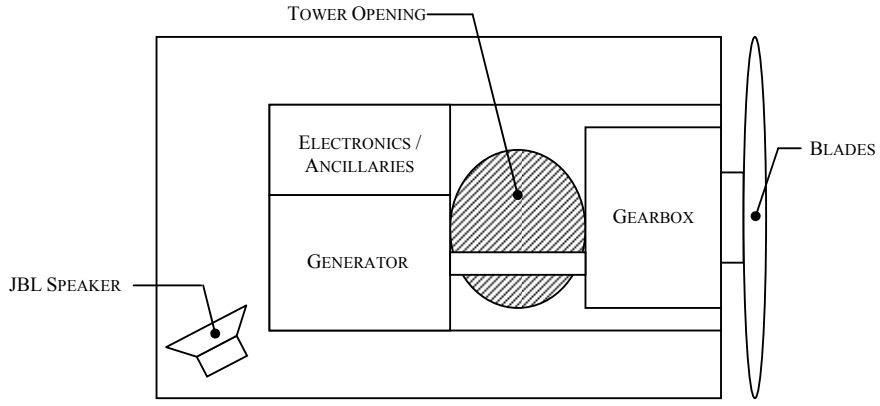

Figure 3.3.1 – Speaker Location Schematic: Plan View of Nacelle

Sound pressure and intensity level measurements (30 second LEQs) were then taken at the locations inside the turbine shown below in figure 3.3.2.

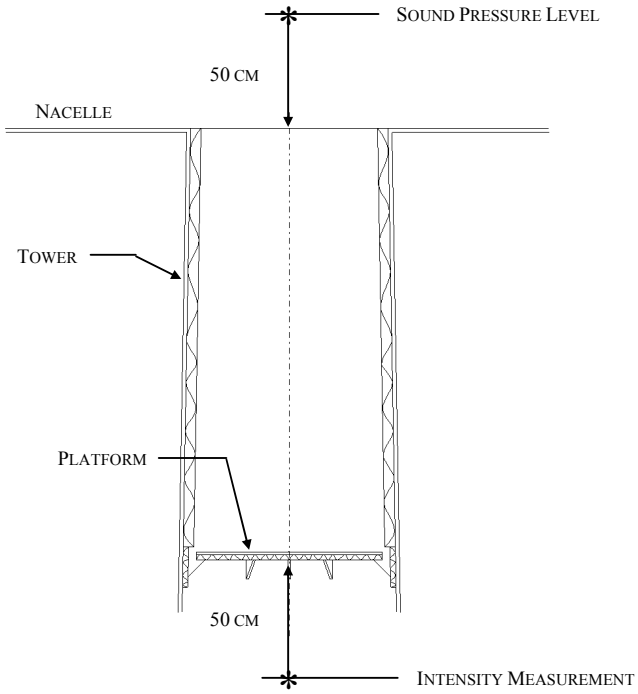

Figure 3.3.2 – Measurement Locations

The transmission loss of the muffler was calculated from a sound pressure level measured in the nacelle 0.5m above the inlet and an intensity measurement taken 0.5m below the outlet. In order to do this it was assumed that the sound field inside the nacelle was diffuse. This assumption was confirmed to be suitable by measuring the sound pressure level at a number of different locations inside the nacelle with the speaker on and finding no significant variation until very close to the source. The transmission loss of the muffler was then calculated using equation 3-3.

$$\textit{Muffler Transmission Loss [dB]} = Lp_{Inlet} - 6 - Li_{Outlet} \qquad (3\text{-}3)$$

The tests were repeated for three different cases –

1. Tower top as built (no muffler installed)
2. Tower with muffler absorption installed but without tower lid.
3. Complete muffler installed.

In order to determine the effectiveness of the muffler in reducing the noise of the operating turbine two further tests were then carried out using the operating turbine as the noise source. These tests were as follows –

4. Attenuation of the complete muffler with the turbine operating.
5. Sound pressure level 100m south of the operating turbine before and after installation of the muffler.

4. Results and Analysis

4.1 Measured Transmission Loss

Figure 3.4.1 below shows the TL of the muffler measured with and without the tower lid compared with the predicted TL, along with the TL measured without the muffler installed in the tower.

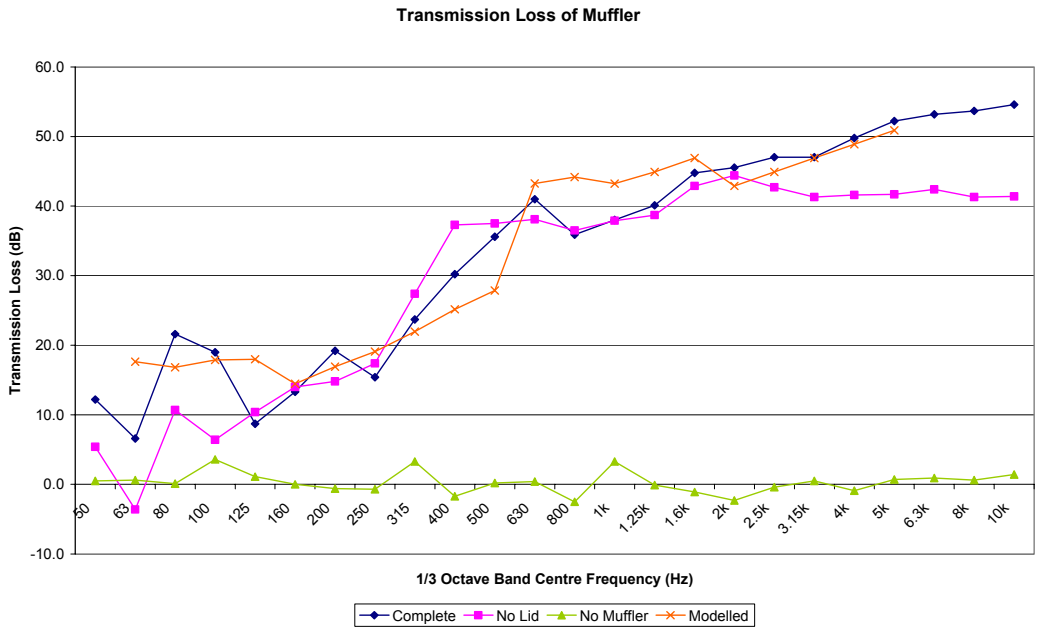

Figure 3.4.1 – Transmission Loss of Muffler

As can be seen from figure 3.4.1, with the tower in the 'as built' condition, the transmission loss between the nacelle and tower was almost zero. Figure 3.4.1 shows that the muffler performed well across the frequency spectrum both with and without the lid in place. However, in the case where the lid was on the muffler a significant improvement was observed in the transmission loss at frequencies greater than 1 kHz. Interestingly the muffler seemed to perform better in the frequency bands of 250 – 500 Hz without the lid in place.

When compared to the modelled transmission loss of the muffler, the measured values were generally found to exceed those predicted, particularly in the 1.25 kHz, 1.6 kHz, and 2kHz frequency bands where the predicted values show a prominent drop. The predicted values were also exceeded significantly at frequencies above 3.15 kHz. However, the model over-predicted the transmission loss of the muffler in the 630 Hz, 800 Hz, and 1 kHz bands, and at some of the frequencies below 160 Hz. The discrepancies between the modelled and measured data are likely to have arisen from a combination of sources. Measurement error is one possible source while the possible inaccuracies in the prediction as outlined previously in section 2.3, are another.

4.2 Muffler Attenuation with Turbine Operating

Figure 3.4.2 shows the TL of the complete muffler measured with the turbine generating compared with that measured using the speaker as a noise source.

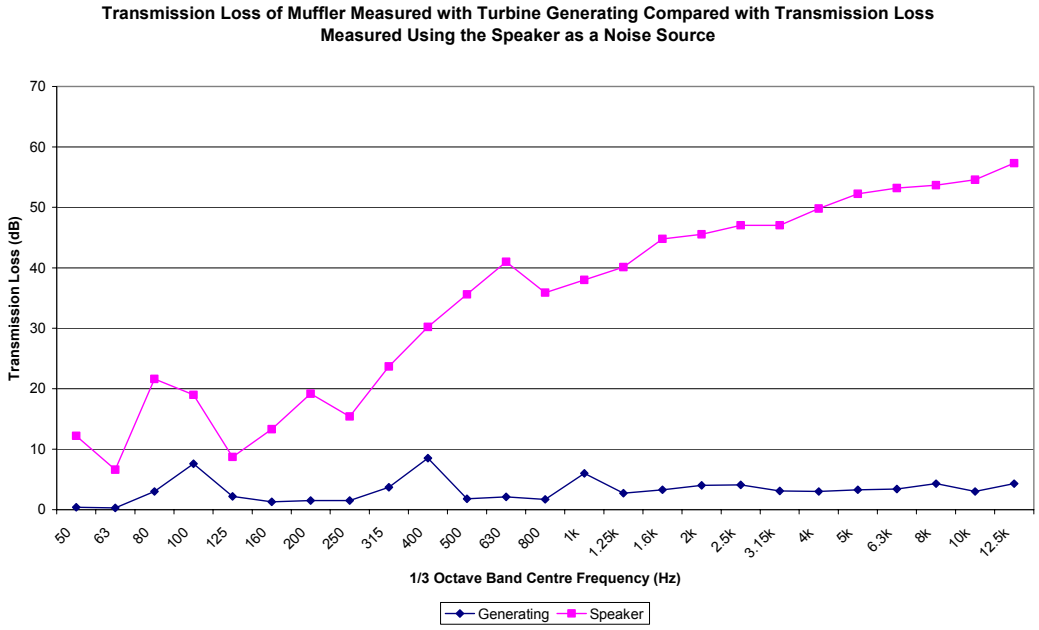

Figure 3.4.2 - Transmission Loss of Muffler with Turbine Generating

The above graph shows that with the generating turbine used as a noise source the measured transmission loss of the muffler was significantly reduced when compared to that measured using the speaker as a noise source. This was attributed to the fact that the speaker produced airborne noise only whereas with the turbine generating there was probably also a large structure-borne sound component. In the case of the generating turbine the noise was clearly bypassing the muffler by way of vibration of the tower wall - which could have been structurally excited by the machinery in the nacelle.

4.3 Far-Field Sound Pressure Levels

Figure 3.4.3 shows the sound pressure levels measured 100m south of the generating wind turbine before and after installation of the muffler at the top of the tower. It can be seen from the levels measured that no significant reduction in the far field sound pressure level was made by installing the muffler. This indicates that either there was a structure-borne component of sound rendering the muffler ineffective as discussed in section 4.2, or that other noise sources were dominating.

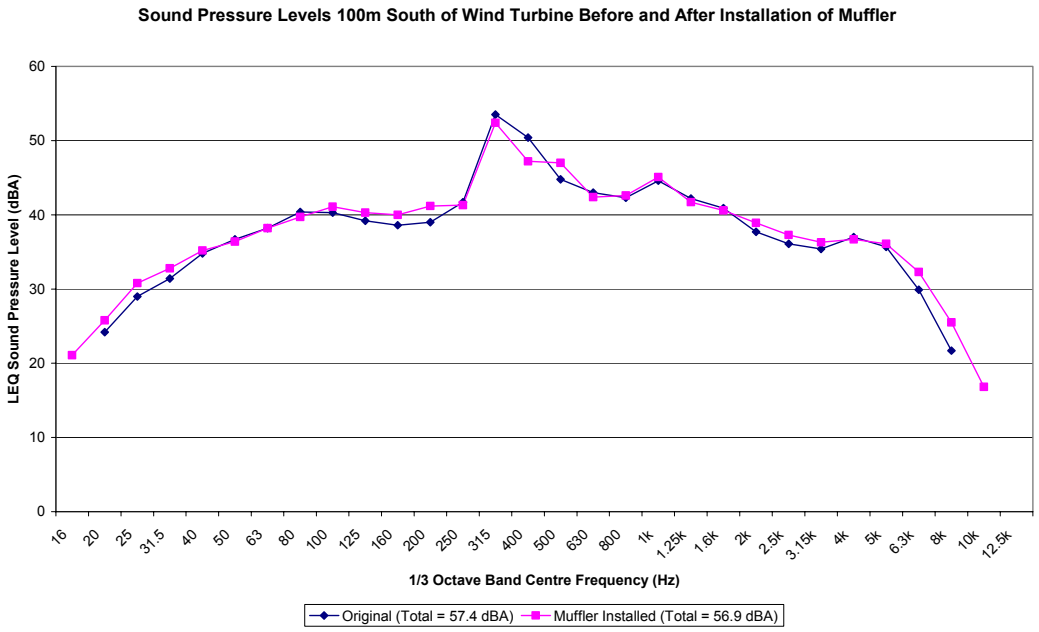

Figure 3.4.3 – Far Field Sound Pressure Levels

5. Conclusion

The tests showed that the muffler was a highly effective means of reducing the airborne sound transmission from the nacelle to the tower in the Windflow 500. However with the turbine operating, the transmission loss measured was significantly reduced and the expected decrease in sound pressure level outside the turbine was not realised. These results indicated that the sound pressure level inside the tower was not due to airborne sound from the nacelle propagating into the tower.

References

[1] Beranek L.L, *Noise and Vibration Control*: Washington, D.C: Institute of Noise Control Engineering, 1988.

[2] Pettersson M.J., "Duct Absorber Design," in *Department of Mechanical Engineering*: University of Canterbury, 2002.

Chapter 4
Tower Noise Investigation

Summary

Given its large surface area, the tubular tower of the Windflow 500 was recognised as being a potentially large contributor to the total sound power of the turbine. This was also supported by observations at the base of the tower where a loud ringing noise generated by vibrations from the machinery in the nacelle could be heard.

An investigation was carried out in order to determine the way in which the tower was vibrating and formulate an appropriate method of reducing the noise produced. It was found that the tower had many free modes of vibration and was easily picking up a strong 311 Hz signal generated by gear tooth meshing in the second stage of the gearbox. Several approaches to reduce the noise from the tower were identified. These included isolation of the nacelle machinery, stiffening of the tower, and damping of the tower. Damping of the tower was thought to be the approach most likely to be successful.

Rubber damping tiles were glued to the inside surface of the tower wall at the points where it was vibrating with the largest accelerations and further sound and vibration measurements were carried out. It was found that the vibration of the tower wall at 311 Hz was reduced significantly while the sound pressure level inside the tower was reduced by up to 9 dBA. However, a reduction in total noise from the wind turbine was not observed at a distance. This supported the finding that noise from the blades was dominating the total noise level produced by the turbine.

Table of Contents

List of Figures

List of Tables

1. Introduction

1.1 Background

The tower was recognised as a significant contributor to the total noise of the wind turbine. Previous work to reduce the transmission of airborne noise from the nacelle to the tower had negligible effect, which indicated that there was likely to be a high degree of structure-borne noise radiated from the tower. This chapter documents and discusses the work carried out to identify and reduce the structure-borne noise from the tower.

2. Vibration Analysis

Vibration analysis of the tower was carried out to determine its vibration levels and confirm that the assumption of structure-borne noise in the tower was correct. Accelerometer measurements were taken at several points on the inside surface of the wind turbine tower using a Commtest VB3000 vibrometer while the wind turbine was operating with steady wind speeds of approximately 10m/s. It was found that the 311 Hz gear meshing frequency of the second planetary stage in the gearbox was dominant in the spectrum (see figure 4.2.1). This verified the tower as a probable path of noise from the machinery in the nacelle.

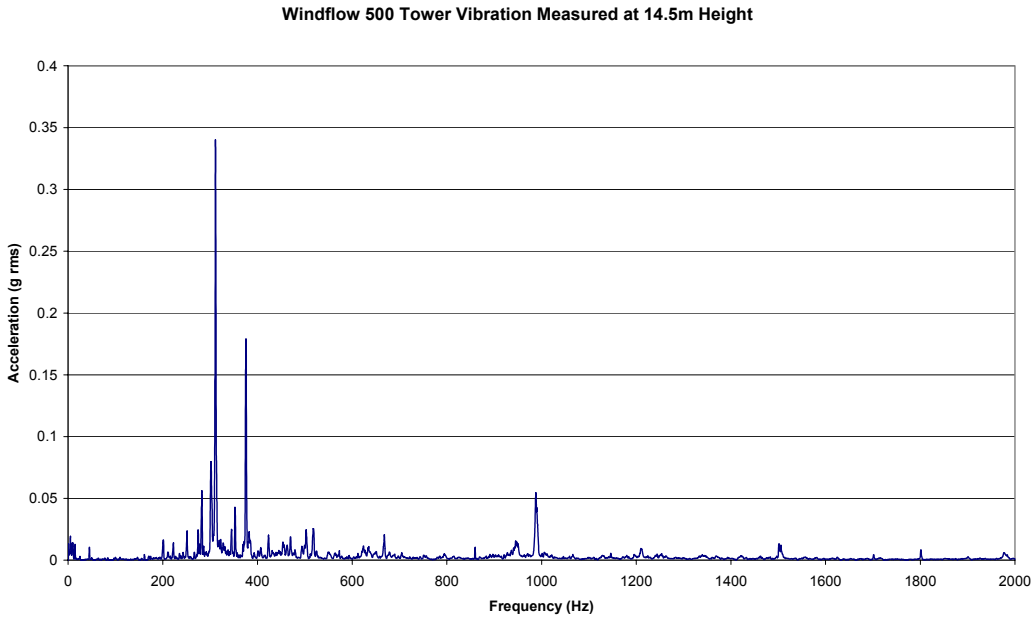

Figure 4.2.1 – Tower Wall Vibration at 14.5m Height

Given that structural vibration of the tower was a likely source of noise, further accelerometer measurements were made on the tower to determine where the largest tower wall accelerations occured. Measurements were taken at 0.5m intervals from the base to the top of the tower approximately 0.6m to the right of the ladder. Measurement locations were marked and labelled to allow later comparisons after a treatment had been applied. The results of the initial vibration scan up the tower for the 311 Hz frequency are shown below in figure 4.2.2.

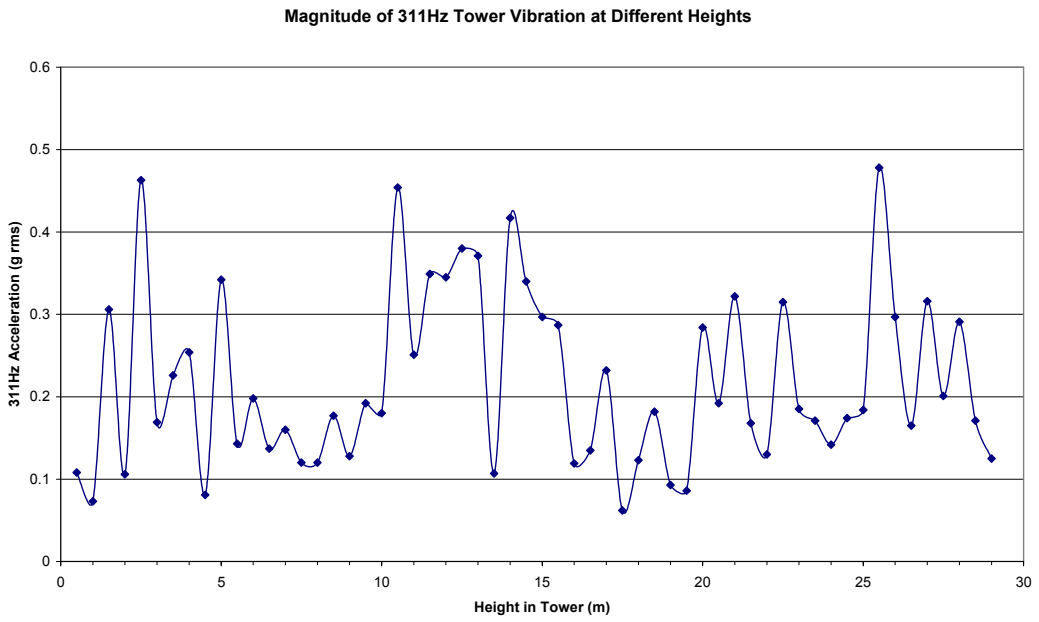

Figure 4.2.2 – Tower Vibration at 311 Hz

As can be seen from the graph the tower was vibrating particularly actively at the heights of 0m to 5m, 10m to 16m, and 25m to 30m.

3. Treatment

3.1 Options Considered

Several options were considered to reduce the structural vibration of the tower. The various alternatives are identified and evaluated below.

3.1.1 Vibration Isolation of Gearbox and Generator from Pallet

The turbine as built had the gearbox and generator rigidly mounted to the pallet (chassis) on solid mounts. The most obvious solution to the problem was to provide some form of vibration isolation between the major rotating components (gearbox and generator) in the nacelle and the pallet on which the machinery was mounted (see figure 4.3.1).

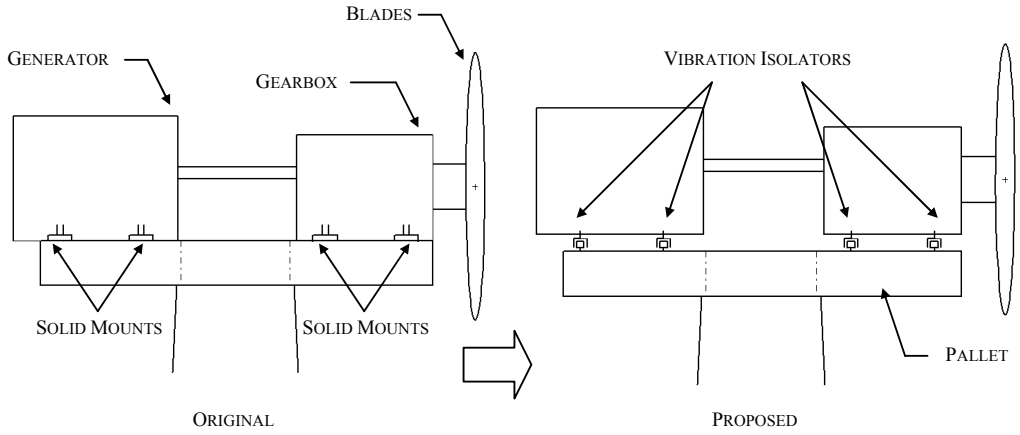

Figure 4.3.1 – Proposed Solution 1 – Gearbox Isolation Schematic

If designed properly it was considered that this solution would be very effective, however several factors detracted from its appeal. The first of these factors was the design time required to develop suitable mounts. The mounts of the gearbox were subject to a wide range of high fluctuating loads acting in a number of modes. Previous experience with similar turbines overseas had shown the difficulties involved in designing vibration mounts for the gearbox with several cases of cracked mounts occurring within relatively short time periods after installation.

In addition to the difficultly involved in the design of the mounts, the mounts would raise the gearbox and generator slightly from its original position, possibly necessitating extensions to pipes, hoses and electrical cables. The expense and difficulty of installation was also a major negating factor.

3.1.2 Vibration Isolation of Entire Nacelle

Another idea suggested to reduce the structurally transmitted vibration to the tower was to vibration isolate the entire nacelle pallet and yaw bearing from the tower (see figure 4.3.2).

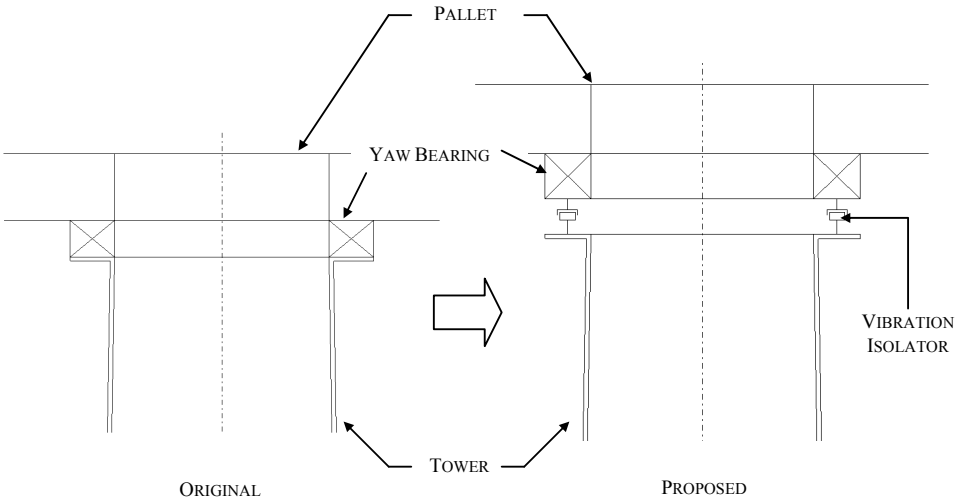

Figure 4.3.2 – Proposed Solution 2 – Cross-Sectional View of Tower / Pallet Joint

As with the design of anti-vibration mounts for the gearbox and generator, the design of the soft mount for the pallet would require careful consideration to ensure all modes of oscillation were accounted for. This would be especially critical for the pallet mount as it is the main joint between the nacelle and tower and failure of it would be catastrophic.

In addition to the design difficulties, manufacture and installation costs would be relatively high.

3.1.3 Structural Bracing / Stiffening of the Tower

Rather than attempting to prevent the transmission of vibration to the tower from the nacelle another approach considered was to reduce the vibration of the tower itself. One possible way of accomplishing this was to stiffen or brace the tower to prevent it vibrating as vigorously. Several configurations were considered including longitudinal and radial stiffeners and combinations of both. Example configurations are shown in figure 4.3.3.

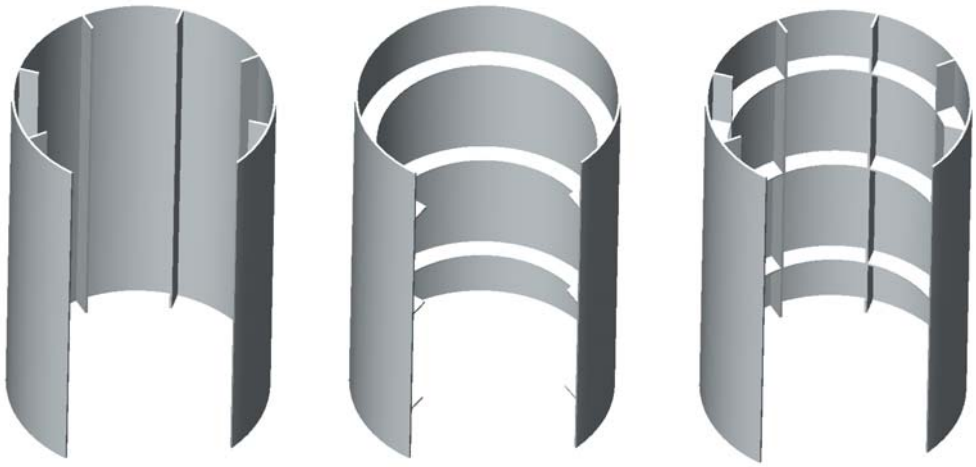

LONGITUDINAL RADIAL COMBINATION

Figure 4.3.3 – Proposed Solution 3 – Structural Stiffeners

The effect of the various stiffener / bracing configurations were modelled by Greg Morehouse of Motivated Design and Analysis using finite element methods (figure 4.3.4 below shows a model of the tower 'as built' vibrating at 311 Hz). A considerable number of modes near to 311 Hz were evident.

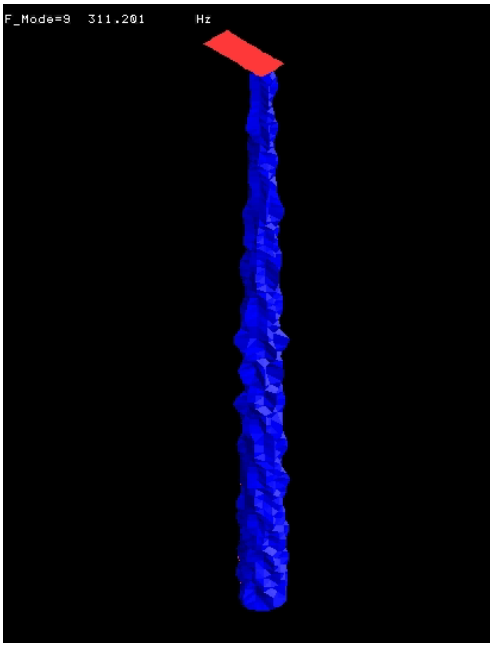

Figure 4.3.4 – Example Finite Element Model

Previous attempts to reduce tower noise with stiffening were conducted by the Wind Energy Group (WEG) in the UK on a turbine similar to the Windflow 500. In this case, radial stiffeners were used to reduce the vibration of the tower, but the approach was found to be unsuccessful.

Given the previous experience of WEG and the large number of modes calculated, structural stiffening of the tower was not pursued.

3.1.4 Structural Damping of the Tower

An alternative to stiffening of the tower to reduce its level of vibration was to introduce damping to the tower. This would be done by applying a damping medium to the inside surface of the tower wall, and would ideally only be required at areas of the tower where the levels of vibration were high.

The main advantage of this approach was that it was a conventional technique used for reducing vibration of surfaces and was therefore likely to be effective. WEG had previously used this technique on the similar MS3 wind turbine with rubber matting as the damping medium and achieved a 7-8 dB tower noise reduction. A further advantage was that it would be relatively cheap and easy to install, depending on the damping medium chosen.

A possible disadvantage of taking this approach was that a large mass of damping material would be expected to be required in order to be effective given the size and thickness of the tower wall. This could add to the expense or possibly make the solution completely impractical.

3.2 Chosen Alternative

Based on the cost and installation considerations, Windflow elected to pursue damping of the tower as a means of reducing the structural vibration.

3.2.1 Damping Medium

Several options were considered to provide the damping medium. Car underseal was suggested as a cost effective material to provide the damping but the thickness of underseal that would be required to have an

effect was expected to be of the order of the thickness of the plate – which was likely to pose problems when trying to apply it to the inside of the tower.

Gluing shaped sandbags to the inside of the tower was also suggested as a cost effective means of providing the damping, but manufacturing and installation of the sand bags in the tower was considered difficult.

Constrained layer damping was investigated briefly but was discarded as a possible method of providing the damping following recommendations that it would not be particularly well suited to the thick plate. It was also very expensive in comparison to the other free layer damping materials investigated.

A playground safety mat manufactured in Oamaru by Numat Industries Ltd was finally chosen as a damping material. The mats were manufactured from shredded recycled rubber and compacted to a density of 16.5 kg/sheet. Each sheet was $1m^2$ x 25 mm thick and could be cut to the required shape with a knife. Figure 4.3.5 shows the structure of the rubber mats.

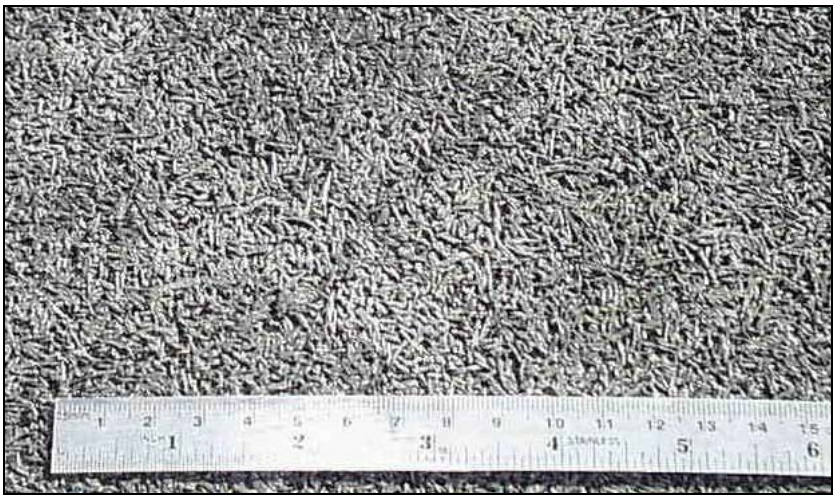

Figure 4.3.5 – Rubber Mat Structure

3.2.2 Areas of Application

The results of the initial vibration scan showed that the tower was vibrating significantly at 311 Hz at the heights of 0m to 5m, 10m to 16m, and 25m to 30m. Given that the vibration was being transmitted from

the top of the tower downwards, if the vibration could be arrested near the top it would not be necessary to provide vibration damping further down the tower. For this reason, sections of rubber were applied to the tower incrementally starting with the top section (25m – 28m) and working downwards. After each section of rubber was added, another vibration scan of the tower was conducted to determine the effect of the added damping and recheck where the areas with the highest vibration levels were. Vibration and noise measurements were always made with the turbine generating in approximately constant 10 m/s winds.

The resulting locations where damping was added were –

- Full circumferential coverage 25m – 28m above ground level inside the tower
- Full circumferential coverage 10m – 12.5m above ground level inside the tower

At each of these locations, two layers of rubber (total = 50 mm thick) were applied. This was done because laboratory experiments applying the rubber onto a simply supported flat steel plate had shown a double thickness to be more effective at damping out 311 Hz vibrations from a mallet impact than an equivalent mass / volume of rubber spread over a wider area.

4. Results and Analysis

4.1 Vibration

The way in which the rubber was applied to the tower wall did not allow accelerometer measurements to be repeated where the rubber had been applied, however the measurements repeated where the rubber was not applied showed significant reductions in the level of vibration at 311 Hz. Figure 4.4.1 shows the reduction in the magnitude of the 311 Hz vibration after each section of rubber was added.

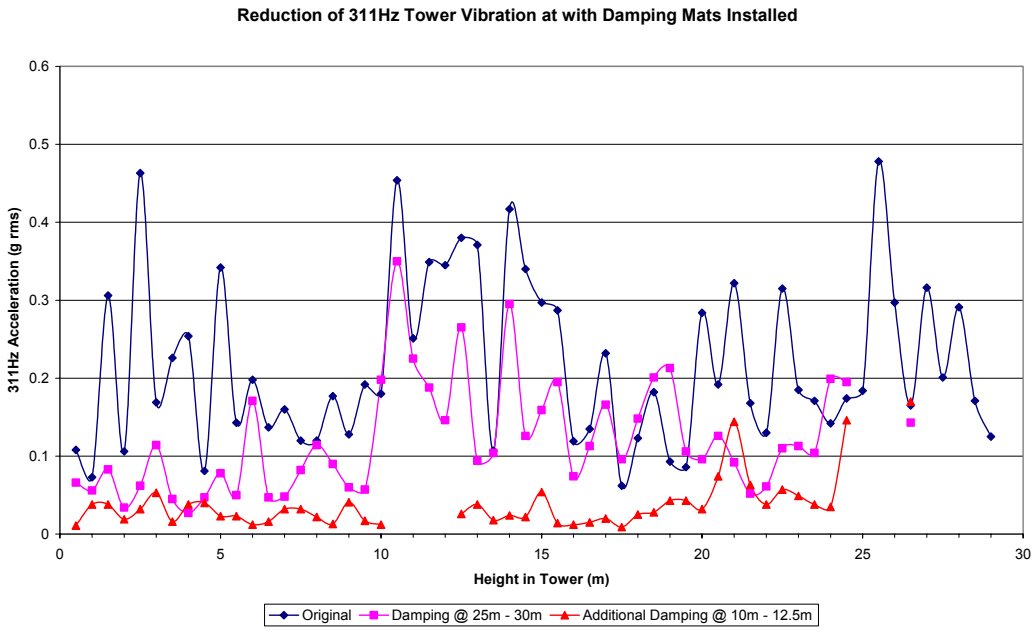

Figure 4.4.1 – Reduction of 311 Hz Tower Vibration

4.2 Noise

Noise analysis was carried out using a Bruel and Kjaer 2260 Investigator Type I sound level meter. Sound pressure levels were measured inside the base of the tower and at several locations around the turbine before and after the tower treatment. In addition to the sound pressure levels, sound intensity measurements were conducted around the lower 6m of the outside surface of the tower before and after the treatment. This was to verify that the structurally transmitted sound from the tower had been reduced rather than only airborne noise inside the tower (which was a possibility given the sound absorbing characteristics of the damping material). The intensity measurements were made using a Bruel and Kjaer Type 3595 Intensity Probe Kit.

After applying the rubber damping to the tower a significant reduction of the sound pressure level measured inside the base of the tower was observed. Original measurements showed levels of approximately 101 dBA. After the treatment, the sound pressure level was measured at 91.7 dBA – a reduction of 9 dBA. Figure 4.4.2 below shows the sound pressure levels measured inside the tower before and after the addition of the rubber, along with the effect observed from covering only the top 4m of the tower.

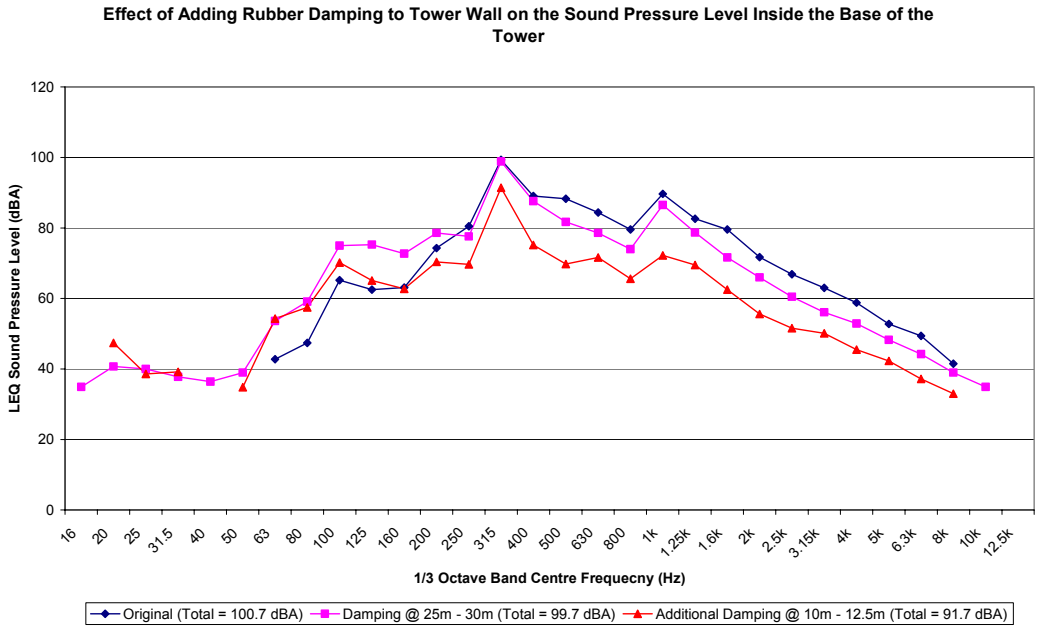

Figure 4.4.2 – Effect of Tower Damping on Sound Pressure Level inside Tower Base

The reduction observed above could be attributed to two factors: i) Reduction in the level of vibration of the tower wall and ii) The increase in sound absorbing material inside the tower which would have had the effect of absorbing some of the airborne sound energy present.

A smaller but still significant reduction of approximately 5 dBA was seen in the sound intensity measurements taken around the tower base (see figure 4.4.3). This reinforced the notion that the damping was effectively preventing the transmission of structure-borne sound down the tower, but also showed that the reduction in sound pressure level observed inside the tower was probably largely due to acoustic absorption rather than structural damping alone – hence the difference in sound level reduction observed between the inside and outside of the tower.

The reduction in sound intensity level meant that the contribution of tower noise to the total sound power of the turbine would have been reduced from 8% – 12% to approximately 3% - 4%.

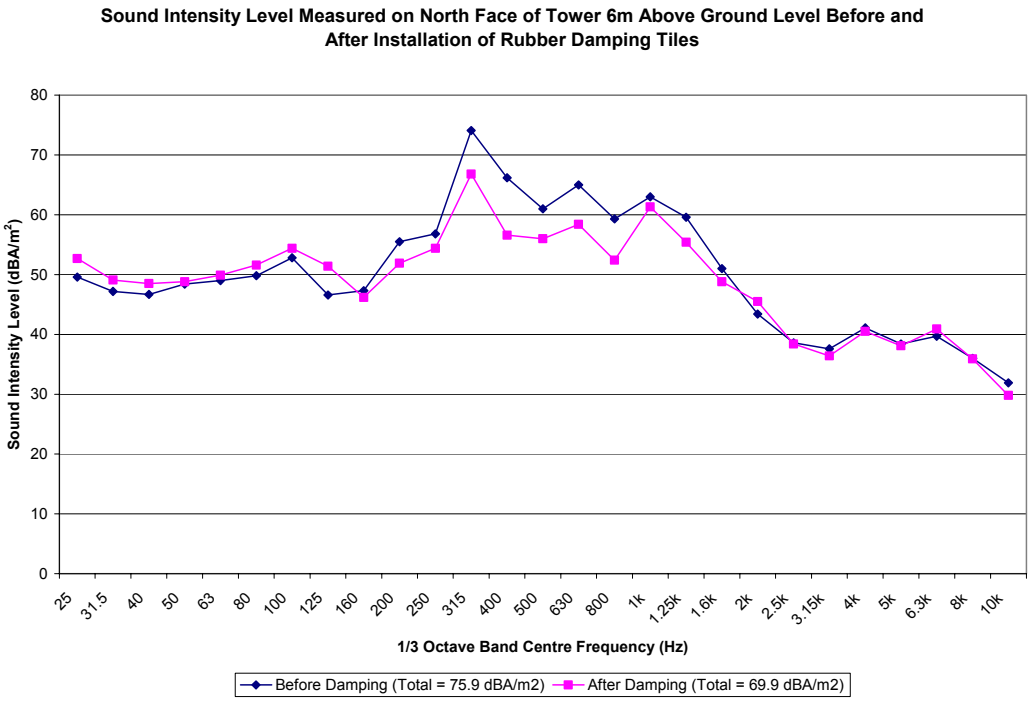

Figure 4.4.3 – Effect of Tower Damping on Sound Intensity Level at Tower Base

In the far field it was found that the sound pressure levels measured before and after the treatment were not appreciably different. The tower was therefore not the major contributor to the total noise radiated from the wind turbine. Table 4.4.1 below shows the levels measured before and after the treatment.

Table 4.4.1 – Sound Pressure Levels from Turbine Before and After Tower Treatment

Distance from Turbine (m)	Before Rubber L_{PA} (dBA)	After Rubber L_{PA} (dBA)
30	67.6	66.3
66	67.0	67.0
90	60.0	61.0
100	57.8	57.0
320	49.7	49.9
1400	32.0	31.2

5. Conclusions and Recommendations

The addition of rubber damping mats to the inside surface of the tower at the three locations of greatest vibration significantly reduced the vibration of the tower wall. This in turn reduced the level of structure-borne sound radiating from the tower. Most notably a reduction of 9 dBA was observed inside the tower base.

The reductions in tower noise observed did not however translate to far field sound pressure level reductions, which indicated that the tower was not the dominant source of noise from the wind turbine.

Given that blade noise was likely to be the major contributor to the total sound power of the wind turbine, a thorough blade noise investigation was considered necessary in order to quantify the level and characteristics of this noise together with the proportion of structurally transmitted to aerodynamically produced blade noise.

Chapter 5
Gearbox Noise Investigation

Summary

It was recognised that tonal noise from the gearbox of the Windflow 500 was a major contributor to the total noise from the wind turbine and had an important influence on the annoyance factor of the noise when observed from nearby residences. Three investigations were undertaken in an attempt to reduce the noise emitted by the gearbox, with a particular emphasis on the tone observed at approximately 311 Hz due to the second stage gear meshing frequency. The objective of this work was to reduce the noise without necessitating the removal of the gearbox from the turbine for modification.

The objective of the first investigation was to evaluate the effects of inserting a flexible coupling on the gearbox output shaft between the gearbox and the generator. The purpose of the coupling was to provide damping for driveline vibrations and inhibit the path of the gearbox vibrations to the turbine structure. Sound pressure levels were measured before and after installing the coupling, both inside the nacelle and at several points in the area around the turbine. It was found that the coupling had no effect on the 311 Hz tone, but did slightly reduce the noise produced at frequencies above 800 Hz. The flexible elements in the coupling are likely to have had a major influence on the frequencies affected by its installation and further work could be done with different flexible element types to see if the coupling could be better tuned to damp the 311 Hz frequency.

The second investigation was of the noise reduction that could be achieved by using a gearbox oil additive in the gearbox. An additive was selected and added to the gearbox as per the additive manufacturer's instructions. Sound pressure levels were then evaluated on a before and after basis as for the flexible coupling investigation. It was observed that a large reduction in sound pressure level was

made at the frequencies between 80 and 200 Hz along with a less significant one at frequencies above 2.5 kHz. In the 315 Hz 1/3 octave band (second stage gear meshing frequency) the reduction observed was within the limits of accuracy of the measurements, and in the 1000 Hz 1/3 octave band (third and fourth stage gear meshing frequencies) the noise level was actually increased. Had the first stage gear meshing frequency of 100 Hz been a problem, the additive may have been more a more successful method of reducing the noise, but for the given situation it was not particularly successful and it was unclear as to whether or not the additive was performing as suggested by the manufacturer.

The third investigation was concerned with the design of the gearbox. It was found through testing of the gearbox at different operating speeds, that a resonance in the gearbox existed in the 318 Hz to 330 Hz region. This resonance region was close to the 311 Hz tone and was considered to be part of the reason that the 311 Hz tone was so prominent. Windflow Technology therefore proposed to further study the gearbox design with a view to shifting the resonance frequency away from the second stage gear meshing frequency. In addition to this, an internal inspection of the gearbox was carried out and it was found that a design error in the second stage was allowing a thrust collar to rub on the gear teeth as they passed. This was thought to be increasing the noise from the second stage so a modification was made to fix the problem. The effect of the modification on sound and vibration levels was then evaluated, however no change was observed.

As a result of these three investigations, no reduction in tonal noise from the gearbox has yet been achieved. However, ongoing work by Windflow Technology and the gearbox manufacturer on the design of the gearbox and its dynamics may provide some tonal noise reduction in the future.

Table of Contents

List of Figures

List of Tables

1. Introduction

1.1 Background

Previous testing had shown that a significant proportion of the noise from the turbine was being generated by the gearbox. In particular, the second step-up stage in the gearbox was creating a prominent tone at a frequency of 310.9 Hz (313.4 Hz gear tooth meshing frequency shifted by the 2.5 Hz planet carrier speed). By reducing the noise and vibration generated by the gearbox, and hence the amount transmitted to the tower, blades and nacelle cladding, the total noise generated by the turbine would be decreased. Along with this, by reducing the magnitude of the tones originating from the gearbox, the annoyance factor of the sound would also be reduced.

1.2 Gearbox Specifications

The gearbox was located inside the nacelle with the input shaft connected directly to the blade hub and the output shaft connected to the generator at the rear of the nacelle. The gearbox itself was bolted to the pallet rigidly via flanges on the side of the casing (see figure 5.1.1).

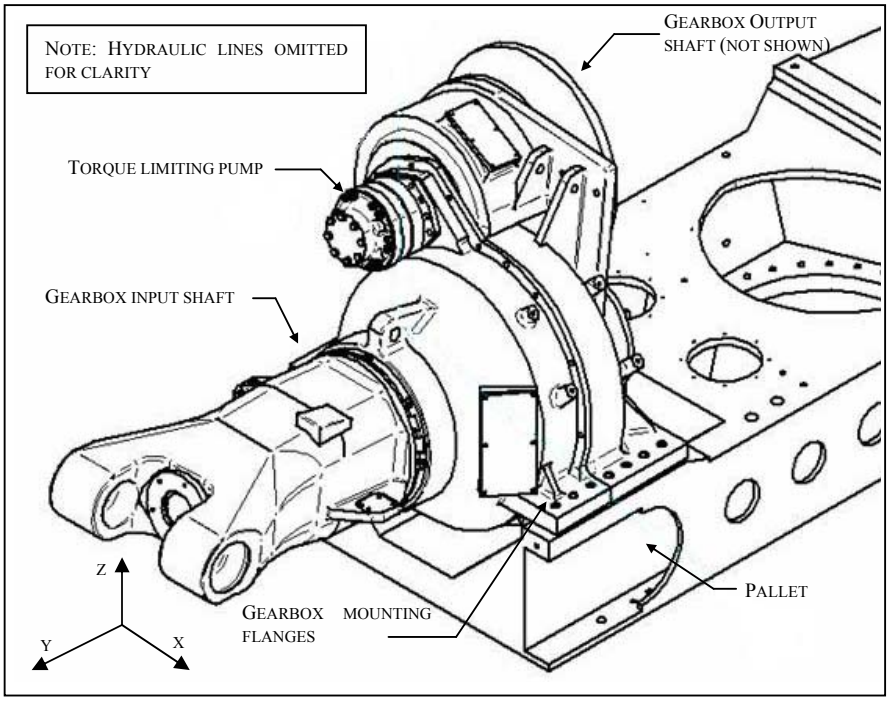

Figure 5.1.1 – Gearbox Mounting

The gearbox consisted of four speed increasing stages and included a torque limiting mechanism on the final stage which allowed slight variations of input shaft speed (typically between 48 and 50 rpm) to occur while maintaining a constant speed of 1500 rpm on the output shaft. This was necessary for the directly on-line synchronous generator to generate alternating current at a frequency of 50Hz. Table 5.1.1 below provides more detailed specifications of the gearbox.

Table 5.1.1 – Gearbox Specifications

Windflow 500 Torque Limiting Gearbox Specifications	
Design	Geoff Henderson
Manufacuturer	AH Gears, Auckland, NZ
Stages	4
Overall Ratio	1:31.1 (Nominal)
Casing Material	Cast Iron
Oil Type	Mobil SHC 632
Oil Quantity	80 Litres
Torque Limiting Pump	3.3 kN.m Radial Piston Motor
Stage 1	
Type	Planetary
Ratio	1:3.11
Planets	8
Planet Teeth	32
Sun Teeth	59
Ring Gear Teeth	125
Input Side (rpm)	
Ring Gear Rotational Speed	0
Carrier Rotational Speed	48.2 (Nominal)
Output Side (rpm)	
Sun Gear Rotational Speed	150.4
Gear Meshing Frequency (Hz)	100.4
Stage 2	
Type	Planetary
Ratio	1:3.11
Planets	4
Planet Teeth	32
Sun Teeth	59
Ring Gear Teeth	125
Input Side (rpm)	
Ring Gear Rotational Speed	0
Carrier Rotational Speed	150.4
Output Side (rpm)	
Sun Gear Rotational Speed	469.1
Gear Meshing Frequency (Hz)	313.4

Stage 3	
Type	Parallel
Ratio	1:2.17
Pinion Teeth	58
Gear Teeth	126
Input Side (rpm)	
Pinion Gear Rotational Speed	469.1
Output Side (rpm)	
Output Gear Rotational Speed	1019.0
Gear Meshing Frequency (Hz)	985.1

Stage 4 (Torque Limiting Stage)	
Type	Planetary
Ratio	1:1.47 (Nominal)
Planets	6
Planet Teeth	32
Sun Teeth	59
Ring Gear Teeth	125
Input Side (rpm)	
Sun Gear Rotational Speed	0.0 (Nominal)
Carrier Rotational Speed	1019.0
Output Side (rpm)	
Ring Gear Rotational Speed	1500.0
Gear Meshing Frequency (Hz)	1002.0

1.3 Objectives

The aim of the investigation was to reduce the noise generated by the gearbox at all frequencies but with particular emphasis on reducing or eliminating the 311 Hz tone from the second stage. A secondary objective of the investigation was to reduce the noise from the gearbox without requiring its removal from the turbine for modification.

2. Noise Reduction Investigation I – Flexible Coupling

2.1 Introduction

It was proposed that a flexible shaft coupling be installed on the high speed shaft between the gearbox and the generator in order to introduce some damping to the gearbox / generator system thereby reducing the driveline vibration and noise originating from the gearbox.

A claw type flexible coupling (Centaflex E-275) manufactured by Centa was selected and installed as shown figure 5.2.1. The coupling utilised compression stressed rubber elements to transmit the torque and provide vibration damping (see figure 5.2.2).

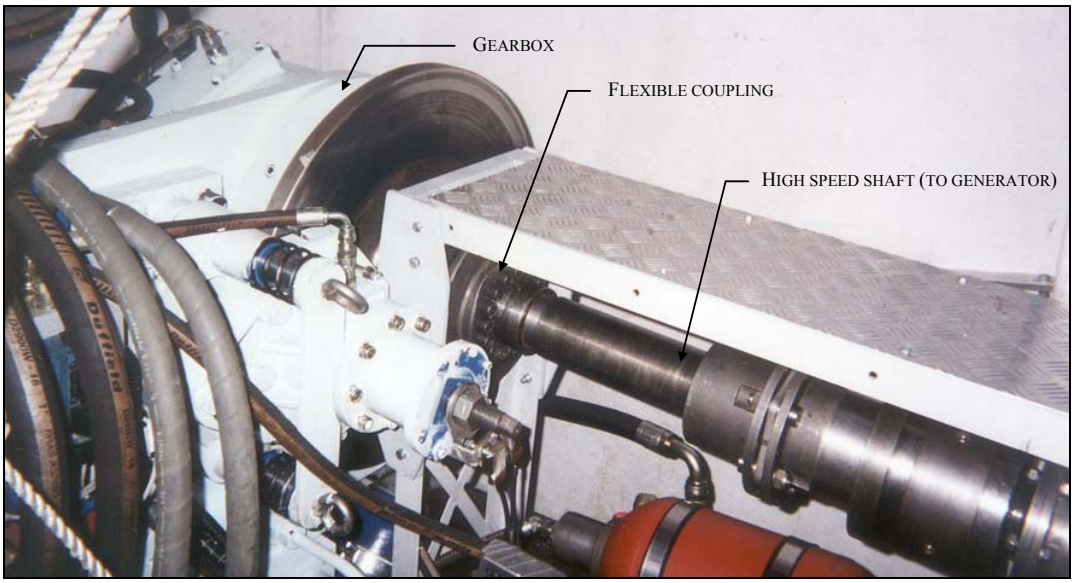

Figure 5.2.1 – Installed Coupling

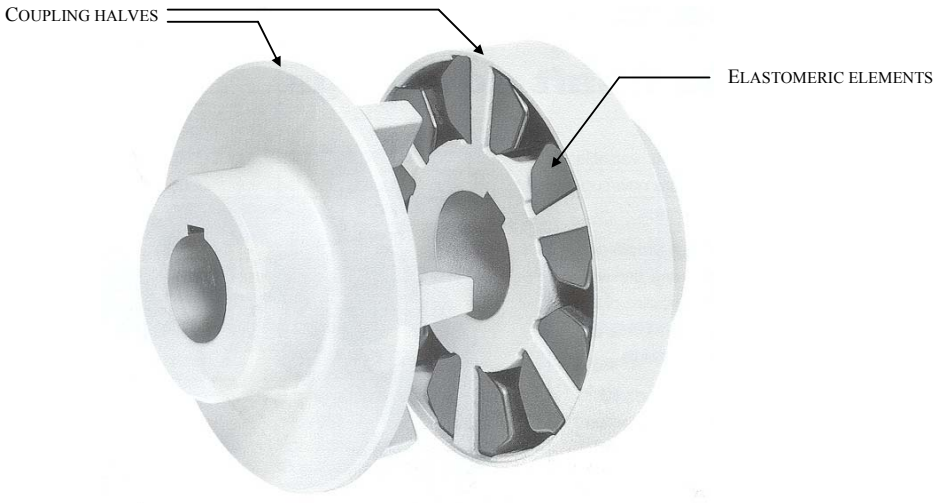

Figure 5.2.2 – Coupling Schematic

2.2 Method of Assessment

A Bruel and Kjaer 2260 Type I sound level meter was used to measure the sound pressure level (30 second L_{eq}) inside the nacelle of the turbine and at the points around the turbine shown in table 5.2.1, before and after the coupling was installed.

Table 5.2.1 – Measurement Locations

Meas #	Location
1	Inside Nacelle
2	30m W of Turbine
3	66m NE of Turbine
4	90m E of Turbine
5	100m S of Turbine
6	320m N of Turbine
7	640m NE of Turbine
8	800m W of Turbine
9	840m NW of Turbine

The measurements were done with the wind blowing at an approximately constant 10 m/s from the NE as measured by the meteorological mast at the wind turbine site 30m AGL.

2.3 Results and Analysis

2.3.1 Sound Pressure Level Variation with Distance

Figure 5.2.3 shows the variation of sound pressure levels measured at various distances from the turbine before and after installation of the coupling, compared with the levels predicted using data from the WEG MS3 wind turbine (a similar design of turbine sited in the UK) [1]. As can be seen from the graph, the sound pressure levels before and after installation of the coupling are similar. In both cases the measured sound pressure levels are above those predicted from the MS3 data.

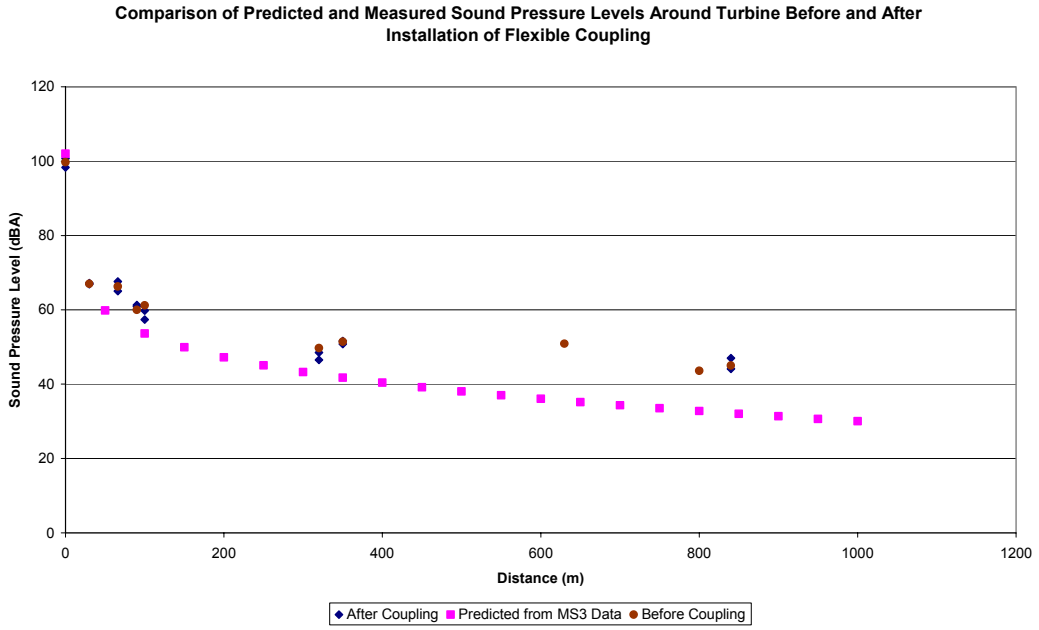

Figure 5.2.3 – Sound Pressure Level Variation with Distance

Variation in the above measurements can largely be accounted for by fluctuations in the background noise level while the measurements were being taken. At distances greater than about 300m, the sound level produced by the turbine is of a similar magnitude to the background noise level - hence the results become particularly sensitive to background noise fluctuations. For this reason the total sound pressure levels measured at each location do not give a truly accurate indication of the noise emitted by the turbine.

2.3.2 Spectral Analysis – Outside Turbine

Figure 5.2.4 shows sound pressure level spectrums taken 90m east of the turbine before and after installation of the coupling.

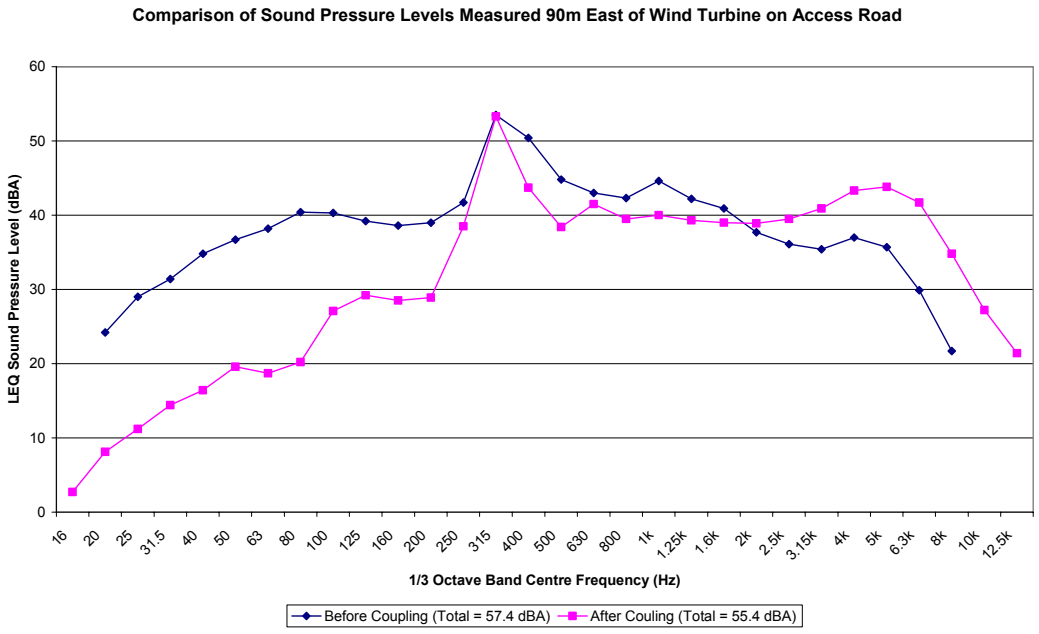

Figure 5.2.4 – Sample Spectrum

As can be seen from the graph, the tonal peak in the 315Hz 1/3 octave band was not reduced – this was also shown in the spectrums measured at the other points in the area of the turbine. The large variations at other frequencies in the spectrum can probably be attributed to differences in the background noise level between measurements. While the tonal noise from the gearbox (315Hz band) usually stood prominently above the background noise level, at other frequencies the sound pressure levels were not sufficiently far above the background noise level to remain uninfluenced by the background noise. This meant that the level of the 315Hz 1/3 octave band was the best gauge of the effectiveness of any modifications that were made.

2.3.3 Spectral Analysis – Inside Turbine

Several sound pressure level measurements were taken inside the turbine at the base of the tower and inside the nacelle. In general the measurements showed a small reduction in sound pressure level at frequencies above 800 Hz. This is illustrated in figure 5.2.5 below, which was measured in the centre of the nacelle.

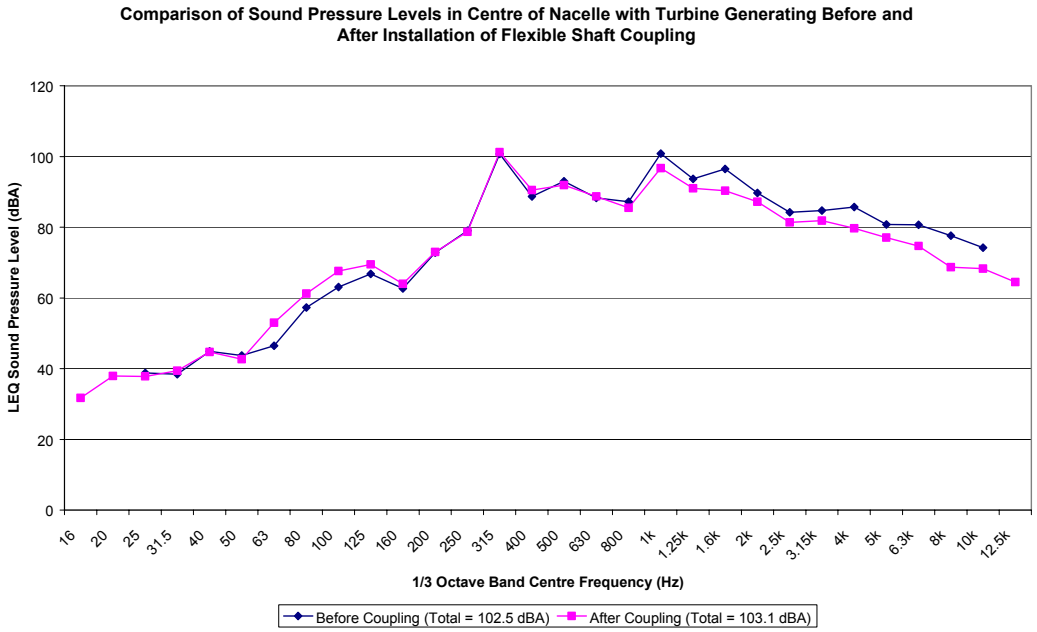

Figure 5.2.5 – Nacelle Spectrum

However, as can be seen from figure 5.2.5 the sound level inside the nacelle at 315Hz was unchanged following installation of the coupling. This along with the results of the measurements taken at a distance indicated that the flexible coupling was neither an effective method of reducing the 311Hz tone originating from the gearbox nor an effective method of reducing the overall noise radiated from the turbine.

3. Noise Reduction Investigation II - Oil Additive

3.1 Introduction

The use of a gearbox oil additive was identified as another possible means of quietening the wind turbine gearbox. While a number of gearbox experts including the gearbox manufacturer recommended that the additive would not be effective in this instance, the failure consequences would be minimal. The oil additive was comparatively low cost and easy to install, not requiring permanent modification of the turbine. The use of a gearbox oil additive was therefore thought to be worthy of further investigation.

Power-Up NNL 690G, an additive designed to reduce noise, vibration and wear in heavy machine gearboxes was selected for use in the investigation. Four litres of the additive were poured into the gearbox oil sump as per the manufacturers' instructions (5% additive to oil ratio). The turbine was then run for approximately half an hour before sound level measurements were made so as to allow the turbine to reach operating temperature and the oil to mix properly with the additive.

3.2 Method of Assessment

Measurements of the sound pressure level at several locations around the turbine were made before and after the addition of the additive, as per the method of assessment previously described in section 2.2, with the difference that the wind speed varied in the range of 6 – 10 m/s.

3.3 Results and Analysis

Figure 5.3.1 shows a comparison of the sound pressure levels measured inside the nacelle before and after the addition of the oil additive to the gearbox.

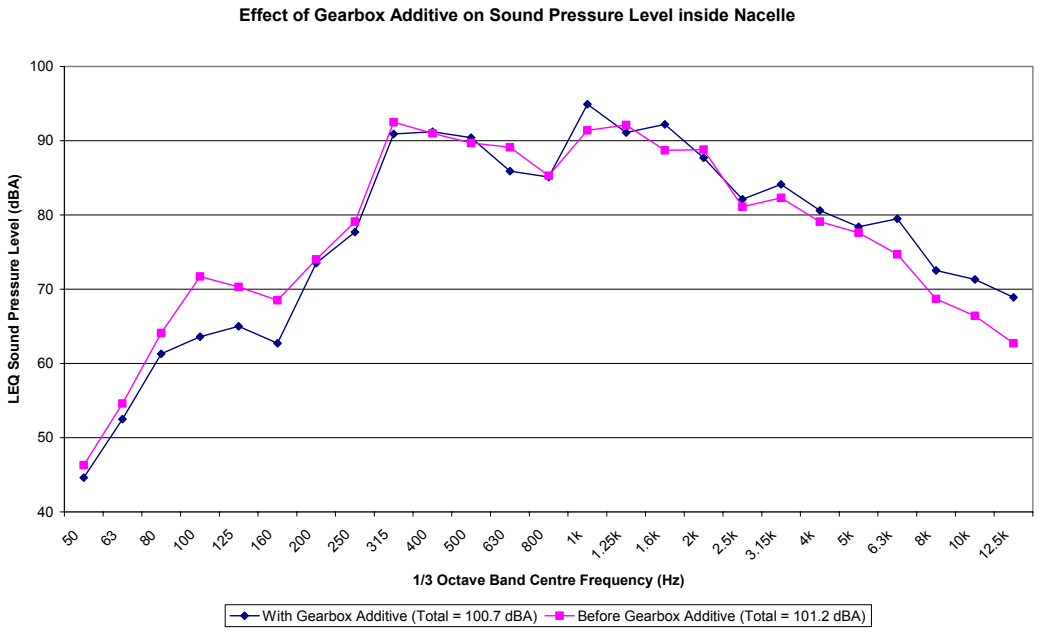

Figure 5.3.1 – Effect of Gearbox Additive on SPL Inside Nacelle

As can be seen from the graph, the sound pressure levels were reduced at frequencies below 400Hz, particularly between 80 and 200Hz. In the 315Hz 1/3 octave band the reduction measured was 1.6 dB – arguably within the limits of the measurement accuracy. In the 1/3 octave bands of 1 kHz, 1.6 kHz and the bands above 2.5 kHz the sound pressure level inside the nacelle increased after the addition of the additive.

Had the additive been working effectively it would have been expected that the noise level particularly at the gear meshing frequencies (100Hz, 315Hz, and 1000Hz bands) would have been reduced, which particularly for the 1000Hz band, is clearly not the case. While the measurements were repeated and checked for consistency as much as possible they still however need to be interpreted with some caution. The gearbox was not the only noise source present during measurement and consequently changes in the noise level from other equipment in the nacelle such as the generator and hydraulic power unit, may have also contributed to the slight reductions and increases observed. The characteristics of the wind and the amount of power produced by the turbine would also have been slightly different during each measurement. On the whole though, the trends observed above were consistent over several measurements.

At the measurement locations in the area around the turbine no change in sound pressure level was observed after the addition of the additive, as would be expected given that there was also no significant change measured inside the nacelle.

The results of this investigation would indicate that as a means of reducing the overall noise level from the gearbox the additive was not particularly successful, however what is clear is that the noise inside the nacelle was significantly reduced at the frequencies between 80 and 160Hz. Had noise from the first stage gear meshing frequency of 100Hz been a problem, the additive would have been an effective means of reducing this. Without understanding the mechanisms at work with the additive installed, it is very difficult to explain why the noise was reduced or increased at the particular frequencies observed and not just at the gear meshing frequencies.

4. Noise Reduction Investigation III – Internal Design

4.1 Introduction

Given the unsuccessful results of the previous investigations it was decided that it would be worthwhile to pursue an attempt to reduce the magnitude of the tone via an internal design change to the gearbox. The first step was to establish the reason(s) why the second stage of the gearbox produced such a prominent tone at the gear meshing frequency while the gear meshing frequencies of the other stages did not exhibit a tone.

4.2 General Approach

4.2.1 Hypothesis I – Gear Tooth Forces

On inspection of the gearbox design it can be seen that the second stage of the gearbox contained only 4 planet gears whereas the first and fourth planetary stages contained 8 and 6 respectively. It was initially thought that this would have resulted in much higher tooth forces being generated in the second stage than the other stages and hence a stronger vibration at the gear meshing frequency. However, tooth forces were calculated for each gearbox stage and it was found that the first stage of the gearbox was subject to the highest tooth forces. This indicated that high tooth forces were not necessarily to blame for the tone observed from the second stage since no major tone was observed at the first stage gear meshing frequency of 100 Hz. It was noted that reducing the tooth forces could still affect the magnitude of the vibration and the opportunity to add extra planet gears to the second stage in order to do this was left as a possibility for further investigation.

4.2.2 Hypothesis II – System Resonance

Another theory was that the gear meshing frequency of the second stage in the gearbox may have been at or near to a resonant frequency of the gearbox or the adjoined mechanical systems. This possibility was investigated both theoretically and experimentally. The theorectical investigation was carried out by Matrix – an Auckland based computational solid mechanics specialist. Matrix looked for resonances in the gearbox casing, pallet and in the wind turbine as a complete system. Matrix's model showed that the gearbox and pallet combination had several high order resonant modes of vibration near to 311 Hz.

Following this an experimental investigation of resonances was conducted. Initially the turbine was run at rotor speeds (speed controlled) from 40 to 56 rpm in 1 rpm increments with no electrical load on the generator. At each speed the x, y, and z accelerations were measured at a point on the gearbox and the sound pressure level 320m from the turbine was recorded. The spectral peak due to the second stage gear meshing frequency was identified for each rotor speed (the gear meshing frequency increases with increasing rotor speed) and the magnitude of the peak was plotted against the rotor rpm. The results of this test showed only a weak correlation with the computational model and were generally inconclusive. It also showed that the 1/3 octave band frequency resolution of the Bruel and Kjaer 2260 sound level meter used for the sound pressure measurements was too wide to satisfactorily distinguish the level of the peak due to the gear meshing frequency. That is the 315 Hz 1/3 octave band upper and lower limits are 385 Hz and 282 Hz respectively, but the gear meshing frequency in the tests ranged from 259 Hz to 363 Hz. Consequently for some rotor speeds the magnitude of the tonal peak was slurred over two 1/3 octave bands resulting in measurements that were not directly comparable.

The same vibration tests were repeated again with a load applied to the generator. The synchronous generator was run in islanded mode (disconnected from the grid) and the generator load was supplied electrically by a fan cooled variable load bank. The load was adjusted for each rotor speed so as to maintain a constant torque on the gearbox (25% of rated) and hence constant tooth forces on the gears. Table 5.4.1 shows the electrical load applied at each speed to maintain constant tooth forces, along with the gear meshing frequency for each rotor speed. Note that the actual load applied at each speed was limited to being adjusted 5kW increments by the load bank.

Table 5.4.1 – Electrical Load Applied at Each Rotor Speed

Rotor Speed (rpm)	2nd Stage GMF (Hz)	Ideal Load Applied (kW)	Actual Load Applied (kW)
40	259	104	105
41	266	107	105
42	272	109	110
43	279	112	110
44	285	115	115
45	292	117	115
46	298	120	120
47	305	122	120
48	311	125	125
49	317	128	130
50	324	130	130
51	330	133	135
52	337	135	135
53	343	138	140
54	350	141	140
55	356	143	145
56	363	146	145

The results of the tests showed that some form of resonance existed in the gearbox near to the nominal second stage gear meshing frequency of 311 Hz. Graphs of the displacement of the gearbox case in the transverse, longitudinal and vertical directions (x, y and z respectively – refer to figure 5.1.1) are shown in figures 5.4.1 – 5.4.3.

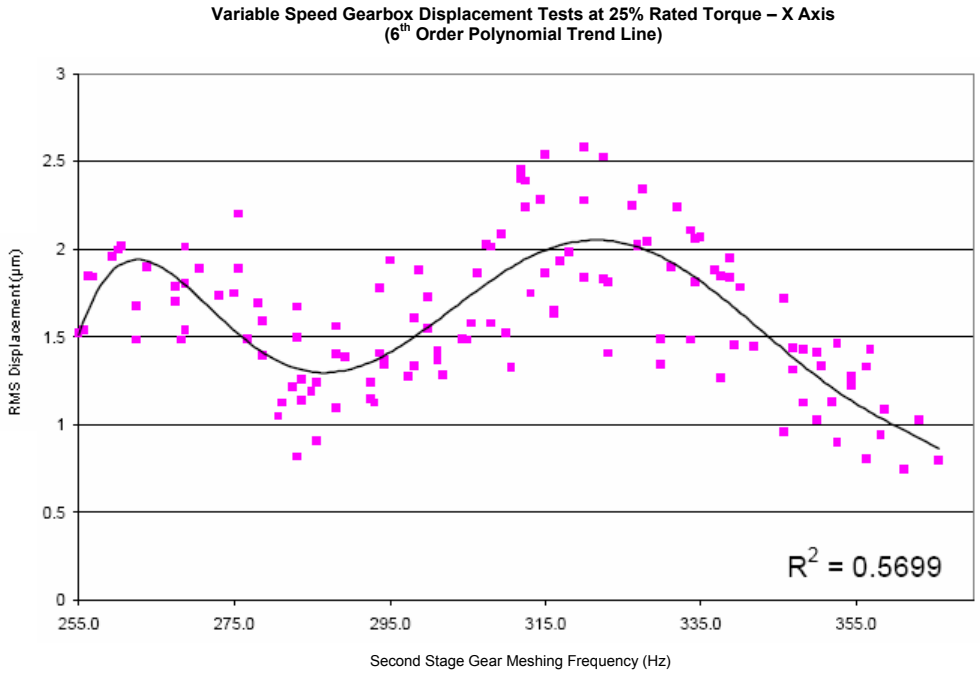

Figure 5.4.1 – X-Axis Gearbox Displacement (Transverse)

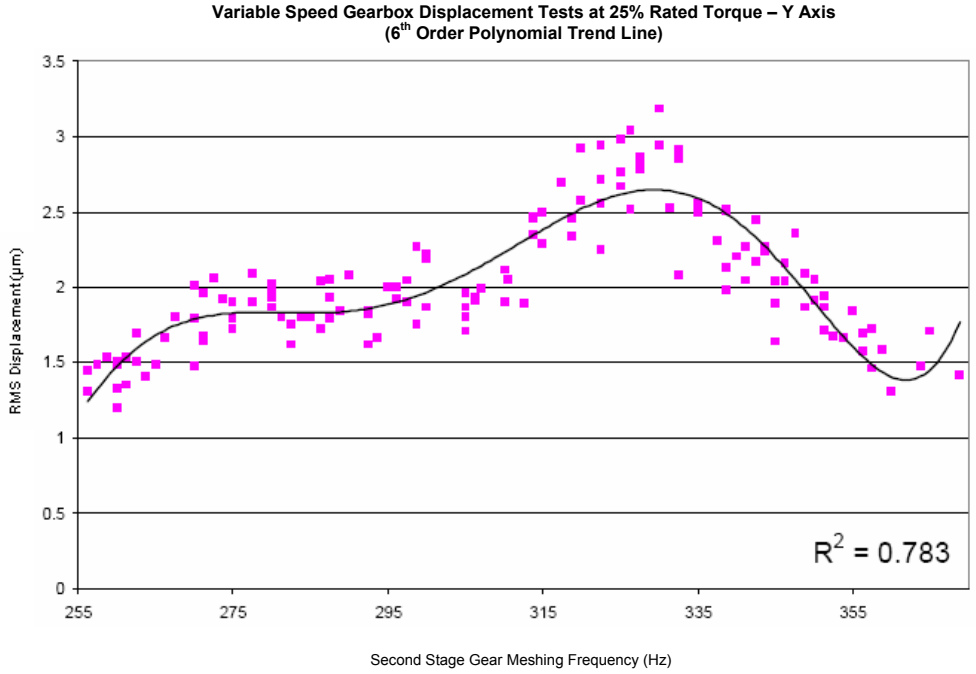

Figure 5.4.2 – Y-Axis Gearbox Displacement (Longitudinal)

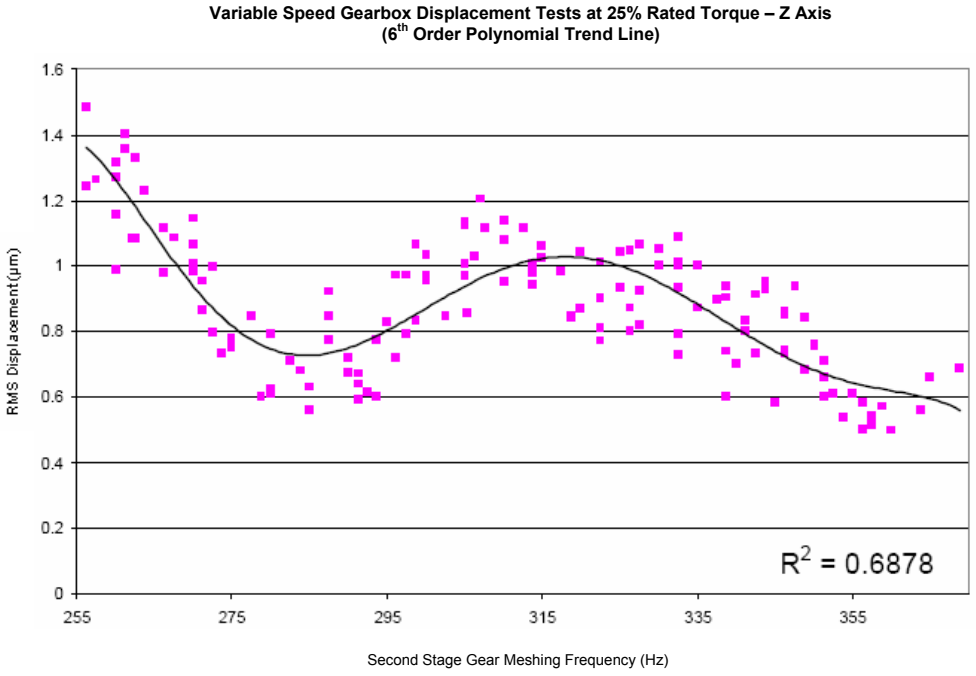

Figure 5.4.3 – Z-Axis Gearbox Displacement (Vertical)

As can be seen from the graphs, the magnitude of the displacement of the gearbox case reached a maximum when the second stage gear meshing frequency was somewhere in the region of 318 Hz to 330 Hz i.e. the area of resonance observed was very close to the nominal gear meshing frequency of the second stage.

Assuming these results were correct and did actually show a resonance then it would be possible to reduce the tonal noise originating from the second stage of the gearbox either by changing the gear meshing frequency to distance it from the resonance region or by changing the design of the gearbox so as to change the frequency of resonance. At the time of writing Windflow Technology was undertaking further research into the idea of altering the gearbox design to move the resonance region away from the gear meshing frequency.

4.3.3 Hypothesis III – Design Error

The third theory suggested was that there was a design or manufacturing error made in the construction of the gearbox which was allowing the unexpectedly high levels of vibration to occur. In order to investigate this without necessitating removal of the gearbox from the turbine, Air New Zealand Engineering Services was contracted to make an internal inspection of the gearbox using an endoscope. The gearbox was inspected for broken or damaged components, abnormal wear and features that differed from those specified in the design.

The endoscope exploration of the gearbox found that a thrust collar used to provide axial alignment for the floating member connecting the first stage sun gear to the second stage planet carrier, had an unusual amount of wear on it (see figure 5.4.1). Further investigation of this found that due to a design error the thrust collar was able to rub on the gear teeth as they passed. Windflow's hypothesis was that the rubbing collar was increasing the level of vibration at the second stage gear meshing frequency and providing a transmission path for the vibration to travel into other parts of the gearbox and turbine.

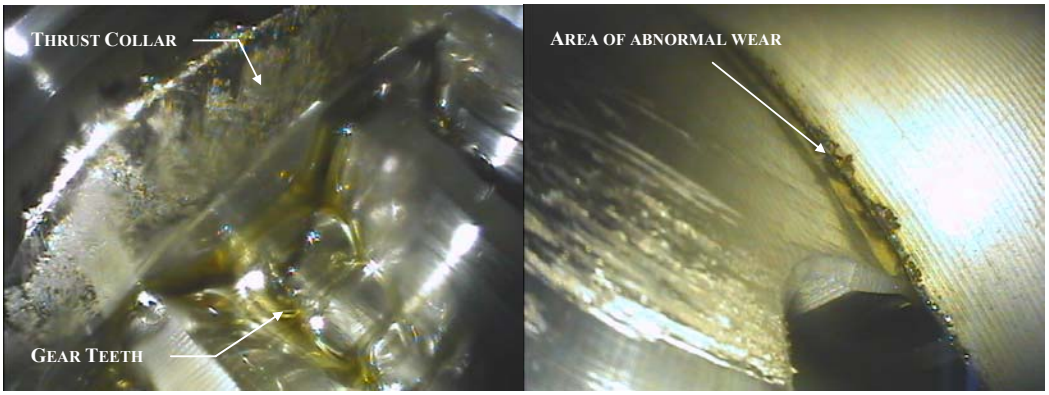

Figure 5.4.4 – Thrust Collar Wear (Endoscope Photographs)

With this evidence in hand the decision was made to remove the gearbox from the turbine. Once removed the gearbox was modified to correct the problem identified and thoroughly inspected to find any other possible noise and vibration inducing faults.

After the modification to the thrust collar was made, the gearbox was re-installed in the turbine and noise and vibration measurements were carried out.

4.3 Method of Assessment

The sound pressure level of the turbine was measured inside the nacelle and at several locations around the turbine as per the method of assessment described in section 2.2. In parallel to this Windflow Technology carried out tests to measure vibration at several points on the gearbox casing.

4.4 Results and Analysis

Figure 5.4.2 shows the sound pressure level in the nacelle with the turbine generating 300 kW of power before and after modification of the gearbox. The graph shows that no change resulted from the modification. This was also shown by the sound level measurements taken at points around the turbine. The vibration measurements taken by Windflow provided confirmation that no improvement had been made to the noise level from the turbine as they too were had not changed since the modification was made.

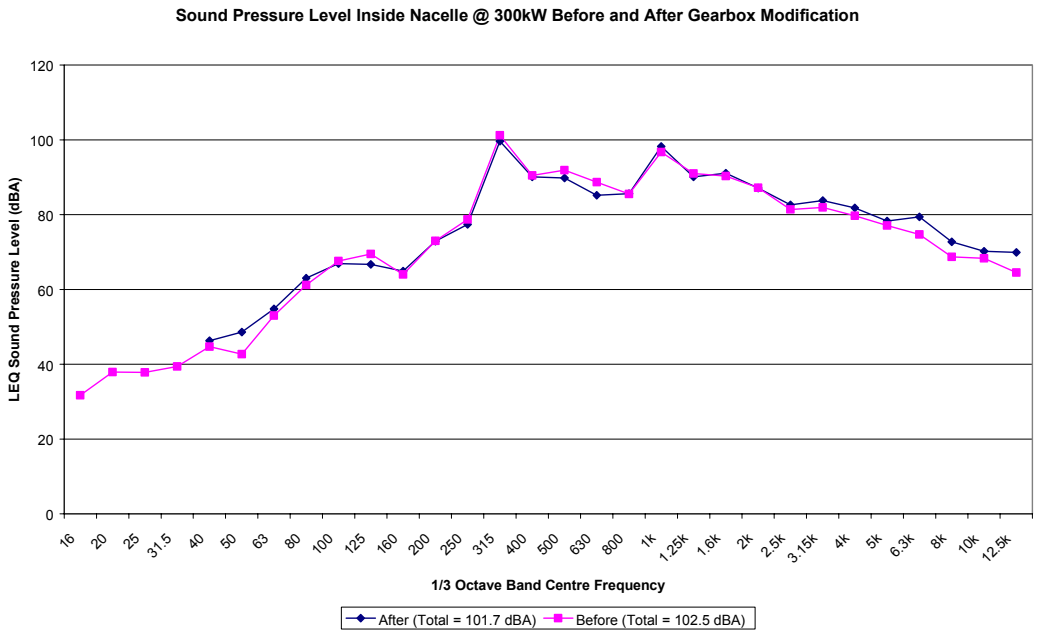

Figure 5.4.5 – SPL Inside Nacelle Before and After Gearbox Modification

These results provided evidence that the cause of the noise and vibration problem had not been correctly identified and further remedial work would need to be carried out to solve it. At the time of writing, no successful method of reducing 311 Hz tone from the gearbox had been found and Windflow Technology was conducting further tests on the gearbox to establish the cause of the abnormal levels of vibration.

5. Conclusions and Recommendations

Three methods of reducing the noise and vibration from the second stage of the gearbox on the Windflow 500 have been tried and tested. The insertion of a flexible coupling between the generator and gearbox to damp out driveline vibration was found to reduce the noise inside the nacelle slightly at high frequencies but not in the 315 Hz 1/3 octave band as intended. Further work on this could be conducted to establish how well suited the rubber elements in the coupling were to damping the 315 Hz vibrations or if there was another alternative that might work better.

The addition of a gearbox oil additive to the gearbox oil was found to reduce the noise at some frequencies while increasing the noise at others. Perhaps surprisingly the noise produced at the gear meshing frequencies remained largely unaffected by the additive (except in the 1000 Hz band where the

noise increased significantly). This indicated that the additive was not performing as suggested by the manufacturer and was not an effective means of reducing the tonal noise from the gearbox.

The third method that was attempted for reducing the noise from the gearbox was to modify the gearbox design to reduce the noise at the source. During an internal exploration of the gearbox it was found that due to a design error a thrust collar in the second stage was rubbing on the gear teeth as they passed. This was thought by Windflow Technology to be the source of the noise problem, so was modified to prevent the rubbing. The results of testing conducted after the modification was made showed no difference from the original sound levels measured. At the time of writing further research was being carried out in order to establish why the tone at the gear meshing frequency of the gearbox second stage was so prominent.

6. References

[1] P.H.Geraets, "Noise and Vibration Measurements on the 33m MS3 Wind Turbine at Carmarthen Bay During November / December 1988," Wind Energy Group WEG 33-6201, 3 January 1989.

Chapter 6
Reduction of Sound Radiation from the Nacelle Cladding

Summary

The amount by which the noise radiated directly from the nacelle could be reduced was investigated. Two conventional noise reduction techniques were evaluated – these were the addition of an acoustic barrier material to the inside of the nacelle cladding and the addition of sound absorbing material inside the cladding.

Acoustop Flexibarrier^{TM}, a mass loaded rubber barrier, was installed on the inside walls of the cladding and sound transmission loss measurements were made on the walls before and after installation. It was found that the barrier material increased the transmission loss of the wall significantly above 400 Hz with a maximum increase of about 12dB at 2.5 kHz. The field results were supported by laboratory data.

In another test, 12m^2 of acoustic grade polyether foam (sound absorbent) was taped to the walls and roof on the inside of the nacelle cladding. A speaker placed inside the nacelle produced pink noise at constant volume and the resulting sound pressure levels inside the nacelle were measured before and after installation of the foam. It was found that the foam reduced the sound pressure level by about 2dB with higher frequencies showing a greater reduction than low frequencies.

While the results showed that it was easily possible to make useful reductions in the noise radiated directly from the nacelle, it was concluded that in the case of the Windflow 500 (and possibly many other turbines), there would be no observable reduction in the overall noise emitted by the turbine since the noise radiated directly from the nacelle contributes only about 1% of the total noise from the turbine.

Table of Contents

List of Figures

1. Introduction

1.1 Background

One way to reduce the noise emitted from a wind turbine is to reduce the sound power radiated by the nacelle. It was decided that a method of reducing the airborne machinery noise transmitted through the nacelle cladding of the Windflow 500 turbine should be investigated. It was proposed that the effects of adding an acoustic barrier material and a sound absorbing medium to the inside of the nacelle cladding be evaluated and the noise reductions achieved quantified for future reference.

1.2 Theory

Sound transmission loss is a measure of the effectiveness of a panel, wall or other surface for preventing the transmission of noise. It is defined as the sound power incident on the panel minus the sound power transmitted through the panel (equation 6-1).

$$STL = L_{W-Incident} - L_{W-Transmitted} \qquad (6\text{-}1)$$

where STL is the sound transmission loss of the panel (dB)

$L_{W\text{-}Incident}$ is the sound power incident on the panel (dB)

$L_{W\text{-}Transmitted}$ is the sound power transmitted through the panel (dB)

When a reverberant field exists on the incidence side of the panel, it can be shown that the sound transmission loss is given by equation 6-2 below –

$$STL = L_{P-Incident} - 6 - L_{I-Transmitted} \qquad (6\text{-}2)$$

where STL is the sound transmission loss of the panel (dB)

$L_{P\text{-}Incident}$ is the sound pressure level measured in the reverberant field on the incidence side of the panel (dB)

$L_{I\text{-}Transmitted}$ is the sound intensity level measured on the surface of the other side of the panel (dB/m^2)

1.3 Objectives

There were two main objectives to the investigation –

1. To determine how much the sound transmission loss of the nacelle cladding could be increased by the addition of an acoustic barrier material to the walls and roof of the cladding.
2. To determine how much the reverberant sound field inside the nacelle could be reduced by the addition of sound absorbing material inside the nacelle, and hence measure the resulting reduction in sound radiated from the outer surface of the cladding.

2. Experimental Method

2.1 Acoustic Barrier Material Investigation

Sound transmission loss measurements were made on each wall of the nacelle cladding using the following method –

1. A JBL EON powered speaker was placed near to the centre of the nacelle as shown below in figure 6.2.1.

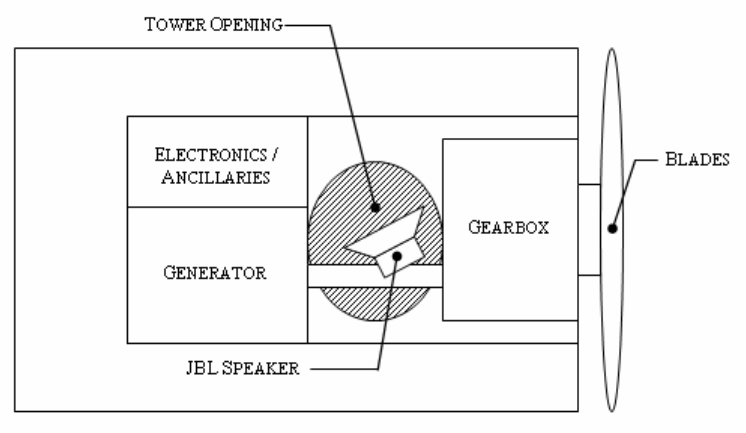

Figure 6.2.1 – Speaker Location

2. A Neutrik Minirator MR1 audio generator was used to create a pink noise signal which was played through the speaker. The speaker volume was adjusted so as to produce a sound pressure level of about 110 dB inside the nacelle.
3. A Bruel and Kjaer 2260 Type I sound level meter was then used to measure the sound pressure level (30 second L_{eq}) at a number of points inside the nacelle. It was found that the sound pressure level measured inside the nacelle was approximately constant regardless of location unless very close to a wall or the speaker. This confirmed that the sound field inside the nacelle was sufficiently reverberant to allow equation 6-2 to be used to calculate the sound transmission loss of the cladding.
4. Sound pressure levels were then measured inside the nacelle 500mm from the surface of interest at several locations on each wall.
5. Following this, the sound intensity levels were measured on the outside of the cladding at the corresponding locations using a Bruel and Kjaer Type 2260 Investigator with a Type 3595 sound intensity probe kit.
6. The sound transmission loss of the cladding was then calculated at each location using equation 6-2.

The sound transmission loss measurements were firstly done with the nacelle cladding in its original condition, and then repeated after installation of the acoustic barrier material. The barrier material was installed as follows –

A mass loaded rubber barrier material called Acoustop Flexibarrier^{TM} supplied by Latimer Acoustics was installed on the walls inside the nacelle. The barrier material had a density of 8 kg/m^2. To decouple the barrier material from the cladding a 50mm air gap was created between the barrier and the wall. This was done by placing a vertical wooden baton every 600mm along the cladding wall and gluing the barrier to them. Care was taken to ensure that all seams, holes and gaps in the barrier were properly sealed with sealing tape.

2.2 Sound Absorbing Material Investigation

A JBL EON powered speaker was set up in the nacelle as described previously in section 2.1. The sound pressure level (30 second L_{eq}) inside the nacelle was measured with the speaker producing random pink noise. This was firstly done with the nacelle in its original condition and then repeated with approximately $12m^2$ of 50mm thick polyether acoustic foam taped to the walls and roof on the inside surface of the cladding.

3. Results

3.1 Effect of Barrier Layer

The addition of the barrier layer to the inside of the nacelle cladding was found to significantly increase the sound transmission loss of the cladding at frequencies above 400 Hz. The increase in transmission loss was found to be up to 12dB at 3.15 kHz. At frequencies below 200 Hz it was unclear from the tests whether or not an improvement had been made by adding the barrier. Figure 6.3.1 below shows the transmission loss of the nacelle port side wall with the barrier layer installed compared to the transmission loss of the wall in its original condition.

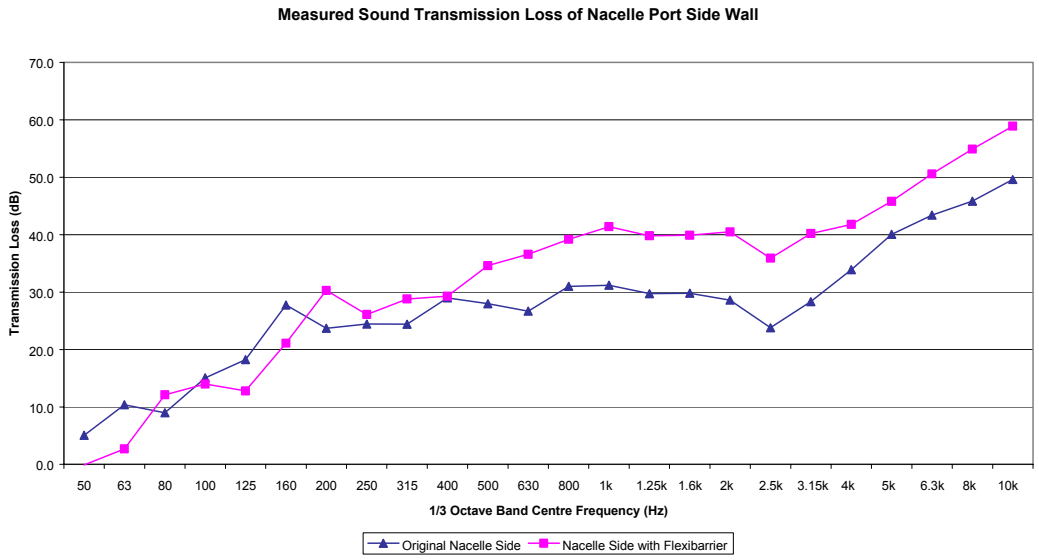

Figure 6.3.1 – Transmission Loss of Nacelle Port Side Wall

Transmission loss measurements on a flat panel of identical material to the nacelle cladding were carried out in the transmission loss suite at the University of Canterbury, prior to construction of the turbine. These measurements were commissioned by Windflow Technology. Figure 6.3.2 compares the transmission loss measurements of the nacelle cladding material with Flexibarrier™ attached in the laboratory tests and installed on the turbine. In the laboratory tests the Flexibarrier™ was bonded directly to the panel whereas an air gap was created when it was installed in the nacelle as described in section 2.1. Figure 6.3.3 shows the same comparison but for the material without Flexibarrier™ attached.

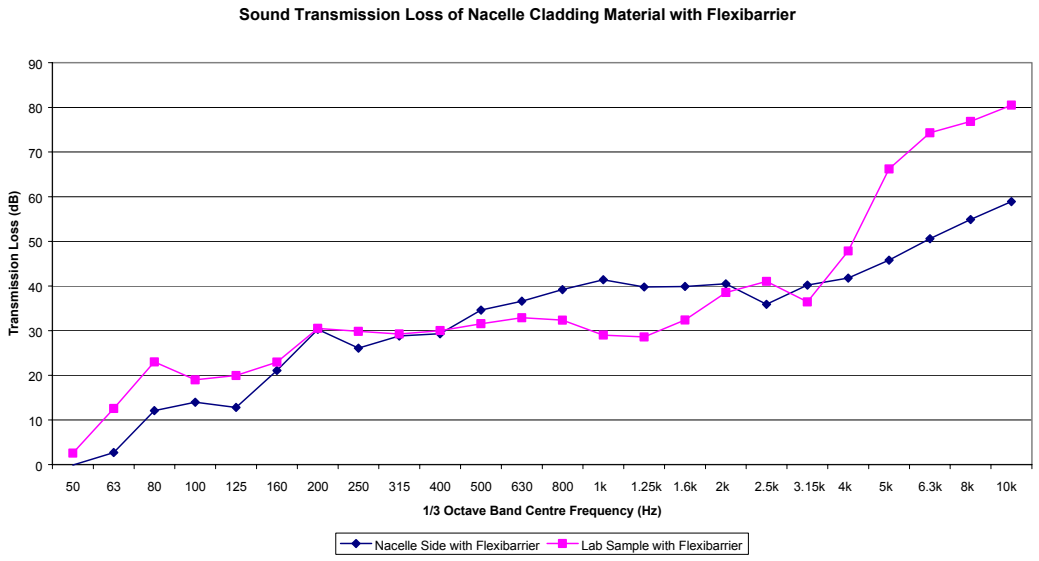

Figure 6.3.2 – Flat Panel Transmission Loss with Flexibarrier™

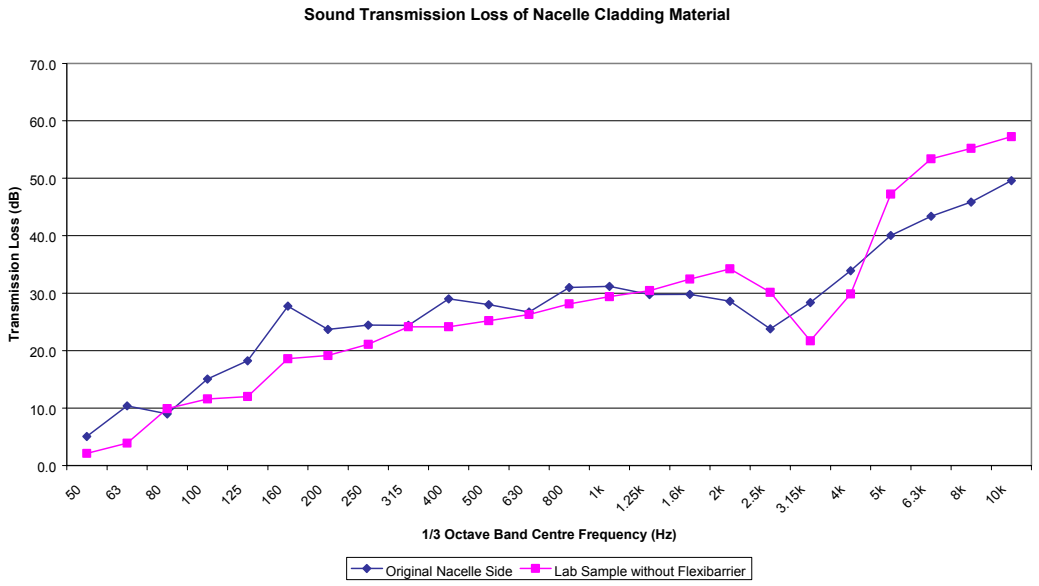

Figure 6.3.3 – Flat Panel Transmission Loss without Flexbarrier™

The laboratory data is generally in agreement with the field measured values however at high frequencies the flat panel in the laboratory clearly out-performed the nacelle cladding. The coincidence dip occurred in the 3.15 kHz 1/3 octave band in the laboratory tests but was shifted to the 2.5 kHz 1/3 octave band in the field measurements. This could have resulted from the material stiffness being slightly different when installed on the nacelle because of the curvature of the panel and the different boundary conditions present.

3.2 Effect of Sound Absorbing Material

The acoustic foam that was installed in the nacelle was found to reduce the total sound pressure level inside the nacelle by over 2dB. The foam was particularly effective at frequencies above 2.5 kHz but made a discernable reduction to the sound pressure level at all frequencies above about 100 Hz. Figure 6.3.4 below shows the sound pressure levels that were measured inside the nacelle before and after installation of the acoustic foam.

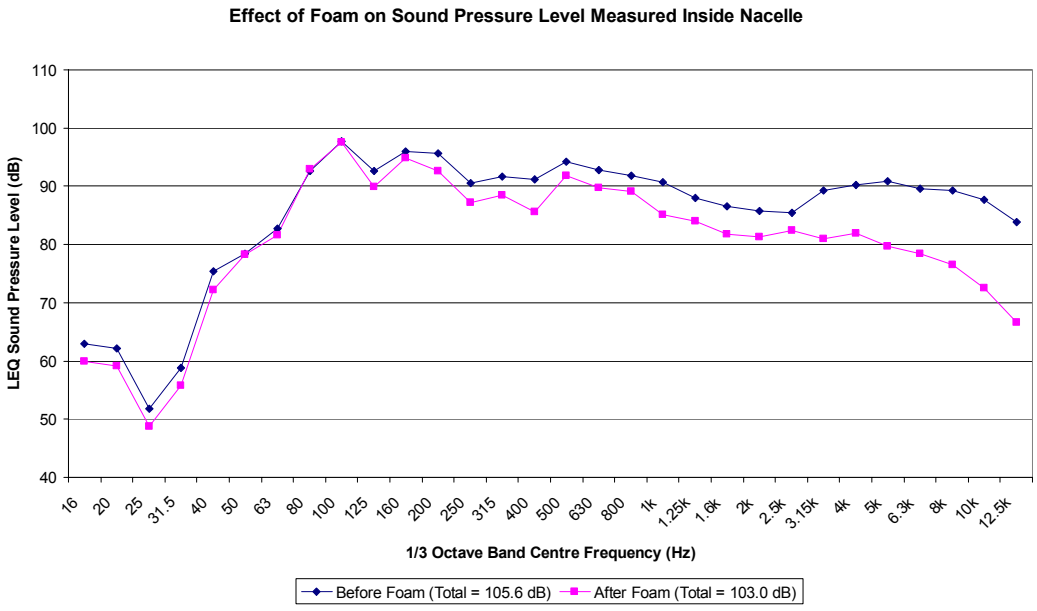

Figure 6.3.4 – Effect of Foam on Sound Pressure Level Inside the Nacelle

4. Discussion

The results of the tests showed that the noise radiated from the nacelle could be reduced considerably from the amount of noise radiated with the nacelle cladding in its original condition. However the addition of a barrier layer or sound absorbing material to the inside of the nacelle cladding is not necessarily an attractive method of reducing the noise level generated from a wind turbine. If the noise from the nacelle was the only noise present in the system then the sound pressure level outside the nacelle would be expected to decrease by the approximately the same amount as any reductions made inside by adding absorbing material. Similarly with transmission loss of the wall it could be expected that a reduction in sound pressure level outside the nacelle would be achieved that was proportional to the increase in transmission loss of the wall. However, the noise radiated directly from the nacelle is not the only contributor to the total noise of a wind turbine. In the case of the Windflow 500 turbine, the nacelle was found to directly radiate about 1% of the total sound power emitted by the turbine. This means that even if the noise radiated from the nacelle was entirely eliminated, the reduction in the total sound power level of the turbine that would be observed would be of the order of one or two tenths of a decibel. Clearly then, reducing the noise radiated directly from the nacelle is not a practical way of reducing the overall noise emitted by wind turbine unless the other larger contributors to the noise from the turbine are significantly reduced.

5. Conclusions and Recommendations

From the investigation it can be concluded that it is possible to decrease the noise radiated directly from the nacelle by 2 -3 dB by reducing the reverberant sound field inside the nacelle using sound absorbent material. Further useful reductions at mid to high frequencies, can be made by installing an acoustic barrier layer inside the nacelle. However, neither of these methods of noise reduction should be implemented unless the nacelle can be proven to be a major source of noise on the turbine – otherwise the noise reduction efforts will have no appreciable effect on the overall noise levels of the turbine.

Chapter 7
Investigation of Structure-Borne Blade Noise

Summary

Blade noise was shown to contribute over 85% of the total sound power produced by the Windflow 500. A preliminary investigation was of the structure-borne component of the blade noise was performed. The structure-borne blade noise largely originates from vibrations transmitted to the blade from machinery in the nacelle. However vibrations caused by pressure fluctuations on the surface of the blade as a result of inflow turbulence also contribute to this noise.

A blade was removed from the turbine and supported horizontally in a cantilever fashion from the blade root. The blade was excited by i) a speaker producing airborne noise inside the hollow blade, which resulted in blade surface vibrations and radiated noise and ii) a rattling impact wrench which excited the structure directly. Noise and vibration measurements were made 21 different points on the blade when it was excited.

The blade was found to be a broad spectrum resonator with no preference as to the frequency of vibration or radiation of noise. Where the foam core was used along the trailing edge of the blade the structure-borne noise levels were reduced significantly. It was found that the vibration and acoustic data correlated well in most cases providing confidence in the tests, however the method used to excite the blade was found to influence the results.

Several possible methods of reducing the structure-borne blade noise were identified including foam filling of the blades. In similar research conducted using a blade in the UK, foam filling was found to

produce noise reductions of up to 13 dB at some frequencies, however the results of tests of the foam filled blades on operating turbines were not reported.

Table of Contents

List of Figures

1. Introduction

1.1 Background

Previous noise measurements of the Windflow 500 showed that over 85% of the noise produced by the turbine was radiated from the blades although the tests did not distinguish the contribution of structure-borne blade noise from the contribution of the aerodynamically produced blade noise. If a significant reduction was to be made in the total noise from the turbine the blade noise needed to be addressed.

Structure-borne blade noise originates from two separate mechanisms. The first mechanism is through the transmission of vibration from the machinery in the nacelle, either along the rotor shaft from the gearbox, into the hub and then to the blades, or along the pitch actuation shaft, through the pitch mechanism and into the blades. The second method of structure-borne noise generation in the blade is due to pressure fluctuations in the air flowing around the blade (caused by both atmospheric and blade induced turbulence) acting on its surface to cause panel vibration and hence radiated noise.

To quantify the level of structure-borne noise from the blades on the operating turbine it would be necessary to measure the vibration of the rotating blade at several points along its surface. Measurements on the rotating blades would require all of the instrumentation to be co-rotating or the use of either radio transmitting accelerometers or a non-contact method of vibration measurement such as a scanning Laser-Doppler vibrometer. Given that the latter were not readily available and the former risked expensive equipment damage if not successfully executed it was decided that a preliminary investigation of the structure-borne blade noise should be carried out while the blades were on the ground during the period when the gearbox was being modified.

1.2 Objective

It was envisaged that the investigation would provide information on which frequencies the blade was vibrating at most readily and the areas of the blade that the most significant noise and vibration levels would occur.

1.3 Construction of the Blade

The 16m long Windflow 500 blades were manufactured from laminated wood and fibre-glass and each weighed approximately 925 kg. The blade had a hollow internal cavity that extended almost its entire length. A cross-sectional view of the blade is shown below in figure 7.1.1.

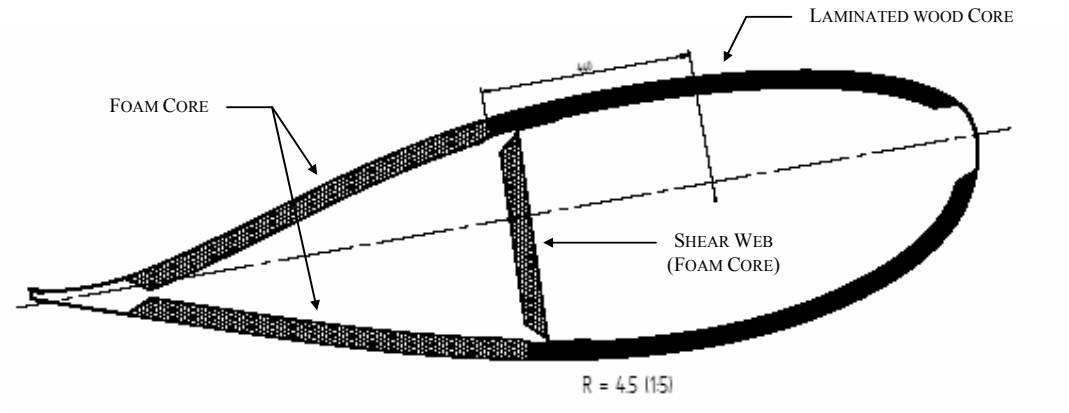

Figure 7.1.1 – Blade Cross-section

As can be seen from the cross-sectional view, the blade utilised a foam core rather than wood near to the trailing edge and for the shear web. The wood / foam interface line ran along the blade 440mm from the twist axis as measured along the local chord line. Figure 7.1.2 shows the resulting area of the aerofoil where the foam core was used.

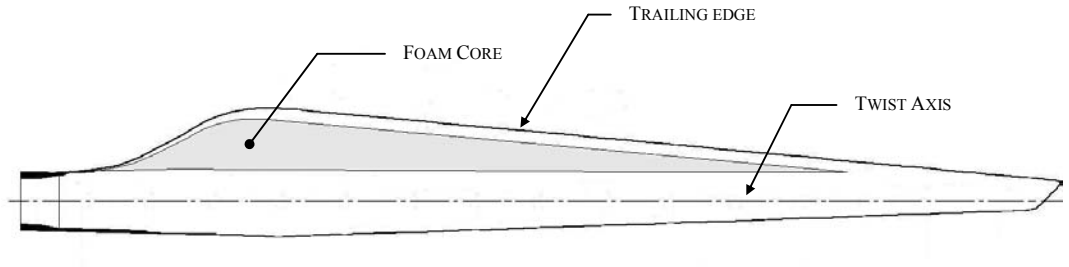

Figure 7.1.2 – Area of Blade with Foam Core

2. Experimental Method

2.1 Set-Up

2.1.1 Blade Support Method

The blade root was mounted to an A-frame which was used as a cantilever support for the blade during testing. The blade was supported horizontally with the trailing edge facing upwards as shown in figure 7.2.1.

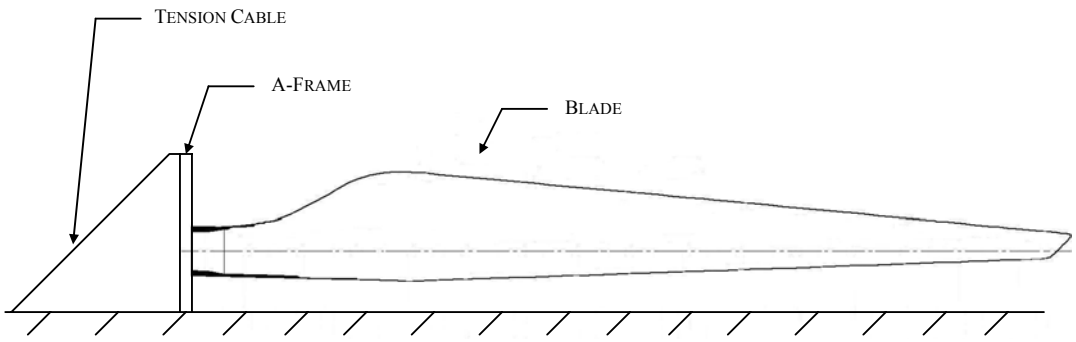

Figure 7.2.1 – Blade Support Method

With the blade supported as shown, two methods of excitation were used to induce vibration in the blade.

2.1.2 Excitation Method I – Speaker

The first method of excitation used a powered speaker (JBL EON Power10) that was placed in a noise box to prevent flanking noise and mounted at the root end of the blade between the uprights of the A-frame with the speaker facing into the internal cavity of the blade (see figure 7.2.2).

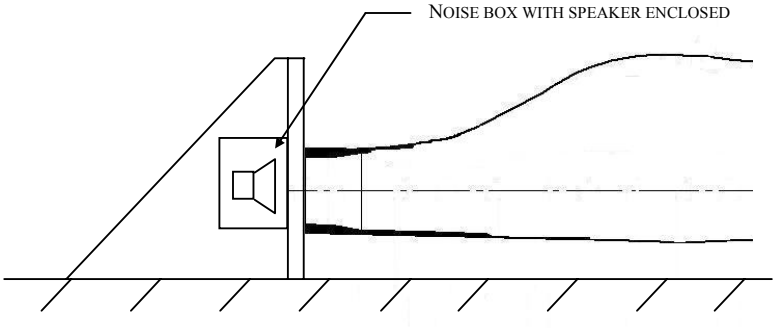

Figure 7.2.2 – Speaker Box Set-up

Three sets of measurements were taken, the first with a pink noise signal, the next with a 100 Hz signal (which was of interest as it was the gearbox first stage gear meshing frequency), and the third with a 315 Hz signal which was close to the gearbox second stage gear meshing frequency.

2.1.3 Excitation Method II – Impact Wrench

The second method of excitation utilised a stalled impact wrench to provide vibration to the blade structure. A nut was welded to the crossbar of the A-frame support and the impact wrench was placed over the nut and supported to prevent it moving when switched on. When switched on the air powered wrench stalled against the welded nut and sat rattling on the A-frame which transmitted to the blade the vibration caused by the wrench (see figure 7.2.3). Note that the opening in the end of the blade was covered for the impact wrench test.

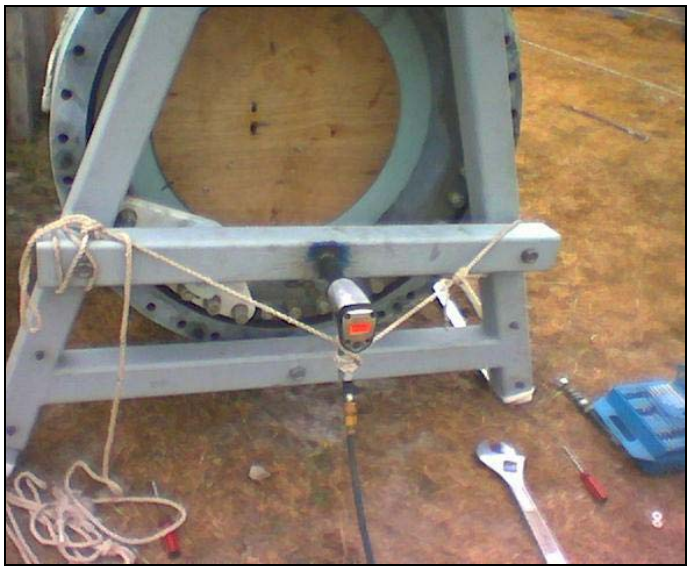

Figure 7.2.3 – Impact Wrench Set-up

2.2 Measurement

2.2.1 Noise Measurement

Sound intensity levels from the blade were measured for each of the input excitations using a Bruel and Kjaer 2260 Investigator with a Type 3595 Sound Intensity Probe Kit. The intensity levels for each input were measured at 21 different points on the pressure side of the blade as shown in figure 7.2.4. Fifteen of

the measurement locations lay along the centreline (twist axis) of the blade and were spaced at 1m intervals.

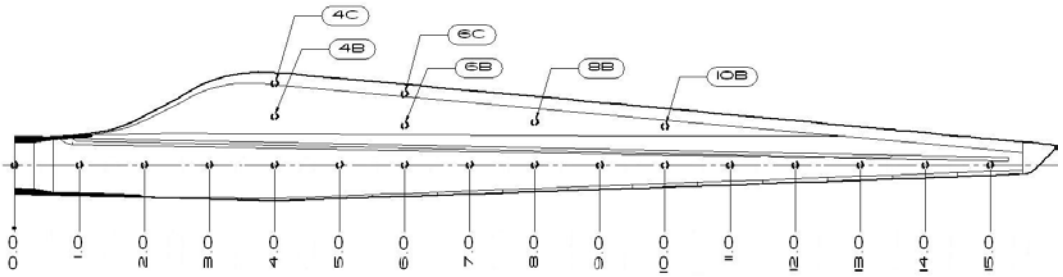

Figure 7.2.4 – Measurement Locations

2.2.2 Vibration Measurement

Vibration measurements (acceleration) along the blade were conducted using a Commtest VB3000 vibrometer. The measurement locations were the same as for the sound intensity levels as described in section 2.2.1.

3. Results and Analysis

3.1 Speaker Excitation Method

The results of the measurements using pink noise from a speaker to excite the blade showed that the blade was vibrating most energetically approximately 8m from the root. This was also reflected in the sound intensity measurements which were at a maximum between 8 and 10m from the root and generally correlated well with the trends observed in the vibration measurements. Figure 7.3.1 shows variation in magnitude of the noise and vibration measurements along the blade, with the blade excited using pink noise.

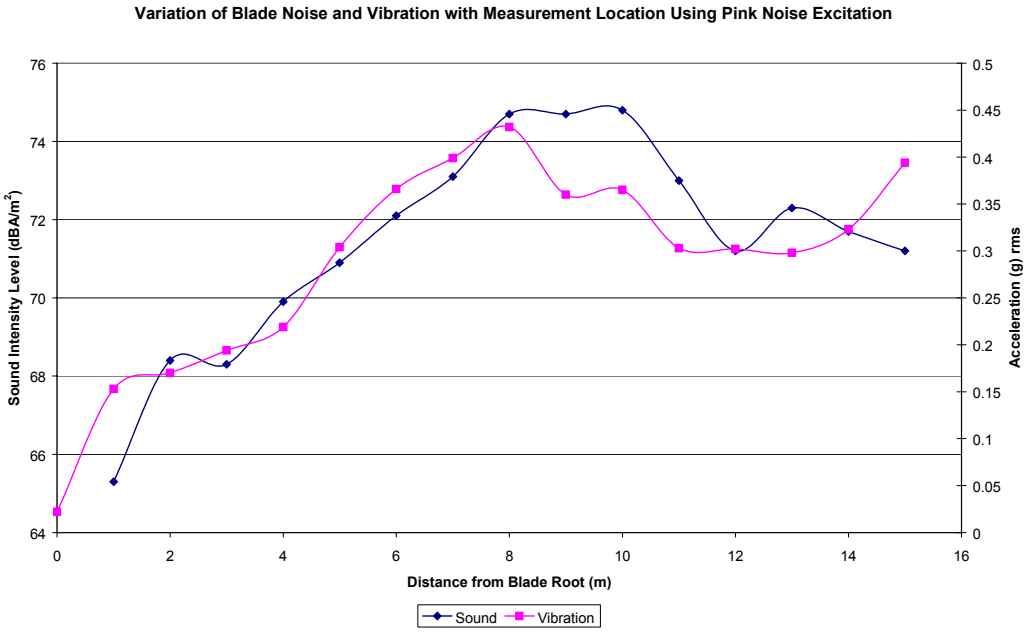

Figure 7.3.1 – Variation of Blade Noise and Vibration (Pink Noise Excitation)

It is interesting to note that the noisiest part of the blade was neither at the root near to the source nor at the widest part of the blade (3 to 4m from root) where one might intuitively expect a high sound intensity level given the shape and size of the surface at this point. The maxima and minima observed in the noise and vibration levels measured are a direct result of the complex geometry and construction of the blade.

In order to begin to establish a relationship between frequency distribution and position on the blade a spectral analysis was conducted in both the longitudinal (span-wise) and transverse (chord-wise) directions. Figure 7.3.2 shows the variation in sound intensity level at each frequency for the measurement points 2, 7, and 15. The graph summarizes the general changes in frequency observed as the longitudinal axis of the blade was traversed.

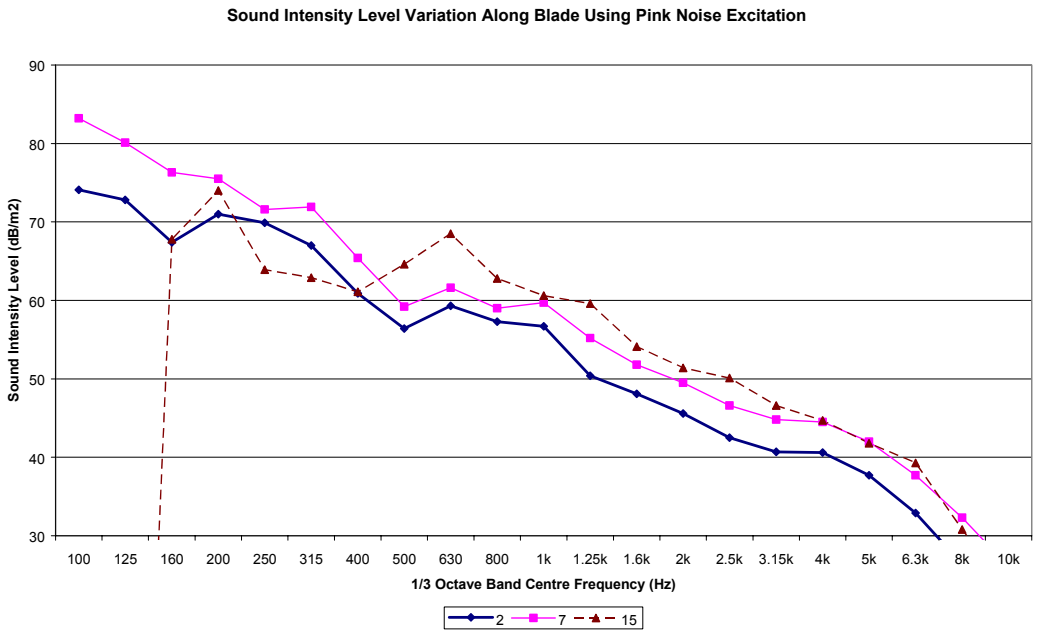

Figure 7.3.2 – Longitudinal Variation of Radiated Noise Using Pink Noise Excitation

As can be seen from the graph, the sound intensity level near to the blade root (point 2) closely follows that of point 7 in the middle of the blade except at a lower level. However near to the tip at (point 15), the graphs shows an increase in sound intensity level at 500 Hz and above, most significantly at 630 Hz. At point 15, below 400 Hz the sound intensity level was generally lower when compared with the other points and at 160 Hz and below was insignificant when compared to the background noise level during testing.

In the transverse direction of the blade the total sound intensity level was found to decrease as the trailing edge was neared. Figure 7.3.3 shows the spectral changes observed 6m from the root as the measurement location was moved from the blade twist axis toward the trailing edge. The changes are typical of those observed for each set of transverse measurements conducted.

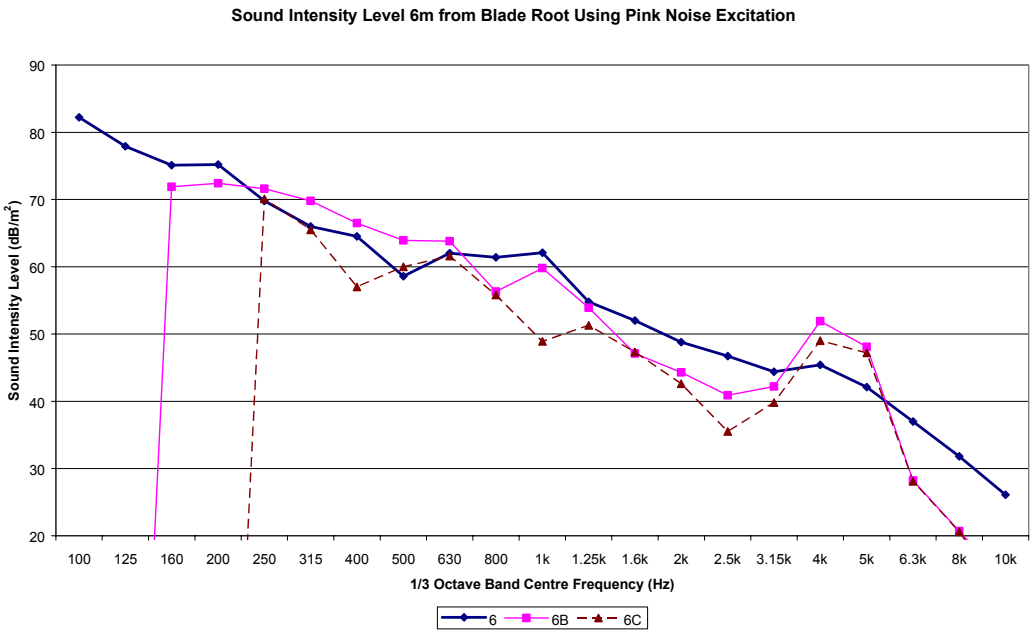

Figure 7.3.3 – Transverse Variation of Radiated Noise Using Pink Noise Excitation

The graph shows that at point 6B the level of noise below 160 Hz was insignificant in comparison to the level of the background level during testing. Nearer to the trailing edge at point 6C the level of noise below 250 Hz was insignificant compared with the background noise level during testing. This observation suggests that the area near to the trailing edge is less susceptible to low frequency vibrations than the larger area near to the twist axis of the blade. This phenomenon would most likely be a function of the changing stiffness of the blade along the chord coupled with the effects of the foam core used in its construction near to the trailing edge, as opposed to the wood used in the main part of the blade. Strangely, blade vibration data gathered simultaneously by Windflow Technology did not completely support the observations made using the sound intensity levels and showed that the area near to the trailing edge readily vibrated at frequencies of 100 – 500 Hz. This is further demonstrated in section 3.2.

In addition to the changes at low frequencies, the sound intensity level between 800 Hz and 3.15 kHz was also significantly reduced. However, in the 4 kHz and 5 kHz 1/3 octave bands the noise level increased near to the trailing edge. Again these effects would be a result of the change in shape, stiffness and construction of the blade at the different measurement locations.

When a tonal excitation was applied to the blade it was found that constructive and destructive interference in the sound waves produced highly fluctuating levels along the length of the blade. These could be heard clearly walking along the length of the blade. As with the pink noise excitation the highest levels of noise and vibration were found to occur at a distance of 6 to 10m from the blade root. Figure 7.3.4 and 7.3.5 show the sound and vibration levels recorded using 100 Hz and 315 Hz excitation frequencies respectively. As can be seen from the graphs the general trends observed with the microphone are supported by the accelerometer measurements.

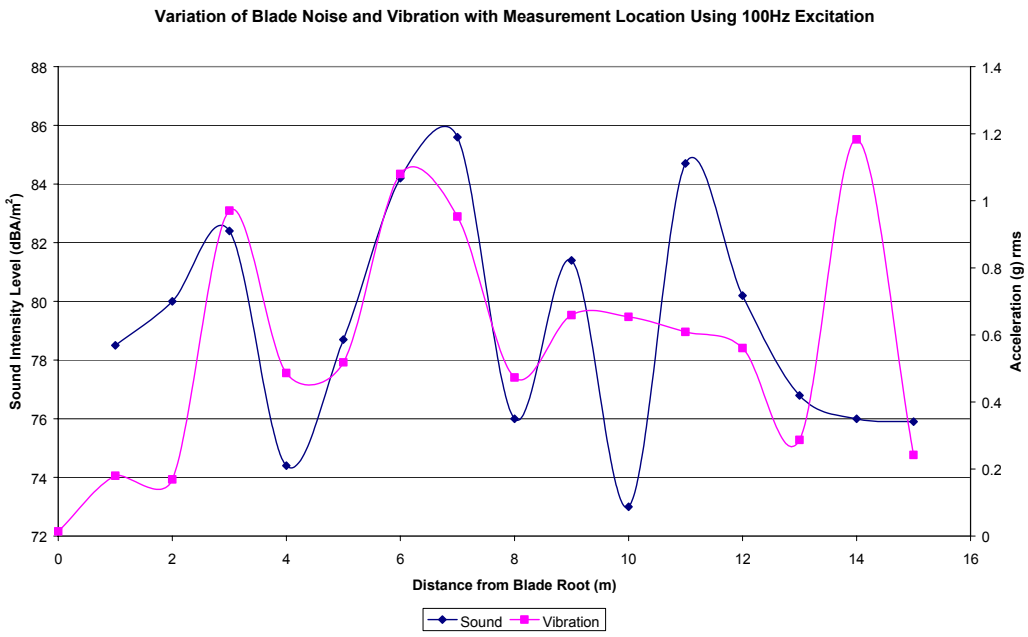

Figure 7.3.4 - Variation of Blade Noise and Vibration (100 Hz Excitation)

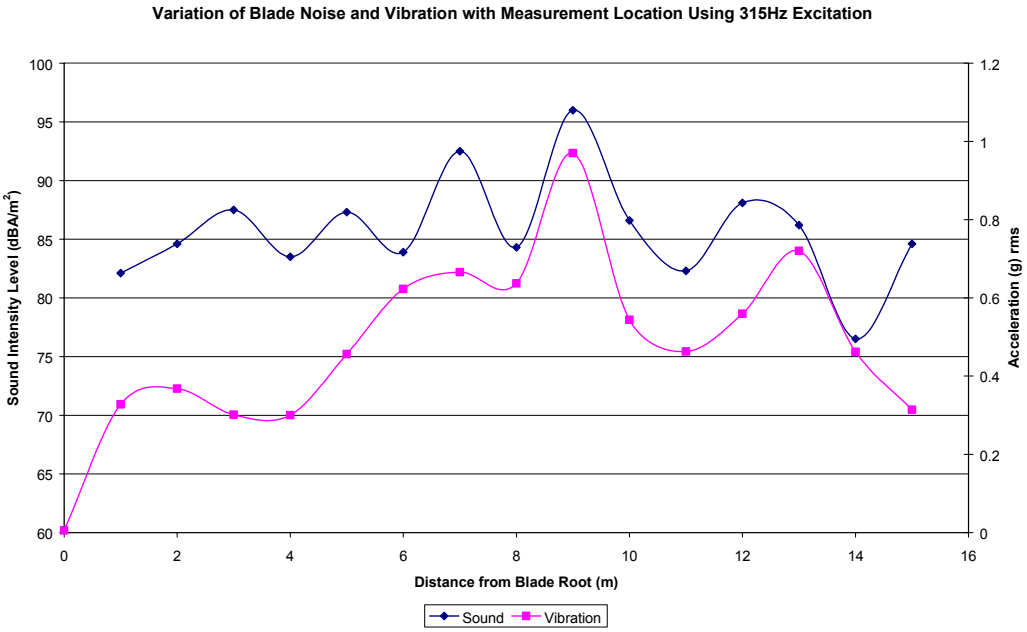

Figure 7.3.5 - Variation of Blade Noise and Vibration (315 Hz Excitation)

3.2 Impact Wrench Excitation Method

Using the impact wrench to excite the blade it was found that the highest levels of noise and vibration occurred near to the root followed by the area 6 - 7m from the root of the blade. Figure 7.3.6 below shows the levels of noise and vibration that were measured.

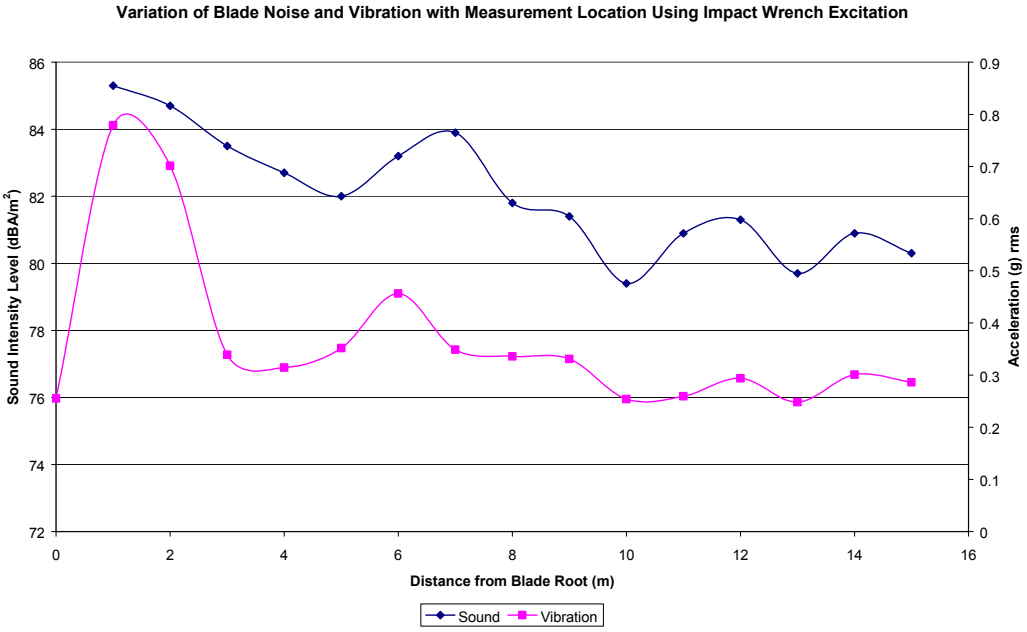

Figure 7.3.6 – Variation of Blade Noise and Vibration (Impact Wrench Excitation)

As for the pink noise excitation of the blade a spectral analysis of the noise was completed in both the longitudinal and transverse directions. Figure 7.3.7 below shows the variations in frequency that occurred along the longitudinal axis of the blade.

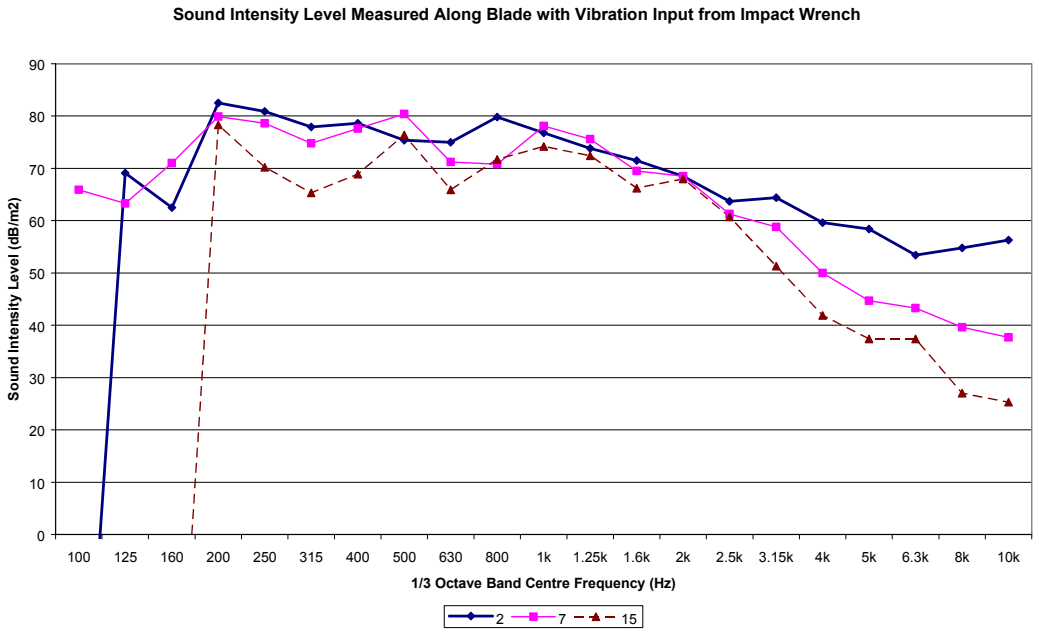

Figure 7.3.7 – Longitudinal Variation of Radiated Noise Using Impact Wrench Excitation

The above figure supports the data gathered using pink noise excitation in the respect that the noise below 200 Hz was significantly reduced near to the tip (point 15). However at other frequencies the noise near to the tip was found to be less than in the other areas of the blade. This does not agree with the results of the tests that used pink noise to excite the blade.

Figure 7.3.8 below shows the variations in frequency that occurred along the transverse axis of the blade 6m from the root using the impact wrench to excite the blade. Clearly near to the trailing edge of the blade the noise is reduced as was observed with pink noise excitation, but whether or not low frequency attenuation is improved is somewhat unclear. Also the increase in noise that was observed toward the trailing edge in the 4 – 5 kHz region using pink noise excitation was not supported by the measurements taken using the impact wrench to excite the blade.

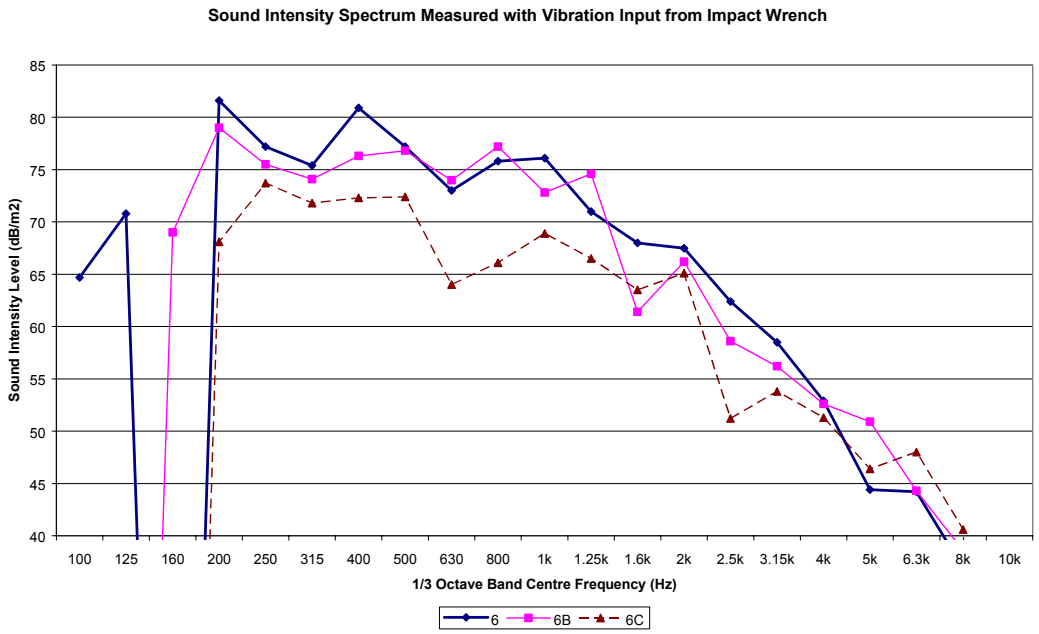

Figure 7.3.8 – Transverse Variation of Radiated Noise Using Impact Wrench Excitation

There are several factors that may contribute to, or explain these discrepancies. To begin with, the mechanisms involved in exciting the structure of the blade are different. In the case where the speaker was used to excite the blade the noise would firstly have been airborne inside the blade and then transferred a portion of its energy to its structure during reflections of the sound waves. This would have created the vibrations in the blade which in turn generated the radiated sound observed on the outside surface i.e. the transmission path of the noise was airborne – structure-borne – airborne. In this instance, the initial airborne sound waves inside the blade had the opportunity to interact before exciting the structure and the constructive and destructive interference of the sound waves inside the blade that may have resulted would have had the capability to produce a significantly different excitation of the blade than if the blade structure was excited directly as in the case of the impact wrench where the transmission path is structure-borne – airborne. Also, in the case of the impact wrench method the levels of noise and vibration near to the root of the blade may well be higher than at the tip because of structural damping of the sound waves as they travel along the blade. This is shown when figures 7.3.1 and 7.3.6 are compared.

Other factors that may have influenced the results relate to with the impact wrench itself. Firstly the impact wrench was powered by a portable air compressor and during testing the pressure of the air supply to the wrench would have varied slightly as the air tank on the compressor emptied and re-filled as a

result of the compressor switching on and off continuously. The changes in air supply were audibly noticeable as a slight change in the rate at which the wrench appeared to be rattling on the A-frame. This would have been detrimental to the consistency of the measurements. In addition, the flanking noise from the impact wrench influenced the measurements and made it difficult to determine if the noise measured was being radiated from the blade surface or directly from the wrench. If the experiment were to be repeated it would be prudent to place the wrench in an enclosure to reduce the level of flanking noise directly from the impact wrench, as was done with the speaker. In the case of pink noise the sound power in each octave band is equal, whereas with the impact wrench the sound power it produces at each frequency would be dependent on the conditions under which it is used and would be likely to fluctuate randomly. This in turn would mean that certain frequencies may not have been represented at sufficient levels in order to achieve an adequate comparison with the pink noise data.

3.3 Possibilities for Structure-borne Blade Noise Reduction

Before any acoustic treatments can be applied to the blade there are several issues that must be addressed. Firstly the treatment must not add too much weight or significantly affect the balance of the blade. The treatment must also be structurally stable enough to withstand the high g-loads that the blades experience (~ 40g at the tip of a Windflow 500 blade under normal operating conditions). Thirdly the treatment should not affect the drainage of rain water and condensation from the inner blade cavity or be able to become water logged and heavy. Finally the treatment would need to be cost effective and easy to fit to the blade during or after manufacture. With these specifications in hand the options for acoustic treatments are somewhat limited.

One possible method of reducing the structural noise and vibration of the blades would be to fill them with a damping medium. Previous research conducted for the Wind Energy Group (WEG) in the UK by SAIC Science and Engineering Ltd. [1] identified several materials that might be suitable as damping media to inhibit structure-borne vibration in wind turbine blades similar to those of the Windflow 500. These included blown Rockwool, melamine foam, shredded melamine foam, polyurethane foam, oasis foam, polystyrene granules and vermiculite granules. Of these materials, Rockwool and vermiculite were found to have an unacceptably high density for the application and showed a tendency to compact towards the blade tip under the high g-loads experienced, melamine was eliminated because it could not

be foamed directly into the blade due to its highly toxic constituents and shredded melamine performed poorly acoustically. Polystyrene was also eliminated because of its poor acoustic performance. Of all the samples, the oasis foam was found to have the best acoustic properties but was physically quite fragile, an extremely efficient water absorber, and it was unclear whether or not oasis could be foamed directly into the blade cavity. This series of eliminations left dense polyurethane foam as the best option since it combined good acoustical and mechanical properties with the desired practical features.

In a second report by SAIC [2] an MS3 wind turbine blade (similar to Windflow 500) was filled incrementally with dense polyurethane foam. The blade was excited using an electromagnetic shaker operating in the region of 100 – 400 Hz. The report found that foam filling of the turbine blade provided an effective means of vibration damping and reduced the surface radiated noise. With the blade completely filled, mean noise reductions of up to 13 dB were recorded at some frequencies; however filling only the last 4m of the tip and the entire trailing edge of the blade was sufficient to produce considerable reductions in noise at certain frequencies. Given the level of noise reduction achieved it is interesting to note that foam of the kind described in the report is generally not regarded as a particularly effective damping medium. The report does not cover testing of the blade on an operating turbine but verbal reports from WEG suggested that foam filling was found to be a successful method of reducing low frequency blade noise (below 400 Hz).

While reverberation times were not formally measured in the present investigation, it was noted subjectively that the interior cavity of the blade was particularly reverberant. This characteristic of the blade suggests that reductions in structure-borne noise from the blade could be made not only from the damping of vibrations, but also by controlling the reverberant sound field inside the blade. In the tested blade condition, sound waves radiating inward from the vibrating blade structure would be reflected by the non-absorptive surface of the inner cavity. The sound pressure level observed inside the blade cavity would therefore be greater than that which would otherwise be measured if the sound field was non-reverberant. Given the greater sound pressure level inside the blade, a larger amount of sound would be transmitted through the blade skin and hence the blade would appear noisier on the outside also. However, by introducing a sound absorbing material to the interior cavity of the blade in order to prevent

reflections and absorb sound energy, the reverberant field could be reduced. This may partly account for the noise reductions observed as foam was added to the blade in the SAIC report [2].

Other alternatives for reducing the structure-borne noise radiated from the blades would be i) to employ a series of resonant absorbers or tuned spring-mass-damper systems at selected locations inside the blade in order to reduce specific problem frequencies in each area; this would require considerably more research in order to produce an effective design, ii) to install a flywheel on the rotor shaft between the gearbox and the blade hub in an attempt to smooth the vibrations from the gearbox thereby preventing their transmission to the blades, iii) to re-engineer the blades using a better damped material and different internal webbing configuration.

4. Conclusions and Recommendations

The blade was shown to be a broad spectrum resonator with little preference for vibrating at any particular frequency. The highest levels of noise and vibration were found to occur 6 to 10m from the blade root. At the locations where the foam core was present along the trailing edge of the blade, low frequency attenuation generally appeared to be improved and the total sound levels were reduced significantly. Vibration and acoustic data were found to correlate well in most cases providing confidence in the test results. The method of blade excitation appears to have a significant effect on results observed.

Previous investigative work carried out on a similar blade in the UK showed that useful reductions in blade noise could be produced by the addition of foam inside the blade. However it is unclear as to whether the reduction is predominantly due to the damping effects of the foam or its sound absorbing qualities. Further work should be carried out to determine if the noise reduction is due to a reduction in the reverberant sound field inside the blade or because of the added damping. Identifying the mechanism at work would provide a better basis for future structure-borne blade noise investigations.

If damping was established as the dominant noise reduction mechanism then further work should be carried out to identify suitable methods of providing damping to the blade since methods such as foam filling are prone to both movement under the high g-loads experienced and water absorption, both of

which can result in blade imbalances. In addition to this, research should be conducted into preventing the transmission of noise and vibration from the nacelle thereby reducing the need for acoustic treatment of the blades.

5. References

[1] SAIC Science and Engineering Ltd., "Investigation of Properties of Materials as Potential Damping Media for Wind Turbine Blades," Cambridge, UK WEG/R073/2857/R1/94, 1994.

[2] SAIC Science and Engineering Ltd., "Measurement of the Effect of Foam Injection on Acoustic Emission from and MS3 Wind Turbine Blade," Cambridge, UK WEG/R073/14M, 1994.

Chapter 8
Investigation of Aero-Acoustic Blade Noise

Summary

This chapter describes a preliminary wind tunnel investigation that was carried out into the aero-acoustic noise produced by the Windflow 500 wind turbine blades. A 2m section of blade was tested in the low noise wind tunnel facility at the University of Canterbury. The noise from the unmodified blade was measured with the blade positioned in the flow at two different locations - (i) the tip, and (ii) 1.5m from the tip.

The results showed that the blade was generating noise over a wide range of frequencies with some frequencies showing tonal characteristics. In particular, noise was shown to be produced aerodynamically in the 315 Hz 1/3 octave band. This indicated that structure-borne noise from the gearbox was not the only contributor to the large amount noise radiated by the blades of the operating turbine in the 315Hz 1/3 octave band.

The influence of the trailing edge of the blade on the noise generated by the blade was investigated. Two serrated trailing edges were tested, both of 3:1 tooth length to width aspect ratio but one with larger teeth than the other. It was found that both serrated trailing edges produced a noise reduction but each affected the flow over the aerofoil differently and performed differently at each frequency. It was determined that the size, aspect ratio, and profile of the teeth probably have a significant influence on the performance of the serrated trailing edge and further investigation of different serrated trailing edges and their effects on the flow around the blade would be required in order to develop a noise reduction solution suitable for use on an actual wind turbine.

Table of Contents

List of Figures

List of Tables

1. Introduction

1.1 Background

Aero-acoustic noise from wind turbine blades is identified in current literature as the dominant source of noise of modern wind turbines. Measurements on the Windflow 500 showed that blade noise was a significant contributor to the total sound power level of the wind turbine (see Chapter 2). This chapter describes the wind tunnel investigation that was conducted into aero-acoustic noise generated by a section of blade from the Windflow 500 turbine.

Theory suggests that the noise level produced by a fan or rotor increases with blade speed proportional to the fifth power of the velocity. The frequency content of the sound may also vary with speed, or may remain unchanged depending on the mechanisms of noise generation present and the flow conditions. For example, in the case of tonal noise caused by vortex shedding from the aerofoil, it would be expected that the frequency of the tone would increase with flow speed since the rate of vortex shedding would also increase. For a circular cylinder this relationship is given by equation 8-1.

$$f_s = \frac{SU}{D} \tag{8-1}$$

where

f_s is the vortex shedding frequency (Hz)

S is the Strouhal number

U is the mean stream velocity (m/s)

D is the diameter of the cylinder (m)

For aerofoils with a chord length and thickness of similar dimensions equation 8-1 can be used with reasonable accuracy to approximate the vortex shedding frequency produced by substituting D with the maximum chord thickness. As the chord length to thickness ratio increases, this relationship becomes more approximate as both the thickness and the length of the chord influence the vortex shedding frequency.

In the case of turbulent boundary layer trailing edge noise (broadband – see Chapter 1, section 3.2), the frequency content of the sound generated would be unlikely to change much with flow speed as long as the flow regime did not change considerably as a result of the change in speed.

Wagner et al. [9] identifies turbulent boundary layer trailing edge noise as the most prominent and easily reduced component of aerodynamic blade noise on wind turbines. One of the most commonly cited methods of reducing turbulent boundary layer trailing edge noise from wind turbine blades is the use of a serrated trailing edge in order to disrupt the interaction of the turbulent boundary layer with the wake of the aerofoil. According to theory by Howe [5] reductions in aerodynamic blade noise of up to 20 dB can be achieved depending on the tooth length to width aspect ratio and the flow conditions. Howe's theory implies that a serrated trailing edge using long narrow teeth will perform better than one with short wide teeth. Figure 8.1.1 shows the reductions predicted by Howe for different tooth aspect ratios assuming a flow speed of 50m/s and a boundary layer thickness of 0.01m.

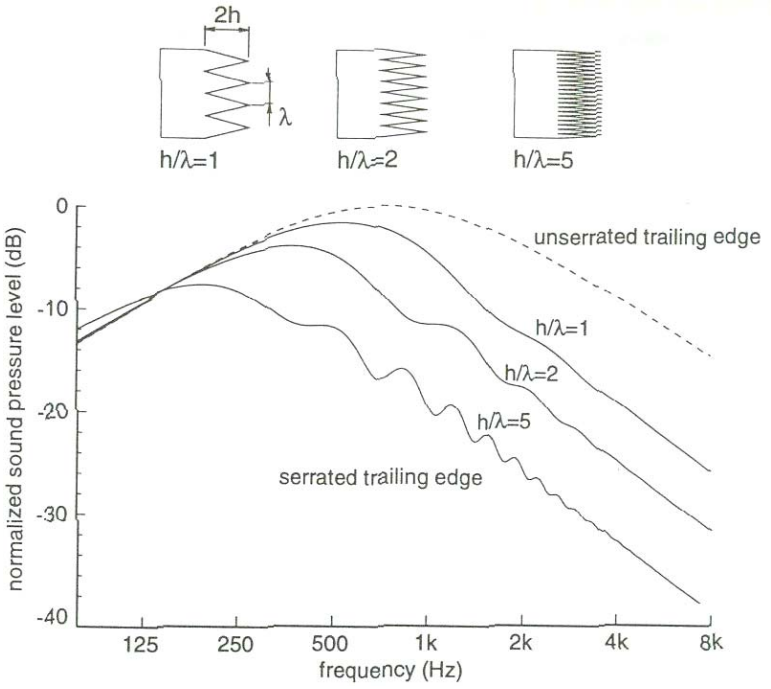

Figure 8.1.1 – Effect of Tooth Aspect Ratio on Serrated Trailing Edge Noise Reduction [5]

In practice it has been found that Howe's theory over predicts the reduction that can be achieved with the use of a serrated trailing edge. Several experimental studies [1-4, 6, 7] have shown that a number of aerofoil and flow parameters not accounted for in Howe's theory can influence reduction achieved. In particular, it was found by Dassen et al. [3] that the tooth aspect ratio was less important than the tooth length itself. Dassen found that the noise reduction that could be achieved using serrated trailing edges increased with tooth length up to a maximum of approximately 6 dB in wind tunnel measurements.

1.2 Windflow 500 Blade Parameters

Each Windflow 500 blade extended 16.6m from the centre of the hub. The profile and twist angle of the blade varied along its length. At a distance of 0.5m from the tip of the blade the profile was defined as having 0 degrees of twist. With the chord line of this profile parallel to the plane of rotation of the blade, the pitch angle of the blade was defined as zero. From the cut-in wind speed (~5.5 m/s) up to wind speeds of 13 m/s the wind turbine blades rotated at an approximately constant rate of 48 rpm set at a pitch angle of 0 degrees (the rotor speed being controlled by the torque limiting gearbox). At wind speeds above 13 m/s (rare in the case of the Gebbies Pass site) the blades were feathered (had pitch angle changed) to maintain the speed of rotation at approximately 48 rpm.

While the pitch angle remained constant at wind speeds up to 13 m/s the actual angle of incidence of the blades varied with wind speed. This was because the angle of incidence of the blades was the result of the vector addition of the velocity of the air relative to each blade due to its rotation and the velocity of the incoming wind (see figure 8.1.2).

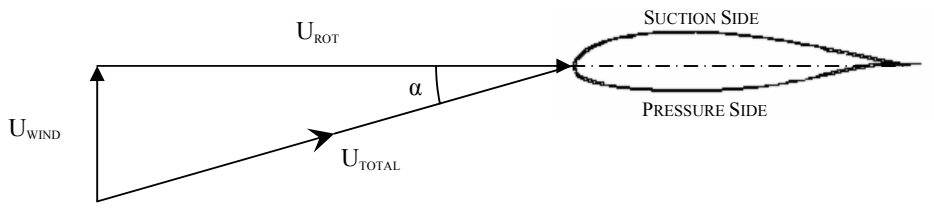

where -

U_{ROT} - Wind speed relative to blade due to rotation of the blade

U_{WIND} – Atmospheric wind speed relative to blade

U_{TOTAL} – Resultant wind speed of airflow relative to the blade

α – Angle of incidence

Figure 8.1.2 – Determination of Angle of Incidence

As a result of the twist of the blades and the variation of their tangential velocity with radius, the angle of incidence also varied along the length of the blades.

A 2.4m section from the tip of a Windflow 500 test blade was obtained for the purpose of this work. The noise generated from airflow over the tip and the aerofoil section 1.5m from the tip was to be investigated. Table 8.1.1 shows the blade parameters relevant to the calculation of the angle of incidence at these locations and table 8.1.2 shows the angle of incidence that would result at a range of wind speeds, assuming normal operating conditions as described earlier.

Table 8.1.1 – Blade Parameters for Calculation of Angle of Incidence

Position	**A**	**B***	**C**
Distance from Tip (m)	0	0.5	1.5
Twist Angle (deg)	0.40	0.00	-0.79
Tangential Velocity (m/s)	83.4	80.9	75.9

* Reference position for pitch angle.

Table 8.1.2 – Angle of Incidence of Blade in Normal Operating Conditions

	Angle of Incidence (deg)		
Wind Speed (m/s)	**A**	**B***	**C**
5	3.8	3.5	3.0
6	4.5	4.2	3.7
7	5.2	4.9	4.5
8	5.9	5.6	5.2
9	6.6	6.3	6.0
10	7.2	7.0	6.7
11	7.9	7.7	7.5
12	8.6	8.4	8.2
13	9.3	9.1	8.9

* Reference position for pitch angle.

The Reynolds number for the aerofoil can be calculated using equation 8-2.

$$\mathrm{Re} = \frac{UL}{\upsilon} \tag{8-2}$$

where

Re is the Reynolds number

U is the mean stream velocity relative to the aerofoil (m/s)

L is a characteristic length (m)

υ is the kinematic viscosity of the air (kg m^{-1} s^{-1})

Depending on the shape of the aerofoil and a number of flow parameters, the length controlling the Reynolds number could take a variety of values. The literature does not clearly define what length should be used in the calculation of the Reynolds number of an aerofoil, but there are three values that are commonly used. These are the length of the chord, the boundary layer thickness of the flow over the aerofoil and the maximum thickness of the chord. As the boundary layer thickness for the flow over the Windflow 500 blade section was unknown the Reynolds numbers were calculated using the chord length and maximum chord thickness only. The results of the calculations are shown in table 8.1.3.

Table 8.1.3 – Reynolds Numbers of Windflow 500 Blade

Position	Maximum Thickness (m)	Chord Length (m)	Reynolds Number L = Max Thickness	Reynolds Number L = Chord Length
B	0.07	0.50	3.83E+05	2.62E+06
C	0.111	0.63	5.46E+05	3.10E+06

* Kinematic viscosity of air taken as 1.543×10^{-5}

The magnitudes of the Reynolds numbers calculated show that the flow over the blade section in normal operating conditions of the turbine would be fully turbulent. Using the above Reynolds numbers the Strouhal number for the aerofoil can be estimated approximately using figure 8.1.3 which shows the Strouhal – Reynolds number relationship for circular cylinders.

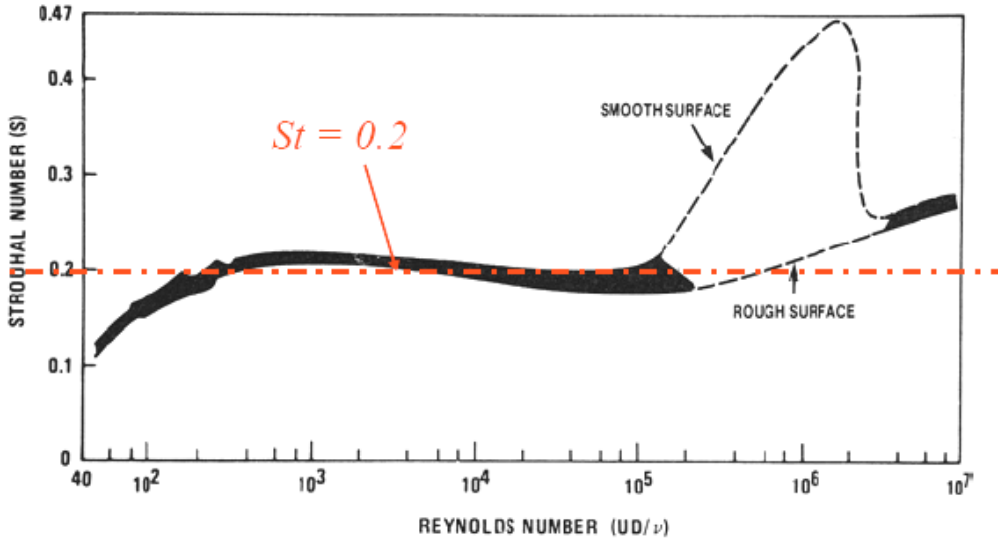

Figure 8.1.3 – Strouhal – Reynolds Relationship for Circular Cylinders (Lienhard 1966) [8]

This results in the Strouhal numbers shown in table 8.1.4 if the values are read from the 'smooth surface' curve.

Table 8.1.4 – Strouhal Numbers of Windflow 500 Blade

Position	Estimated Strouhal Number L = Max Thickness	Estimated Strouhal Number L = Chord Length
B	0.34	0.27
C	0.37	0.26

The vortex shedding frequency of the blade can then be estimated using equation 8-1. The calculations were done assuming the length controlling the rate of vortex shedding (*D*) was the chord length, and also assuming that the controlling length was the maximum thickness of the chord. Table 8.1.5 shows the vortex shedding frequencies that were calculated for the Windflow 500 blade.

Table 8.1.5 – Calculated Vortex Shedding Frequencies of Windflow 500 Blade

		Estimated	Vortex Shedding Frequency (Hz)	
Position	**Airspeed (m/s)**	**Strouhal Number**	**D = Max Thickness**	**D = Chord Length**
B	80.9	0.34	377	55
B	80.9	0.27	299	44
C	75.9	0.37	253	45
C	75.9	0.26	178	31

1.3 Objective

This investigation was designed as a preliminary study of the blade noise from the Windflow 500. There were two main aims for the investigation –

(i) To establish the level and frequency distribution of the aero-acoustic noise produced the tip section of a Windflow 500 wind turbine blade.

(ii) To determine if the noise level from the blade could be reduced with the addition of a serrated trailing edge.

2. Experimental Method

A 2.4m long section from the tip of a Windflow 500 test blade was mounted on stands at the 0.77m x 0.77m outlet of the low noise wind tunnel in the Department of Mechanical Engineering at the University of Canterbury. The stands were constructed so as to allow the angle of incidence and section of the blade in the airflow to be adjusted. The leading edge of the blade was placed 200 mm from the exit of the tunnel and the microphone was placed out of the airflow 750mm below the trailing edge. The experiments were conducted at two positions on the blade -

(i) *Main Span* - Blade tip positioned 1.5m from the centreline of the tunnel (referred to in tables as position C).

(ii) *Tip* - Blade positioned so that 0.6m of the tip extended into the air flow from the tunnel (referred to in tables as position B).

Figure 8.2.1 and 8.2.2 show the set-up for each test position.

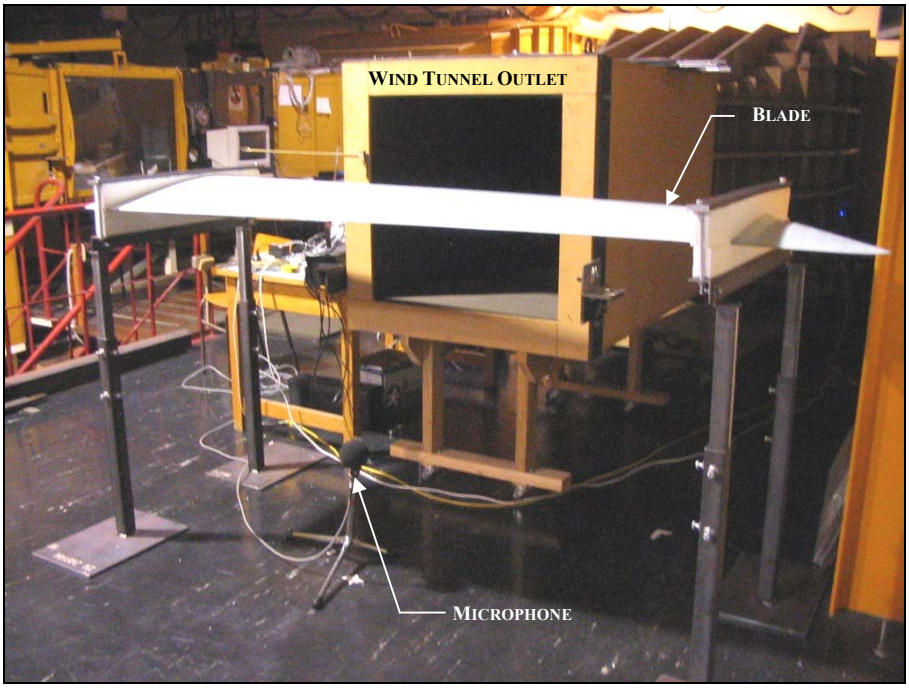

Figure 8.2.1 – Set-Up for Main Span Test

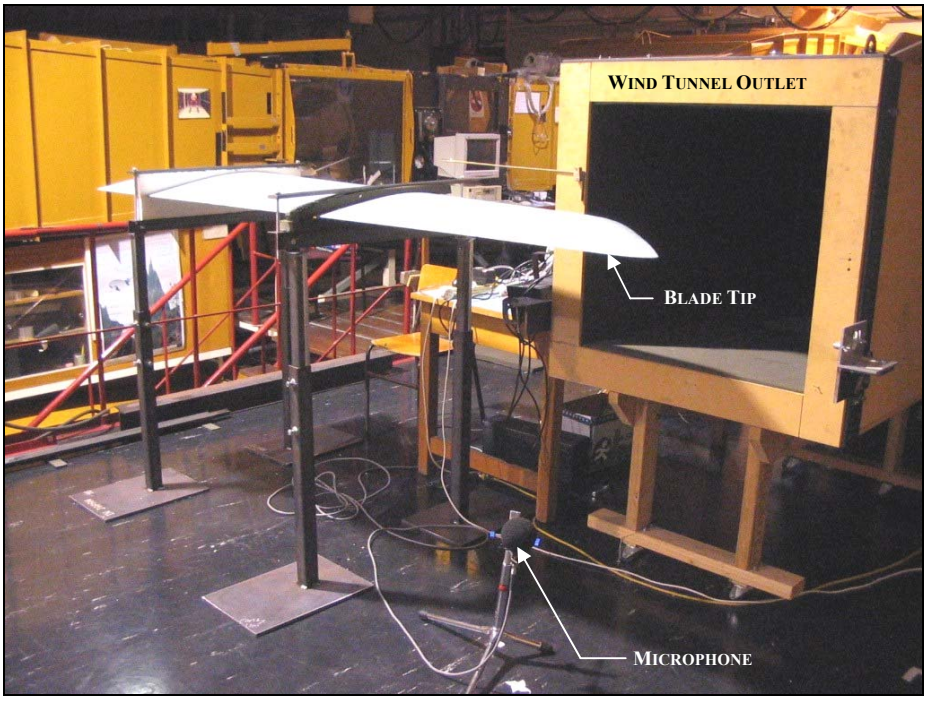

Figure 8.2.2 – Set-Up for Tip Test

The wind tunnel was unable to produce airflow speeds as high as those experienced by the tip on the operating turbine but could be run at sufficiently high speeds so as to achieve similar flow conditions (based on Reynolds number). The wind tunnel was set to run at 40 m/s and the noise produced by the blade was measured in 1/3 octave bands using a Bruel and Kjaer 2260 Investigator. Measurements were conducted with the angle of incidence set at 0, 3, 6, 9, and 12 degrees. This covered the range of angles that would be encountered in the normal operating conditions of the turbine. With the blade set at an angle of incidence of 6 degrees, the noise from the blade was also measured with the air speed set to 20, 30, and 45 m/s in order to establish the way in which the air speed of the wind tunnel affected the noise produced by the blade. This provided an indication as to whether the results of the experiments would still be valid for the higher flow speeds present on the operating turbine. The background noise level was measured for each airflow speed with the blade removed from the flow (microphone position unchanged). Each measurement was repeated 3 times at the same setting to ensure that repeatable results were being achieved.

Table 8.2.1 shows the Reynolds numbers calculated for the aerofoil at each of the flow speeds tested in the wind tunnel (as in section 1.3, Reynolds numbers have been calculated using both the chord length of the aerofoil, and the maximum thickness of the chord).

Table 8.2.1 – Reynolds Numbers for Wind Tunnel Investigation

Airspeed		**Reynolds Number**	
(m/s)	**Position**	**L = Max Thickness**	**L = Chord Length**
20	B	9.46E+04	6.48E+05
	C	1.44E+05	8.17E+05
30	B	1.42E+05	9.72E+05
	C	2.16E+05	1.22E+06
40	B	1.89E+05	1.30E+06
	C	2.88E+05	1.63E+06
45	B	2.13E+05	1.46E+06
	C	3.24E+05	1.84E+06

* Kinematic viscosity of air taken as 1.543×10^{-5}

As can be seen from the Reynolds number, the flow over the aerofoil is still likely to be fully turbulent even at the reduced flow speeds imposed by the wind tunnel, with the exception of the flow over the aerofoil at 20 m/s which is probably in the transition region between laminar and turbulent flow.

Table 8.2.2 shows for each of the flow speeds tested in the wind tunnel the estimated Strouhal number and vortex shedding frequency (should vortex shedding be present) for the flow over the aerofoil. The Strouhal numbers were obtained using figure 8.1.3.

Table 8.2.2 – Estimated Vortex Shedding Frequencies for Wind Tunnel Investigation

Airspeed (m/s)	Position	Estimtated Strouhal Number	Vortex Shedding Frequency (Hz) D = Max Thickness	D = Chord Length
20	B	0.20	55	8
	B	0.39	107	16
	C	0.21	38	7
	C	0.44	79	14
30	B	0.21	86	13
	B	0.44	181	26
	C	0.26	70	12
	C	0.47	127	22
40	B	0.24	132	19
	B	0.46	252	37
	C	0.30	108	19
	C	0.47	169	30
45	B	0.25	154	23
	B	0.47	290	42
	C	0.31	126	22
	C	0.46	186	33

To enable any interesting features of the flow to be visualised, each section of the aerofoil to be tested in the flow was tufted with cotton threads. On the main span of the blade section 7 rows were placed along the span of the blade with a spacing of 50mm. Each tuft was approximately 30mm in length and each row of tufts covered the entire length of the chord from leading edge to trailing edge. The same tuft size and spacing was utilized across the 0.5m tip section of the blade. Tufts were placed on both the suction and the pressure side of the aerofoil. Figure 8.2.3 illustrates the placement of the tufts on the blade.

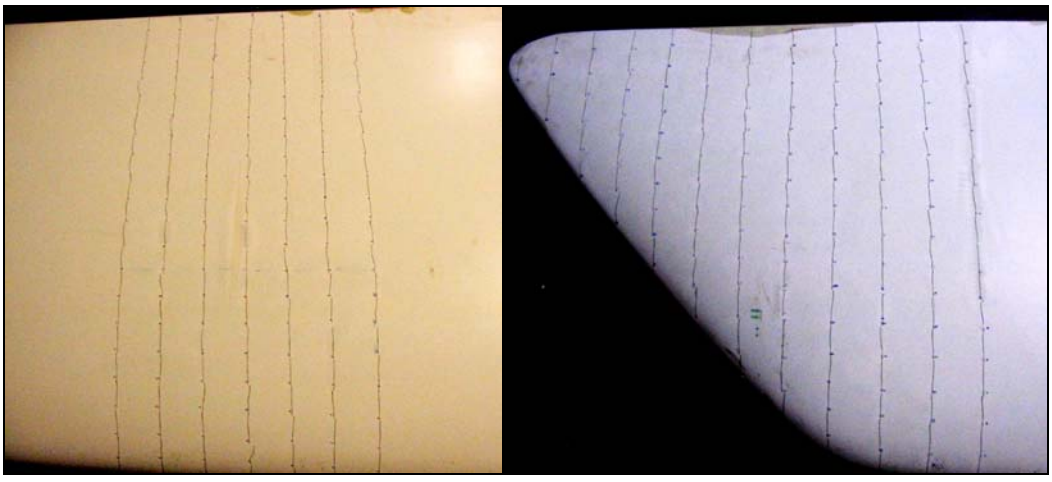

(I) MAIN SPAN (II) TIP SECTION

Figure 8.2.3 – Tufted Test Sections

Four sets of experiments were conducted –

(i) Main span of the blade section unmodified.

(ii) Tip of the blade unmodified.

(iii) Main span of the blade section with a small toothed serrated trailing edge attached.

(iv) Main span of the blade section with a large toothed serrated trailing edge attached.

For experiments (iii) and (iv), serrated trailing edges with a tooth length to width aspect ratio of 3:1 were wire cut from 2mm thick stainless steel and attached to the trailing edge of the blade as shown in figure 8.2.4.

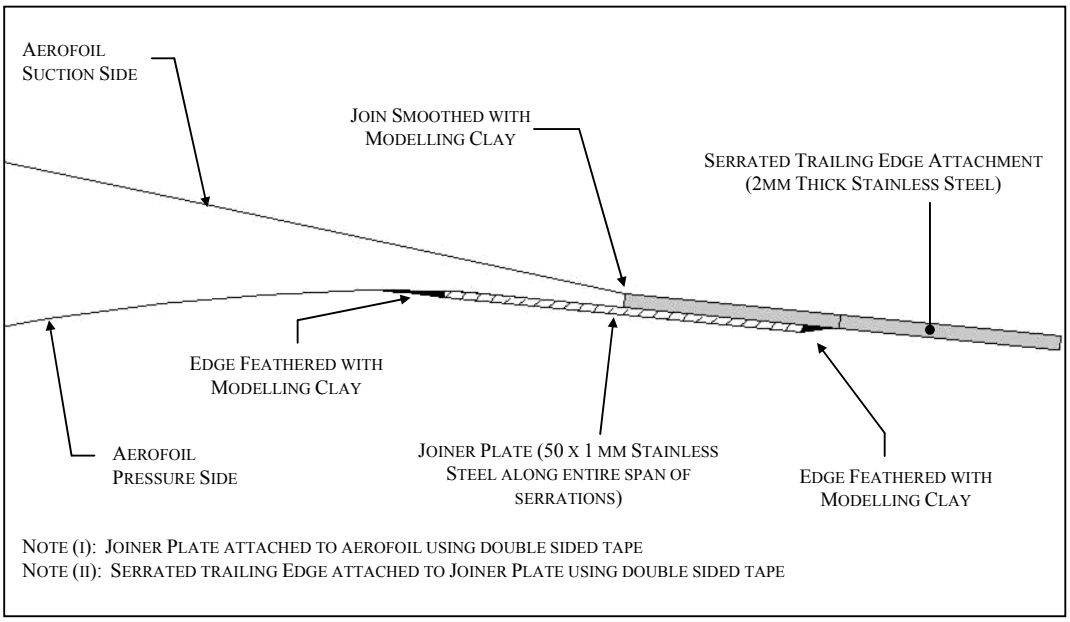

Figure 8.2.4 – Serrated Trailing Edge Attachment Method

The serrations spanned 1m along the trailing edge and were centred 1.5m from the tip of the blade. The serrations consequently spanned the entire airflow from the wind tunnel with the blade in the 'Main Span' test position.

For experiment (iii) the small toothed serration shown in figure 8.2.5 was used.

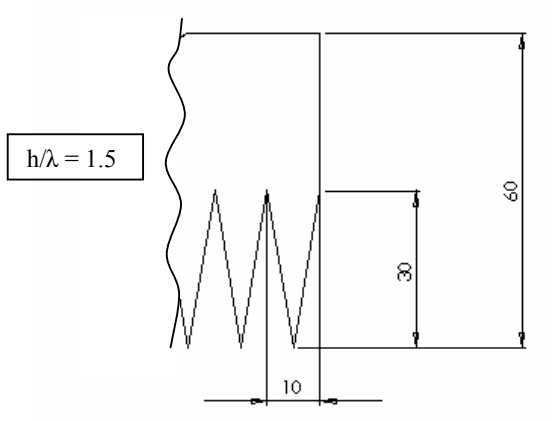

Figure 8.2.5 – Small Toothed Serration Dimensions (mm)

For experiment (iv) the larger toothed serration shown in figure 8.2.6 was used.

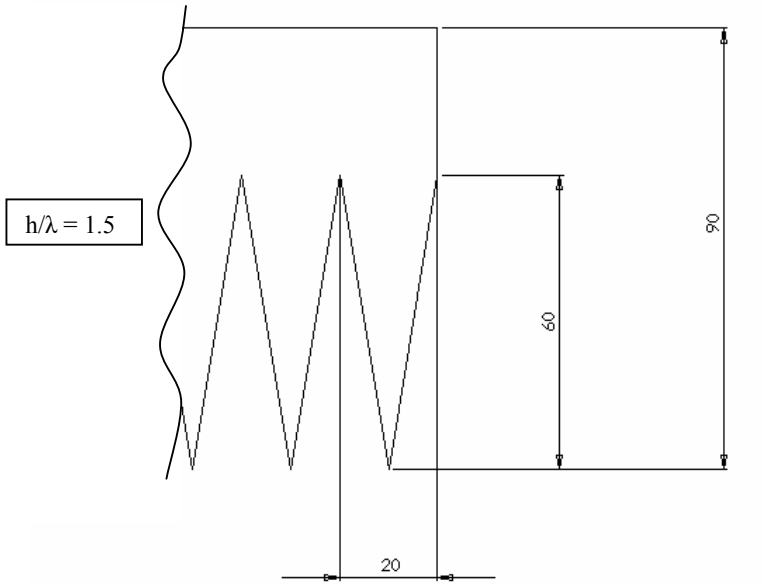

Figure 8.2.6 – Large Toothed Serration Dimensions (mm)

The use of the small and large toothed serrations increased the effective chord length of the aerofoil by 60mm and 90mm respectively.

3. Results

3.1 Main Span of Blade Unmodified

3.1.1 Sound Pressure Level

Figure 8.3.1 shows the sound pressure level that was measured with the blade at each angle of incidence. The total sound pressure level (dB Lin) is given in the key below the abscissa. The figure also shows the background noise level measured with the wind tunnel set at a flow speed of 40 m/s.

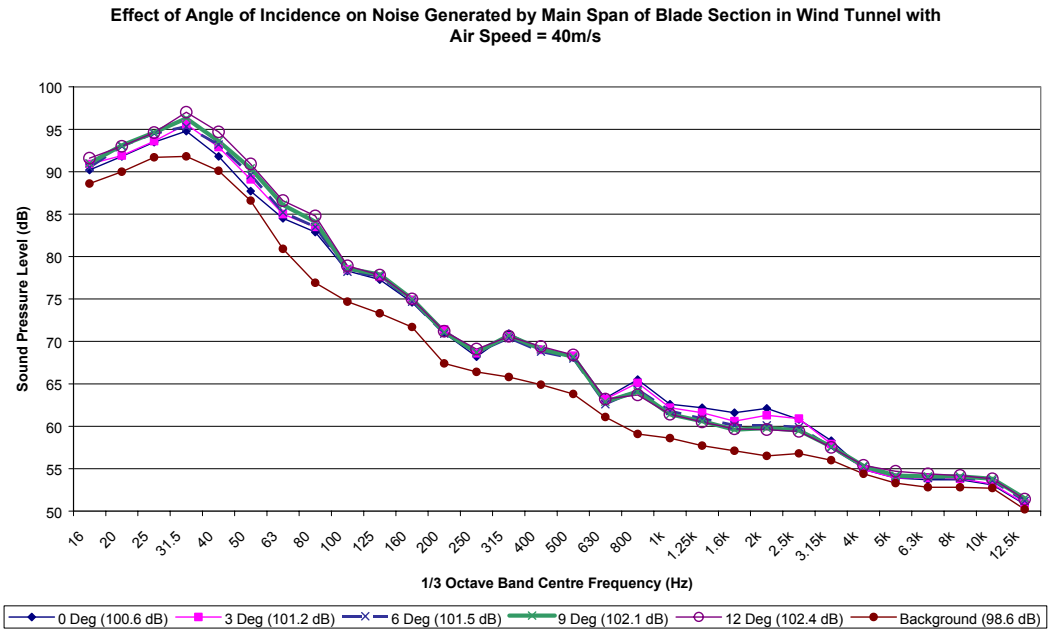

Figure 8.3.1 – Variation of Main Span Sound Pressure Level with Angle of Incidence

Figure 8.3.2 shows more clearly the differences measured for each angle of incidence setting. The figure shows normalized sound pressure for each frequency. The normalized level was calculated by arithmetically subtracting the background noise level from the measured sound pressure level for each angle of incidence setting i.e. the normalized level is the number of decibels that the blade noise was above the background noise.

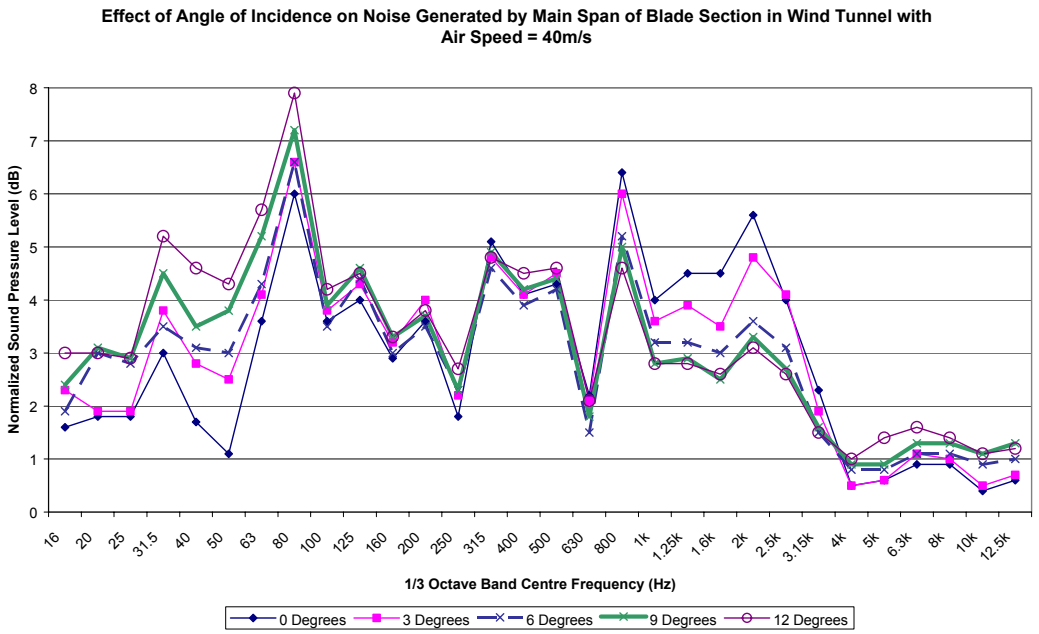

Figure 8.3.2 – Normalized Sound Pressure Level from Main Span of Blade Section

Figure 8.3.3 shows the effect of air speed on the noise produced by the main span of the blade section at 6 degrees angle of incidence.

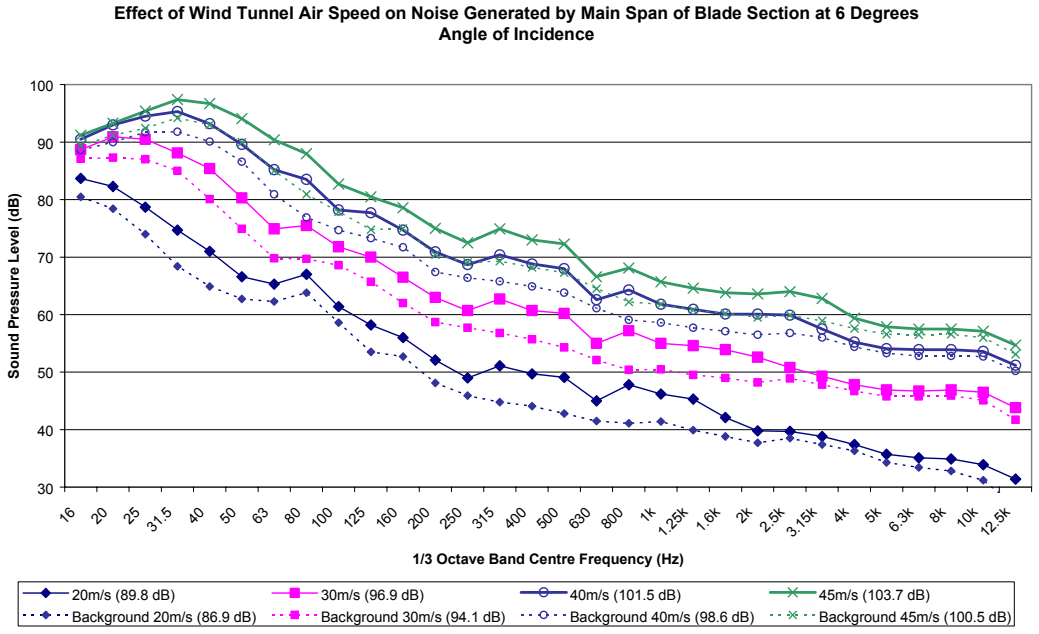

Figure 8.3.3 – Effect of Air Speed on Noise Generated by Main Span of Blade Section

The increase in background and blade generated noise with wind tunnel air speed was found to fit well to a logarithmic curve as shown in figure 8.3.4.

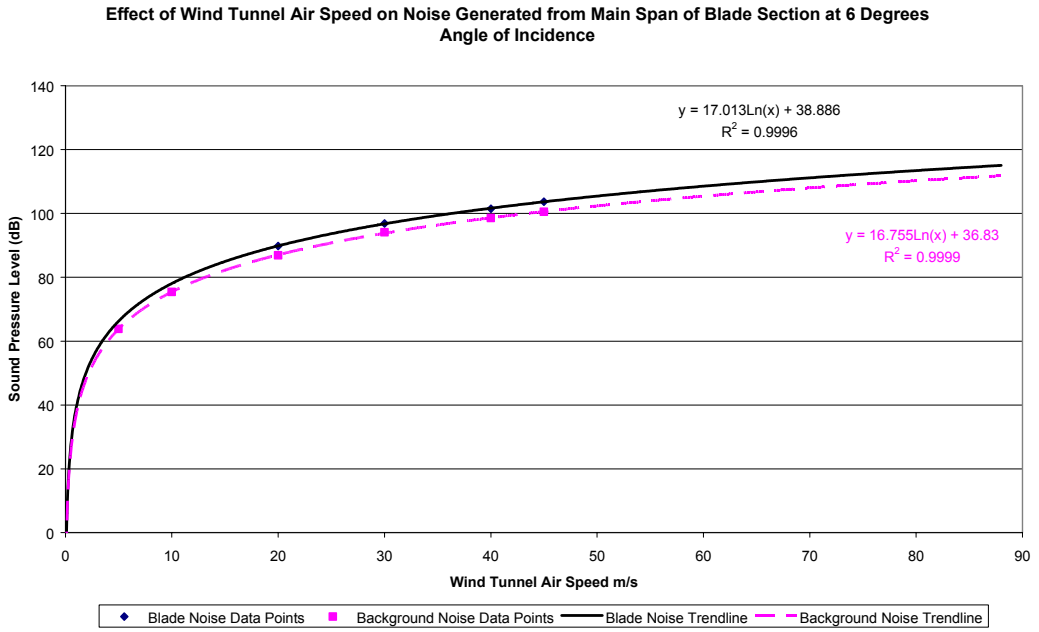

Figure 8.3.4 – Curve Fitting of the Effect of Air Speed on Background and Blade Noise

3.1.2 Flow Visualisation

The tufts on the main span of the unmodified blade showed no separation of the flow on either side of the aerofoil at 0, 3, 6, and 9 degrees angles of incidence. With the aerofoil set to 12 degrees angle of incidence the two rows of tufts nearest the trailing edge on the suction side of the aerofoil began to flutter violently indicating separation of the flow close to the trailing edge. Figure 8.3.5 shows the cotton tufts on the suction side of the aerofoil at (i) 9 degrees angle of incidence and (ii) 12 degrees angle of incidence.

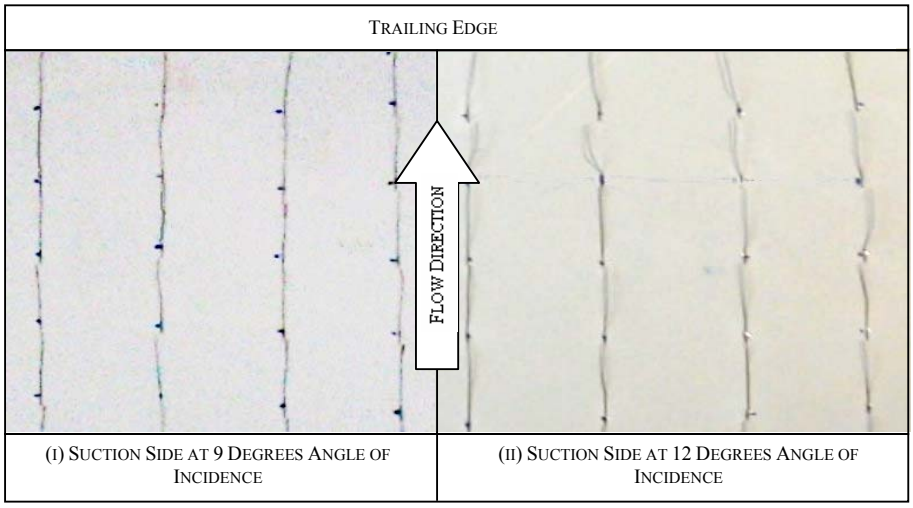

Figure 8.3.5 – Flow Visualisation of Main Span of Blade Section

3.2 Tip of Blade Unmodified

3.2.1 Sound Pressure Level

Figure 8.3.6 shows the effect of angle of incidence on the noise generated by the tip of the aerofoil in the wind tunnel with the airflow speed set to 40m/s.

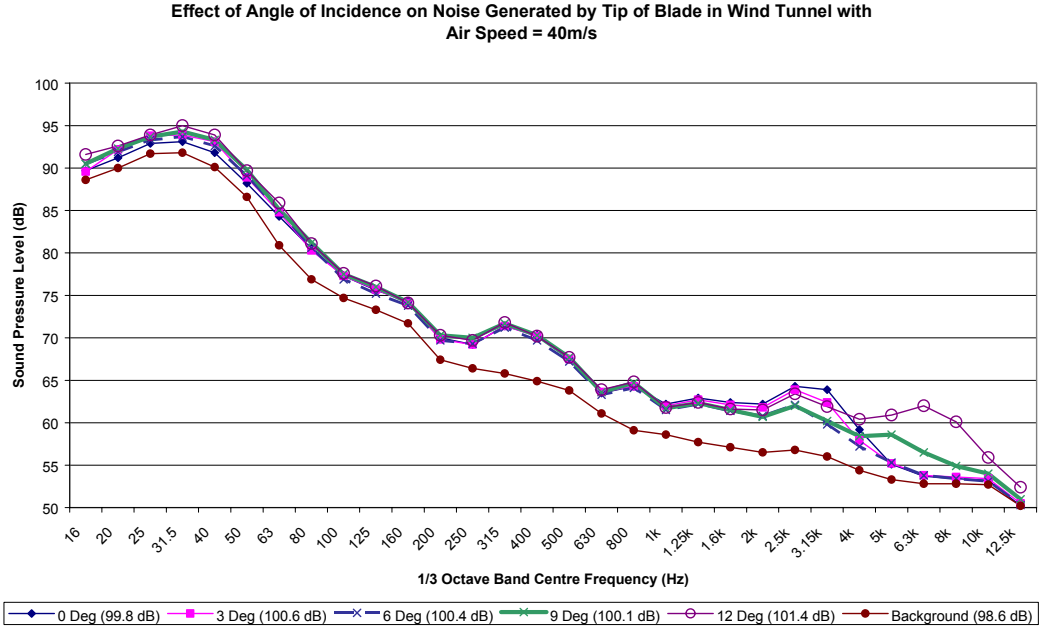

Figure 8.3.6 – Variation of Blade Tip Noise with Angle of Incidence

Figure 8.3.7 shows the normalized sound pressure level from the tip of the blade at different angles of incidence, which more clearly distinguishes the changes in sound pressure level that occurred.

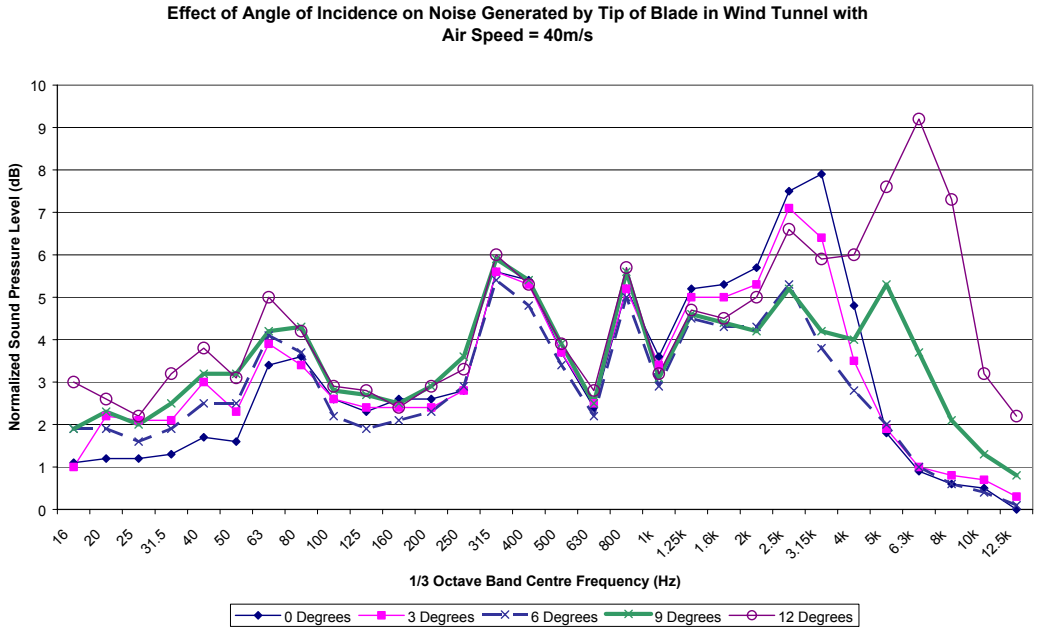

Figure 8.3.7 – Normalized Sound Pressure Level from Tip of Blade

Figure 8.3.8 shows the effect of flow speed on the noise generated by the tip of the blade at 6 degrees angle of incidence.

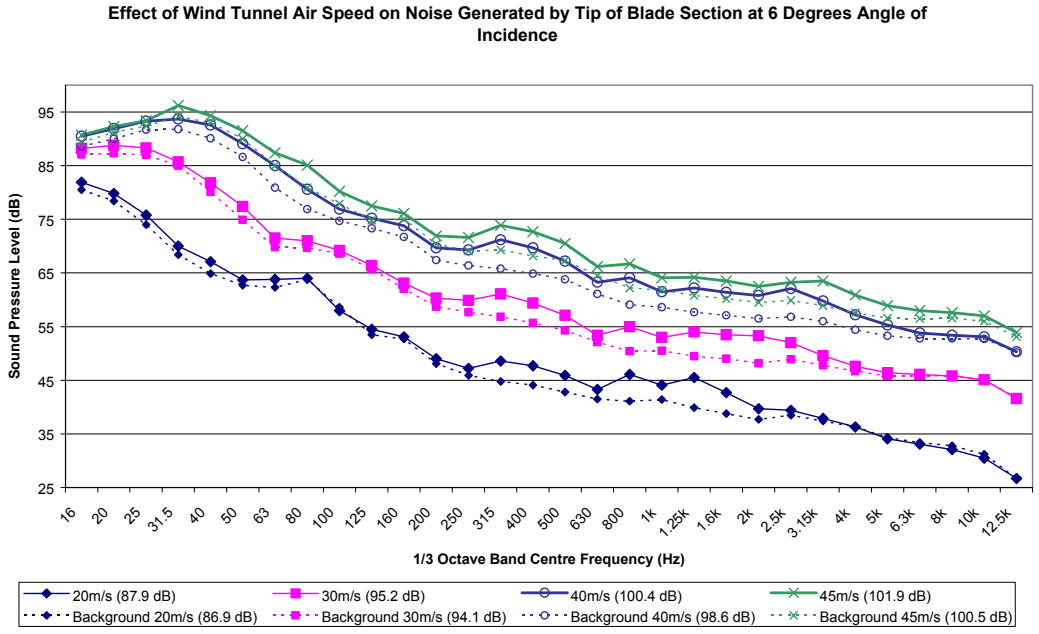

Figure 8.3.8 – Effect of Air Speed on Noise Generated by Tip of Blade

3.2.2 Flow Visualisation

The tufts on the pressure side of the aerofoil showed that the flow remained attached and flow directly from the leading edge to the trailing edge at all angles of incidence. On the suction side of the aerofoil the majority of the tufts showed attached flow at 0, 3, 6, and 9 degrees angle of incidence, with the exception of the tufts furthest from the tip end which fluttered in the flow and pointed towards the tip. This effect became more prominent with increasing angle of incidence. At 12 degrees angle of incidence it was found that the flow across the entire section in the flow was beginning to separate near the trailing edge, and the single tuft right on the tip showed fully separated flow at that point. Figure 8.3.9 shows a comparison of the cotton tufts on the suction side of the tip at (i) 0 degrees and (ii) 12 degrees angle of incidence with an airflow speed of 40m/s.

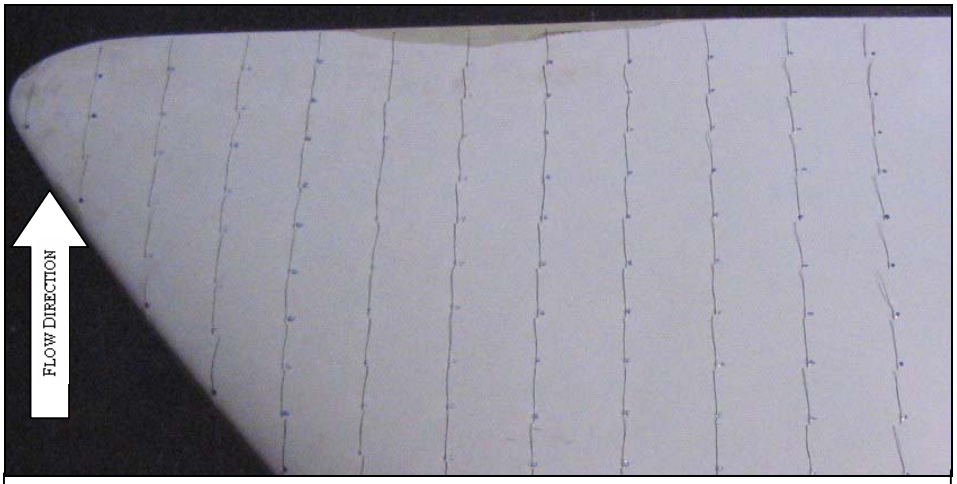

(I) SUCTION SIDE AT 0 DEGREES ANGLE OF INCIDENCE

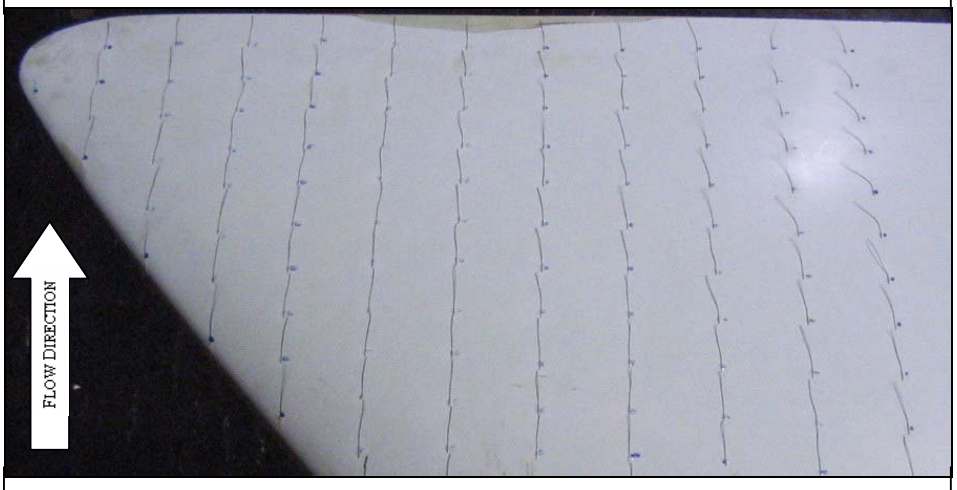

(II) SUCTION SIDE AT 12 DEGREES ANGLE OF INCIDENCE

Figure 8.3.9 – Flow Visualisation of Tip of Blade.

3.3 Comparison with Field Data

Figure 8.3.10 shows a comparison of a blade noise measurement made in the field with the noise produced by the 'main span' area and 'tip' of the blade section at 9 degrees angle of incidence in the wind tunnel. The field measurement was obtained with the microphone placed approximately 4m from the root of the blade (radially) and a distance of 1m behind it. The microphone remained stationary while the blades rotated. The measurement was conducted over a period of 30 seconds (~48 blade passes) with the turbine operating in a 10 – 13 m/s wind (~9 degrees angle of incidence). This comparison is very approximate and is discussed further in section 4.3.

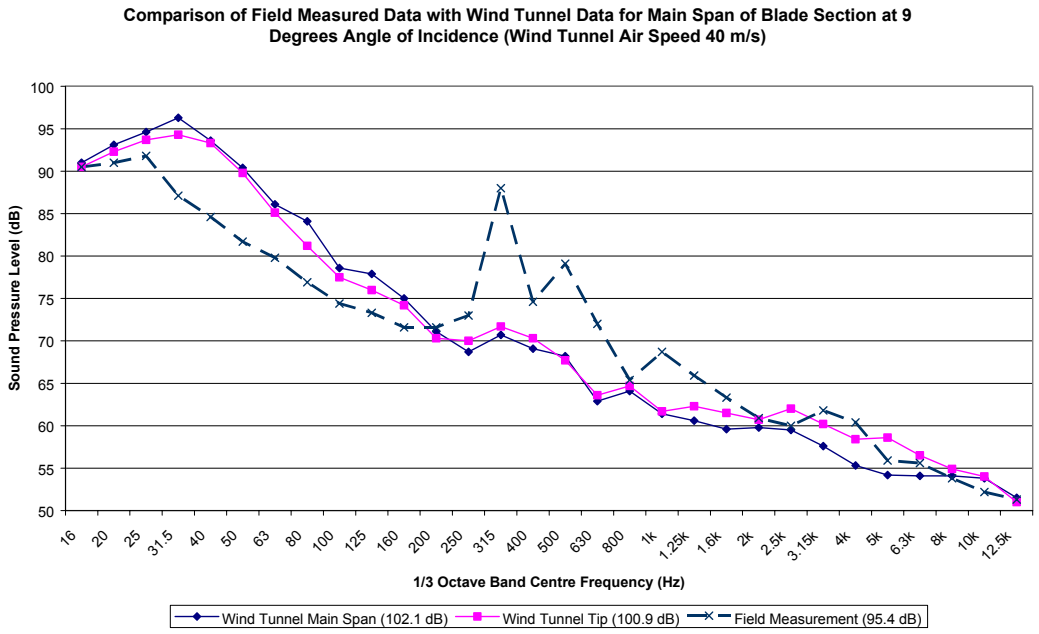

Figure 8.3.10 – Comparison of Wind Tunnel and Field Data

3.4 Effect of Serrated Trailing Edges

3.4.1 Sound Pressure Level

Figure 8.3.11 shows the sound pressure levels that were measured at each angle of incidence tested, with the main span of the aerofoil in a 40m/s airflow and the trailing edge modified with the small toothed serrations.

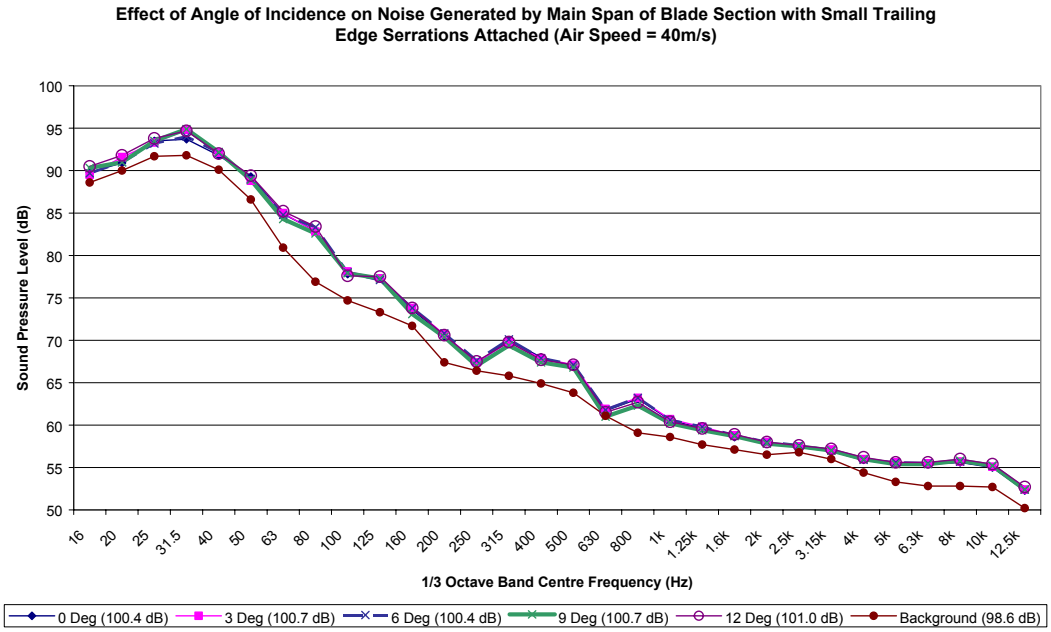

Figure 8.3.11 – Noise Measured with Small Toothed Trailing Edge Serrations

The normalized sound pressure level in figure 8.3.12 shows more clearly the differences observed at each angle of incidence.

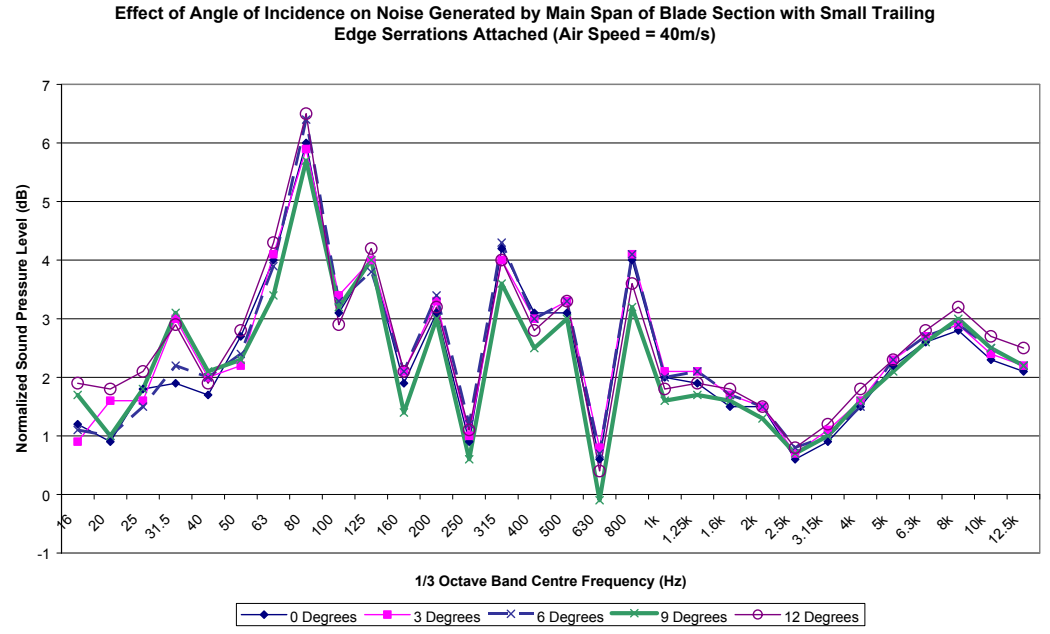

Figure 8.3.12 – Normalized SPL with Small Toothed Trailing Edge Serrations

Figure 8.3.13 shows the sound pressure levels that were measured at each angle of incidence tested with the main span of the aerofoil in a 40m/s airflow and the trailing edge modified with the large toothed serrations.

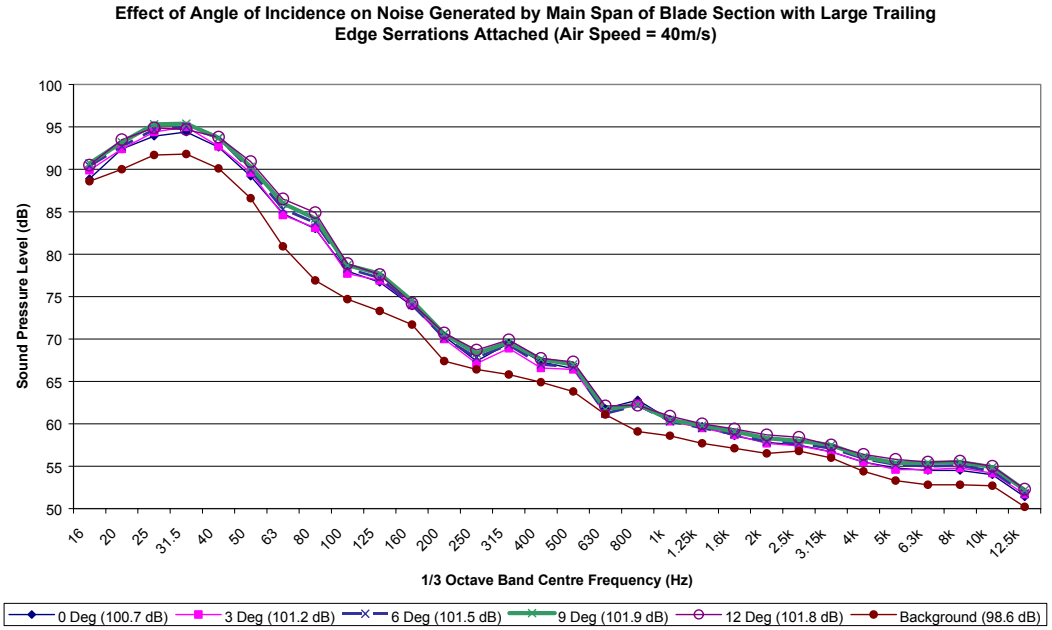

Figure 8.3.13 - Noise Measured with Large Toothed Trailing Edge Serrations

Figure 8.3.14 illustrates more clearly the differences observed at each angle of incidence, using a normalized sound pressure level.

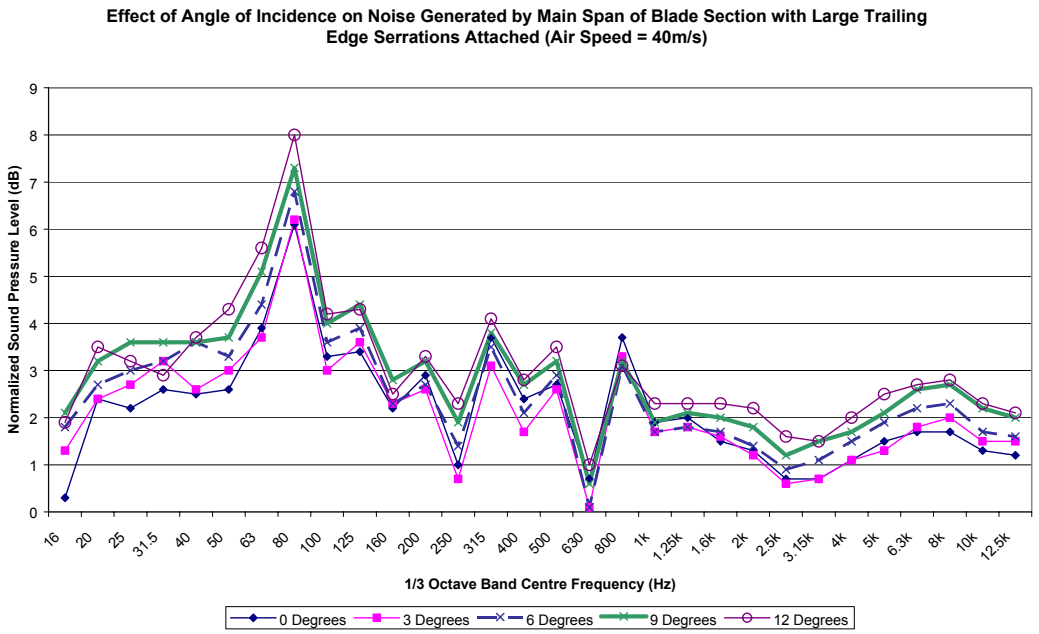

Figure 8.3.14 – Normalized SPL with Large Toothed Trailing Edge Serrations

3.4.2 Comparison with Unmodified Blade

Figure 8.3.15 shows the differences observed between the sound pressure levels measured for each of the three trailing edge conditions at 6 degrees angle of incidence with a 40 m/s airflow speed.

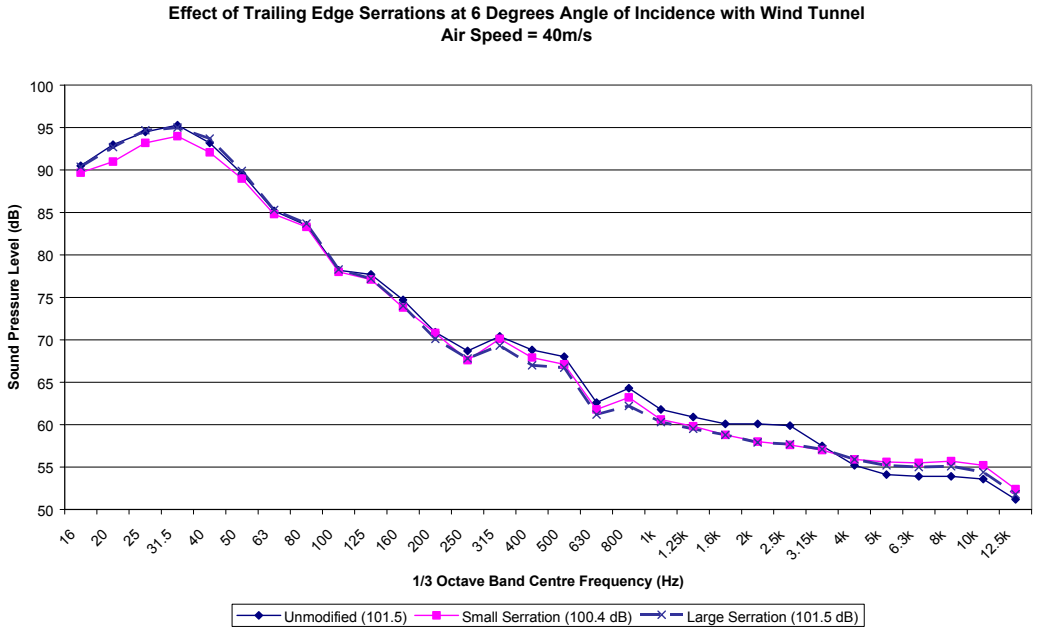

Figure 8.3.15 – Effect of Trailing Edge Serrations on Sound Pressure Level

Figure 8.3.16 shows the reduction of sound pressure level that was achieved at 6 degrees angle of incidence using each of the serrated trailing edges. The reduction was calculated by arithmetically subtracting the sound pressure level produced by the blade with the serrated trailing edge attached, from the sound pressure level produced by the blade in unmodified form, for each 1/3 octave band. Note that a positive reduction indicates a decrease in sound pressure level when compared with the sound pressure level produced by the blade in its unmodified form.

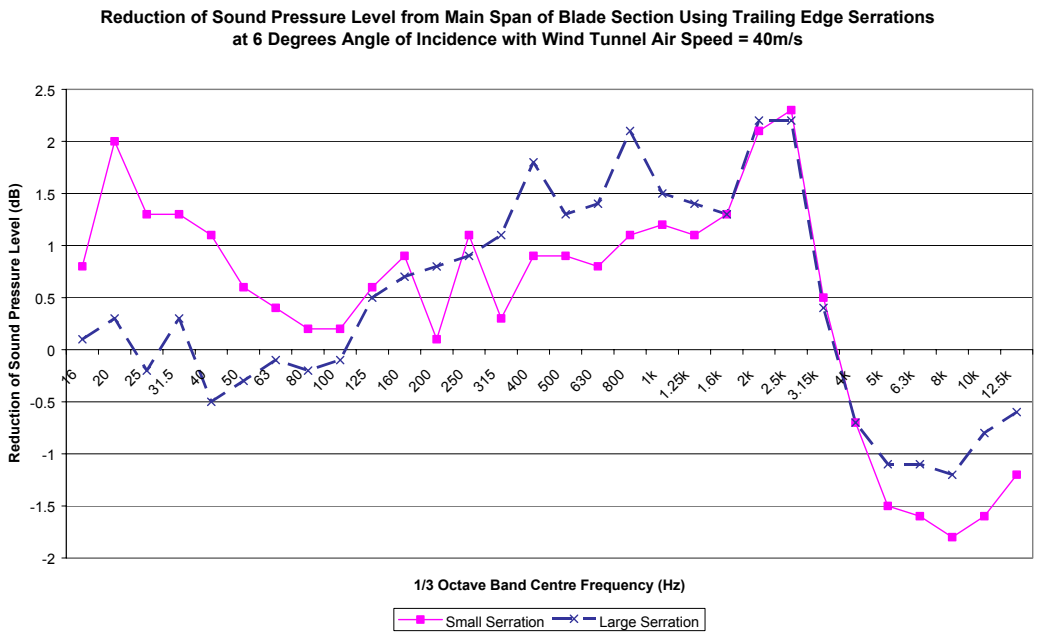

Figure 8.3.16 – Reduction in Sound Pressure Level Produced by Trailing Edge Serrations

A full set of graphed comparisons showing the effect of the serrated trailing edges at each angle of incidence can be found in Appendix A.

3.4.3 Flow Visualisation

With the small toothed serrated trailing edge attached the cotton tufts on the aerofoil showed no signs of flow separation on either the suction or pressure side of the aerofoil at any of the angles of incidence tested. Figure 8.3.17 illustrates this, showing the tufts near to the trailing edge on the suction side of the aerofoil at 0 and 12 degrees angle of incidence in a 40 m/s flow.

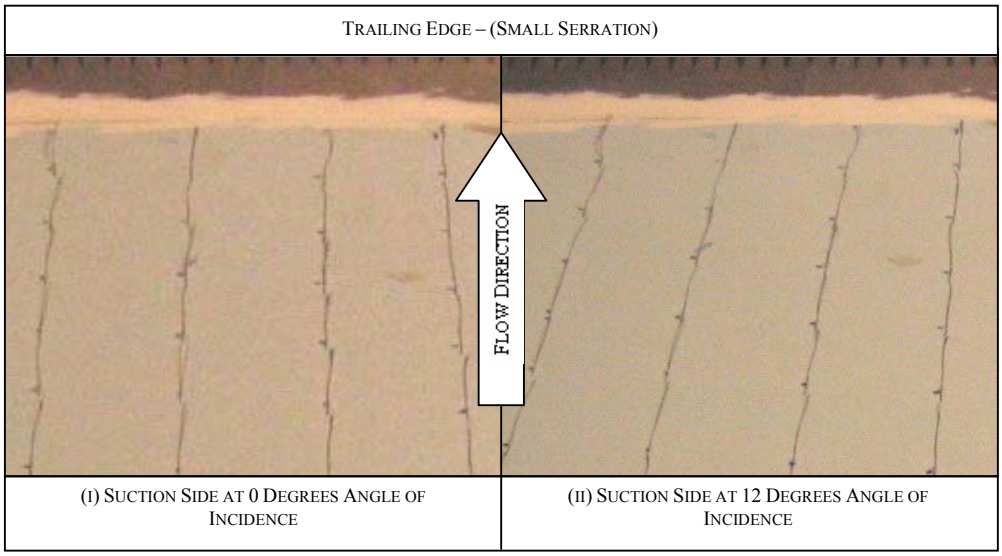

Figure 8.3.17 – Flow Visualisation Using Small Toothed Serrated Trailing Edge

With the large toothed serrated trailing edge attached the tufts showed no flow separation on the pressure side of the aerofoil at any of the angles of incidence tested. On the suction side of the aerofoil the flow remained attached at 0, 3, and 6 degrees angle of incidence but separated from the aerofoil near to the trailing edge with it set at 9 and 12 degrees angle of incidence. Figure 8.3.18 shows the state of the tufts near to the trailing edge on the suction side of the aerofoil at (i) 6 degrees and (ii) 9 degrees angle of incidence with an airflow speed of 40 m/s.

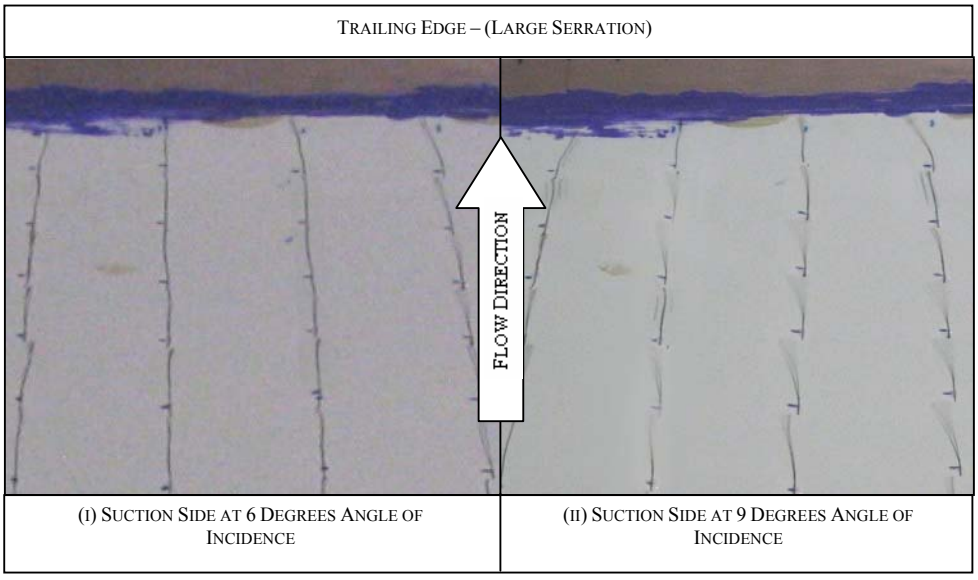

Figure 8.3.18 – Flow Visualisation Using Large Toothed Serrated Trailing Edge

4. Discussion

4.1 Main Span of Blade Unmodified

The noise generated by the 'main span' of the blade section was found to be dominated by low frequencies with various peaks throughout the spectrum, most notably in the 1/3 octave bands of 31.5 Hz, 80 Hz, 315 Hz, 500 Hz, 800 Hz and 2 kHz. It was found that the total noise generated with the main span of the blade section in the airflow increased by about 2 dB between 0 and 12 degrees angle of incidence. This was probably a result of increased flow irregularity in the wake of the blade as the angle of incidence increased and the onset of flow separation from the aerofoil occurred. However, while the noise at most frequencies increased with angle of incidence, the sound pressure level measured in each of the 1/3 octave bands from 800 Hz to 3.15 kHz was significantly reduced. It is difficult to provide an explanation of this phenomenon without an in-depth study of the flow over the aerofoil at each angle of incidence.

The frequency content of the spectrum measured was found not to be affected significantly by the airflow speed, except between 1.6 kHz and 4 kHz (see figure 8.3.3) for which the measured sound pressure level increased slightly (relative to background noise level) with the increasing flow speed. The fact that the frequency content of the spectrum remained relatively constant for different flow speeds indicates that noise produced by flow speed dependent mechanisms such as vortex shedding was not dominant in the noise generated by the aerofoil.

It was found that the relationship between the wind tunnel airflow speed and both the background noise level and the blade noise level fitted extremely well to a logarithmic curve. Extrapolating this curve, it could be expected that if the blade was tested in the wind tunnel under the same conditions but with the flow speed set at ~80 m/s as for the operating turbine, the background noise level would be approximately 116 dB and the measured noise level from the blade would be approximately 118 dB.

4.2 Tip of Blade Unmodified

Low frequency noise was found to dominate the sound pressure levels measured from the tip of the blade. Various peaks were observed throughout the spectrum, most notably in the 1/3 octave bands of 40 Hz, 63 Hz, 315 Hz, 800 Hz, and 2.5 kHz (see figure 8.3.7). The total noise generated by the tip of the blade

increased by about 1.5 dB between 0 and 12 degrees angle of incidence. As for the main span of the blade section, this was probably a result of increased flow irregularity in the wake of the blade as the angle of incidence increased and the onset of flow separation occurred. At the tip of the aerofoil the flow was found to separate at a lower angle of incidence than for the main span. The cotton tufts were beginning to show signs of separation at 9 degrees angle of incidence, and at 12 degrees angle of incidence showed separation near to the trailing edge of the aerofoil. This result is reflected in the sound pressure levels measured. Above 1 kHz the sound pressure level in each 1/3 octave band was found to decrease with increasing angle of incidence except that at 9 degrees angle of incidence sound pressure level above at 3.15 kHz and above increased, and at 12 degrees angle of incidence the sound pressure level above 1.6 kHz was significantly increased (particularly at 6.3 kHz) when compared with the angles of incidence that showed no flow separation. This indicates that separation of the flow considerably influences the sound produced at higher frequencies. However, during normal operation of the turbine it would be unusual for the angle of incidence to be greater than 9 degrees and therefore additional noise created by separation of the flow would be unlikely to be present. Even if it were to occur, the high frequency of the additional noise produced would be readily attenuated by a number of mechanisms.

The frequency content of the spectrum measured was found not to be affected significantly by the airflow speed, except between 1.6 kHz and 5 kHz for which the measured sound pressure level increased slightly (relative to background noise level) with increasing flow speed. At 45 m/s the sound pressure level shows a small peak at 31.5 Hz that is not present at lower speeds. This could possibly indicate that as the flow speed increases above 45 m/s the dominant mechanisms of noise generation begin to change – however this remains purely speculative without further testing at higher flow speeds. From the data gathered, the frequency content of the spectrum could be said to have remained relatively constant for different flow speeds, indicating that noise produced by flow speed dependent mechanisms such as vortex shedding was not dominant in the noise generated by the aerofoil.

An interesting observation made during testing was the direction that the cotton tufts faced at greater angles of incidence. It was found that as the angle of incidence increased the rows of tufts furthest from the tip near to the trailing edge on the suction side of the aerofoil began to point toward the tip. This could possibly be attributed to end effects at the tip causing a span-wise flow along the aerofoil toward

the tip. The fact that only the tufts furthest from the tip reacted in this way could be due to the reduction in Reynolds number that occurs as a result of the smaller chord size nearer to the tip. The lower Reynolds number would mean that the flow was less turbulent and the tufts would therefore be less likely to show span-wise flow effects. Another possible explanation for the observation is that wall effects from the wind tunnel outlet were influencing flow on that side of the test section. However, when the tip was shifted across the flow so that the tufts in question were more centralised in the jet the effect remained, which would not be expected if it was wall effects from the tunnel influencing the flow.

4.3 Comparison with Field Data

When the wind tunnel measurements of noise from the blade are compared with a measurement taken on the operating turbine it can be seen that the frequency content of each measurement is similar. The peaks at 315 Hz and 500 Hz are present in both spectrums, but the peaks at 31.5 Hz and 800 Hz on the wind tunnel measurements are not present on the field measurement, instead being replaced with peaks at 25 Hz and 1 kHz. The general level of noise at low frequencies was much lower (relative to the other frequencies in the spectrum) on the field measurement. However it is clearly not a good comparison. The measurements in the wind tunnel were taken with the microphone placed 750 mm below the trailing edge of the blade whereas in the field the microphone was not in a fixed position relative to the blade (since the blade was rotating) and was approximately 1m from the trailing edge each time the blade passed. This would have had the effect of reducing the level of noise that was measured compared to that if the microphone was stationary relative to the blade. The field measurement was taken only 4m from the root of the blade whereas the wind tunnel measurements used a section near the tip. The larger chord and slower airflow speed nearer to the root of the blade would have influenced both the frequency content and the level of the spectrum measured. Finally, the field measurement would have also included the noise radiated as a result of structure-borne noise from the blade, which could have increased the noise measured at certain frequencies.

Despite these differences the comparison provided confidence that the wind tunnel investigation produced results that related reasonably well to the actual situation. Perhaps most significantly, the wind tunnel tests showed that the blades were generating aerodynamic noise in the 315 Hz 1/3 octave band. This indicated that the large amount of 315Hz noise radiated from the blades was not entirely due to structure-

borne noise transmitted from the gearbox as previously thought and could possibly be reduced to some extent by modifying the aerodynamics of the blade.

4.4 Effect of Serrated Trailing Edges

With the small serrated trailing edge attached to the blade it was found that the total sound pressure level increased by only 0.6 dB from 0 to 12 degrees angle of incidence. With the large serrated trailing edge attached the sound pressure level was found to increase by about 1 dB from 0 to 12 degrees angle of incidence. When compared with the increase of noise with angle of incidence for the unmodified blade, it can be seen that the use of the serrated trailing edges reduced the influence of the angle of incidence on the level of noise produced by the aerofoil.

At 0, 3, and 6 degrees angle of incidence the large toothed serration produced a greater noise reduction than the small toothed one, but at 9 and 12 degrees angle of incidence when the flow was found to be separated for the large toothed serration, the small toothed serration performed better. Below 100 Hz the small toothed serration was generally found to perform better. At low angles of incidence a reduction of up to 4.5 dB was observed at 2.5 kHz for both trailing edges. This reduction decreased with increasing angle of incidence to about 1 – 2 dB at 12 degrees. Above 3.15 kHz both trailing edges were found to increase the noise produced by the aerofoil, but the increase was less for the large serration than for the small serration. In practice a slight increase at these high frequencies would probably be of little consequence since the noise at those frequencies would be rapidly attenuated.

The flow phenomena causing the noise reductions and increases observed at certain frequencies are undoubtedly very complex and related to the size, aspect ratio, and profile of the teeth. The two serrated trailing edges tested here appear to have achieved the reductions observed through different mechanisms. This is evident because the flow across the unmodified blade separated near to the trailing edge at 12 degrees angle of incidence, while the blade with the large toothed serration attached showed signs of flow separation at only 9 degrees angle of incidence and the blade with the small toothed serration showed no signs of flow separation at any of the angles of incidence tested. Clearly further investigation of the flow over the aerofoil with each modification should be conducted in any future work. The effects of each

modification on the actual performance (lift / drag) of the aerofoil would also need to be investigated before a solution such as this could be incorporated into the blades for an actual turbine.

4.5 Quality of Results

Ideally, to ensure that the sound pressure level of the data gathered is unaffected by background noise, the background noise level should be at least 10 dB below the blade noise level. During testing it was found that the noise produced by the blade at each frequency was typically 2 – 7 dB above the background noise level. However, in this instance the absolute level of the noise measured was of less interest than the actual frequencies produced and their relative contributions, which could be determined reasonably accurately despite the higher than ideal background noise levels.

A small portion of the background noise was due to noise from the fans of the wind tunnel, but the majority of the noise was found to be flow noise. One of the main sources of the noise was a deflector that was placed near to the end of the wind tunnel in order to redirect the flow over a wall near to the tunnel exit (see figure 8.4.1).

Figure 8.4.1 – Airflow Deflector

The deflector was buffeted by the flow at high air speeds and consequently produced a lot of low frequency flow noise, particularly with the aerofoil set at higher angles of incidences where the wake was more turbulent and much more deflected downwards.

Despite relatively high levels of background noise, the results were found to be highly repeatable. Consecutive measurements on the same day were found to be within ± 0.1 dB at each frequency, while measurements repeated on different days were found to be within ± 0.3 dB of one another at each frequency. The larger difference between measurements on different days could most likely be attributed to differences in atmospheric conditions.

5. Conclusions and Recommendations

In unmodified form, the noise produced by the blade increased with increasing angle of incidence. It was found that the blade produced noise over a wide range of frequencies with tonal peaks observed in several 1/3 octave bands. One such peak was found to occur in the 315 Hz 1/3 octave band, which indicated that the large amount of noise radiated from the blades of the operating turbine at this frequency was not entirely due to structure-borne noise transmitted from the gearbox as previously thought. The spectral results of the wind tunnel tests were found to agree reasonably well with field measurements, despite difficulties in comparison.

Modifying the blade with serrated trailing edges was found to reduce the total noise produced as expected but was also found to increase the noise generated by the blade at frequencies above 3.15 kHz. In general the large toothed serrated trailing edge was found to perform better at low angles of incidence while the small toothed one performed better at high angles. Analysis of the flow over the aerofoil with each of the trailing edge modifications showed that the flow was vastly different in each case. Further investigation would be required into the size, aspect ratio and profile of the teeth, along with the effects of the modifications on the performance of the aerofoil (lift / drag) if a worthwhile reduction in aerodynamic blade noise was to be achieved using serrated trailing edges.

6. References

[1] Braun K., et al., "Noise Reduction by Using Serrated Trailing Edges," presented at EWEA Conference, Dublin Castle, Ireland, 1997.

[2] Braun K., et al., "Serrated Trailing Egde Noise (STENO)," presented at EWEA Conference, Nice, France, 1999.

[3] Dassen T., Parchen R., et al., "Results of a Wind Tunnel Study on the Reduction of Airfoil Self-Noise by the Application of Serrated Blade Trailing Edges," presented at EWEA Conference, Goteborg, Sweden, 1996.

[4] Hagg F., van Kuik G., Parchen R., and van der Borg N., "Noise Reduction on a 1MW Size Wind Turbine with a Serrated Trailing Edge," presented at EWEA Conference, Dublin Castle, Ireland, 1997.

[5] Howe M., "Noise Produced by a Sawtooth Trailing Edge," *J. Acoust. Soc. Am.*, vol. 90, pp. 482 - 487, 1991.

[6] Jakobsen J. and Andersen B., "Aerodynamical Noise from Wind Turbines - Experiments with Full Scale Rotors, Change of Pitch, Trailing Edges, and Tip Shapesq," DELTA Acoustics and Vibration AV 590/95, 1995.

[7] Klug H., Osten T., et al., "Aerodynamic Noise from Wind Turbines and Rotor Blade Modification," presented at EWEA Conference, Goteborg, Sweden, 1996.

[8] Lienhard, J.H., 1966. "Synopsis of Lift, Drag, and Vortex Frequency Data for Rigid Circular Cylinders". Bulletin 300, Washington State University.

[9] Wagner S., Bareiss R., and Guidati G., *Wind Turbine Noise*: Springer, 1996.